5-2010

Liquefaction Analysis of Three Pleistocene Sand Deposits that did not Liquefy During the 1886 Charleston, South Carolina Earthquake based on Shear Wave Velocity and Penetration Resistance

Aaron Geiger
Clemson University, ajgeiger@gmail.com

LIQUEFACTION ANALYSIS OF THREE PLEISTOCENE SAND DEPOSITS THAT DID NOT LIQUEFY DURING THE 1886 CHARLESTON, SOUTH CAROLINA EARTHQUAKE BASED ON SHEAR WAVE VELOCITY AND PENETRATION RESISTANCE

A Thesis
Presented to
the Graduate School of
Clemson University

In Partial Fulfillment
of the Requirements for the Degree
Master of Science
Civil Engineering

---

by
Aaron James Geiger
May 2010

Accepted by:
Dr. Ronald D. Andrus, Committee Chair
Dr. C. Hsein Juang
Dr. Bradley J. Putman

This research was supported by the National Science Foundation, under the NSF grant number CMS-0556006. Any opinions, findings, conclusions, or recommendations are made by the author of this thesis and do not necessarily reflect the views of the National Science Foundation.

ABSTRACT

The results of geotechnical investigations at three sites located in the South Carolina Coastal Plain are presented in this thesis. The three sites are called the Hobcaw Barony Borrow Pit site located near Georgetown, SC; the Rest Area Ponds site near Walterboro, SC; and the Lowcountry Sand & Gravel site, also near Walterboro. Near-surface sand deposits at these sites ranged in geologic age from 200,000 to greater than 1,000,000 years. These three sites lie well outside the region of most liquefaction effects observed following the 1886 Charleston earthquake. Investigations conducted at the sites include seismic cone penetration tests with pore pressure measurements (SCPTu), dilatometer tests (DMT), standard penetration tests (SPT), seismic crosshole tests, and fixed piston sampling. Laboratory investigations on samples collected include grain size, Atterberg limit, and consolidation tests.

Sand layers most susceptible to liquefaction are identified at each site. For these critical sand layers, ratios of measured V_s to V_s estimated (MEVR) using relationships proposed by Andrus et al. (2004a) are 1.28, 1.13, and 1.36 at the Borrow Pit, Rest Area Ponds, and Lowcountry Sand & Gravel sites, respectively. These MEVRs suggest geotechnical ages of 16,000, 240, and 152,000 years for each site, respectively, based on the MEVR-time relationship presented in Andrus et al. (2009).

The critical sand layers at each site are evaluated for liquefaction potential using shear wave velocity-based and penetration-based cyclic resistance ratio

(CRR) curves adjusted for age/cementation. The results of the evaluation indicate low probability of liquefaction at the three sites during the 1886 Charleston earthquake. Based on the 2% probability of exceedance in 50 years earthquake scenario suggested by the 2008 USGS Hazard Map, moderate liquefaction is predicted for the Borrow Pit and Rest Area sites and marginal liquefaction is predicted at the Lowcountry Sand & Gravel site. Predictions based on shear wave velocity and penetration are in good general agreement with each other when age/cementation corrections are applied.

DEDICATION

I dedicate this thesis to all my dear friends and family, especially my mother, father and brother, for their continued love, support, and fellowship in all my endeavors.

ACKNOWLEDGMENTS

First I would like to graciously thank my advisor Dr. Ronald Andrus for being my mentor since 2006. His guidance, patience, and positive support were greatly appreciated and I don't feel I could have had a better adviser. I also would like to thank my committee members Dr. C. Hsein Juang and Dr. Bradley Putman for serving on the committee and for taking the time to review my thesis. In addition, I give thanks to Billy Camp and many others at S&ME for their support of this study and for providing the necessary field equipment to complete my research.

I would also like to thank the National Science Foundation for funding my research for the past two and a half years. In addition, special thanks are given to George Askew and Jeff Vernon of the Baruch Institute of Coastal Ecology and Forest Science, Charles Byrd of the SCDOT, and Roger Walker of Lowcountry Sand & Gravel, Inc. for providing sites for geotechnical study. I also thank the assistance of the many current and former graduate students throughout this project, especially Ronald Boller, Hossein Hayati, Tehereh Heidari, Md. Akhter Hossain, and Shimelies Aboye for their assistance and guidance in the data collection and analysis for this research.

Finally, I thank my friends and my family for their support during all my endeavors, especially my mother, father, and brother. I also want to thank my dearest friend Jenny Tate for being there for me during my research and for giving me encouragement whenever I was in need.

TABLE OF CONTENTS

Table of Contents (Continued)

Table of Contents (Continued)

LIST OF TABLES

List of Tables Continued

Table Page

List of Tables Continued

Table Page

List of Tables Continued

Table Page

List of Tables Continued

Table Page

LIST OF FIGURES

List of Figures Continued

Figure Page

List of Figures Continued

Figure Page

List of Figures Continued

Figure Page

List of Figures Continued

Figure Page

List of Figures Continued

Figure Page

List of Figures Continued

Figure Page

List of Figures Continued

CHAPTER ONE

INTRODUCTION

1.1 Liquefaction Overview

Liquefaction is an important hazard to consider in seismic hazard analyses of sites. Liquefaction occurs when the soil skeleton collapses and the load carried by the grain-to-grain contacts is transferred to the pore water, usually initiated by earthquake shaking. The increase in pore pressure reduces effective stress, causing the soil to lose strength and bearing capacity. Liquefaction typically occurs in granular material, such as sand. Liquefaction-induced ground failures can cause structural damage and potentially loss of life. There are many factors that can affect the susceptibility and potential of liquefaction. One of these factors is the age of the deposit.

1.2 Liquefaction Potential and Aged Soils

Currently, the most widely used procedure for analyzing liquefaction potential is the simplified procedure originally proposed by Seed and Idriss (1971) and subsequently updated by many others (e.g., Seed et al. 1985; Robertson and Wride 1998; Andrus and Stokoe 2000; Youd et al. 2001; Juang et al. 2002; Cetin et al. 2004; Moss et al. 2006; Idriss and Boulanger 2008). The procedure involves determining an earthquake's loading on soil, known as the cyclic stress ratio (CSR), and a soil's capacity to resist liquefaction, known as the cyclic resistance ratio (CRR). The factor of safety against liquefaction is determined by dividing CRR by CSR. A number of charts have been proposed to estimate CRR based on penetration resistances or small-strain shear wave velocities and values of CSR calculated for locations that did or did not liquefy. The curves separating CSR values for cases of liquefaction from cases of no liquefaction are called CRR curves. Sites that plot above the curve are likely to liquefy under the given earthquake loading.

One limitation to most CRR curves is that they are primarily based on young soil deposits with ages of less than 1000 years (Youd et al. 2001). In fact, Hayati and Andrus (2009) found that many of the liquefaction cases are from deposits that are less than 50 years old. Thus corrections may be necessary to account for older soil deposits.

Youd and Perkins (1978) and Seed (1979) both suggest an increase in liquefaction potential with an increase in the age of the deposit. In the past 20 years, there has been a series of studies conducted that have led to a suggestion for a correction factor that accounts for the influence of age, cementation, and stress history on CRR (Troncoso et al. 1988, Lewis et al. 1999, Arango et al. 2000, Leon et al. 2006, Hayati et al. 2008, Hayati and Andrus 2008b, 2009). This correction can be applied by:

$$CRR_k = CRR * K_{DR} \quad (1.1)$$

where CRR_k is the deposit resistance-corrected CRR and K_{DR} is the correction factor.

Hayati and Andrus (2009) proposed the following equation based on age for estimating K_{DR}:

$$K_{DR}=0.13\log_{10}(t)+0.83 \qquad 1.2$$

where *t* is either the age of the deposit or the time since the last critical disturbance (i.e. liquefaction). It was the belief of Hayati and Andrus (2009) that a critical disturbance in a soil would cause the grain-to-grain contacts in the soil to "reset", which would cause a disturbed soil to geotechnically act more like a young soil deposit than an older one. This poses a problem for sites where there is little to no information on past earthquakes to determine time since the last critical disturbance. With that in mind, a property to estimate the age of a soil has been proposed and is defined as the measured to estimated velocity ratio (MEVR).

MEVR is determined by obtaining shear wave velocities from in situ testing and dividing them by velocities calculated using the following penetration resistance-based empirical equations from Andrus et al. (2004a):

$$(V_{s1})_{cs}=87.6[(N_1)_{60cs}]^{.253} \qquad 1.3$$

$$(V_{s1})_{cs}=62.6[(q_{t1N})_{cs}]^{.231} \qquad 1.4$$

where $(N_1)_{60cs}$ and $(q_{t1n})_{cs}$ are the clean sand and overburden stress-corrected SPT blowcount and cone tip resistance, respectively. Andrus et al. (2009) characterizes Equation 1.4 as a relationship for six year old deposits. Because Equations 1.3 and 1.4 were derived from the measurements at the same site, Equation 1.3 is likely also for deposits of about six years old.

Presented Figure 1.1 is the relationship between MEVR and the time since initial deposition or critical disturbance proposed by Andrus et al. (2009) It is seen that MEVR increases significantly with time.

As an alternative to Equation 1.2, Hayati and Andrus (2009) presented the following equation to replace time in Equation 1.2 with MEVR:

$$K_{DR}=1.08*MEVR-0.08 \quad 1.5$$

This equation allows for the estimation of K_{DR} without needing to know the age or time since last critical disturbance.

In Equation 1.5, MEVR attempts to account for all the diagenetic processes that occur over time in a soil deposit. Friedman and Sanders (1978, p.145) characterized diagenetic processes as involving compaction, addition of new material, removal of material, transformation by change of mineral phase, and transformation by replacement of one mineral phase by another. These diagenetic processes can have a significant effect on liquefaction resistance.

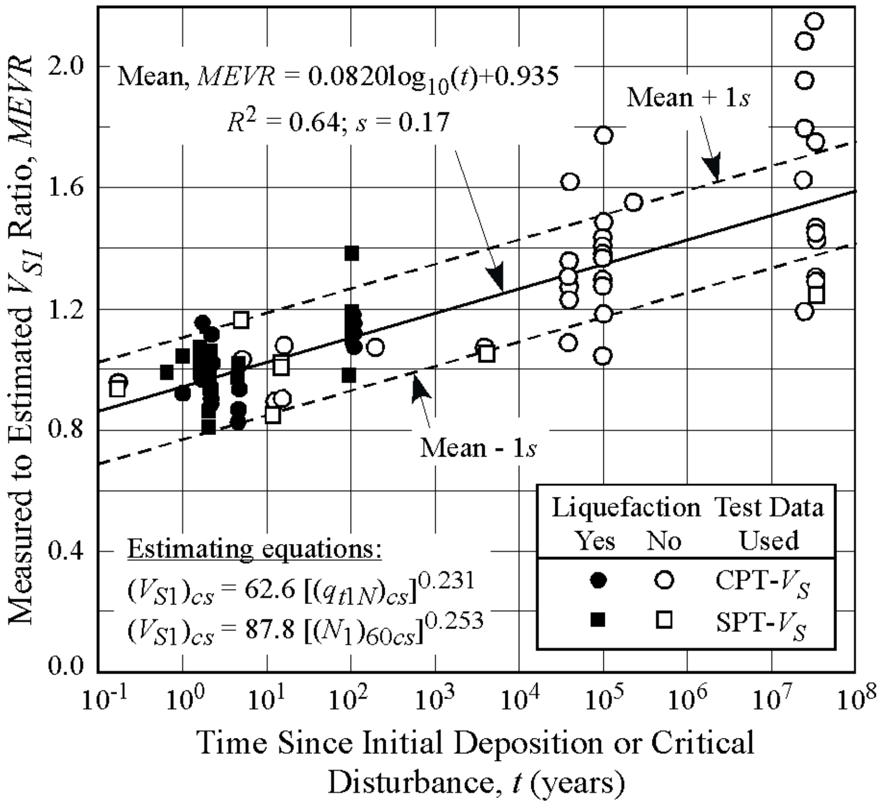

Figure 1.1 Relationship between MEVR and time since initial deposition or critical disturbance as presented by Andrus et al. (2009) based on estimating equations by Andrus et al. (2004a).

1.3 Purpose of Research

The relationship between MEVR and geotechnical age shown in Figure 1.1 is well supported by case studies performed in young or recently disturbed soils. As for older soils, however, Figure 1.1 shows scatter for older sites. In addition, there is a significant lack of case studies between ages of 100,000 and 1,000,000,000 years. In order to improve our understanding of MEVR, additional case studies are needed. The South Carolina Coastal Plain is a good source for these case studies because of the August 31st, 1886 Charleston earthquake and the geology, which provides many unique regions of varying soil types and ages.

The search for case studies for this thesis focused on finding sites with near-surface sand deposits with geologic ages between 100,000 and 1,000,000,000 years. Specifically, sand deposits that are susceptible to liquefaction but did not liquefy in 1886 were desired. These sand deposits are tested for liquefaction potential using shear wave velocity-based CRR curves and penetration resistance-based CRR curves.

1.4 Scope and Organization

This research is part of a National Science Foundation-sponsored project to create case studies and to investigate the behavior and liquefaction potential of aged sands. Clemson University, the University of South Carolina, and S&ME, Inc. are all partners on the project. At Clemson, the goal has been to develop geotechnical investigation sites at locations throughout the South Carolina coastal region that did not liquefy in 1886. This thesis focuses on three of those sites; one near Georgetown, SC and two near Walterboro, SC. At the sites, seismic cone penetration testing with pore pressure measurements (SCPTu), standard penetration testing (SPT) with split spoon sampling, Hvorslev and Osterberg fixed-piston sampling, dilatometer testing (DMT), and seismic crosshole testing were conducted. Additionally, grain size analyses, Atterberg limit tests, and consolidation tests were performed at Clemson. The objective of the testing is to characterize the soil deposits at the sites in order to evaluate liquefaction susceptibility and potential.

Chapter 2 outlines the field and laboratory testing procedures for all testing conducted at the three sites, as well as the procedures for reduction of test data. Chapter 3 presents the results of the investigations performed at the Hobcaw Borrow Pit site near Georgetown. Chapters 4 and 5 present the results of investigations of the Rest Area Ponds site and Lowcountry Sand & Gravel site, respectively, located near Walterboro. Chapter 6 is devoted to the liquefaction evaluation procedure for each of the three sites. Finally, Chapter 7 summarizes the findings of this thesis research and proposes future studies to be conducted. Three appendicies (A-C) present detailed test results for each of the three sites. The fourth appendix (D) contains tabulated CPT penetration data for all three sites.

CHAPTER TWO

TEST METHODOLOGY

This chapter presents the testing procedures performed at the three geotechnical investigation sites. It also includes procedures and assumptions used in reducing the experimental data and references the ASTM standard for each test.

2.1 Seismic Cone Penetration Test

The seismic cone penetration tests with pore pressure measurements (SCPTu) were performed according to ASTM D 5778. In the tests, a 15 cm^2 electric piezocone penetrometer was hydraulically pushed through the ground at a rate of 2 cm/s. The SCPTu apparatus included load cells behind the tip and near the sleeve to determine tip resistance (q_t) and sleeve friction (f_s). It also had a saturated pore pressure transducer behind the cone tip for determining pore water pressure (u_2). This transducer used a filter that had been saturated in vacuum oil for several days, according to the test operator, to provide a good coupling between the pore water pressure in the soil and the transducer. Values of q_t, f_s, and u_2 were recorded by computer at a rate of 27 samples per meter.

In addition to the equipment previously mentioned, two geophones were placed inside the cone rods 1.00 m apart. These geophones received seismic waves generated at the surface by the source, which was a hammer striking a horizontal plank on the ground surface as shown in Figure 2.1. With both geophones, true interval velocity measurements were made.

Figure 2.1 SCPTu truck rig's front leveling jack, which also serves as the source of the seismic energy for true interval velocity measurements.

Figure 2.2 Data acquisition station and hydraulic assembly inside the cone truck.

2.1.1 Test Setup

Details of SCPTu testing at the Hobcaw Borrow Pit site are given in Boller (2008). At the two Walterboro sites, S&ME provided a tire-mounted truck rig for conducting SCPTu's (see Figure 2.1). At each cone sounding location, the truck used hydraulic jacks to become level for testing. After the rig was level, the cone penetrometer was lowered through an opening on the underside of the truck and then pushed into the ground using a hydraulic assembly inside the truck, which is also where the data acquisition station was located, as is seen in Figure 2.2.

During the testing process, the operators stopped pushing the cone at relatively regular intervals to conduct seismic velocity testing. An automatic solenoid hammer struck a metal plank in the truck's front jack. The energy traveled through the ground and was received by both geophones. The locations of the geophones are shown in Figure 2.3. Two hits were made in opposite directions, which was done to obtain two different sets of signals that were 180° out of phase with each other, creating a butterfly pattern.

2.1.2 SCPTu Seismic Data Reduction

For this thesis, true interval velocity measurements were taken for all SCPTu's. This means that two geophones received signals from a single hit, as opposed to pseudo interval velocity measurements where only one geophone is used and two hits are required. In the pseudo-interval method, significant differences are more likely to occur in wave forms which can lead to interpretation errors. However, wave forms generated from one hit are likely to be more similar, which can lead to reduced errors in the calculated velocity.

To determine the velocity, the distances between the source and receivers and the travel time must be known. The velocity from SCPTu can be calculated using the equation in Figure 2.4 and the distances displayed.

Figure 2.5 is a representative set of signals for a given depth collected during a SCPTu. With two signals, the goal is to look for the time shift of similar points between the top and bottom signals. The points considered are most commonly the first arrival, the first peak, and the first crossover. First arrivals are determined by finding the point in the wave form at which the strong shear wave appears to arrive. This is usually seen as a sudden increase or decrease from the initial flat portion of the wave form. First peaks are initial maximum or minimum values in a wave form. They usually come soon after the first arrival. Finally, the first crossover is the point after the first peak where the voltage returns to the initial value. The point at which this occurs is the first crossover.

For the Walterboro Rest Area and Lowcountry Sand & Gravel sites, the first arrival was not used as a reference point due to the difficulty in selecting distinct arrival points. Therefore, only first peak and first crossover points after the initial shear wave were used. Travel time for each wave was determined by subtracting the time it takes the wave to reach the top geophone from the time it takes the wave to reach the bottom geophone. Because two hits were used at each depth, a total of four travel times were determined. After determining the distance the wave traveled from the top geophone to the bottom geophone, the velocities were determined using the equation in Figure 2.4. The four velocities were averaged together to obtain a single shear wave velocity for the test depth.

After obtaining an average velocity, the velocities were corrected for overburden stress and fines content. Youd et al. (2001) recommended that the following overburden stress correction be used:

$$V_{s1}=V_s\,(P_a/\sigma_v')^{0.25} \qquad 2.1$$

where V_{s1} is the overburden stress-corrected shear wave velocity, σ'_v is the vertical effective stress, and P_a is atmospheric pressure of 100 kPa. Juang et al. (2002) suggested using the following equations to adjust the velocity to a clean sand equivalent, $(V_{s1})_{cs}$:

$$(V_{s1})_{cs}=K_{cs}V_{s1} \quad 2.2$$

where K_{cs} is defined by the following equations:

$$K_{cs}=1.0,\ FC \leq 5\% \quad 2.3a$$

$$K_{cs}=1+(FC-50)T,\ 5\% < FC < 35\% \quad 2.3b$$

$$K_{cs}=1+30T,\ FC \geq 35\% \quad 2.3c$$

where FC is the fines content and T is defined by the following equation:

$$T = 0.009-0.0109(V_{s1}/100) + 0.0038(V_{s1}/100)^2 \quad 2.4$$

Fines content determined from laboratory testing was used where applicable. At the Lowcountry Sand & Gravel site however, no samples were taken for analysis. Thus, the fines contents for this site were estimated using the following relationship suggested by Robertson and Wride (1998):

$$FC = 1.75I_c^{3.25} - 3.7,\ 1.26 \leq I_c \leq 3.5 \quad 2.5$$

where I_c is the soil type behavior index, which will be explained further in the section on SCPT penetration data reduction.

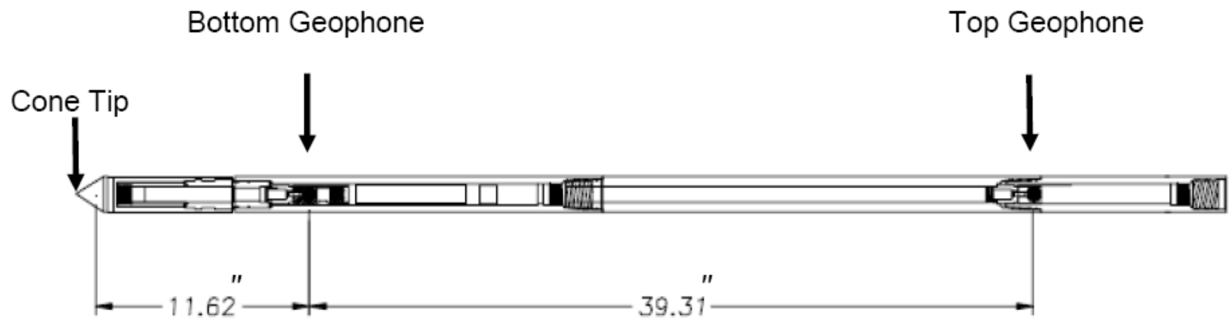

Figure 2.3 SCPTu probe with locations of geophones for true interval shear wave velocity calculations (Boller 2008).

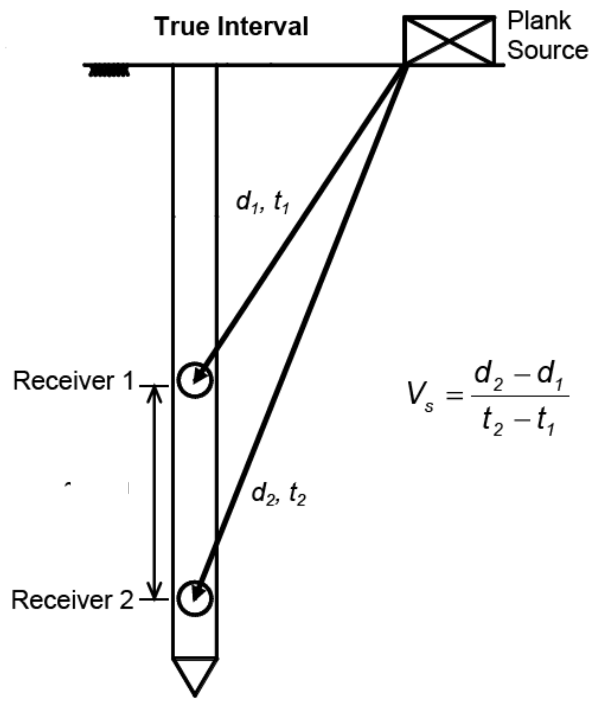

Figure 2.4 Diagram of true interval method used for calculating shear wave velocity (Boller 2008).

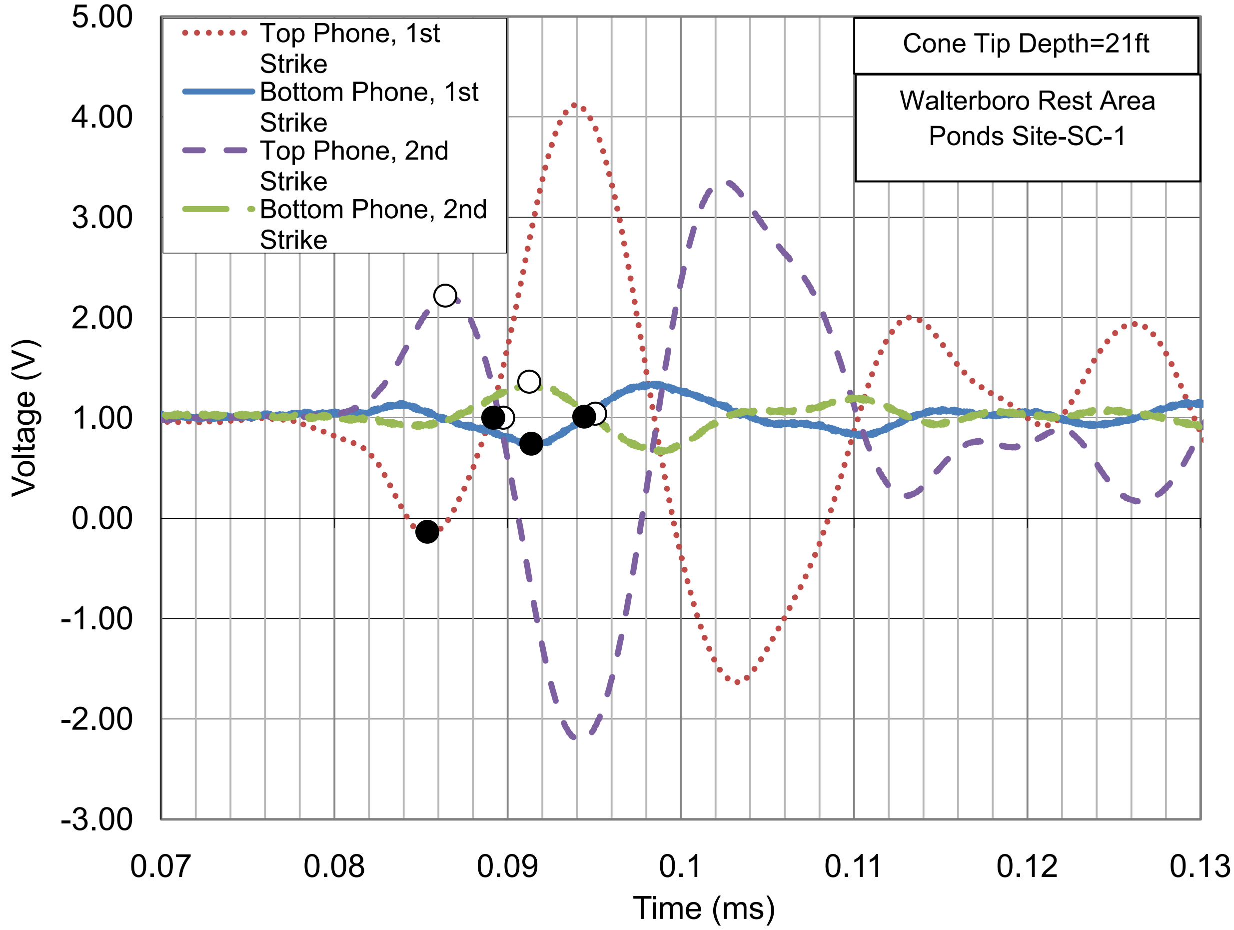

*Peak and crossover points used for determining travel times are highlighted with circles. White circles are the 2nd strike. Black circles are the 1st strike.

Figure 2.5 Typical true interval time histories for SCPTu testing.

2.1.3 SCPTu Penetration Data Reduction

Various index properties were calculated from the q_t, f_s, and u_2 measurements and are presented in summary tables in Chapters 3, 4, and 5. These indexes are used for determining liquefaction susceptibility and potential. The index properties included are stress-corrected normalized cone tip resistance (q_{t1N}), friction ratio (FR), normalized friction ratio (F_N), normalized cone tip resistance (Q_t), normalized cone pore pressure ratio (B_q), and soil behavior type index (I_c). Robertson and Wride (1998) and Youd et al. (2001) present the following equations for determining these values:

$$q_{t1N} = (q_t/P_a)\,(P_a/\sigma'_v)^n \qquad 2.6$$

$$FR = (f_s/q_t) * 100\% \qquad 2.7$$

$$F_N = (f_s/(q_t - \sigma_v)) * 100\% \qquad 2.8$$

$$Q_t = [(q_t - \sigma_v)/P_a]\,(P_a/\sigma'_v)^n \qquad 2.9$$

$$B_q = (u_2 - u_0)/(q_t - \sigma_v) \qquad 2.10$$

$$I_c = [(3.47 - \log Q_t)^2 + (1.22 + \log F_N)^2]^{0.5} \qquad 2.11$$

where P_a is a reference stress of 100 kPa, σ_v is the vertical total stress, n is an exponent that ranges from 0.5 for sand to 1.0 for clay, and u_0 is the hydrostatic pressure determined by multiplying the depth below the groundwater table by the unit weight of water. These six equations all produce dimensionless values.

Finally, Robertson and Wride (1998) suggested a clean sand correction for q_{t1N}. These corrective equations are:

$$(q_{t1N})_{cs}=K_c q_{t1N} \qquad 2.12$$

where K_c is calculated by:

$$K_c=1.0,\ Ic\leq1.64 \qquad 2.13a$$

$$K_c=-0.403I_c^4+5.581I_c^3-21.63I_c^2+33.75I_c-17.88,\ I_c>1.64 \qquad 2.13b$$

2.2 Dilatometer Test

The flat plate dilatometer test (DMT) was performed using equipment owned and operated by S&ME in accordance with ASTM D 6635 01. The DMT involved pushing a tapered blade into the ground at a rate of roughly 20 mm/sec. The pushing was temporarily halted at 0.3 m (1.0 ft) intervals for testing. The DMT is conducted using nitrogen gas pressure to cause a metal membrane to expand out and deform the soil. The pressures at deformations of 0.05 mm and 1.1 mm were recorded, these pressures are called the lift off pressure (P_0) and expansive pressure (P_1), respectively. After obtaining these pressures, the plate was returned to zero deformation. The pressure at this point is called closing pressure (P_2). The readings were taken in 15-30 second intervals, though sometimes P_2 was unobtainable.

Figure 2.6 shows the DMT control box with pressure gages. The beginning of the DMT included determining the membrane stiffness correction factors (ΔA and ΔB). For these baseline tests, vacuum pressure was applied to the membrane with a syringe. A buzzer went off when the membrane collapsed to a distance of 0.05 mm. This pressure is ΔA. The pressure was then increased to a deformation of 1.1 mm. The buzzer went off again at this point. This pressure was ΔB. Both baseline correction factors were remeasured at the end of the DMT. The correction factors were averaged to obtain one ΔA and one ΔB value.

Figure 2.6 Dilatometer control box with pressure gages.

After establishing the initial baseline correction factors, the DMT was conducted every 0.3 m (1.0 ft). At each test depth, the dilatometer was expanded to a 0.05 mm deformation. The buzzer went off at this deformation, and the lift off pressure, A, was recorded. The deformation was then increased to 1.1 mm. Again, the buzzer went off and the expansive pressure, B, was recorded. The pressure was then slowly released, allowing the deformation to return to zero. This pressure is the closing pressure, C. The values of P_0 and P_1 were determined using the following equations presented by Marchetti (1980):

$$P_0=1.05(A+\Delta A-Z_m)-0.05(B-\Delta B-Z_m) \quad 2.14$$

$$P_1=B-\Delta B-Z_m \quad 2.15$$

where Z_m is the zero correction for the gauge.

2.2.1 DMT Data Reduction

The results of the DMT data reduction can be found in Appendix B and C for the Walterboro test sites and in Boller (2008) for the Hobcaw Borrow Pit site. The pressure readings from the DMT are used to obtain various geotechnical indexes and coefficients. These include the DMT material index (I_D), the horizontal stress index (K_D), the at-rest earth pressure coefficient (K_0), and the DMT constrained modulus (E_D). Marchetti (1980) recommended the following equations for determining I_D, K_D, and E_D:

$$I_D = (P_1-P_o)/(P_o-u_o) \quad 2.16$$

$$K_D = (P_1-u_0)/\sigma'_v \quad 2.17$$

$$E_D = 34.7(P_1 - P_0) \quad 2.18$$

For K_0, two different equations were used. For soils with $I_D<1.2$, K_0 was determined using the following equation (Marchetti, 1980):

$$K_0 = (K_D/1.5)^{0.47} - 0.6 \quad 2.19$$

For soils with $I_D \geq 1.2$, K_0 was determined using an equation originally presented by Baldi et al. (1986) based on natural sand deposits along the Po River. This equation was recommended by Marchetti et al. (2001) for natural sand deposits and can be expressed as:

$$K_0 = 0.376 + 0.095\, K_D - 0.005\, (q_t/\sigma'_v) \quad 2.20$$

2.3 Fixed Piston Sampling

At the Hobcaw Borrow Pit and the Walterboro Rest Area Ponds sites, fixed piston samples were obtained. At Hobcaw, a Hvorslev-type fixed piston sampler was used to obtain samples. At the Walterboro Rest Area Ponds site, an Osterberg-type fixed piston sampler (see Figure 2.7) was used. The Hvorslev fixed-piston sampler required the use of inner rods, whereas the Osterberg fixed-piston sampler did not and was easier to use. In addition, the vacuum created within the thin walled tubes was much easier to release in the Osterberg sampler than in the Hvorslev sampler.

The fixed piston tubes were immediately capped at the bottom. The bottom caps had small holes in them to allow the samples to drain. After draining overnight, hot wax was poured on the top of the sample. The tubes were capped on the top and black tape was used to seal the seams between the caps and tubes. The tubes were always kept vertical or near vertical during handling in the field and transporting them back to the laboratory. The tube samples were transported by car in a wooden frame. Foam was used to cushion the tubes against the frame and to reduce the effects of driving vibrations on the samples.

Figure 2.7 Osterberg sampler used at the Walterboro Rest Ponds site.

2.4 Standard Penetration Test

Standard penetration tests were conducted using equipment owned and operated by S&ME following ASTM D 1586. The SPT is a common field test method used to investigate the density and consistency of soils. It consists of a hammer falling a constant distance and striking an anvil connected to drill rods and a split spoon sampler. The split-spoon sampler was driven a distance of 0.46 m (1.50 ft) and the number of blows for each six inch interval was recorded. Due to the effect of possible disturbance and soil falling from the borehole wall, the blowcount in the top six inches is disregarded. Borehole depth measurements before pulling the drill rods and after inserting the SPT sampler indicated that soil falling from the borehole wall was minimal. The blowcounts from the two deepest six inch intervals were added together to obtain the blowcount (*N*) for that particular depth range.

SPT's were conducted at the Hobcaw Borrow Pit and Walterboro Rest Area sites using a CME 550X mud rotary drill with a 11.43 cm (4.5 in.) drill bit. High viscosity bentonite drilling mud was pumped through the drill bit to wash out trimmings and to prevent the borehole walls from collapsing. These trimmings were collected in a drilling mud box. Once the drill bit had reached a specified testing depth, it was replaced with the SPT split spoon sampler. Chalk was used to mark six inch intervals on the SPT rods. Attached to the rod at the ground surface was an apparatus with accelerometers and strain gages for determining the hammer system's energy efficiency for each blow. This apparatus is seen in Figure 2.8. An automatic trip hammer then activated to simulate the dropping a 140lb hammer for a distance of 76.2 cm (30 in.) for each blow. The number of blows for each six inch interval was recorded. After completing a test at a given depth, the SPT probe was replaced by the drill bit and drilling recommences. The split spoon sampler was opened and the sample was observed and stored. At the Hobcaw site, the samples were stored in plastic freezer bags, whereas glass jars were used to store some of the samples from the Walterboro Rest Area Ponds site, in addition to plastic bags.

2.4.1 SPT Data Reduction

Based on the work of many investigators, Youd et al. (2001) recommended that the *N* values be corrected for various test conditions. One of these was hammer energy efficiency (C_E). The correction for rod length (C_R) is not necessary as it was included in the energy efficiency measurements and the energy correction. Corrections for borehole diameter (C_B), and type of sampler (C_S) both equal one. N was corrected by the following equation to obtain N_{60}:

$$N_{60}=N*C_E*C_B*C_S \qquad 2.21$$

In addition, N_{60} was corrected for overburden stress (C_N). This correction was determined by the following equation presented by Kayen et al. (1992):

$$C_N=2.2/(1.2+\sigma'_{vo}/P_a) \qquad 2.22$$

where P_a is equal to 100 kPa. The stress-corrected blowcount ($(N_1)_{60}$) was determined by the following equation:

$$(N_1)_{60}=N_{60}*C_N \qquad 2.23$$

In addition to the overburden-stress correction, a clean sand correction was applied to obtain $(N_1)_{60cs}$. Youd et al. (2001) recommended the following set of equations for the clean sand correction:

$$(N_1)_{60cs}=\alpha+\beta(N_1)_{60} \qquad 2.24$$

where α and β are coefficients determined by the following equations:

$$\alpha=0.0 \text{ for } FC\leq5\% \qquad 2.25a$$

$$\ln(\alpha)= (91.76-190/FC^2),\ 5\%<FC<35\% \qquad 2.25b$$

$$\alpha=5.0,\ FC\geq35\% \qquad 2.25c$$

$$\beta=1.0,\ FC\leq5\% \qquad 2.26a$$

$$\beta=0.99+FC^{1.5}/1000,\ 5\%<FC<35\% \qquad 2.26b$$

$$\beta=1.2,\ FC\geq35\% \qquad 2.26c$$

Figure 2.8 SPT energy measuring equipment that was attached to the rods.

2.5 Seismic Crosshole Test

The seismic crosshole test was performed according to ASTM D 4428. This test was conducted in order to determine compression (P), vertical shear (SV), and horizontal shear (SH) wave velocities. To do this, three inclinometer casings were installed in the boreholes at the Hobcaw Borrow Pit and Walterboro Rest Area Ponds sites. The inclinometer casing had four grooves on the inside of the casing designed to be used as tracks for spring-loaded wheel assemblies on probes. The four grooves within the inclinometer casing were spaced evenly at 90° intervals. Each casing was inserted into a borehole and cemented in place using grout. The three casings were oriented such that one set of grooves were aligned with the boreholes in the same direction.

The seismic crosshole test consists of a source in one of the casings producing waves of stress energy. The source contains three electromechanical solenoid hammers that hit in the up, down, and horizontal directions and one accelerometer to determine the time that the waves leave the source. The two receivers each contain three geophones in the radial, vertical, and transverse directions. They were in the other two casings at the same depths as the source. Figure 2.9 presents a diagram showing how the source, trigger accelerometer, and geophones are oriented in the casings. Figure 2.10 is a photograph of the source and the receivers. The three probes are connected to a signal analyzer, as shown in Figure 2.11, and the pressure manifold, as seen in Figure 2.12. The pressure is provided by a bicycle pump. The analyzer is used to collect the data, and later, reduce the data.

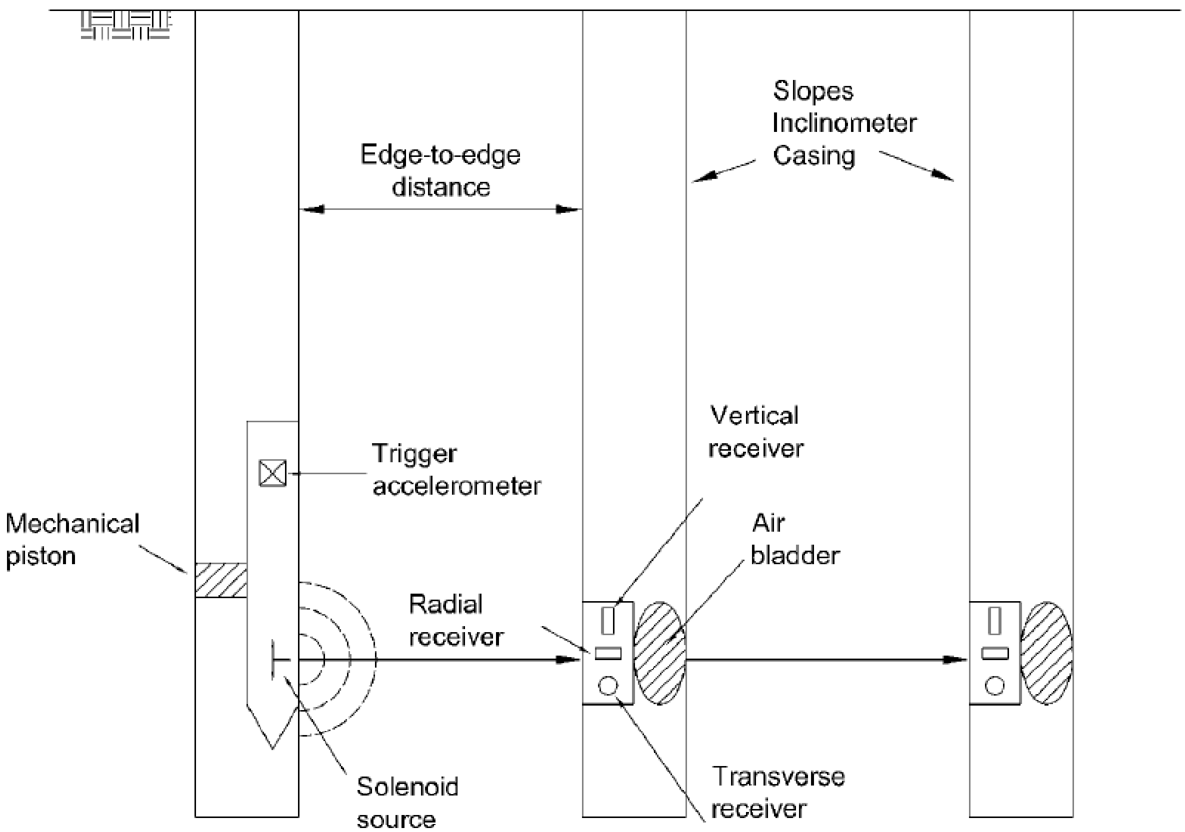

Figure 2.9 Schematic for seismic crosshole test setup in the casings (Hayati 2009).

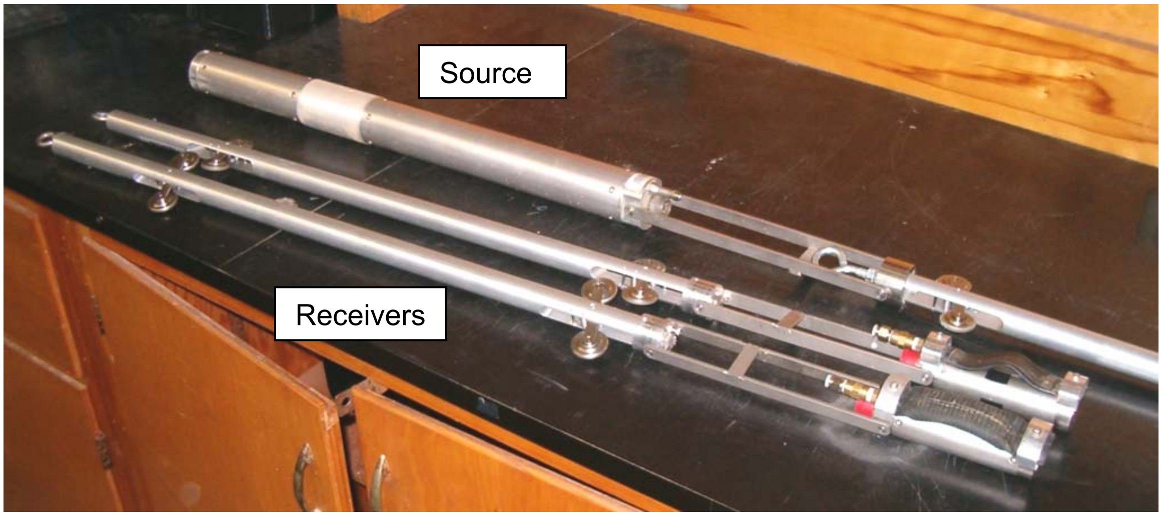

Figure 2.10 Source and receiver assemblies used for seismic crosshole testing.

Figure 2.11 Agilent Technologies dynamic signal analyzer used for collecting and analyzing seismic crosshole test data.

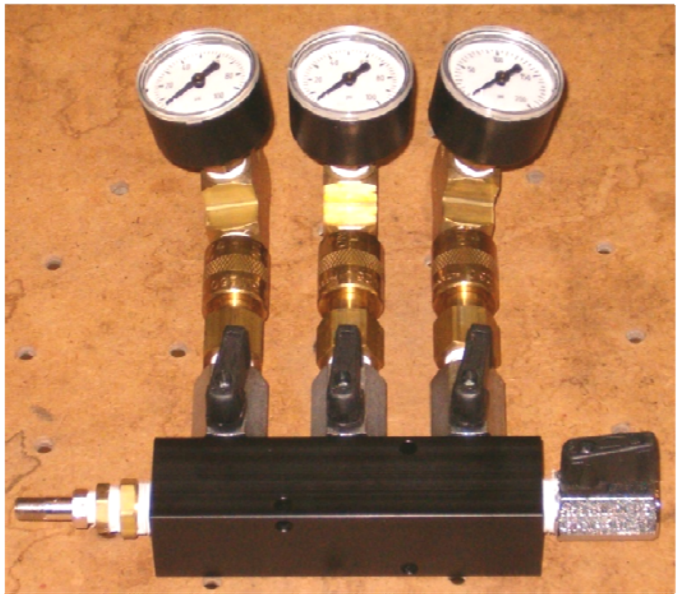

Figure 2.12 Pressure manifold for seismic crosshole testing.

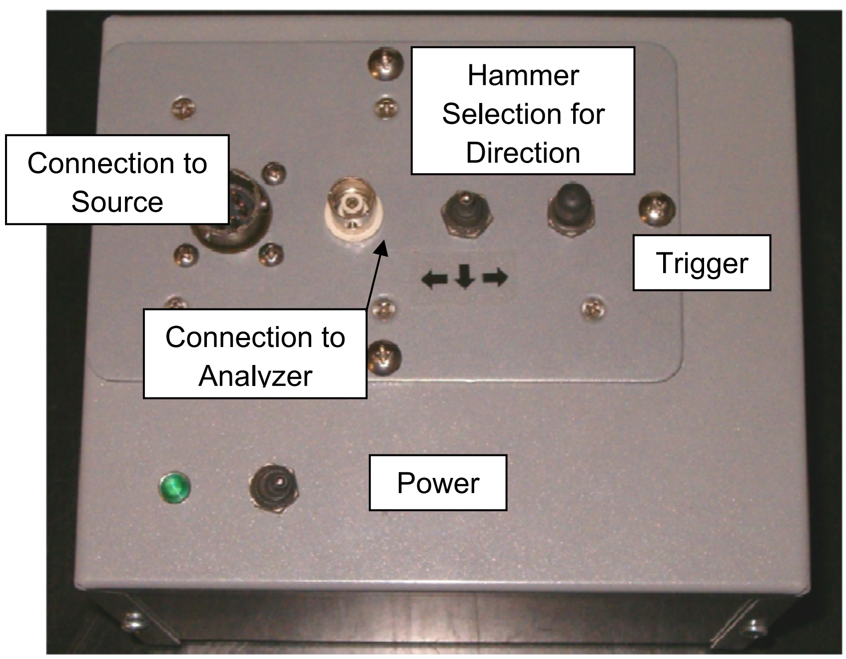

Figure 2.13 Solenoid hammer control box used in seismic crosshole testing.

2.5.1 Test Procedure

The crosshole tests were performed with an Agilent Technologies dynamic signal analyzer and source/receiver equipment manufactured by Olsen Instruments. The solenoid hammer source was connected to the analyzer via a control box, seen in Figure 2.13, which controlled the orientation of the hit and also initiated the hit. The receivers both were directly connected to the analyzer. In addition to the data cables, the geophone probes also had air bladders that were connected to a pressure apparatus.

For testing, each apparatus was lowered into the casings to a selected depth. Clamps were used to hold the probes in place until the pressure tubes were inflated. The source was oriented in various directions depending upon what wave was being measured. P wave testing required that the source be directed toward the receivers. P waves were produced using the horizontal solenoid and SV waves were produced using the downward and upward hitting solenoids. For SH waves, the source was rotated 90° both clockwise and counterclockwise so that the horizontal solenoid was hitting transverse to the borehole array. Once the source and receivers were aligned for a specific wave type, a bicycle pump was used to pressurize air bladders in the receiver probes and a piston in the source. The pressures were controlled through a pressure manifold as seen in Figure 2.12. This was done to ensure that the source and receivers were firmly against the wall of the casing. Once the signal analyzer was prepared for collecting data, the solenoid hammer was activated, producing stress energy. Multiple hits were conducted to try to obtain a relatively clean signal.

2.5.2 Seismic Crosshole Data Reduction

To analyze the results, the trigger and arrival signals were recalled on the signal analyzer back in the laboratory. On each signal, the point at which the wave arrived was identified as best as possible. If it was impossible to identify the wave's arrival, the records were classified as poor and not used. For the trigger signals and the P wave signals, the arrival point was the first major up or down in the signal. For SV "left" (direction of switch on the control box) and SH counterclockwise wave arrival signals, the first wave arrival generally exhibited a major up in the record. For SV "right" and SH clockwise wave arrival signals, the first wave arrival generally exhibited a major down in the record. A sample set of SH records is shown in Figures 2.14 and 2.15.

For seismic crosshole, there are various methods with which to obtain wave velocities, just as there are pseudo and true interval measurements for downhole testing. The two primary types are direct and interval measurements. Direct measurement means a measurement of travel time between the source and a receiver. With this measurement, there are external factors that may require corrections to be made to the travel time. One such correction applied to this work is the velocity of P and S waves through the grout used to secure the casings. With interval measurement, the source is ignored and the two arrival times for two receivers are used to determine travel time. Effects of grout and borehole disturbance cancel out in interval measurements. However, it is difficult sometimes to get a strong, usable signal in the 2nd receiver.

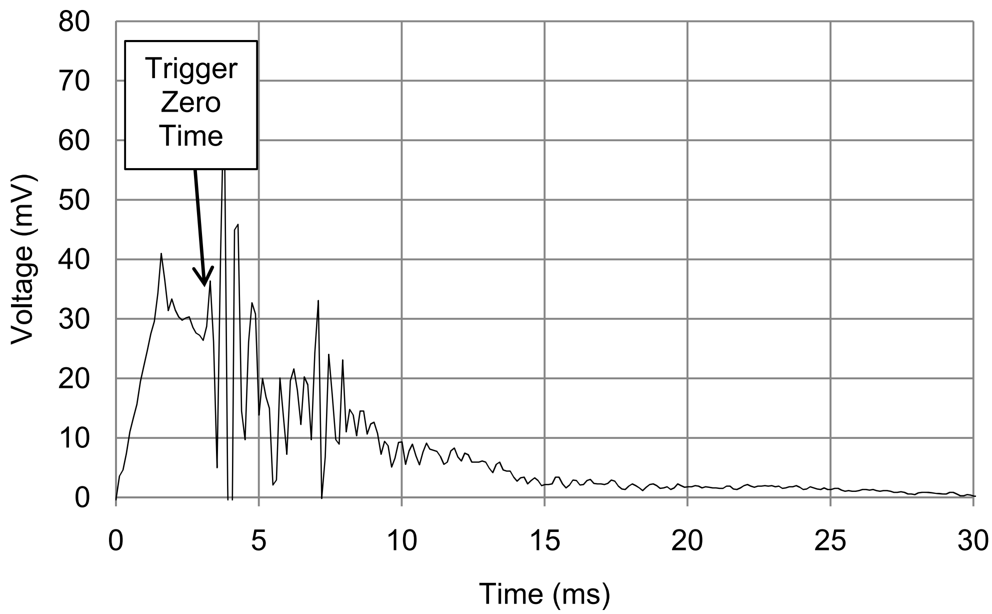

Figure 2.14 Time history from the trigger accelerometer for a SH wave test at the Hobcaw Borrow Pit site at a depth of 1.8 m (6 ft).

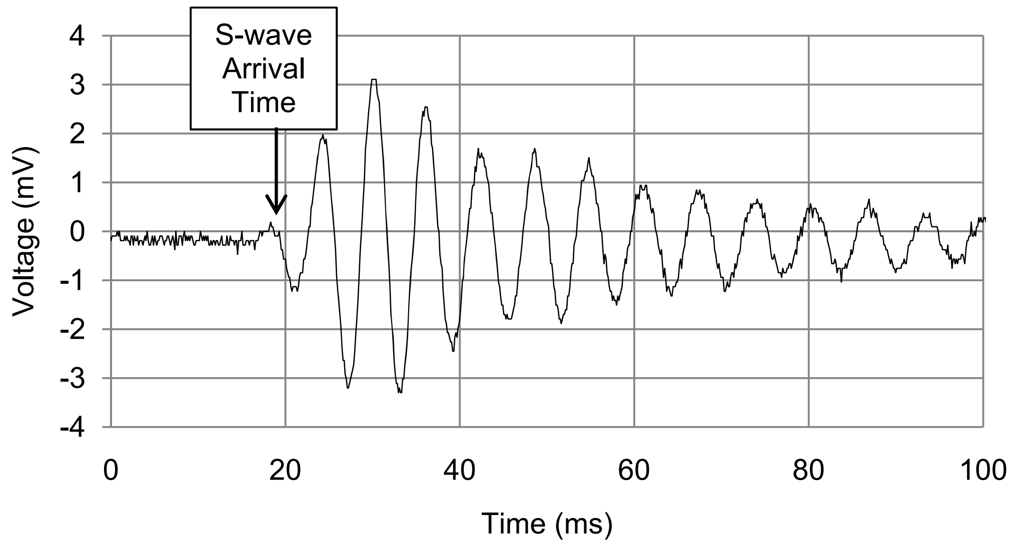

Figure 2.15 Time history from the near transverse receiver for a SH wave test at the Hobcaw Borrow Pit site at a depth of 1.8 m (6 ft).

2.5.3 Inclinometer Survey

In order to determine accurate compression and shear wave velocities, the distance between each casing must be accurately known. While this distance is known at the surface, it can change below the surface due to any deviations of the borehole casings from vertical. A slope inclinometer survey was used to determine these deviations as is required by ASTM D4428-D4428M. The apparatus used for this survey is a Slope Indicator system produced by Durham Geo Slope Indicator (DGSI), consisting of an inclinometer probe and a digital data collection device, both of which can be seen in Figure 2.16.

The first part of the survey involved orienting the probe in the correct set of grooves. The A0 direction is in the direction of B-2 and B-3 when standing from

B-1, and the B0 direction is 90° clockwise from A0. The probe was lowered to the bottom of the casing. Readings were taken at 0.6 m (2 ft) intervals by the data collection box. After completing a survey in one direction, it was performed again in the 180° direction (i.e., A180 or B180). The algebraic difference between A0 and A180 was the combined A reading. The same was done for B0 and B180 to get a combined B reading. A total of four surveys were conducted for each borehole in order to obtain average A and B readings.

The readings collected by the data collection box are in device-specific reading units. They must be converted into lateral displacement values. Equation 2.27 is provided by DGSI to convert the readings into displacements for a survey with 0.6 m (2 ft) intervals:

$$Displacement = 24\ in.\left(\frac{Current\ Combined\ Reading - Initial\ Combined\ Reading}{2 * 20{,}000}\right) \quad 2.27$$

The displacements were used to determine the corrected distances between the casings. Plots of the displacements of each borehole casing for the Hobcaw Borrow Pit site are presented in Appendix A.

Figure 2.16 Digitilt Slope Inclinometer system manufactured by DGSI.

2.6 Laboratory Investigations

Samples used for laboratory testing were collected from either split spoon or fixed piston samplers at the Hobcaw Borrow Pit and Walterboro Rest Area Ponds sites. The laboratory investigations performed included sieve analyses with some hydrometer tests, Atterberg limits, and one-dimensional consolidation tests.

2.6.1 Grain Size Analysis

Sieve analyses were conducted in a similar manner as specified in ASTM D 421. Before sieving the soil, the samples were washed over a #200 wash sieve to remove as much fines from the sample as possible. This wash material and soil retained on the wash sieve were dried for 24 hours. After drying, the soil retained on the wash sieve was cooled and lightly tamped to break the soil apart. The standard U.S. sieves used for the analysis were the #4, #10, #20, #40, #60, #80, #100, and #200. The sample was placed in the sieve stack that was shaken in a sieve shaker for 8-10 minutes. Each sample portion was then weighed. The fine material passing the #200 sieve during washing was included in determining the gradation of the sample. For clayey split-spoon samples, the soil passing the #40 sieve was saved for Atterberg limit testing.

Hydrometer testing was performed on three samples from the Hobcaw Borrow Pit site. Each test was conducted in accordance with ASTM D 422 except that a constant temperature bath was not used. However, temperatures were recorded and they fluctuated very little. ASTM 152-H type hydrometers were used for the tests. Each sample was saturated for 8-12 hours in a 4% solution of sodium hexametaphosphate (Calgon) and distilled water. Two 1000 cm^3 graduated cylinders were used for testing. Each test was run for 48 hours. After reducing the hydrometer readings, the gradation was combined with the gradation from standard sieve analysis, disregarding the first three hydrometer readings to obtain a smooth gradation curve. The hydrometer test results are presented in Appendix A.

2.6.2 Atterberg Limits

Samples that exhibited clayey behavior were tested for Atterberg limits following the general procedures given in ASTM D 4318. For both the liquid limit (LL) and the plastic limit (PL) tests, only material finer than the #40 sieve was used. A summary of these test results are in the appendicies.

PL was determined using a glass plate for rolling the soil into threads. Only a few samples had enough fines content to be rolled without falling apart at the first roll due to high amounts of sand. The soil was hand-rolled to a thickness of 3.2 mm (1/8 in.). If it broke at this thickness, the sample was dried and its moisture content was determined. This was done three times to obtain an average PL.

LL was determined using a Casagrande LL device. Soil was placed in the device with an approximate depth of 8 mm. A standard LL grooving tool was used to make a groove through the sample. The test involved turning a crank at a rate of approximately two revolutions per second. The test was completed when the groove was closed a distance of 12.7 mm (1/2 in.). The number of blows it took to do this was recorded, along with the moisture content of the particular sample. Three tests were conducted to obtain samples with blow numbers above 25, around 25, and below 25 as best as possible. LL is considered to be the moisture content at a blow number of 25. LL was obtained from a plot of moisture content versus the logarithm of the blow number.

2.6.3 One-Dimensional Consolidation Test

This test was performed following the general procedures of ASTM D 2435. The consolidation procedure chosen for testing was an incremental one dimensional consolidation test using the GeoTAC testing system. The system consists of a GeoJac loading frame, an 8.9 kN (2,000 lb) load cell, a deformation sensor, a consolidation cell, and the GeoTAC's Sigma-1 ICON program for collecting data. A photograph of the GeoTAC system is shown in Figure 2.17. Before testing, the system was calibrated for machine deflection using a stainless steel sample machined to be the same size as a test sample.

Samples from the fixed piston tubes were used for consolidation testing. They were carefully trimmed into a consolidation ring having approximately a 6.35 cm (2.5 in.) inner diameter and a 2.54 cm (1 in.) height. They were trimmed and very gently pushed into the ring to minimize disturbance to the sample. Once the samples were completely trimmed, two pieces of moist filter paper were placed on opposite sides to help prevent loss of material into the porous stone during testing. In the consolidation cell, a saturated porous stone was placed in the base. The sample with ring and filter paper was placed on top next. Another saturated porous stone was placed on top of the stack. The upper piece of the consolidation cell was then screwed into place and the loading platen was set upon the top to complete the cell setup.

The cell was aligned with the load cell on the GeoJac frame. The loading piston was lowered into place. Once seating had begun to prevent swelling, water was poured into the cell to fill it to the top and completely saturate the sample. The loading schedule for the samples was vertical loads of 6.0, 12.0, 23.9, 47.9, 95.8, 191.5, 383.0, 766.1, 1532.2, and 766.1 kPa (125, 250, 500, 1000, 2000, 4000, 8000, 16000, 32000, 8000, and 2000 psf). This loading schedule was automated using the computer program. Each load was maintained until the completion of primary consolidation, which was generally less than 80 minutes.

After completing the test, the data were converted into plots of void ratio versus the logarithm of effective vertical stress. Using these plots, the preconsolidation pressure (σ_c') was obtained using Casagrande's (1936) graphic procedure. With σ_c' and the calculated value of effective vertical stress for the sample depth, the overconsolidation ratio (OCR) of the sample was determined by the following equation:

$$\sigma_c' / \sigma_v' = OCR \qquad 2.28$$

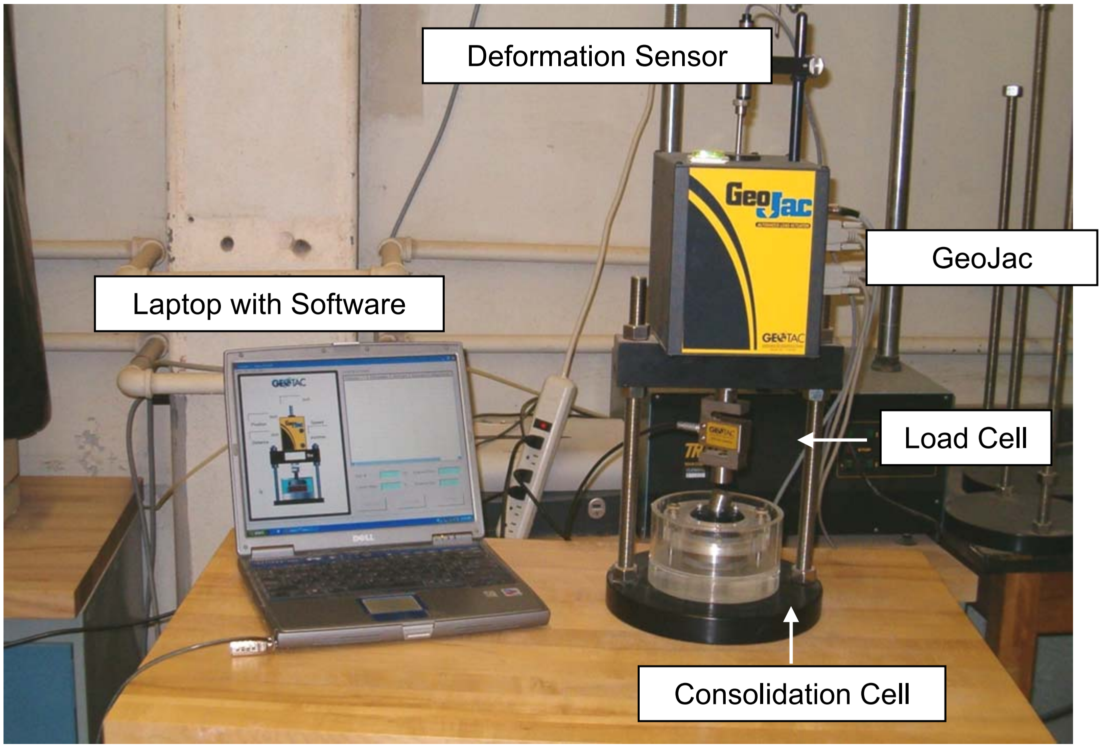

Figure 2.17 GeoTAC equipment used in the one-dimensional consolidation test.

CHAPTER THREE

INVESTIGATIONS AT THE HOBCAW BARONY BORROW PIT SITE

Geiger et al. (2010) presented summary results and analysis for studies at the Hobcaw Barony Borrow Pit, including the previous studies conducted by Boller (2008) and Geiger (2009) at the site. Those papers did not include finalized seismic crosshole test results. This chapter now presents the seismic crosshole results in full for the first time and updates the previous studies at the Hobcaw Borrow Pit site.

3.1 Introduction

The Hobcaw Barony Borrow Pit site is located within Hobcaw Barony, a 17,500 acre outdoor laboratory owned and operated by the Belle W. Baruch Foundation. The site is just east of Georgetown and is located on a peninsula set between the Waccamaw River and the Atlantic Ocean, as seen in Figure 3.1. Clemson University and the University of South Carolina both operate research centers at Hobcaw Barony for forestry, wildlife, and coastal research. The foundation made available an area within a borrow pit located west of the Bellefield House and Stables just off of Airport Road for geotechnical experimentation.

The Hobcaw Barony area lies well outside the zone of 1886 liquefaction craterlets identified by Dutton (1889). No reports of liquefaction in the Hobcaw Barony area during the 1886 Charleston earthquake were found by Martin and Clough (1990) and Lewis et al. (1999). There have been no paleo-liquefaction studies conducted in the immediate area.

Figure 3.1 Map presented in Geiger et al. (2010) showing the Hobcaw Barony and surrounding area with locations of the site and selected boreholes from the geologic investigation by May (1978).

Figure 3.2 Satellite image of the Hobcaw Borrow Pit site as presented by Boller (2008).

3.2 Geology

As discussed by May (1978), Hobcaw Barony was formed on the east by beach barriers and tidal flats. The area has many beach ridges that are inland. These are the result of repeated wave action from the changing coastline, depending on whether the Atlantic Ocean was receding or the coastline was advancing. May (1978) suggests that the sands making up the higher ground are 100,000 to 200,000 years old. McCartan et al. (1984) also estimates the surficial sands to be 200,000 years old.

A geological cross-section of the Hobcaw Barony area by May (1978) is presented in Figure 3.3. The profile is based off of investigations conducted in four boreholes. The locations of these boreholes are shown in Figure 3.1. The surface consists of Pleistocene deposits, ranging in thickness from 9 to 15 m (29.5 to 49.2 ft). Below this is the Black Mingo Formation, which is a Tertiary-aged formation. It is approximately 58 m (190.3 ft) thick. Beneath the Black Mingo is the Peedee Formation, a Paleocene-aged deposit. It begins approximate 66 m (216.5 ft) below the surface. The vast majority of the geotechnical investigations at Hobcaw took place in the Pleistocene deposits. Stiple (1957) characterized the Black Mingo and Peedee formations as sand to sandstone and black to gray sand, respectively. Both regions have interbedded silts and clays.

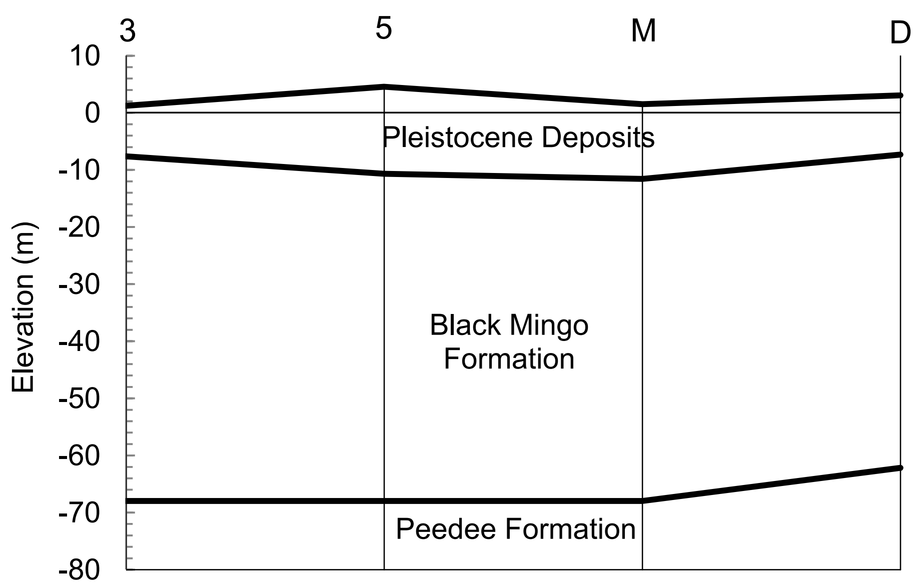

Figure 3.3 Geologic profile based off of boreholes 3, 5, M, and D shown in Figure 3.1 (adapted from May 1978; as presented by Boller 2008).

3.3 Investigations

Figure 3.4 presents a map of the locations of all field tests performed as part of the investigations at the Hobcaw Borrow Pit site. Three SCPTu's and one DMT were conducted by Boller (2008). All remaining investigations were conducted as part of this study. Three oak trees were used as references for developing the site map in Figure 3.3.

The SCPTu's and DMT took place on July 25, 2007. A track-mounted cone rig pushed all SCPTu's to refusal and the DMT to 10.4 m (34.1 ft) (Boller 2008). On August 4-6, 2008, a CME 550X drilling rig was brought in to conduct SPTs, split spoon sampling, and Hvorslev-type fixed piston sampling in boreholes B-1, B-2, and B-3. The SPTs were conducted to a depth of 11.4 m (37.5 ft). Fixed piston samples were taken from B-2 and delivered to the University of South Carolina for cyclic triaxial testing. Fixed piston samples were taken from B-3 as well. The fixed piston samples were brought back to Clemson for further investigation. The samples were placed in a refrigerator until February 2010 when consolidation tests were performed. A standpipe was installed in B-4 to determine the change in the groundwater table. Seismic crosshole testing was performed on November 4, 2008. An inclination survey was conducted on January 19, 2010.

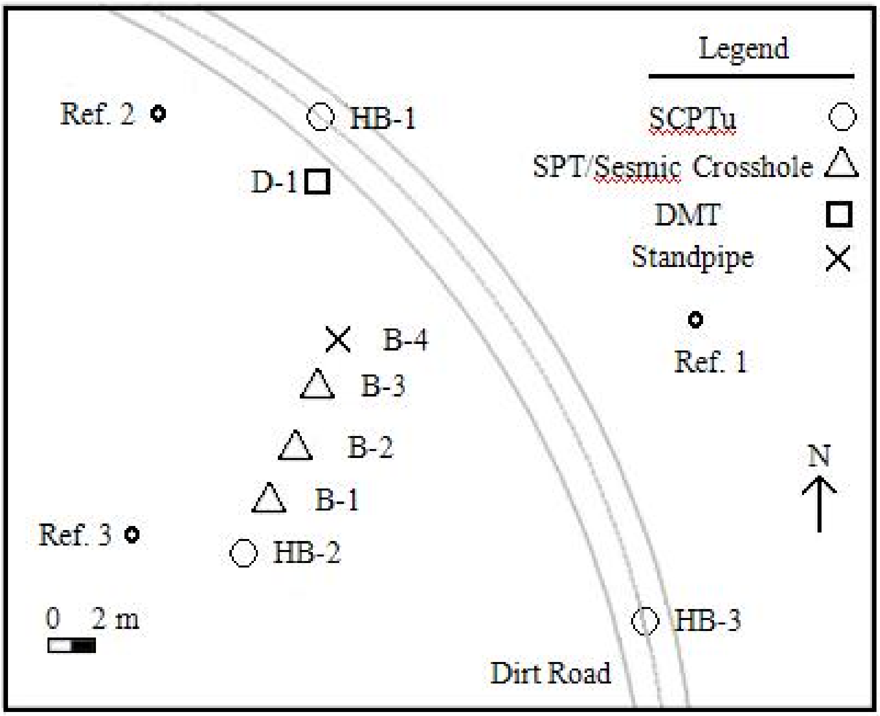

Figure 3.4 Site map for the Hobcaw Borrow Pit site (Modified from Boller 2008)

3.4 Results

The DMT and SCPTu's conducted by Boller (2008) are referenced and summarized in this chapter. SCPT tabulated data are presented in Appendix D, though composite profiles for each cone sounding are not presented in this thesis. Detailed test results conducted for this study are presented in Appendix A and will be summarized and referenced as needed in this chapter.

3.4.1 CPT Stratigraphy and Properties

Figure 3.5 presents profiles of q_t and FR for the three cone soundings conducted at the site. There are three distinct layers in the top 12 m (39.4 ft). Table 3.1 presents average cone indexes for each of these layers. Some of these indexes are plotted on the soil behavior classification charts by Robertson (1990) presented in Figure 3.6.

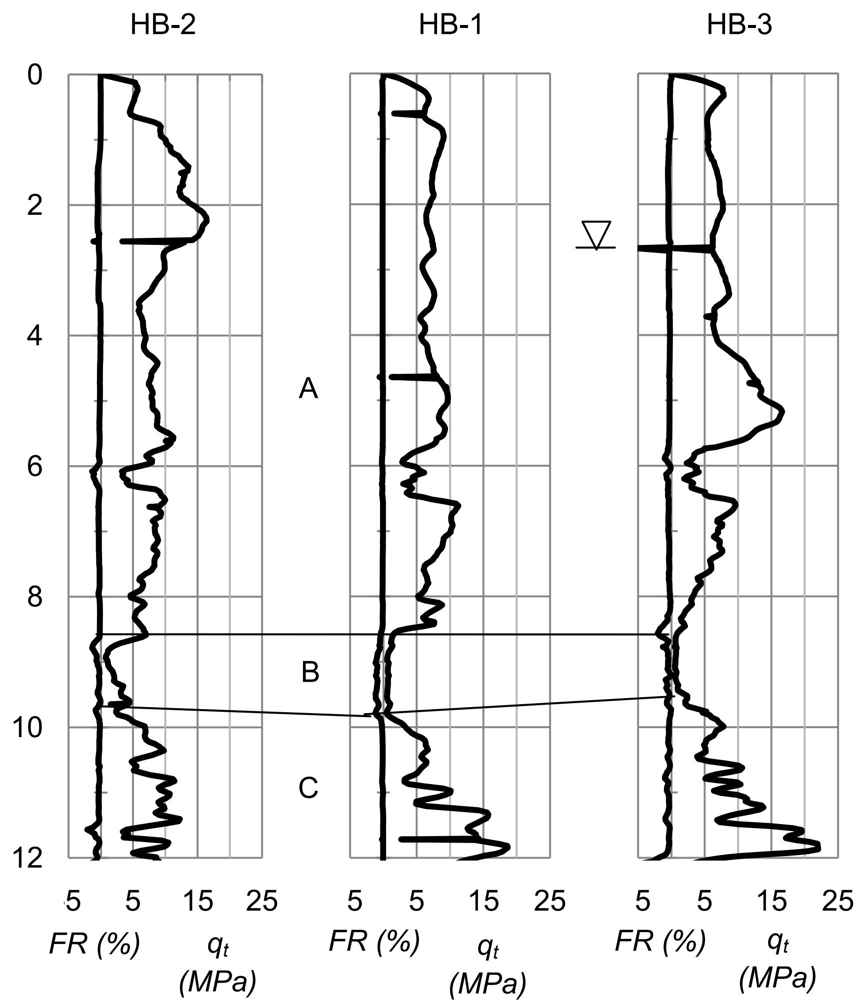

Figure 3.5 SCPTu cross-section for SCPTu's at the Hobcaw Borrow Pit site, modified from Boller (2008).

Layer A extends from the ground surface down to a depth of approximately 8.8 m (28.9 ft). The groundwater table is located in this layer and, during the time of this study, varied between 2.0 and 2.5 m (6.7 and 8.5 ft). The section of Layer A below the groundwater table is used for analysis. This portion of Layer A had an average q_t of 6.9 MPa and an average FR of 0.27%. In addition, pore pressures were slightly below hydrostatic pressure, indicating dilative behavior during the advancement of the cone. The CPT-based soil identification chart by Robertson (1990), presented in Figure 3.6, identifies Layer A materials as clean sand to silty sand, which agrees with the borehole samples collected.

Layer B extends from a depth of 8.8 m (28.9 ft) to a depth of 9.6 m (31.5 ft). Layer B has an average q_t and FR of 0.71 MPa and 0.64%, respectively. Pore pressures were above hydrostatic pressure, indicating the presence of significant amounts of fines. Figure 3.6 suggests that Layer B varies from clay to silty sand.

Layer C begins at a depth of 9.6 m (31.5 ft). Figure 3.5 does not indicate the bottom surface of Layer C, but deeper measurements in SCPT HB-1 (Boller 2008) indicate that the bottom of Layer C is approximately 12 m (39.4 ft). This layer has an average q_t and FR of 8.7 MPa and 0.64%, respectively. The pore pressures were not greater than the hydrostatic pressure. The soil identification chart in Figure 3.6 indicates that Layer C materials consist of clean sand to silty sand.

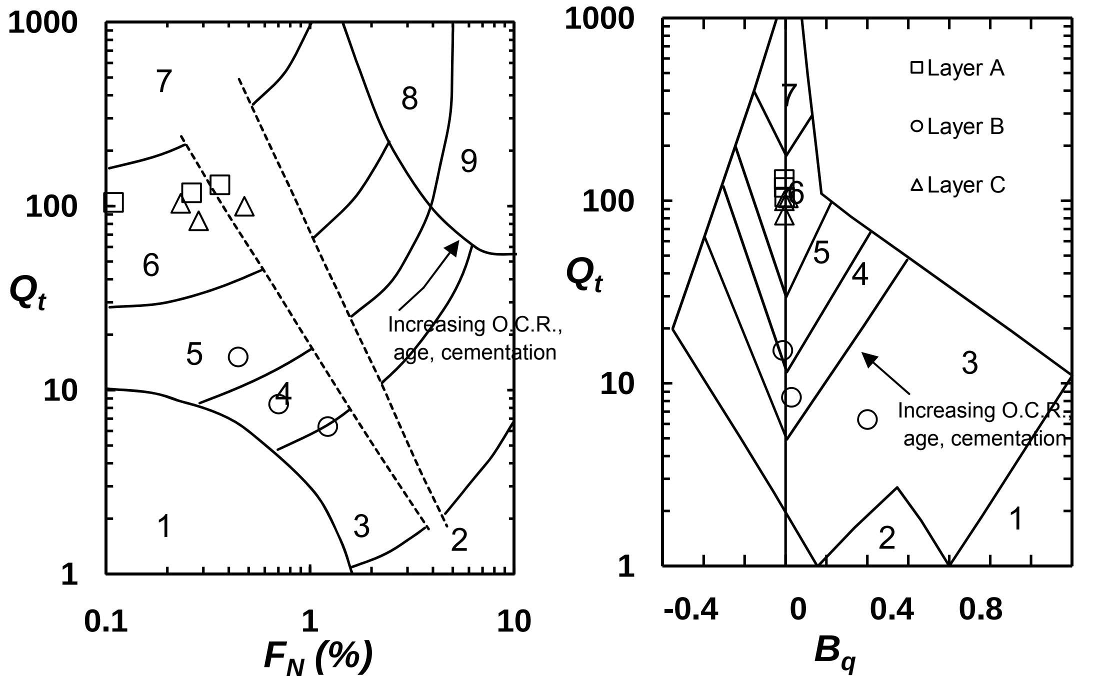

Zone	Soil behavior type	Zone	Soil behavior type
1.	Sensitive, fine grained;	6.	Sands: clean sands to silty sands;
2.	Organic soils, peats;	7.	Gravelly sand to sand;
3.	Clays: clay to silty clay;	8.	Very stiff sand to clayey sand;
4.	Silt mixtures: clayey silt to silty clay;	9.	Very stiff fine grained
5.	Sand mixtures: silty sand to sandy silt;		

N.C. = Normally Consolidated
O.C.R. = Overconsolidation Ratio

Figure 3.6 Soil behavior type classification charts by Robertson (1990) with data from the Hobcaw Borrow Pit site modified from Boller (2008).

Table 3.1 Average values of CPT properties at the Hobcaw Borrow Pit site modified from Boller (2008).

ID	Depth (m)	q_{t1N}	I_c	B_q	q_{t1Ncs}
Layer A					
HB-1	3.2-8.9	78.2	1.66	0.006	81.4
HB-2	2.7-8.9	80.8	1.65	0.007	83.8
HB-3	2.4-8.7	85.9	1.61	0	85.9
Layer B					
HB-1	8.9-9.8	6.1	3.12	0.509	49.2
HB-2	8.9-9.3	6.5	3.09	0.535	50.1
HB-3	8.7-9.6	7.1	3.05	0.496	49.1
Layer C					
HB-1	9.8-13.0	78.6	1.79	0.015	89.2
HB-2	9.3-12.2	74.8	1.84	0.058	84.3
HB-3	9.6-12.0	77.8	1.82	0.022	88.5

3.4.2 DMT Results

Figures 3.7 and 3.8 present the results of the DMT conducted in D-1 as presented by Boller (2008). Figure 3.7 presents profiles of DMT material index (I_D), DMT horizontal stress index (K_D), estimated at rest earth pressure coefficient (K_0), and DMT constrained modulus (E_D) with depth. Boller (2008) determined K_0 using different relationships than those presented in Chapter 2. These relationships are presented in Boller (2008). These results are those as determined by Boller (2008).

Boller (2008) identifies average values of K_0 for Layers A, B, and C of 0.69, 0.98, and 0.61, respectively. These indicate that horizontal stresses and/or stiffnesses are less than the vertical stresses and/or stiffnesses in each of the layers. However, Layer B has very similar vertical and horizontal stresses.

Figure 3.8 presents a soil type identification chart with data from D-1. Boller (2008) determined, as seen in Figure 3.7, that Layer A is a medium dense to dense silty sand to sand. Layer B appears to be a soft silty clay to clay. Layer C is indicated as being a low to medium dense silty sand or sandy silt. These assessments generally agree well with the CPT-based identifications.

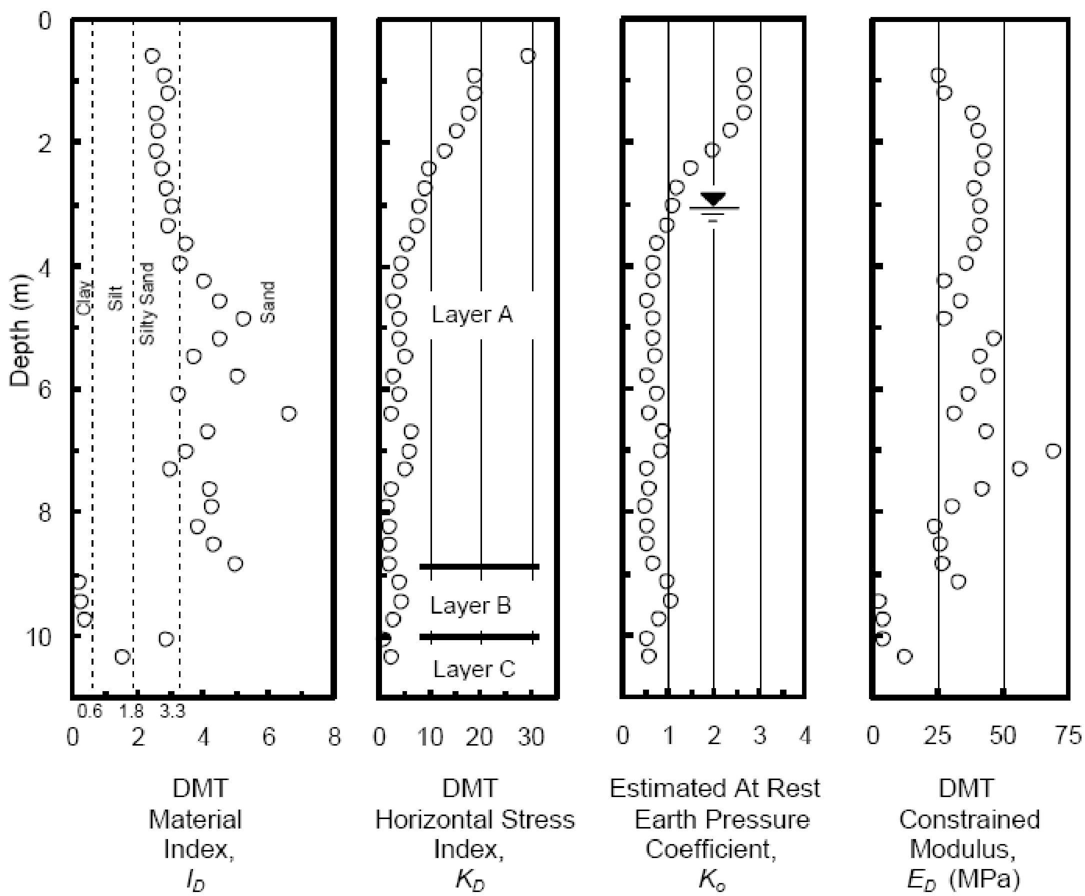

Figure 3.7 Results of DMT D-1 at the Hobcaw Borrow Pit site as presented in Boller (2008).

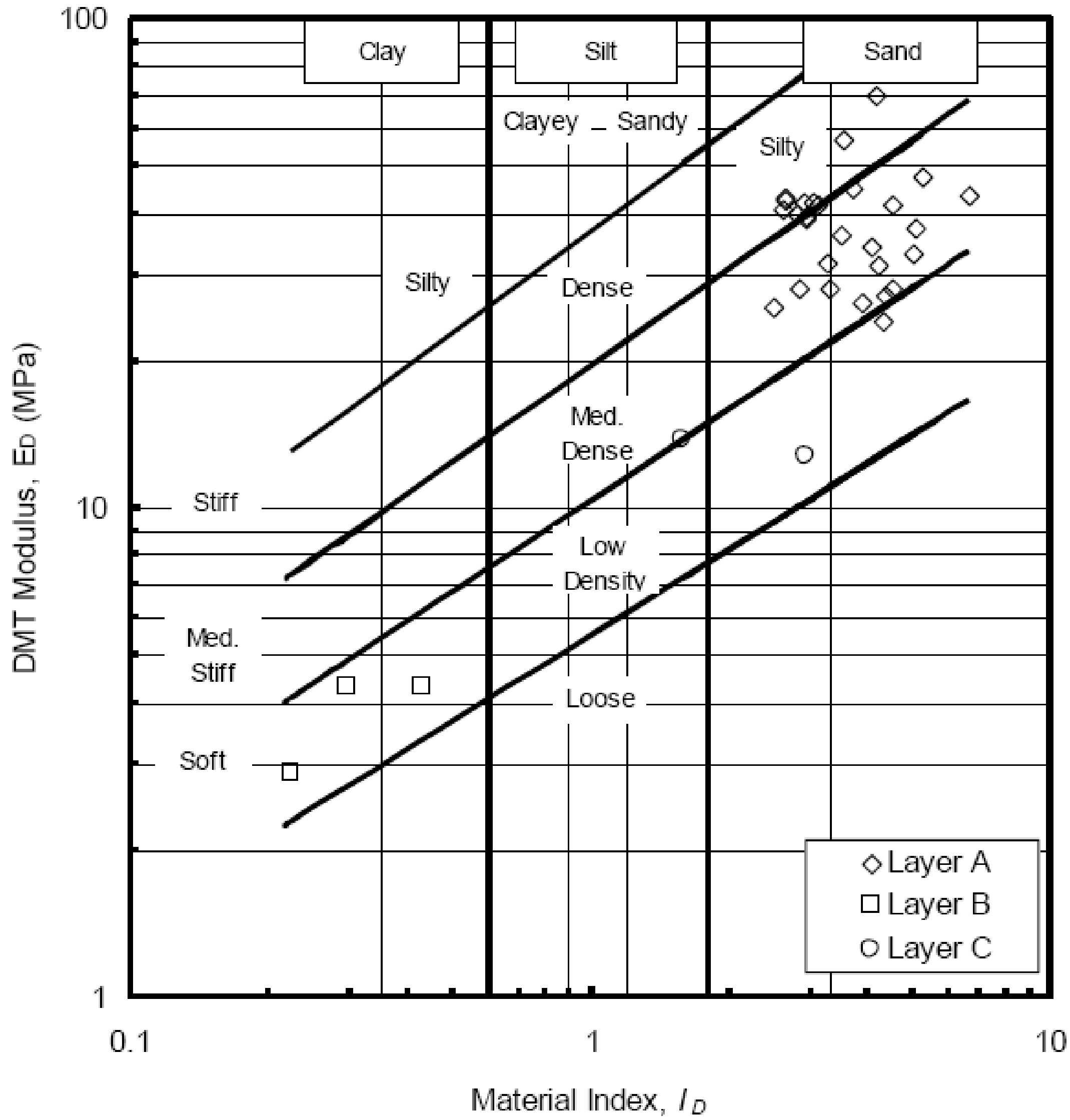

Figure 3.8 DMT modulus and material index chart (ASTM D 6635) from DMT results at the Hobcaw Borrow Pit site as presented by Boller (2008).

3.4.3 SPT Results

Figure 3.9 presents a SPT profile using corrected blowcount, N_{60}. Table 3.2 presents average corrected SPT blowcounts. The highest blowcount occurs at a depth of just below 5 m (16.4 ft), which coincides with an increase in tip resistance seen in HB-2, the closest SCPT to B-1. The blowcounts corrected for overburden stress and fines content, $(N_1)_{60cs}$, are used for liquefaction evaluation in Chapter 6.

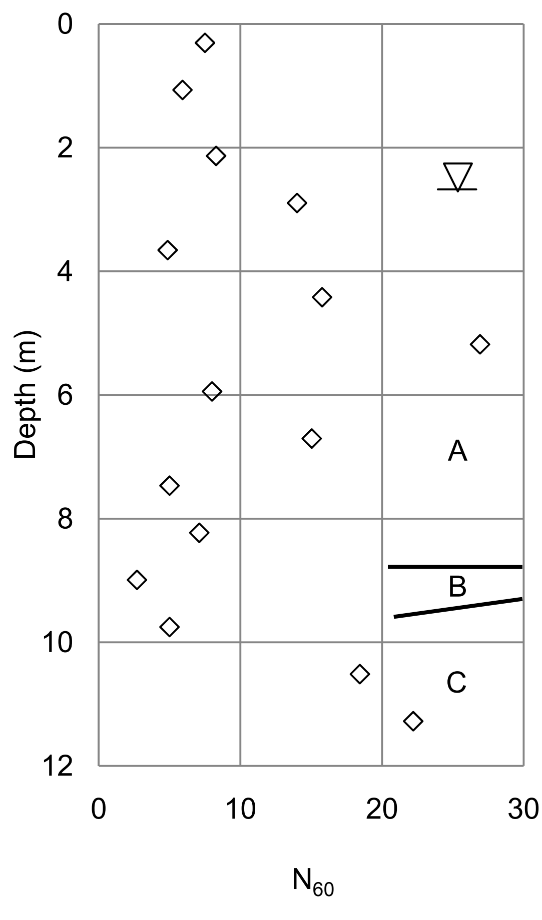

Figure 3.9 SPT corrected blowcount profile in B-1 at the Hobcaw Borrow Pit site.

Table 3.2 Average values of SPT properties at the Hobcaw Borrow Pit site.

Layer	Depth (m)	$(N_1)_{60}$ (blows/0.3m)	Fines Content (%)	$(N_1)_{60cs}$ (blows/0.3m)
A	2.7-8.9	13	6.0	14
B	8.9-9.3	4	21.3	7
C	9.3-12.2	15	7.8	15

3.4.3 Velocity Results

Figures 3.10, 3.11, and 3.12 present P, S_H, and S_v wave velocities for seismic crosshole testing using the direct and interval methods and S-wave velocities for seismic downhole testing using the true interval method. The measured S-wave velocities from seismic downhole testing are presented in Boller (2008).

The P-wave velocities in Figure 3.10 below the water table are all very near 1,500 m/s (5,000 ft/s), which is the velocity of P-waves in water. This indicates that the soil below the groundwater table is completely saturated or very nearly saturated. The results also indicate that the seismic crosshole data were reduced properly and that correct distances between the source and receivers were used.

For S_H waves, the profile in Figure 3.11 does show fairly constant velocities in the top 10 m and an increase at just over 10 m (32.8 ft). This may indicate that Layer C is experiencing higher horizontal stresses than the more shallow layers.

Figure 3.12 presents one profile of direct SV-wave crosshole velocities, one profile of interval SV-wave crosshole velocities, and three profiles of true interval seismic downhole velocities. These profiles are in generally good agreement. Tables 3.4 and 3.5 present average velocities for values in each layer.

MEVR was calculated for each measured velocity using either an SPT-based or CPT-based relationship to estimate velocity (see Chapter 1) and presented in Figure 3.13. These MEVRs range from 1.21 to 1.38. The expected mean MEVR for a 200,000 year-old site is 1.37 using the relationship shown in Figure 1.1. In addition, MEVR for the same aged deposit may be expected to have an MEVR as high as 1.54 or as low as 1.20. The portion of Layer A below the groundwater table has an average MEVR of 1.28. This falls within the expected range of MEVR. No average MEVR is presented for Layer B from seismic downhole results because the layer is less than a meter thick, which is the distance between geophones. This MEVR falls within the expected range. Finally, Layer C has an average MEVR of 1.21, which is within the expected range. The MEVR’s for Layers A and C are not too far apart, indicating good agreement for similar layers.

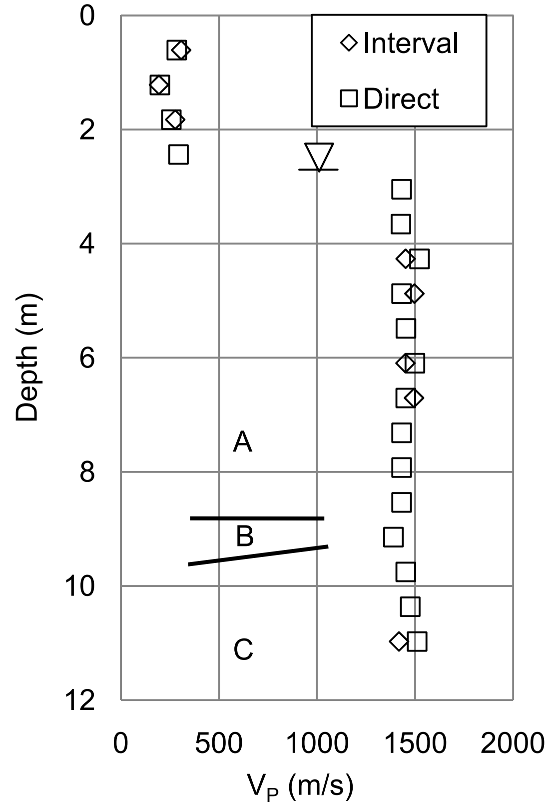

Figure 3.10 P-wave velocity profiles for seismic crosshole measurements at the Hobcaw Borrow Pit site.

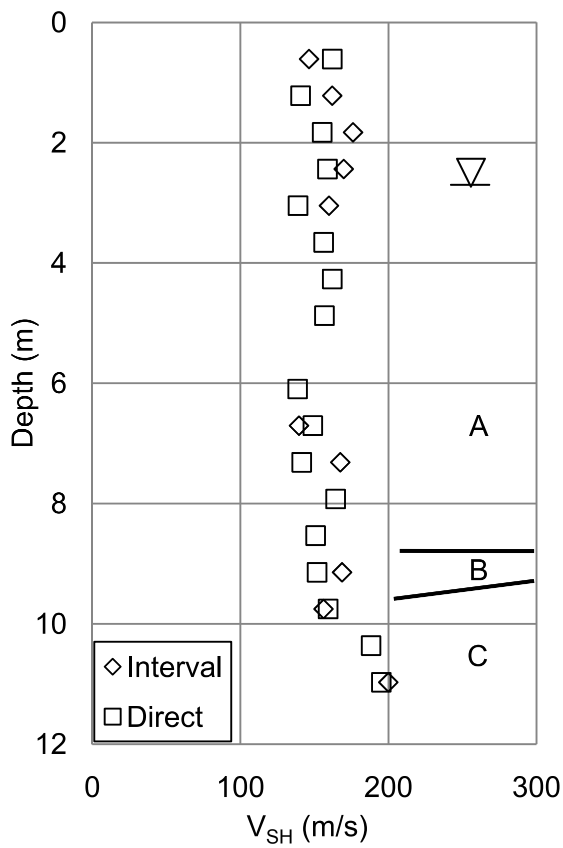

Figure 3.11 V_{SH} wave velocity profiles for seismic crosshole measurements at the Hobcaw Borrow Pit site.

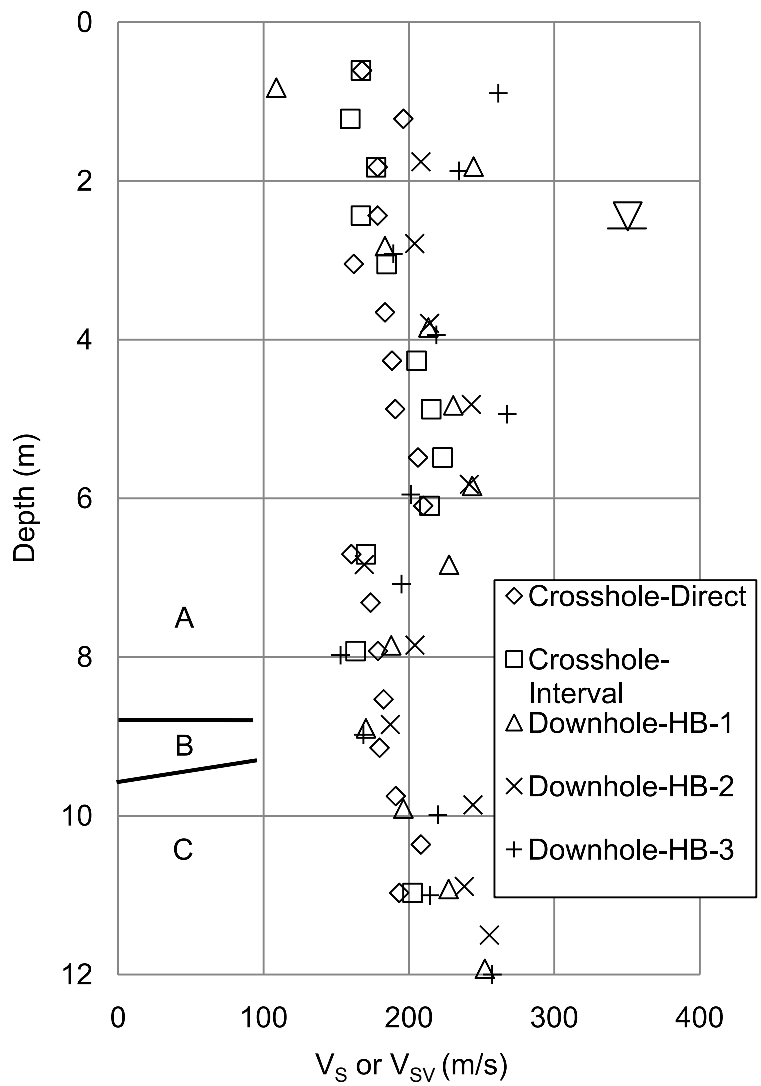

Figure 3.12 V_{SV} profiles for seismic crosshole and V_s profiles for downhole measurements for the Hobcaw Borrow Pit site.

Table 3.3 Summary of seismic downhole S-velocity calculations for the Hobcaw Borrow Pit site.

ID	Depth (m)	V_s (m/s)	V_{s1} (m/s)	$(V_{s1})_{cs}$ (m/s)	*MEVR*
Layer A					
HB-1	3.2-8.9	221	235	236	1.36
HB-2	2.7-8.9	213	234	235	1.34
HB-3	2.4-8.7	213	234	235	1.28
Layer B					
HB-1	8.9-9.8	-	-	-	-
HB-2	8.9-9.3	-	-	-	-
HB-3	8.7-9.6	-	-	-	-
Layer C					
HB-1	9.8-13.0	218	204	206	1.21
HB-2	9.3-12.2	246	234	238	1.38
HB-3	9.6-12.0	242	227	231	1.34

Table 3.4 Summary of seismic crosshole S_V wave calculations for the Hobcaw Borrow Pit site.

ID	Depth (m)	V_{sv} (m/s)	V_{sv1} (m/s)	$(V_{sv1})_{cs}$ (m/s)	*MEVR based on CPT-Est.* V_s	*MEVR based on SPT-Est.* V_s
Layer A						
Direct	3.2-8.9	183	197	197	1.15	1.30
Interval	2.7-8.9	195	214	214	1.22	1.31
Layer B						
Direct	8.9-9.8	180	178	184	1.20	1.37
Interval	8.9-9.3	-	-	-	-	-
Layer C						
Direct	9.8-13.0	183	208	211	1.19	1.18
Interval	9.3-12.2	197	190	191	1.13	1.04

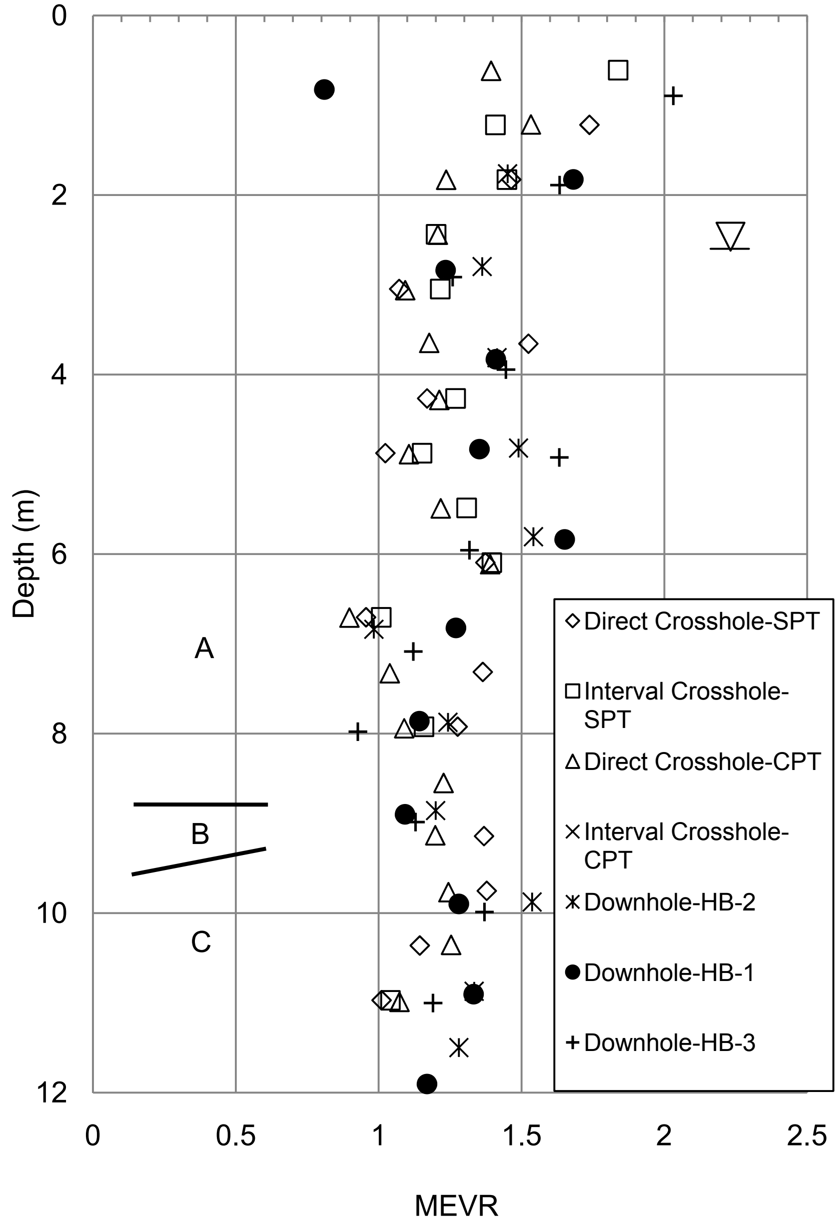

Figure 3.13 MEVR profile using velocities obtained from seismic crosshole and downhole-measured velocities and estimated velocities from equations proposed by Andrus et. al. (2004a).

3.4.4 Laboratory Index Properties

A variety of laboratory tests were performed on samples collected from the boreholes at the Hobcaw Borrow Pit site. Grain size analyses and Atterberg limits were used in determining classifications using the United Soil Classification System (USCS).

Layer A consists of poorly graded sand with silt to poorly graded sand (SP-SM to SP). Figure 3.14 presents the grain size distribution for Layer A, which also indicates a poorly graded condition. These results agree well with the CPT and DMT identifications. No Atterberg limits were obtained, as the samples were all non-plastic. A consolidation test was performed on a sample collected from fixed piston sampling in B-3, but an overconsolidation ratio (O.C.R.) was unable to be determined because primary consolidation was completed very quickly. Layer A has an estimated dry unit weight of 17.3 kN/m^3 (110 lb/ft^3) and saturated unit weight of 19.2 kN/m^3 (122 lb/ft^3).

Layer B is a thin layer with significant fines content. Two hydrometer tests were conducted in Layer B to assist with the classification. Layer B is classified as a SP-SM with thin layers of silt of high plasticity (MH). These classifications generally agree well with CPT and DMT identifications. Consolidation tests performed on fixed piston samples from Layer B suggest that Layer B has an average overconsolidation ratio (O.C.R.) of 2.40. This would indicate a highly overconsolidated layer, though it is important to note that the samples tested were refrigerated from August 2008 to February 2010, which may have an impact on the sample. A saturated unit weight of 16.7 kN/m^3 (106 lb/ft^3) is estimated for Layer B.

Layer C contains SP-SM and is non-plastic, which is very similar to Layer A and is also similar to the CPT and DMT identifications. Layer C also has an estimated saturated unit weight of 19.2kN/m^3 (122 lb/ft^3).

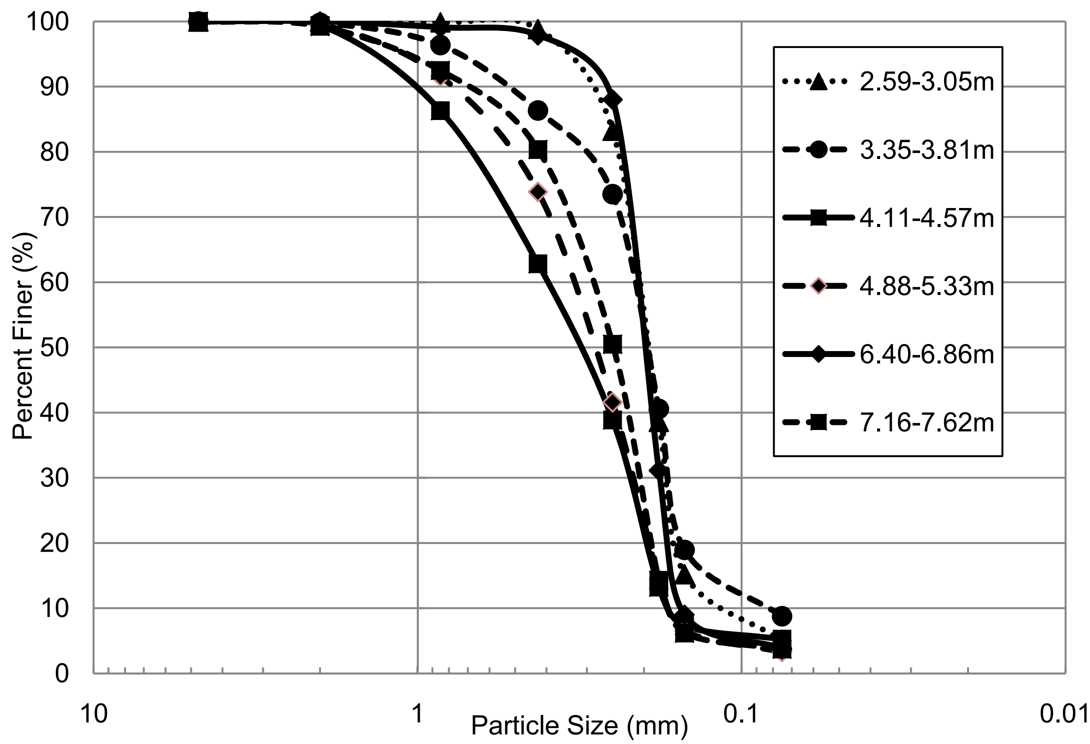

Figure 3.14 Grain size distribution curve for Layer A at the Hobcaw Borrow Pit site.

3.5 Summary

The Hobcaw Barony Borrow Pit site has an estimated age of 200,000 years (May 1978, McCartan et al. 1984). This site is likely a barrier beach sand deposit. Near-surface sediments can be divided into three distinct layers in the top 12 m (39.4 ft). Layer A extends down to about 8.8 m (28.9 ft) and is classified as SP-SM. The groundwater table is in Layer A and varied from 2.0 to 2.6 m (6.7 to 8.6 ft) during the time of this study. Layer B ranges in depth from 8.8 to 9.6 m (28.9 to 31.5 ft) and is SP-SM with interbedded layers of MH. The MH samples are highly overconsolidated. Layer C lies between depths of 9.6 and 12.0 m (31.5 and 39.4 ft) and is classified as SP-SM.

The expected mean MEVR for a 200,000 year-old site is 1.37 based on the relationship presented in Figure 1.1. The plus/minus one standard deviation MEVRs range is 1.20 to 1.54. Layers A and C are both within the expected range with average MEVR's of 1.28 and 1.21, respectively. Layer B has an average MEVR of 1.20, which is at the bottom of the plus/minus one standard deviation range. Overall, data from this site supports the MEVR relationship presented in Figure 1.1.

CHAPTER FOUR

INVESTIGATIONS AT THE WALTERBORO REST AREA PONDS SITE

4.1 Introduction

The Rest Area Ponds site is located behind a rest area on Interstate-95 northbound at mile marker 47 near Walterboro. A map showing the location of the town of Walterboro and the Rest Area Ponds site is presented in Figure 4.1. A satellite image showing the location of the site relative to I-95, the rest area, and the ponds is presented in Figure 4.2. When the South Carolina Department of Transportation (SCDOT) built the rest area, they built two sewage treatment ponds for the rest area. However, the ponds have never beenused for sewage treatment. The area around the ponds is fenced off to discourage public access. SCDOT made an area adjacent to the ponds available for geotechnical investigations, which are shown in Figure 4.3.

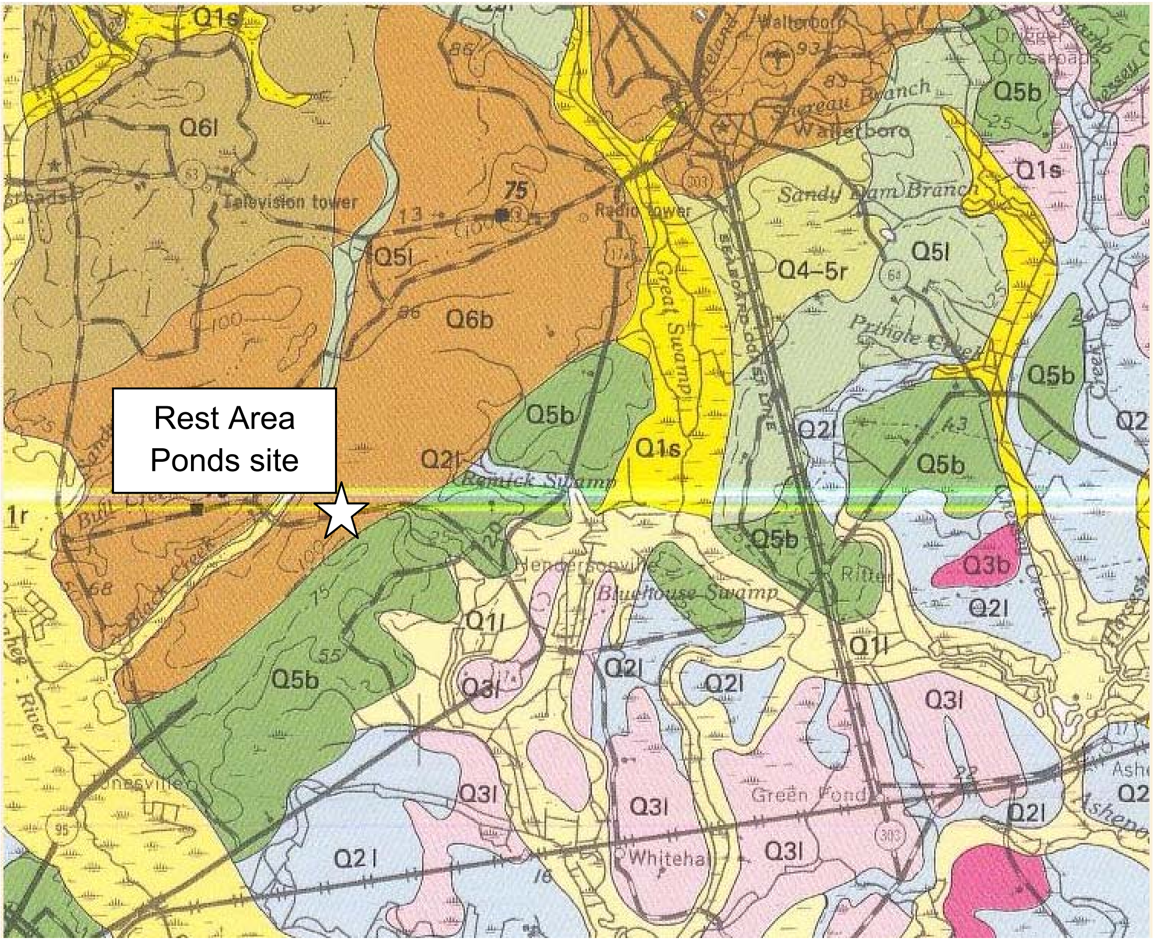

Figure 4.1 Geologic map by McCartan et al. (1984) showing the location of the Rest Area Ponds site.

Figure 4.2 Satellite image of the Rest Area Ponds site.

4.2 Geology

The Walterboro Rest Area Ponds site is located in the geologic unit designated Q6b on the map by McCartan et al. (1984), as shown in Figure 4.1. McCartan et al. characterized Q6b as beach sand deposits with an age of at least 1,000,000 years.

The Rest Area Ponds site lies well outside the zone of 1886 craterlets reported by Dutton (1889, Plate XXVIII). Thus, it is unlikely that liquefaction occurred at the site in 1886.

Figure 4.3 Photograph of testing area at the Rest Area Ponds site.

4.3 Investigations

On June 25, 2009, three SCPTu's and one DMT were conducted at the Rest Area Ponds site. The test locations, identified as SC-1, SC-2, and SC-3, are presented on the site map in Figure 4.4. The pond, fence, and entrance gate are used as references. Their locations are indicated in Figure 4.4.

The SCPTu's were pushed to refusal in SC-1 and to depths of 12.2 m (40 ft) in SC-2 and SC-3, temporarily stopping every 1 m (3.3 ft) to add a new rod and make shear wave velocity measurements. The DMT was pushed to 11.6 m

(38 ft), stopping every 0.3 m (1.0 ft) to make measurements. On October 13-14, 2009, a CME 550X drilling rig was brought in to conduct SPT's, split-spoon sampling, and Osterberg-type fixed-piston sampling. The three boreholes, identified as B-1, B-2, and B-3, are shown on the site map in Figure 4.4. SPT's were conducted in B-3 to a depth of 11.4 m (37.5 ft). Seven fixed-piston samples were taken from B-1. The first four were delivered to the University of South Carolina for cyclic triaxial testing. The three remaining samples were brought back to Clemson. These three fixed piston tubes were stored in the laboratory until consolidation tests were performed on select samples in February 2010. Split-spoon samples were used for grain size analysis and Atterberg limits. A standpipe was also installed at B-4 (see Figure 4.4) to determine the change in the groundwater table for future investigations. Inclinometer casings were installed in each borehole and are shown in the photograph presented in Figure 4.5.

Seismic crosshole testing was performed on January 18, 2010 at B-1, B-2, and B-3 and an inclination survey was conducted on January 19, 2010. The seismic crosshole tests were conducted as part of another thesis study and are not present in this report.

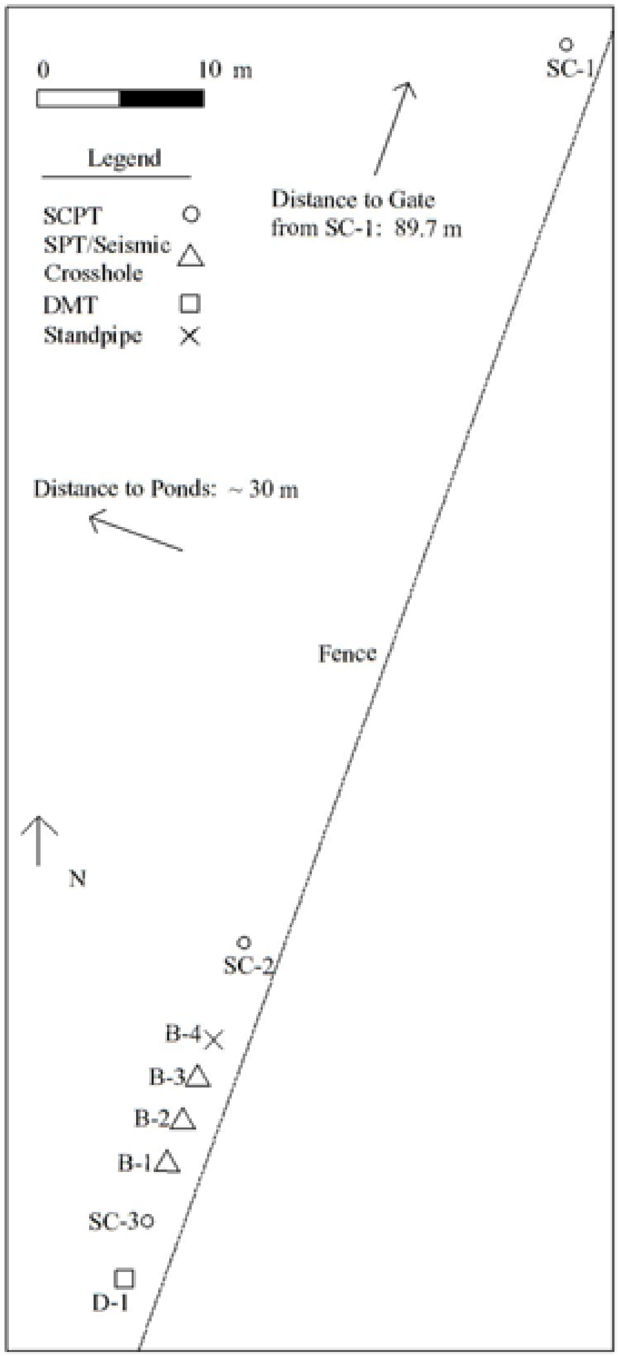

Figure 4.4 Site map for the Rest Area Ponds site.

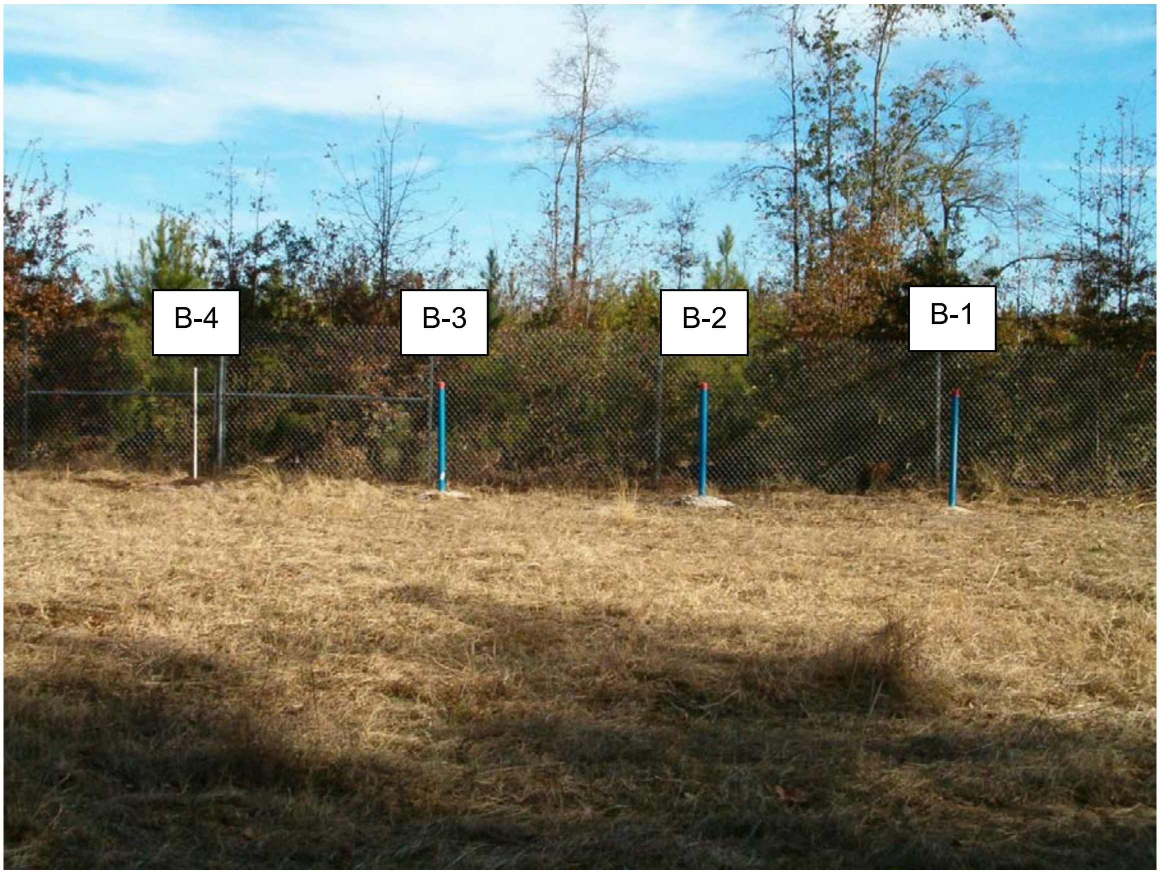

Figure 4.5 Photograph of borehole locations with inclinometer casings at the Rest Area Ponds site.

4.4 Results

The following section includes data from all of the investigations mentioned in the previous section except for the seismic crosshole testing and the inclination survey. All other test results are presented in detail in Appendix B and tabulated SCPTu data are presented in Appendix D.

4.4.1 CPT Stratigraphy and Properties

Presented in Figure 4.6 are profiles of q_t and FR for each of the three cone soundings conducted at the site. The top 12 m (39.4 ft) contains six distinct layers. Some of the cone indexes are plotted on the soil behavior charts by Robertson (1990) presented in Figure 4.7

Layer A extends from the ground surface down to an average depth of 1.8 m (5.9 ft). Layer A has very high q_t which averages 14.7 MPa. It also has an average FR of 0.62% and the cone pore pressure does not exceed the hydrostatic pressure. The soil identification charts in Figure 4.7 identify this layer as clean to silty sand. It is also known that during the construction of the site, some fill material was added to the area. In addition, while conducting sounding SC-1, a metal plate was punctured by the cone tip, likely left over from construction.

Layer B is located between depths of 1.8 m and 2.7 m (5.9 ft to 8.8 ft). Tip resistance is low in Layer B, averaging 3.7 MPa. Layer B also has an average FR of 0.74%. Cone pore pressures do not rise above hydrostatic pressure.

Figure 4.7 indicates that the material in Layer B varies from clean sand to sandy silt. The groundwater table is within this layer. The groundwater table was observed at a depth of 2.3 m (7.5 ft) the day after drilling. However, the depth of the groundwater table has varied from 1.7 to 2.8 m (5.7 to 9.3 ft) between visits to the site.

Layer C extends from a depth of 2.7 m (8.8 ft) to 5.9 m (19.2 ft). In SC-2 and SC-3, the tip resistance is fairly consistent throughout the depth (see Figure 4.6). However, SC-1 indicates the upper half of Layer C to have a very high average tip resistance of 22 MPa, whereas the lower half is similar to tip resistances seen in SC-2 and SC-3. Therefore, Layer C was separated into sublayers C1 and C2 for SC-1. The depth separating these sublayers is 4.4 m (14.4 ft). Sublayer C1 has the previously mentioned average q_t of 22.0 MPa and an average FR of 0.85%. Sublayer C2 and Layer C in SC-2 and SC-3 have an average q_t of 8.1 MPa with an average FR of 0.71%. Again, cone pore pressures do not rise above hydrostatic pressure. Figure 4.7 indicates that Layer C consists of clean to silty sand.

Located between depths of 5.9 and 6.6 m (19.2 and 21.8 ft) is Layer D. It is a thin layer with very low average q_t of 1.8 MPa. The average FR is 2.36%. Cone pore pressure rose above hydrostatic pressure for the layer, suggesting significant fines content. Figure 4.7 suggests that materials in Layer D vary from silty clay to clean sand.

Layer E is about as thick as Layer D, beginning at a depth of 6.6 m (21.8 ft) and ending at 7.5 m (24.6 ft). Layer E has average q_t and FR values of 2.3 MPa and 0.45%, respectively. The cone pore pressures did not rise above hydrostatic pressure. Figure 4.7 indicates that Layer E consists of silty sand to sandy silt.

Layer F is located between depths of 7.5 and 10.2 m (24.6 to 33.5 ft). It has average q_t and FR values of 0.41 MPa and 1.46%, respectively. Cone pore pressures are above hydrostatic pressure. Layer F is classified as a clay to silty clay by Figure 4.7.

Finally, Layer G begins at a depth of 10.2 m (33.5 ft). SC-1 was pushed deep enough to encounter the bottom of Layer G as shown in Figure B.1. The bottom depth of Layer G is 14.9 m (48.9 ft). Using the data available from Layer G, the average values of q_t and FR are 2.6 MPa and 1.76%, respectively. Cone pore pressures fluctuate in Layer G, suggesting thin interbedded silt and clay layers. Figure 4.7 supports this belief and identifies Layer G as having materials varying from clay to silty sand.

Below Layer G, Layers H, I, and J are identified in SC-1's composite profile (see Figure B.1). These layers are not considered for this study.

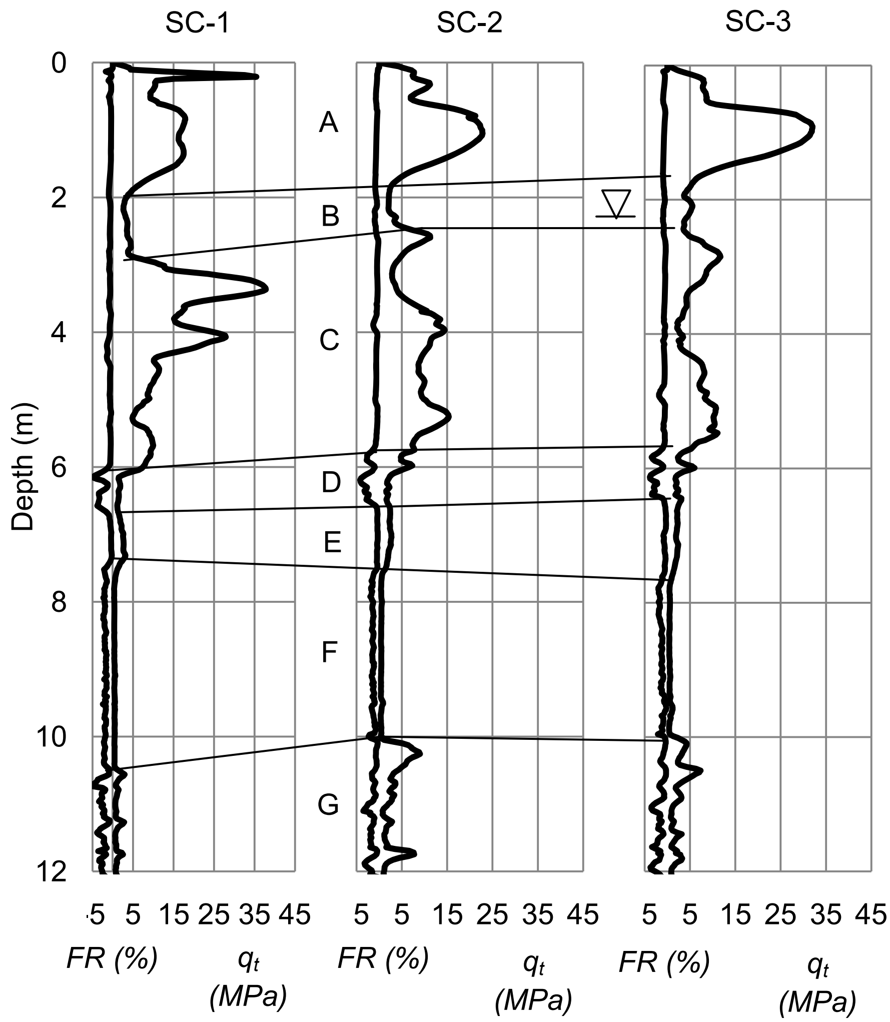

Figure 4.6 SCPT cross-section of the Rest Area Ponds site.

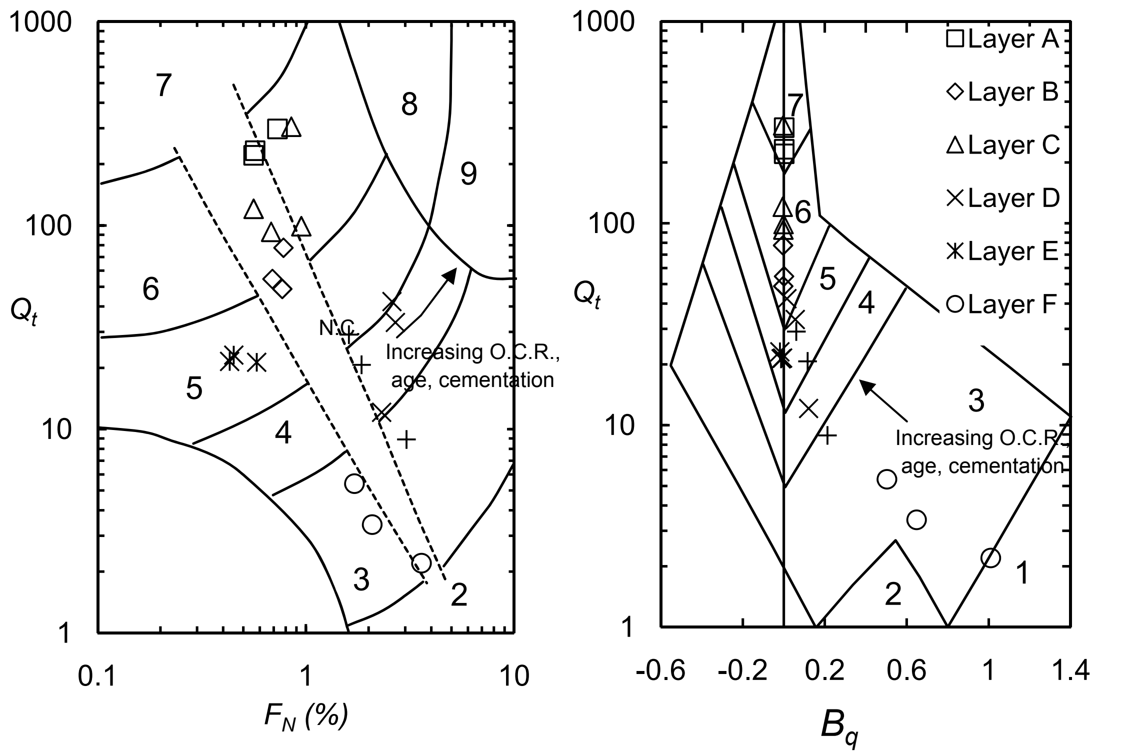

Zone	Soil behavior type	Zone	Soil behavior type
1.	Sensitive, fine grained;	6.	Sands: clean sands to silty sands;
2.	Organic soils, peats;	7.	Gravelly sand to sand;
3.	Clays: clay to silty clay;	8.	Very stiff sand to clayey sand;
4.	Silt mixtures: clayey silt to silty clay;	9.	Very stiff fine grained
5.	Sand mixtures: silty sand to sandy silt;		

N.C. = Normally Consolidated
O.C.R. = Overconsolidation Ratio

Figure 4.7 Soil behavior type classification charts by Robertson (1990) with data from the Rest Area Ponds site.

Table 4.1 Summary of CPT indexes for the Rest Area Ponds site.

ID	Depth (m)	q_{t1N}	Q_t	F_N (%)	I_c	B_q	q_{t1Ncs}
Layer A							
SC-1	0-2.0	382.7	220.8	0.56	1.4	0.002	385.9
SC-2	0-1.8	388.9	232.7	0.57	1.34	0.002	390.3
SC-3	0-1.6	466.7	297.7	0.73	1.37	0.002	467.4
Layer B							
SC-1	2.0-2.9	55.3	54.6	0.69	2.03	0.001	74.4
SC-2	1.8-2.5	49.7	48.8	0.77	2.12	-0.003	72.6
SC-3	1.6-2.6	80.4	77.7	0.78	1.93	-0.004	97.8
Layer C							
SC-1, C1	2.9-4.4	306.3	305.4	0.85	1.53	-0.003	310.0
SC-1, C2	4.4-6.2	100.3	99.2	0.95	1.87	-0.001	117.2
SC-2	2.5-5.7	121.8	120.8	0.56	1.71	-0.005	128.4
SC-3	2.6-5.7	94.13	93.1	0.68	1.86	-0.002	107.2
Layer D							
SC-1	6.2-6.9	13.4	12.1	2.31	2.84	0.121	68.0
SC-2	5.7-6.6	43.7	42.3	2.59	2.49	0.015	108.6
SC-3	5.7-6.4	34.8	33.4	2.69	2.55	0.056	102.7
Layer E							
SC-1	6.9-7.4	23.0	21.5	0.43	2.30	-0.006	45.0
SC-2	6.6-7.5	24.5	23.1	0.45	2.29	-0.019	46.2
SC-3	6.4-7.6	22.7	21.3	0.58	2.36	-0.013	48.5
Layer F							
SC-1	7.4-10.6	3.7	2.2	3.59	3.68	1.01	56.9
SC-2	7.5-10.0	5.1	3.4	2.08	3.33	0.648	55.1
SC-3	7.6-10.1	7.1	5.4	1.71	3.16	0.503	53.2
Layer G							
SC-1	10.6-14.9	10.5	8.9	3.04	3.11	0.213	68.5
SC-2	10.0-12.1	30.9	29.1	1.61	2.53	0.061	73.1
SC-3	10.1-12.8	22.5	20.7	1.85	2.66	0.116	69.2

4.4.2 DMT Results

The DMT was performed at D-1 next to SCPTu sounding SC-3 (See Figure 4.4). Figures 4.8 presents plots of DMT material index (I_D), DMT horizontal stress index (K_D), estimated at rest earth pressure coefficient (K_0), and DMT constrained modulus (E_D). Average values of these properties for each layer are presented in Table 4.2. Figure 4.9 presents the DMT results on a soil type chart. These plots provide additional insight to the CPT layering identified previously.

Layer A has a very high average K_0 of 7.68. This indicates that the horizontal stresses and/or stiffnesses are much higher than vertical. Layers B, C, D, and E all have average K_0 greater than two. The results indicate that these layers exhibit higher horizontal stresses and/or stiffnesses, but not nearly as high as Layer A. Layers F and G have average K_0 below one, indicating that the vertical stresses and/or stiffnesses are greater than horizontal.

Figure 4.9 indicates that Layer A has a wide range of soil types. It ranges from a medium dense sandy silt to a very dense sand. Layer B is shown in Figure 4.9 to vary from dense sandy silt to a medium dense sand. Layer C is shown by Figure 4.9 to be a dense sand to silty sand. Layer D is indicated as being a low to medium dense silty sand. Layer E is a silty sand with low density. Layer F has a wide range of soil types, varying from silty sand of low density to very soft clay. Finally, Layer G varies from silty sand of medium density to soft silty clay.

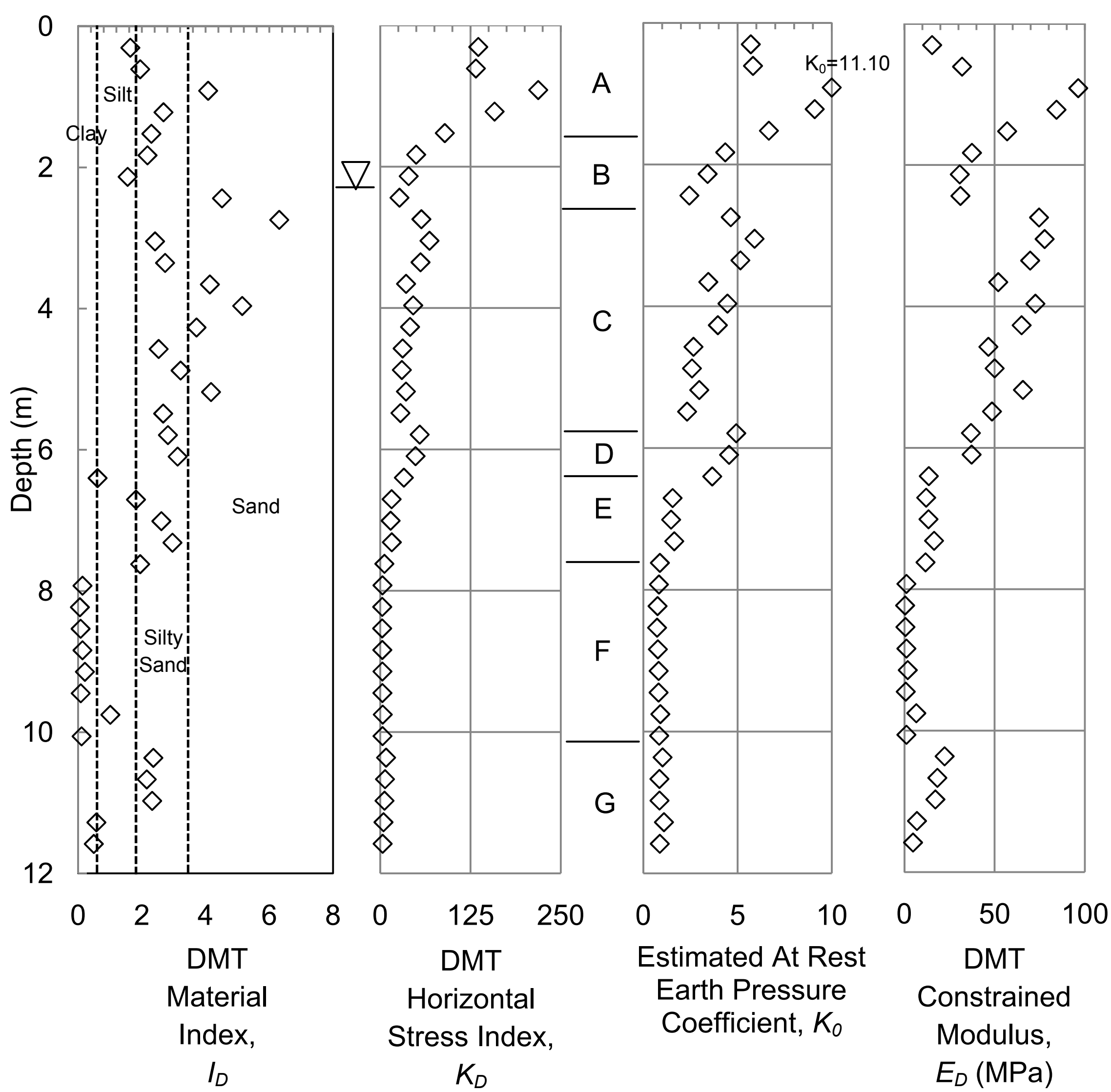

Figure 4.8 Results of DMT D-1 conducted at the Rest Area Ponds site.

Table 4.2 Summary of DMT indexes for D-1 at the Rest Area Ponds site.

Layer	Depth (m)	Material Index, I_D	DMT Horizontal Stress Index, K_D	Estimated at Rest Earth Pressure Coefficient, K_0	DMT Constrained Modulus, E_D (MPa)
A	0-1.6	2.53	146.95	7.68	56.98
B	1.6-2.6	2.75	38.69	3.41	33.07
C	2.6-5.7	3.70	42.92	3.81	62.24
D	5.7-6.4	2.97	51.86	4.74	37.08
E	6.4-7.6	2.00	19.82	2.09	13.89
F	7.6-10.1	0.45	3.46	0.82	3.07
G	10.1-12.8	1.33	5.40	0.93	11.81

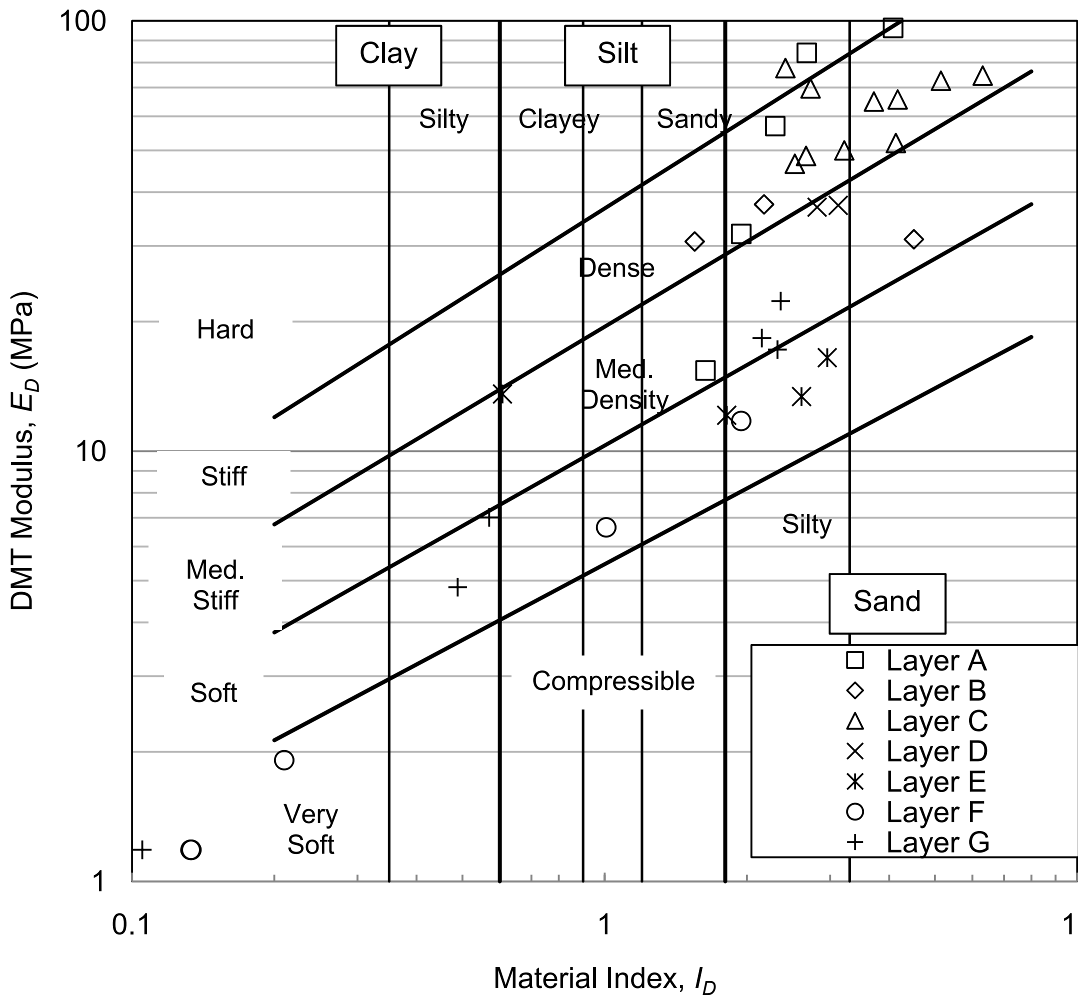

Figure 4.9 DMT modulus and material index chart (ASTM D 6635) with data from D-1 at the Rest Area Ponds site.

4.4.3 SPT Results

SPT's were conducted in borehole B-3 at the Rest Area site. Figure 4.10 presents a SPT profile using corrected blowcount, N_{60}, and Table 4.3 presents average calculated SPT properties. There are no blowcounts for Layer F, as the SPT hammer and rods were heavy enough to sink through the 1.5 ft range. This was recorded as "weight of hammer" for blowcount in the boring log in Appendix B. The fines content for the clean sand correction was determined from grain size analysis that will be presented later in this chapter.

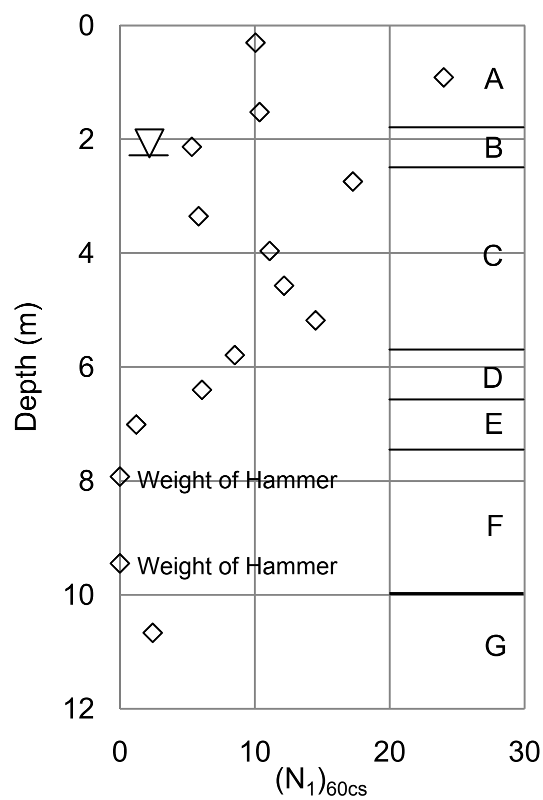

Figure 4.10 SPT profile for B-3 at the Rest Area site.

Table 4.3 Summary of SPT properties at the Rest Area Ponds site.

Layer	Depth (m)	$(N_1)_{60}$ blows/0.3m	Fines Content (%)	$(N_1)_{60cs}$ blows/0.3m
A	0-1.8	24	9.7	25
B	1.8-2.5	15	10.0	16
C	2.5-5.7	15	8.6	15
D	5.7-6.6	8	30.7	9
E	6.6-7.5	1	12.1	3
F	7.5-10.0	-	17	-
G	10.0-12.1	2	10.9	3

4.4.4 Shear Wave Velocity

Figure 4.11 presents a profile of true interval S-wave velocities for seismic downhole testing in SC-1, SC-2, and SC-3 at the Rest Area Ponds site. Table 4.4 presents a summary of velocities for each layer. The corrected S-wave velocity, $(V_{s1})_{cs}$, is obtained using procedures presented in Chapter 2. Values of Vs varied fairly uniformly with depth, ranging from about 100 m/s at a depth of 1 m to about 250 m/s at a depth of 11 m.

MEVRs were calculated using CPT-based estimated velocity for each downhole test. In addition, MEVR was calculated using an SPT-estimated velocity with measured velocity data from SC-2, which is nearest to B-3. Profiles of MEVR are presented in Figure 4.12. The averages for layers greater than 1 m thick are summarized in Table 4.4. If a layer is less than 1 m, average velocity measurements of shear wave velocity will not be presented, as the measurement interval for downhole testing is 1 m. For this reason, Layers B, D, and E are not presented in Table 4.4.

Based on Figure 1.1, a mean MEVR of 1.42 is expected for a 1,000,000 year-old soil deposit. The MEVR that is one standard deviation below the mean is 1.25, and the MEVR for one standard deviation above the mean is 1.59. Layer A has an average MEVR of 0.96, well below the expected range. This MEVR suggests that the region is either younger than 6 years or was disturbed in recent history. The latter of these is more likely because the construction of the site and addition of fill could easily have disturbed the soil.

Layer C in SC-2 and SC-3 and Sublayer C2 in SC-1 have an average MEVR of 1.13, which is well below the expected range. This may be due to diagenetic processes or local disturbance. Sublayer C1 in SC-1 has an average MEVR of 0.89. This is similar to the situation in Layer A. Both layers have very high corrected tip resistances and both ended up having lower MEVRs. This would suggest that the density of a material may have an impact on the MEVR that isn't covered by the relationship shown in Figure 1.1.

Layer F has an average MEVR of 1.31, which falls within the expected range. There are no MEVR's for Layer F using SPT data because the only SPT's conducted in Layer F did not produce blowcounts. Finally, Layer G has an average MEVR of 1.21, which falls just below the expected range of MEVR.

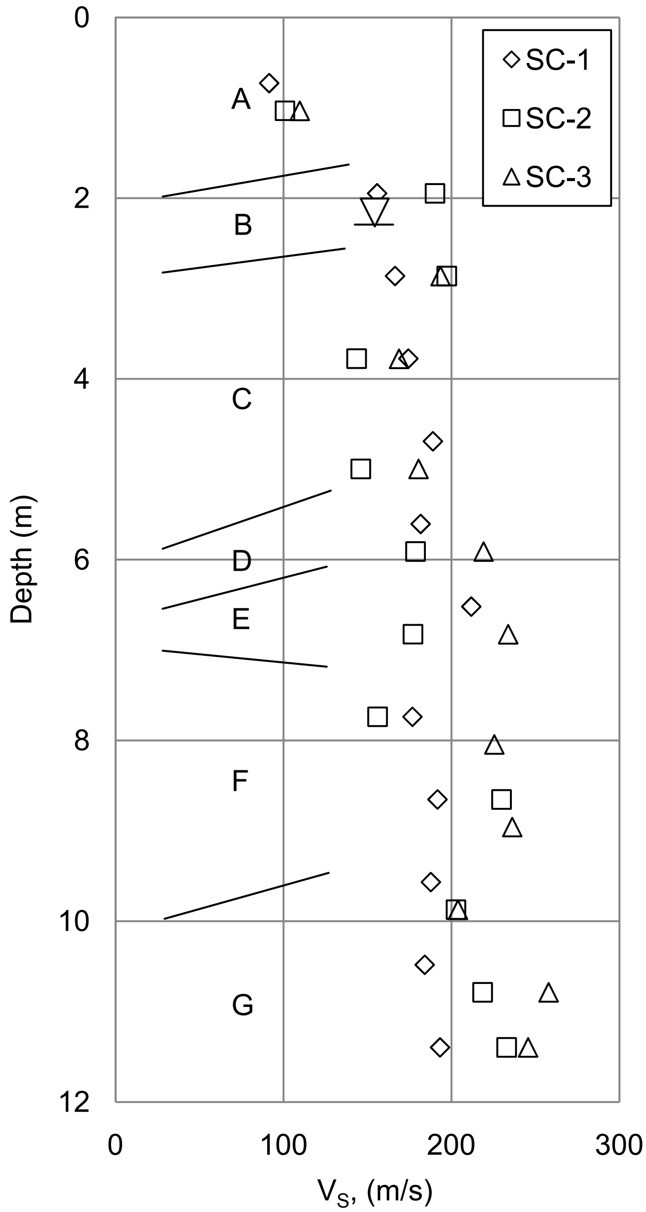

Figure 4.11 V_S profiles for seismic downhole measurements for the Rest Area Ponds site.

Table 4.4 Summary of S wave velocity calculations for the Rest Area Ponds site.

ID	Depth (m)	V_s (m/s)	V_{s1} (m/s)	$(V_{s1})_{cs}$ (m/s)	*MEVR*
Layer A					
SC-1	0-2.0	124	205	208	0.91
SC-2	0-1.8	101	175	176	0.69
SC-3	0-1.6	110	195	197	0.75
B-3	0-1.8	101	150	151	1.50
Layer C					
SC-1, C1	2.9-4.4	174	208	210	0.89
SC-1, C2	4.4-6.2	185	209	212	1.06
SC-2	2.5-5.7	162	195	198	1.09
SC-3	2.6-5.7	181	217	220	1.21
B-3	2.5-5.7	159	180	182	1.15
Layer F					
SC-1	7.4-10.6	185	170	173	1.10
SC-2	7.5-10.0	196	200	207	1.32
SC-3	7.6-10.1	222	225	235	1.50
B-3	7.5-10.0	-	-	-	-
Layer G					
SC-1	10.6-14.9	183	159	161	0.97
SC-2	10.0-12.1	226	219	223	1.34
SC-3	10.1-12.8	252	244	252	1.54
B-3	10.0-12.1	219	209	213	0.97

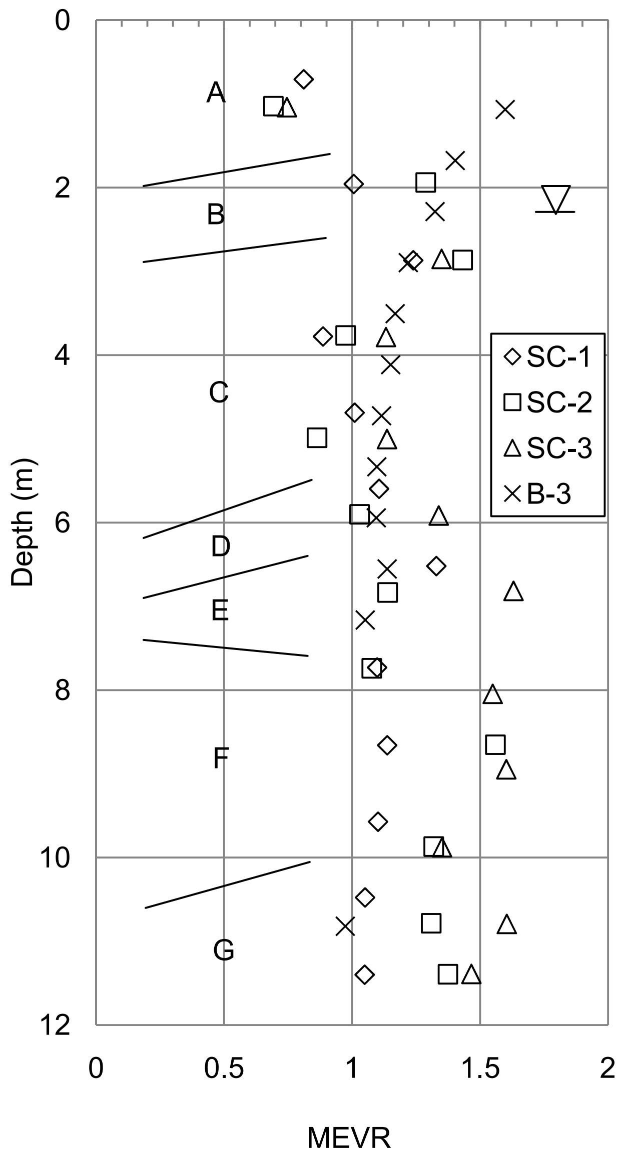

Figure 4.12 MEVR profile for the Rest Area Ponds site using velocities obtained from seismic downhole-measured velocities and estimated velocities using equations proposed by Andrus et al. (2004a).

4.4.5 Laboratory Investigations

A variety of laboratory tests were performed on samples collected from boreholes at the Walterboro Rest Area Ponds site. Grain size analyses and Atterberg limits were used in determining classifications using the United Soil Classification System (USCS). Consolidation tests were conducted on fixed piston samples from B-1.

Layer A consists of poorly graded sand with silt (SP-SM), which agrees well with CPT and DMT classifications. The samples were all non-plastic, so no Atterberg limits were obtained. This layer did contain organic content at the surface. Layer A is likely fill material and is assumed to have a dry unit weight of 17.3 kN/m^3 (110 lb/ft^3).

Layer B is a very dark colored layer with soil that was difficult to cut upon first observation. This layer classifies as SP-SM, which agrees well with CPT and DMT classifications. Layer B is non-plastic as well. Layer B is assumed to have a dry unit weight of 17.3 kN/m^3 (110 lb/ft^3) and a saturated unit weight of 18.9 kN/m^3 (120 lb/ft^3). It is thought that this layer is the original ground surface.

Layer C contains poorly graded sand to poorly graded sand with silt (SP to SP-SM), which agrees well with CPT and DMT classifications. This layer is non-plastic and generally brown in color. Layer C's saturated unit weight is assumed to be 18.9 kN/m^3 (120 lb/ft^3). Figure 4.13 presents the particle size distribution for Layer C. Layers C and B are believed to be the beach sand deposit identified on the map by McCartan et al. (1984).

Layer D contains white silty sand to clayey sand (SM to SC), which agrees well with CPT and DMT classifications. Layer D also appears to be dessicated, as a sample from the layer broke apart during trimming for consolidation testing. It is estimated to have a saturated unit weight of 18.4 kN/m^3 (117 lb/ft^3).

Layer E is a white silty sand (SM), which agrees well with CPT and DMT classifications. Layer E is also non-plastic. This layer is very similar to Layer D except for the decreased fines content. The layer's saturated unit weight is assumed to be 18.4 kN/m^3 (117 lb/ft^3).

Layer F contains gray silty sand to poorly graded sand with silt (SM to SP-SM), though CPT and DMT classifications suggest this to be clay to silty clay. Some of the soil in this layer is plastic enough to obtain Atterberg limits. Consolidation tests were also conducted in this layer from fixed piston samples collected from B-1. These tests indicate the layer is slightly overconsolidated with an average OCR of 1.62. The estimated saturated unit weight for this layer is 18.9 kN/m^3 (120 lb/ft^3).

Layer G is a gray poorly graded sand with silt (SP-SM), which agrees well with CPT and DMT classifications. Layer G is also non-plastic. The layer has an assumed unit weight of 18.9 kN/m^3 (120 lb/ft^3).

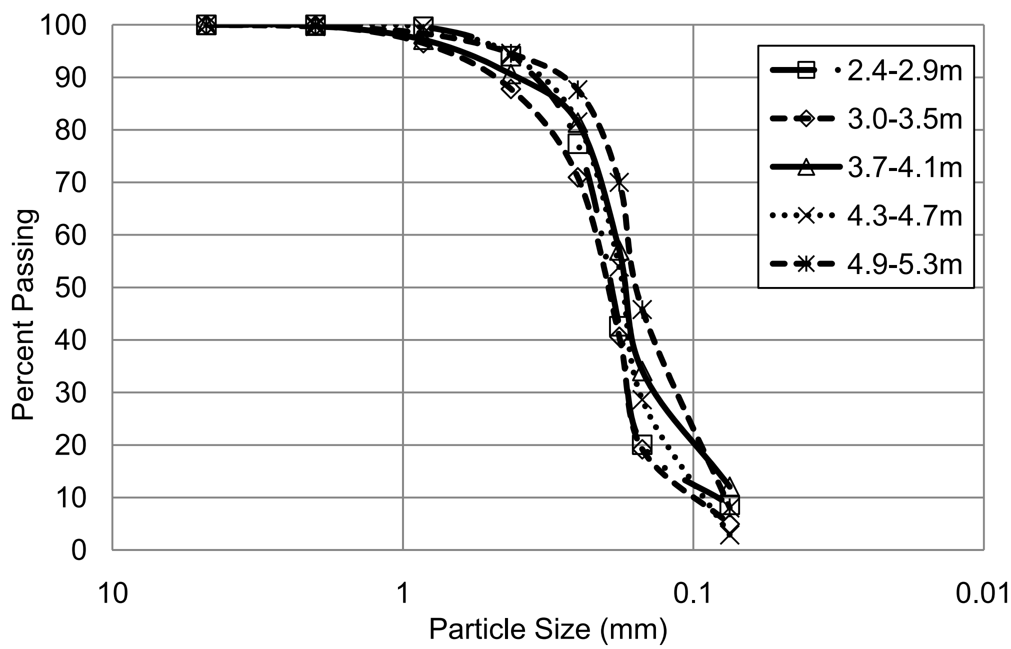

Figure 4.13 Grain size distributions for Layer C at the Rest Area Ponds site.

4.5 Summary

The Walterboro Rest Area Ponds site has surface soils that McCartan et al. (1984) estimates to be at least 1,000,000 years old. Three SCPTu's and one DMT were conducted at the site. In addition, SPT, seismic crosshole, and Osterberg-type fixed piston sampling were conducted to further investigate the site. Grain size analyses, Atterberg limits, and consolidation tests were performed in the laboratory back at Clemson.

The site has seven identified layers in the top 12 m (39.4 ft). Layer A is a dense layer that classifies as SP-SM. Layer B is also SP-SM, though it is less dense than Layer A. The water table is located in Layer B at an average depth of 2.3 m (7.5 ft), although seasonal fluctuations are significant. Layer C consists of

SP to SP-SM. Layer D is SM to SC with low density. Similarly, Layer E is SM with low density. Layer F is SP-SM with interbedded fine-grained material and is less dense than other layers. Layer F is also slightly overconsolidated. Finally, Layer G is medium dense SP-SM.

Based on DMT indexes, Layer A has an average K_0 of 7.68. This indicates that Layer A is either experiencing very high horizontal stresses or that it is very stiff in the horizontal direction. Layers B, C, D, and E have average K_0 higher than two, but not nearly as high as Layer A. Layers F and G both have average K_0 less than one, indicating that vertical stresses are higher than horizontal stresses.

Shear wave velocities were measured at SC-1, SC-2, and SC-3 using the true-interval downhole method. The velocities were corrected and used to determine MEVRs for each test location. Figure 1.1 suggests that the mean expected MEVR for a 1,000,000 year-old soil is 1.42. The plus/minus one standard deviation range of MEVR is 1.25 to 1.59. Layers A, C, and G have MEVR's of 0.98, 1.13, and 1.21, respectively. These all are less than 1.25, the minus one standard deviation of MEVR. Layer F has a MEVR of 1.31, which does fall within the expected range.

CHAPTER FIVE

INVESTIGATIONS AT THE WALTERBORO LOWCOUNTRY SAND & GRAVEL SITE

5.1 Introduction

The Lowcountry Sand & Gravel site is located about 5.6 km (3.5 mi) southeast of Walterboro, just off of Route 303. The site is owned by Lowcountry Sand & Gravel, Inc. A map showing the locations of the town of Walterboro, Route 303, and the Lowcountry Sand & Gravel site is presented in Figure 5.1.

In Figure 5.2, the test site can be seen next to a large man-made pond, which Lowcountry Sand & Gravel, Inc. provided for geotechnical investigation. Figure 5.3 is a photograph of the site during testing taken from the opposite lake shore.

Over the years, mining operations at the site have consisted of stripping off of finer grained soils above the groundwater table and dredging coarse sand deposits that lie below the groundwater table. Based on mining operations at the time of this study, the site has been graded down from its original elevation by about 3.4 m (11 ft). A photograph of mining operations is presented in Figure 5.4.

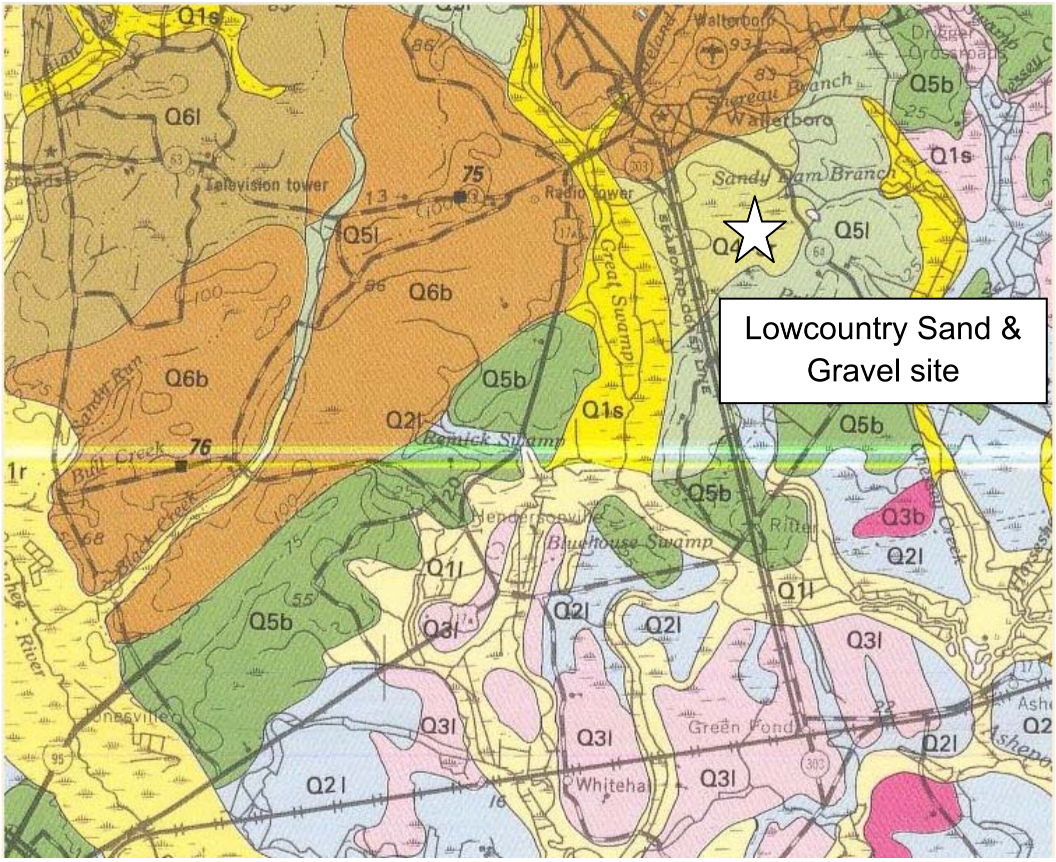

Figure 5.1 Geologic map by McCartan et al. (1984) showing the location of the Lowcountry Sand & Gravel site.

5.2 Geology

The Lowcountry Sand & Gravel site is located in the geological unit designated as Q4-5r on the map by McCartan et al. (1984), as shown in Figure 5.1. McCartan et al. characterized Q4-5r as fluvial deposits with age around 450,000 years. The Lowcountry Sand & Gravel site lies well outside the zone of 1886 craterlets reported by Dutton (1889, Plate XXVIII). Thus, it is unlikely that liquefaction occurred at the site in 1886.

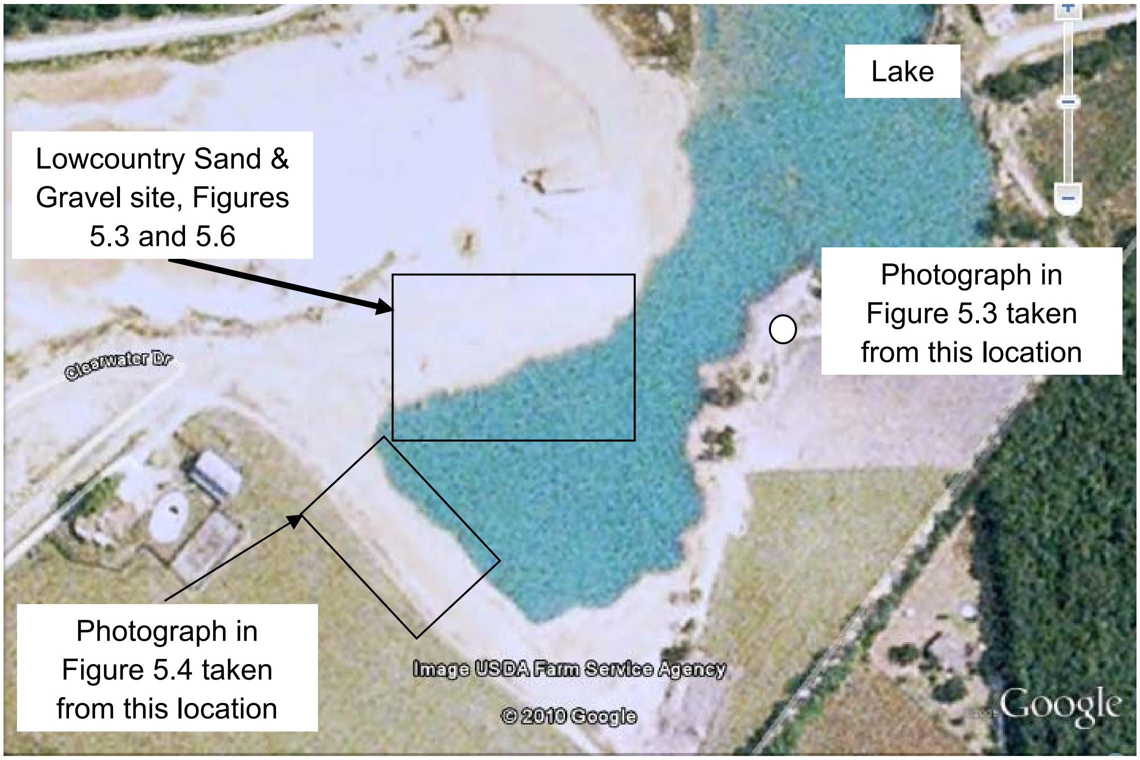

Figure 5.2 Satellite image showing the location of the Lowcountry Sand & Gravel site.

Figure 5.3 Photograph of testing area at the Lowcountry Sand & Gravel site. The cone truck is located at SC-1L.

Figure 5.4 Mining operations at the Lowcountry Sand & Gravel site.

5.3 Investigations

On June 25, 2009, three SCPTu's and one DMT were performed at the Lowcountry Sand & Gravel site. The test locations, identified as SC-1L, SC-2L, SC-3L, and D-1L, are presented on the site map in Figure 5.5. Two nearby utility poles were used as references, which are indicated in Figure 5.5 as well.

SC-1L was pushed to refusal, which was at a depth of 21.3 m (70.0 ft). SC-2L and SC-3L were both pushed to depths of 9.4 m (31.0 ft), temporarily stopping every 1 m (3.3 ft) to add a new rod and make shear wave velocity measurements. The DMT was pushed to a depth of 11.6 m (38.0 ft), stopping every 0.3 m (1.0 ft) to make measurements.

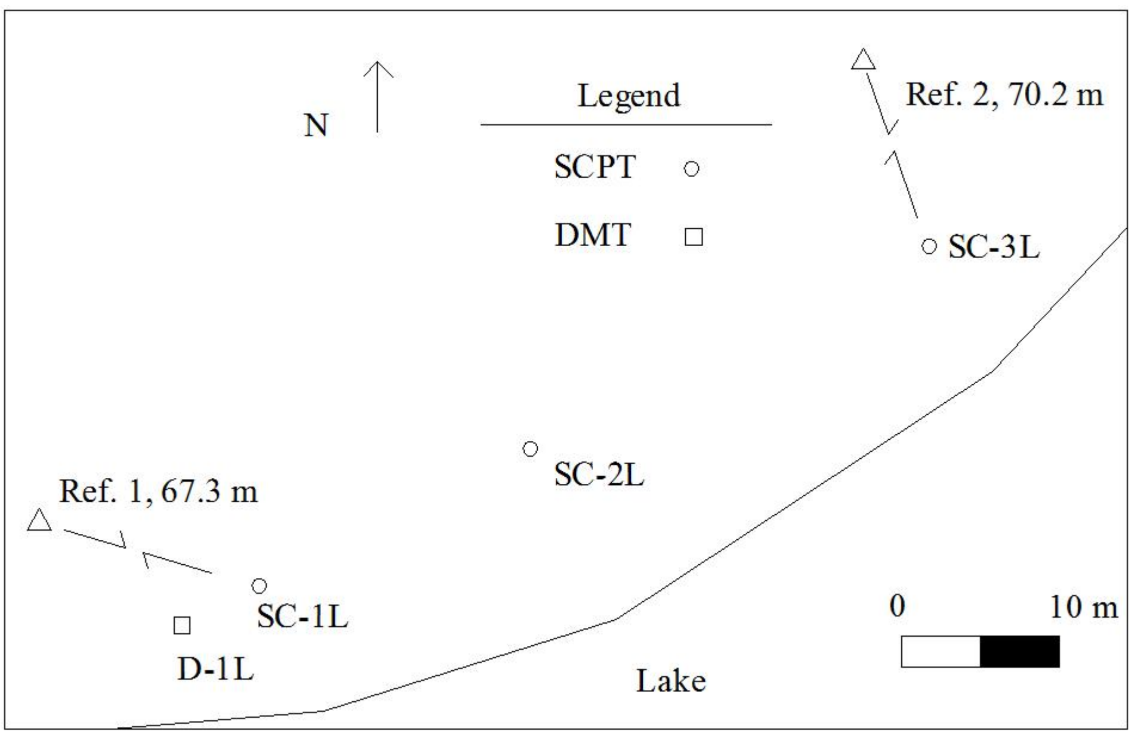

Figure 5.5 Site map for the Lowcountry Sand & Gravel site.

5.4 Results

This section presents results from the SCPTu's and DMT conducted at the Lowcountry Sand & Gravel site. More detailed test results, including composite CPT profiles, are presented in Appendix C. Tabulated SCPTu data are presented in Appendix D.

5.4.1 CPT Stratigraphy and Properties

Presented in Figure 5.6 are profiles of q_t and FR for the three cone soundings conducted at the site. The top 10 m (33 ft) contains at least seven distinct layers. Table 5.1 presents average cone indexes for six of the layers. Some of the cone indexes are plotted on the soil behavior classification charts by Robertson (1990) presented in Figure 5.7.

As illustrated in Figure 5.6, Layer A extends from the ground surface down to a depth of 2.4 to 2.6 m (7.9 to 8.5 ft) and has an average q_t of 19.7 MPa and an average FR of 0.61%. Figure 5.7 indicates that Layer A consists of either clean sand to silty sand to gravelly sand. The groundwater table is located within Layer A at a depth of 1.5 m (4.9 ft).

Layer B is a thin layer that is present at SC-1L and SC-2L (see Figure 5.6), but not at SC-3L. At SC-1L and SC-2L, Layer B's bottom surface is nearly level, ranging in depth from 2.8 to 2.9 m (9.2 to 9.5 ft). Layer B has an average q_t of 1.6 MPa and an average FR of 2.20%. Cone pore pressures in Layer B do not increase much above hydrostatic pressure. The soil classification chart by Robertson (1990) shown in Figure 5.7 indicates that Layer B materials are most likely silty sand to clayey silt.

Layer C lies directly below Layer B at SC-1L and SC-2L. The profiles of q_t suggest that the density of Layer C materials (see Figure 5.6) varies significantly across the site with an average q_t of 21.6 MPa and FR of 0.37% at SC-1L to an average q_t of 8.3 MPa and FR of 0.55% between SC-2L and SC-3L. There is no significant rise in measured cone pore pressure for this layer (See Appendix C), suggesting sandy material. Figure 5.7 identifies this layer as between a gravelly sand and a silty sand.

Layer D varies in thickness from 2.9 m (9.5 ft) at SC-1L to 1.3 m (4.3 ft) at SC-3L. The top of Layer D is nearly flat, with depths ranging from 4.2 to 4.3 m (13.8 to 14.1 ft). The bottom of Layer D dips to the southwest from depths of 5.6 to 7.0 m (18.4 to 23.0 ft). Layer D has an average q_t and FR of 1.1 MPa and 2.86%, respectively. The pore pressures measured in this layer are above hydrostatic pressure, suggesting higher fines content. Figure 5.7 indentifies Layer D as clay to clayey silt. Based on the finer grained materials and slope of the bottom of Layer D, Layer D represents the filling of a low-lying area, possibly a paleo-river channel..

Below Layer D the stratigraphy becomes rather interesting. In SC-3-L, there is a region of very high q_t values, some of which approach 30 MPa. At the other two locations, q_t is much lower, averaging 3.4 MPa. For this reason, the region is divided into two layers. Layer E is the region of high tip resistance. Layer E extends from a depth of 5.6 m to 9.5 m (18.4 to 31.2 ft) in SC-3L and exhibits average values of q_t and FR of 19.0 MPa and 0.40%. Figure 5.7 identifies this layer as a gravelly sand to silty sand.

Layer F extends down to 9.4 m (30.8 ft) in SC-1L and SC-2L. It has average q_t and FR values of 3.4 MPa and 1.56%, respectively. The pore pressure values fluctuate in this layer, indicating some interbedded fines content. Figure 5.7 characterizes this layer as clayey silt to silty sand to sandy silt. The frequent fluctuations in q_t and FR suggest that Layer F might be an overbank deposit with interbedded fines content, formed from seasonal flooding.

Below Layer F, Layers G, H, and I are identified in SC-1L's composite profile (see Figure C.1). Layer I exhibits cone pore pressure approaching 8.2 MPa. This layer, located at a depth of 16.2 m (53.2 ft), is believed to be the Cooper Marl, a very stiff Tertiary-age unit present throughout much of the coastal plain around Charleston.

Table 5.1 Summary of CPT properties for Layers A-F at the Lowcountry Sand & Gravel site.

ID	Depth (m)	q_{t1N}	Q_t	F_N (%)	I_c	B_q	q_{t1Ncs}
Layer A							
SC-1L	0-2.4	219.8	198.1	0.53	1.57	0.001	222.1
SC-2L	0-2.5	702.5	450.1	0.67	1.33	0.002	704.8
SC-3L	0-2.6	440.7	318.8	0.61	1.42	0.003	447.7
Layer B							
SC-1L	2.4-2.9	31.8	30.1	1.23	2.39	0.019	71.1
SC-2L	2.5-2.8	24.0	22.1	4.01	2.81	-0.006	99.2
Layer C							
SC-1L	2.9-4.2	328.1	327.2	0.38	1.28	0.000	329.3
SC-2L	2.8-4.3	116.6	115.6	0.60	1.71	0.000	123.6
SC-3L	2.6-4.1	140.6	139.7	3.70	1.67	0.000	148.0
Layer D							
SC-1L	4.2-7.0	16.6	15.0	3.48	2.96	0.282	83.5
SC-2L	4.3-6.3	14.3	12.7	2.95	2.92	0.133	81.5
SC-3L	4.1-5.6	19.6	18.1	3.70	2.93	0.194	89.0
Layer E							
SC-3L	5.6-9.5	215.9	214.3	0.40	1.49	0.000	218.7
Layer F							
SC-1L	7.0-9.4	32.7	31.0	1.86	2.49	0.018	81.4
SC-2L	6.3-9.4	41.6	40.0	1.47	2.32	0.043	80.0

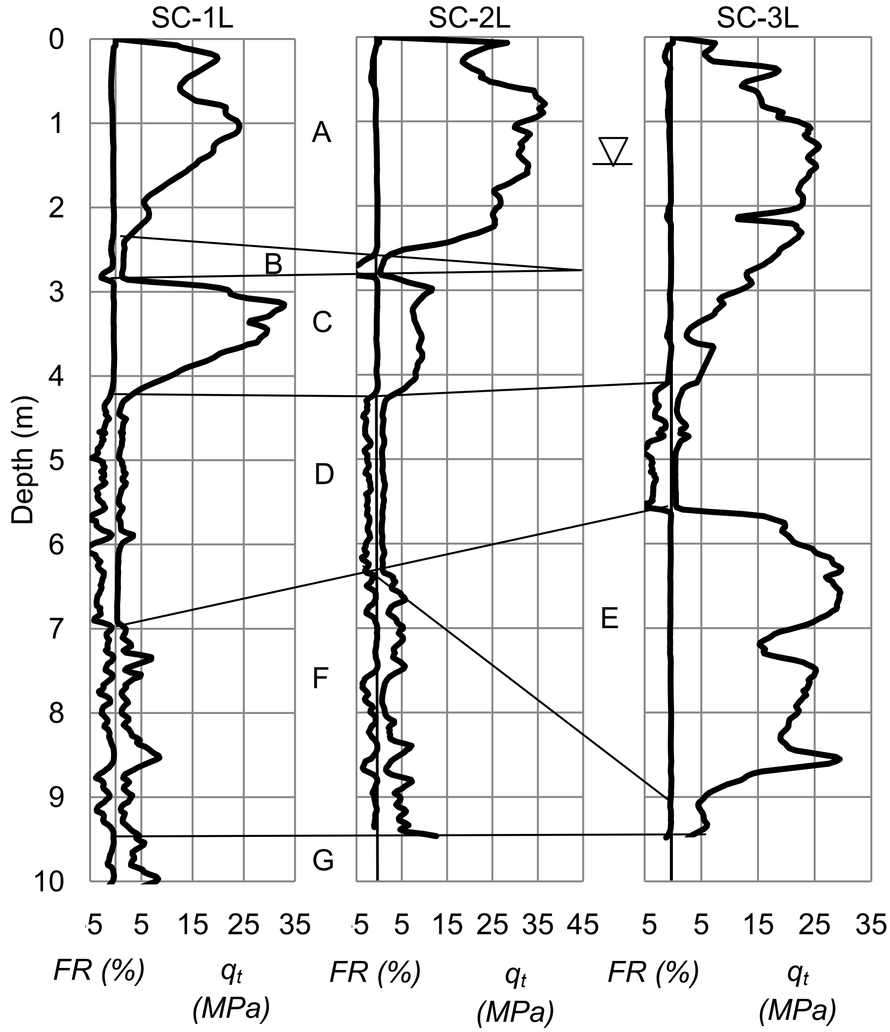

Figure 5.6 SCPT cross-section of the Lowcountry Sand & Gravel site.

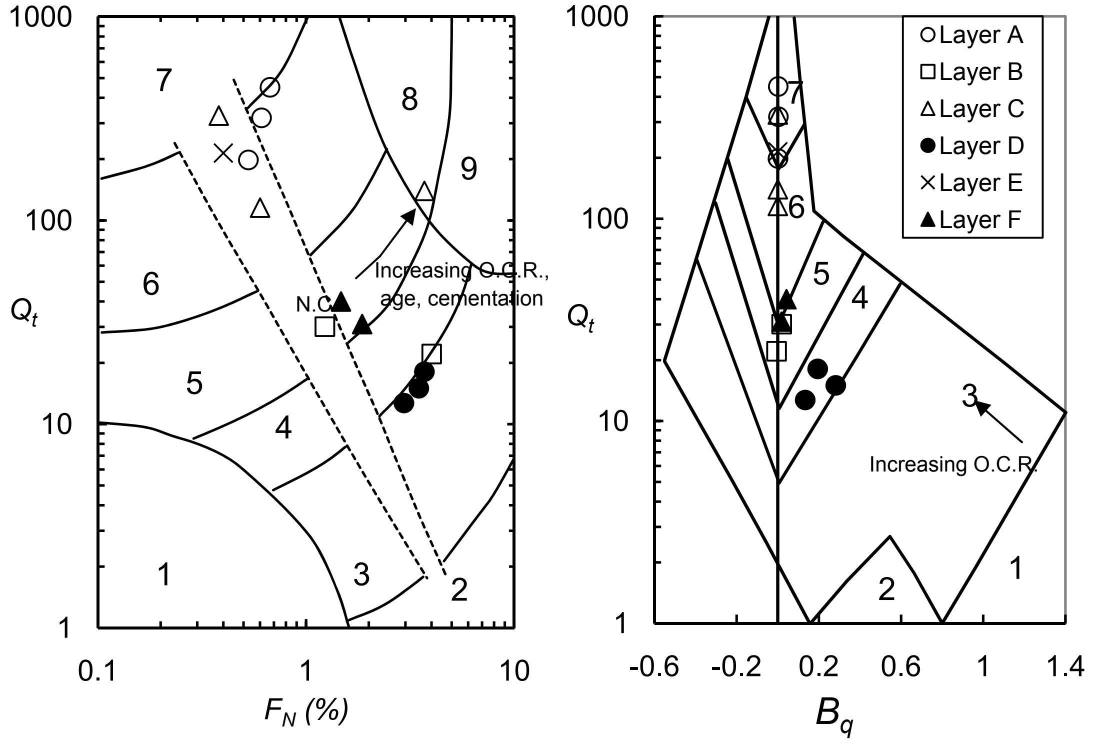

Zone	Soil behavior type
1.	Sensitive, fine grained;
2.	Organic soils, peats;
3.	Clays: clay to silty clay;
4.	Silt mixtures: clayey silt to silty clay;
5.	Sand mixtures: silty sand to sandy silt;
6.	Sands: clean sands to silty sands;
7.	Gravelly sand to sand;
8.	Very stiff sand to clayey sand;
9.	Very stiff fine grained

N.C. = Normally Consolidated
O.C.R. = Overconsolidation Ratio

Figure 5.7 Soil behavior type classification charts by Robertson (1990) with data from the Lowcountry Sand & Gravel site.

5.4.2 DMT Results

The DMT was performed at D-1L next to SCPTu sounding SC-1L (See Figure 5.5). Figures 5.8 presents plots of DMT material index (I_D), DMT horizontal stress index (K_D), estimated at rest earth pressure coefficient (K_0), and DMT constrained modulus (E_D). Average values of these properties for each layer are presented in Table 5.2. I_D and E_D are properties that indicate the type of material and the density or stiffness of that material. K_D was used to estimate the lateral at rest earth pressure, K_0, at each test depth. Figure 5.9 presents the DMT results on a soil type chart. These plots provide additional insight to the CPT layering identified previously.

Layers A and B have the highest estimated K_0 values, with averages of 8.57 and 4.46, respectively. These estimates of K_0 suggest high lateral stresses and/or high stiffnesses in Layers A and B. Layers C, D, F, G, and H have much lower K_0 values of 0.77, 1.90, 1.54, 1.40, and 1.98, respectively. These K_0 values suggest lower lateral stress and/or lateral stiffness than the top two layers, though horizontal stresses/stiffnesses are still relatively high in Layers D, F, G, and H.

Based on the DMT soil behavior index chart in Figure 5.9, Layer A materials classify as a dense sand to silty sand, which agrees with the CPT-based classification. This classification agrees well with the CPT-based classification of clean sand to silty sand. The one reading in Layer B suggests dense sand, which is in general agreement with the CPT-based classification.

Layer C classifies as sand to silty sand with medium density, which agrees with the CPT-based classification. Layer D varies from a medium dense silty sand to a soft silty clay, which is supported by the CPT classification charts. As D-1L is nearest SC-1L, Layer E does not exist in the soil profile. Layer F materials classify as silty sand to sandy silt, which agrees with the CPT-based classification. Layer G material classifies as a medium dense to dense sand. Layer H materials vary from dense sandy silt to dense sand.

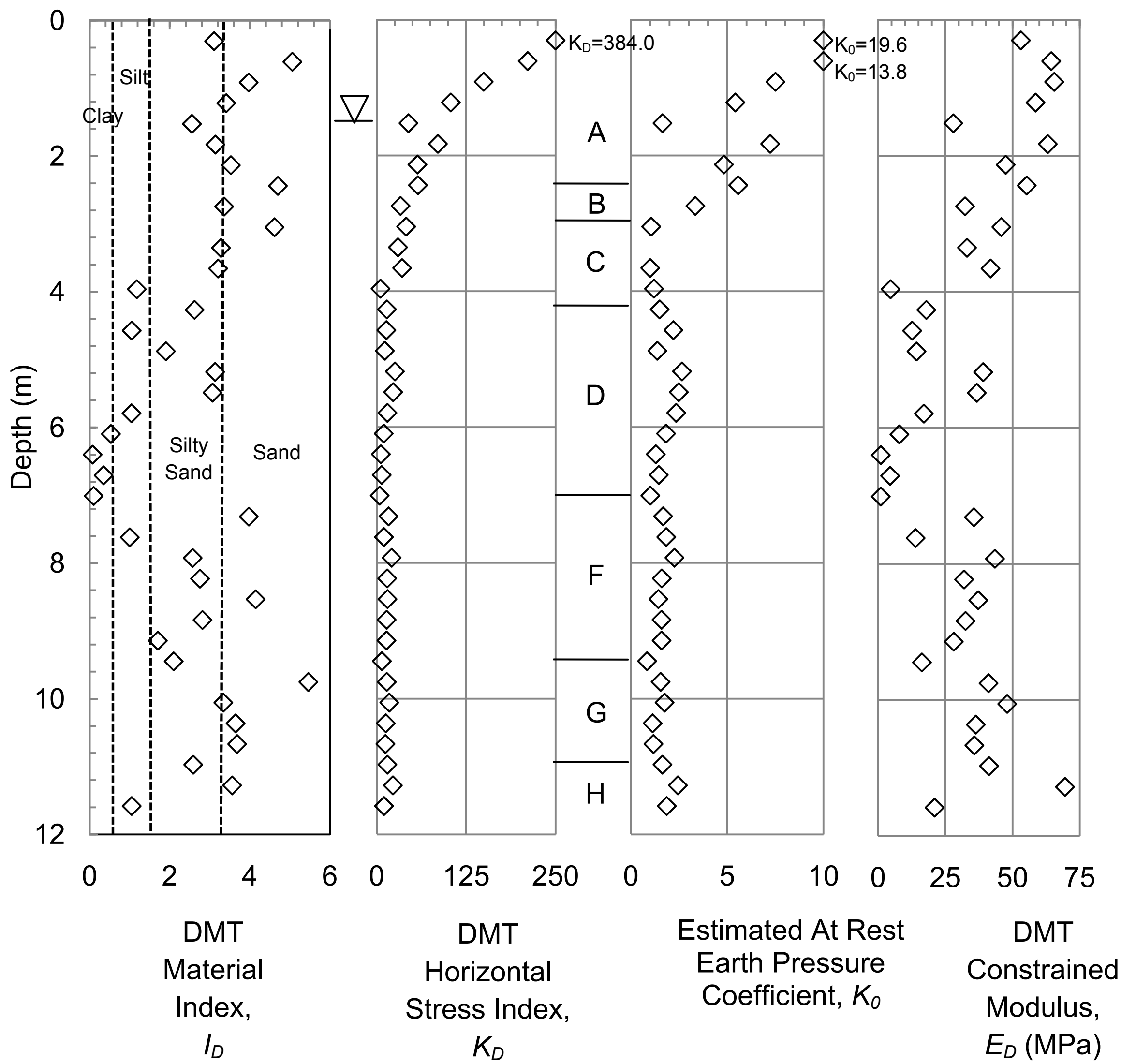

Figure 5.8 Results of DMT D-1L conducted at the Lowcountry Sand & Gravel site.

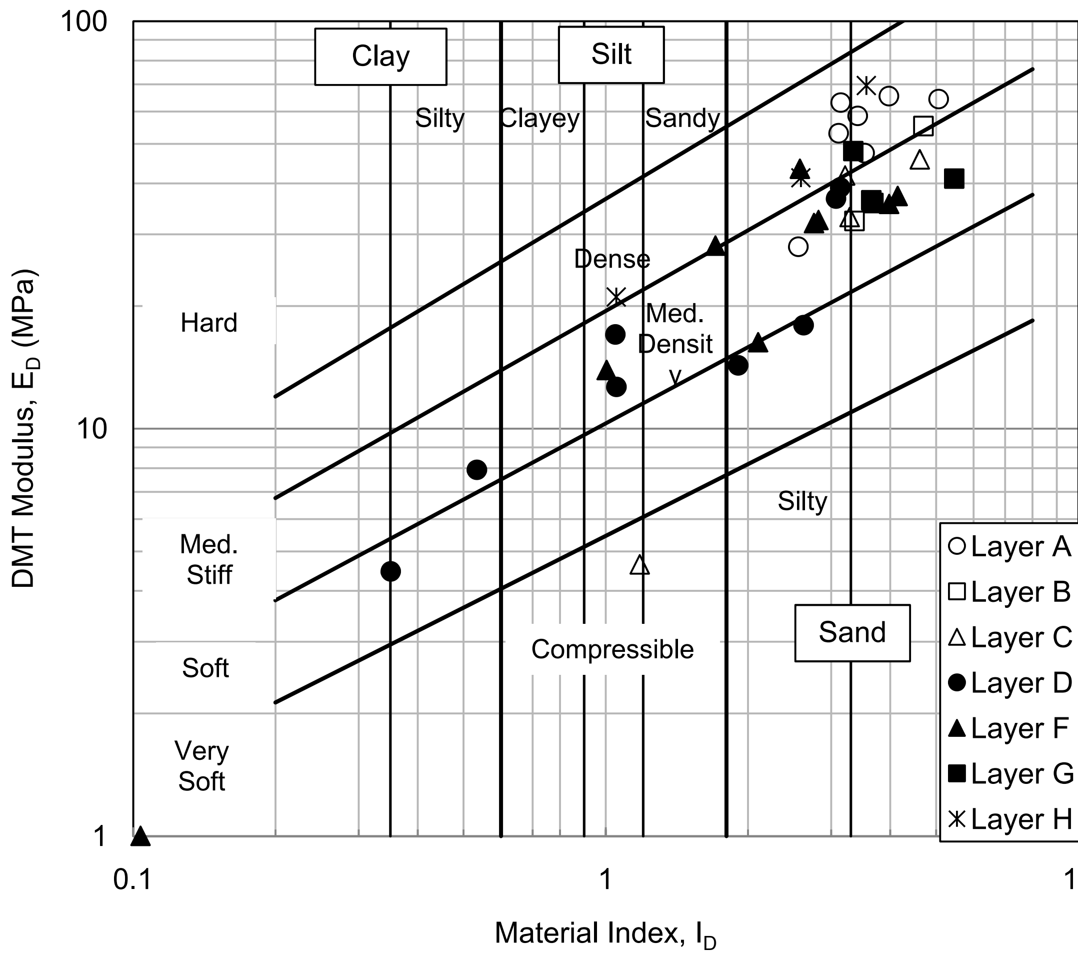

Figure 5.9 DMT modulus and material index chart (ASTM D 6635) with data from D-1L at the Lowcountry Sand & Gravel site.

Table 5.2 Summary of DMT calculations for D-1L at the Lowcountry Sand & Gravel site.

Layer	Depth (m)	Material Index, I_D	DMT Horizontal Stress Index, K_D	Estimated at Rest Earth Pressure Coefficient, K_0	DMT Constrained Modulus, E_D (MPa)
A	0-2.4	3.54	147.88	8.57	54.31
B	2.4-2.9	4.03	45.45	4.46	438.23
C	2.9-4.2	3.07	27.88	0.77	313.41
D	4.2-7.0	1.53	13.88	1.90	167.94
F	7.0-9.4	2.35	12.87	1.54	266.94
G	9.4-11.0	4.03	14.10	1.40	40.32
H	11.0-11.6	2.40	15.89	1.98	43.94

5.4.3 Velocity Results

Figure 5.10 presents profiles of true interval S-wave velocities for seismic downhole testing in SC-1L, SC-2L, and SC-3L at the Lowcountry Sand & Gravel site. Presented in Table 5.3 is a summary of S-wave velocities for Layers A-F. Figure 5.10 shows that Vs below the water table varies from 150 m/s to 250 m/s. In general, the velocities measured from the three cone soundings are in general agreement with each other. There is some variation where the soil type is varied between cone soundings at the same depth. The corrected S-wave velocity, $(V_{s1})_{cs}$, is obtained using procedures presented in Chapter 2. Values of $(V_{s1})_{cs}$ are used for liquefaction analysis (Chapter 6) and to determine MEVR.

MEVR (see Chapter 1) is calculated using CPT-based estimated velocity for each downhole test. Profiles of MEVR are presented in Figure 5.11. The averages for Layers A-F are summarized in Table 5.3.

Based on Figure 1.1, a mean MEVR of 1.40 is expected for a 450,000 year-old soil deposit. The MEVR that is one standard deviation below the mean is 1.23, and the MEVR for one standard deviation above the mean is 1.57. Layer A has an average MEVR of 0.86, which is well below the expected range. This would indicate that Layer A is either barely a year old or has recently been disturbed. The latter is the more likely reason, as mining operations could have easily disturbed Layer A.

Layer B is less than 1 m (3.3 ft) thick, which is the thickness required for a velocity measurement. Therefore, no average MEVR was presented for this layer.

Layer C has an average MEVR of 1.36, which is very close to what was expected. Layer C is a layer with varying density. It has already been seen in Layer A that areas of high tip resistance can produce low MEVRs. In the case of Layer A, this is believed to be affected by mining disturbance. The same could be true for the portion of Layer C at SC-1L which exhibits a higher tip resistance and low MEVR.

Layer D has an average MEVR of 1.80, which falls above the expected range. This may be a result of disturbance or diagenetic processes. Also, the estimating equations used in calculating MEVR by not be appropriate for Layer D because those equations are based on sands, whereas Layer D has fine-grained material.

Layer E has an average MEVR of 0.92, which corresponds to a time of less than just over half a year. This is a curious result because it was believed that a sandy layer would have a MEVR that was closer to the expected range. Diagenetic processes and local disturbance may have had an impact on Layer E.

Layer F has an average MEVR of 1.35, well within the expected range. This is different from the MEVR obtained for Layer E, further highlighting the horizontal variation present at the site. Layer E is only different from Layer F in that it has a much higher average tip resistance.

Figure 5.11 indicates that many MEVRs in Layers G and H are below an MEVR of 1, the MEVR expected for a soil that is just over six years old or was critically disturbed just over six years ago. What makes these layers different from the more shallow layers is that Layers F, G, and H have significant amounts of fine-grained material. This poses a problem in that the estimating equations by Andrus et al. (2004a) used to calculate MEVR are based on velocities of sand and not silt and/or clay. In addition, diagenetic processes could again be affecting the MEVRs.

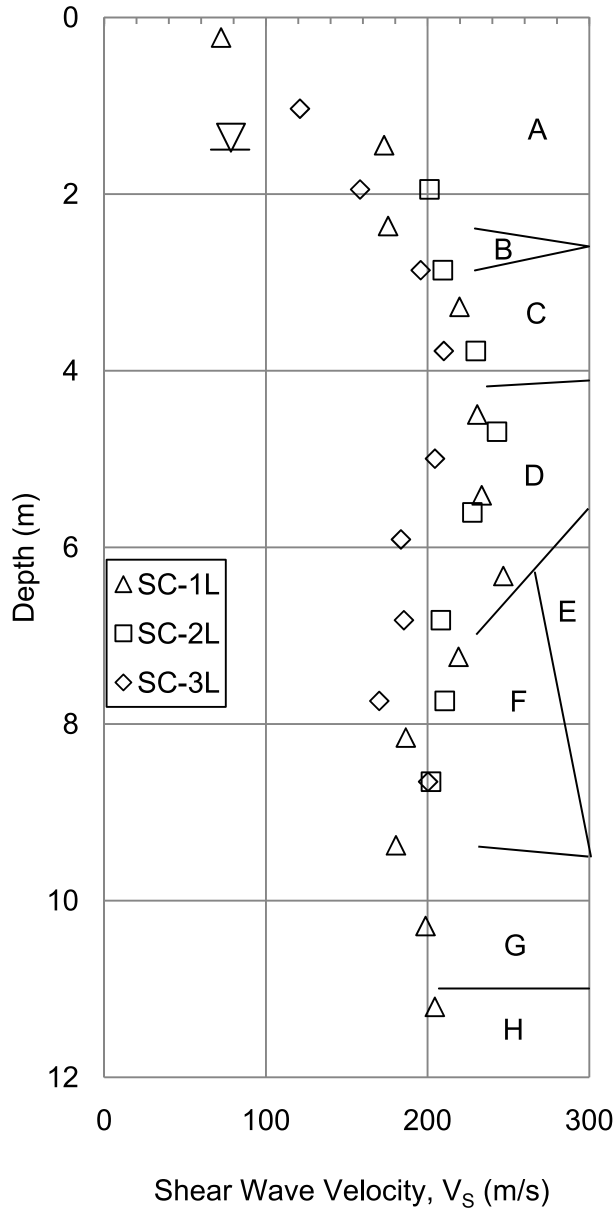

Figure 5.10 V_S profiles for seismic downhole measurements conducted at the Lowcountry Sand & Gravel site.

Table 5.3 Summary of S_V wave velocity calculations for Layers A-F at the Lowcountry Sand & Gravel site.

ID	Depth (m)	V_s (m/s)	V_{s1} (m/s)	$(V_{s1})_{cs}$ (m/s)	*MEVR*
Layer A					
SC-1L	0-2.4	123	156	157	0.78
SC-2L	0-2.5	201	272	272	1.05
SC-3L	0-2.6	140	181	181	0.75
Layer B					
SC-1L	2.4-2.9	-	-	-	-
SC-2L	2.5-2.8	-	-	-	-
SC-3L	-	-	-	-	-
Layer C					
SC-1L	2.9-4.2	198	245	248	1.16
SC-2L	2.8-4.3	220	272	288	1.52
SC-3L	2.6-4.1	203	205	269	1.40
Layer D					
SC-1L	4.2-7.0	237	263	360	2.08
SC-2L	4.3-6.3	235	267	354	2.04
SC-3L	4.1-5.6	205	176	138	1.29
Layer E					
SC-3L	4.1-9.5	185	197	198	0.92
Layer F					
SC-1L	7.0-9.4	203	211	229	1.32
SC-2L	6.3-9.4	207	218	234	1.37

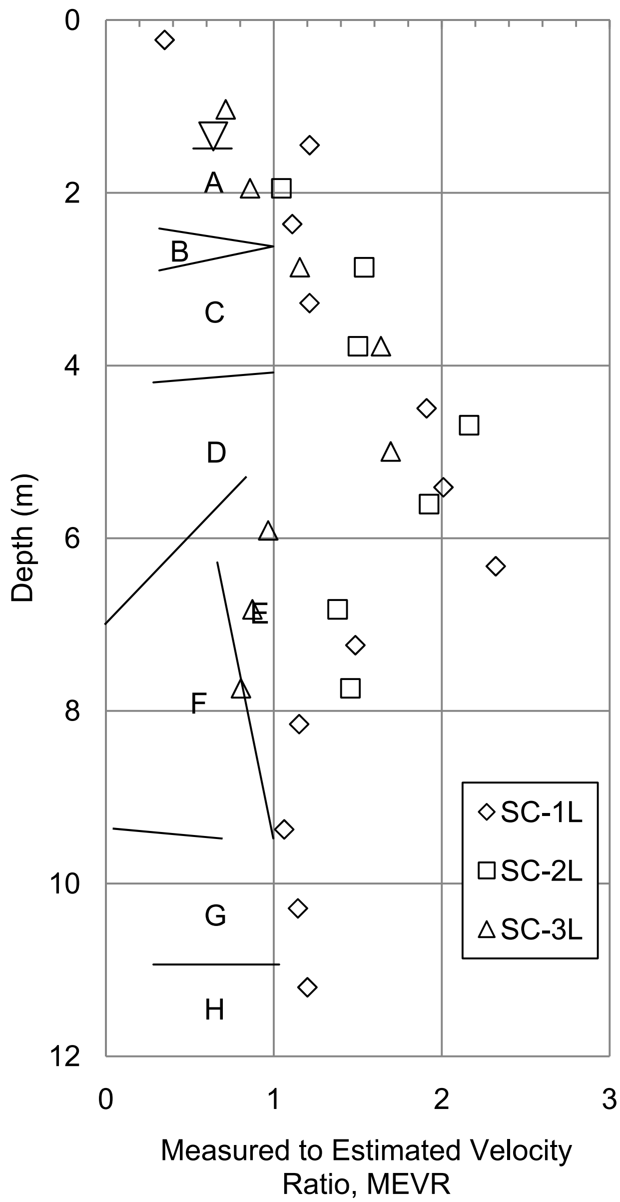

Figure 5.11 MEVR profile for the Lowcountry Sand and Gravel site using velocities obtained from seismic downhole-measured velocities and estimated velocities using equations proposed by Andrus et. al. (2004a).

5.5 Summary

The Lowcountry Sand & Gravel site has an estimated age of 450,000 years, based on the geologic map by McCartan et al. (1984). Three SCPTu's and one DMT were performed at the site. The SCPTu profiles indicate that the site is a fluvial deposit with soil types ranging from silty clay to coarse sand.

Seven distinct layers are identified in the top 12 m (39.4 ft) from the CPT and DMT investigations. Layer A is dense sand with an average tip resistance of 19.7 MPa. Layer B likely consists of more silty sand and exhibits lower cone tip resistances. The thickness and density of Layer C varies across the CPT cross-section, having the highest tip resistance in SC-1L and reduced tip resistance in the other two locations. Layer C is a medium dense sand to silty sand. Layer D consists of silty sand to clayey silt. Layer F is a silty sand to sand layer with reduced tip resistance and appears to be an overbank deposit, formed from seasonal flooding. Layer E is a sand with a high average tip resistance of 19.0 MPa. Finally, Layer G is a dense sand to silt.

Layers A and B both exhibit very high K_0, indicating high lateral stresses and/or stiffnesses. Layers D, F, G, and H exhibit K_0's above 1, but much lower than Layers A and B. Layer C is the only unit with an average K_0 below 1, suggesting that the horizontal stresses and/or stiffnesses are less than the vertical.

Shear wave velocities were measured at SC-1L, SC-2L, and SC-3L using the true-interval downhole method. The velocities were corrected and used to determine MEVRs for each test location. Figure 1.1 suggests that the mean expected MEVR for a 450,000 year-old soil is 1.40. The range of expected MEVRs is 1.57 to 1.23, these being the MEVR's that are one standard deviation above and below the mean MEVR of 1.40. Layers C and F were the only layers to have average MEVRs within this range. These layers are both clean to silty sands with average corrected tip resistances greater than 80 and less than 150. Layer D has an average MEVR of 1.80, well above the expected range. This may be a result of diagenetic processes. In addition, the use of V_{s1} estimating equations may be inappropriate here, as Layer D has significant fine-grained material and the equations are based on velocities in sand. Layers A and E both exhibit average MEVR's of less than 1.00. Both of these layers are sand layers with very high corrected tip resistances greater than 200. The reason for the low MEVR's in Layer A may be due to recent disturbance at the site or diagenetic processes.

From the analysis of the soil and stratigraphy, Layer C is identified as being the critical sand layer for liquefaction research because it is fairly thick and saturated, exhibits lower corrected tip resistance, and is close to the surface. Layer C's average MEVR of 1.36 will be used for liquefaction analysis in Chapter 6. The other layers identified at the site will be investigated in Chapter 6 for their liquefaction susceptibility only.

CHAPTER SIX

LIQUEFACTION PREDICTION

6.1 Introduction

To assess the liquefaction potential of a site, one needs to consider the condition of the soil and the likelihood and estimated strength of seismic activity. There are two terms that are used in liquefaction predictions: susceptibility and potential. Liquefaction susceptibility is determining whether a soil layer is capable of liquefying, no matter the size of the seismic event. Liquefaction potential is different in that it is used to determine whether a soil will liquefy given a specific earthquake loading. For this research, a susceptibility analysis is conducted first. Afterwards, the layer most likely to liquefy is selected for liquefaction potential analysis. Earthquake scenarios are determined for the analysis and then used to develop a set of CRR curves for determining liquefaction potential.

This chapter outlines the evaluation procedure and presents the related results for each of the three geotechnical experimentation sites.

6.2 Liquefaction Susceptibility

There are four general criteria that influence liquefaction susceptibility. The four criteria are history, geology, composition, and state (Kramer 1996, pp.

351-355). History is simply whether the soil has or has not liquefied in past events. If liquefaction has happened at the site in the past, then the site is more likely to experience it again in the future. The geology criteria include depositional environment and groundwater conditions. Sands deposited by low energy wind and water flows are often highly susceptible, for example. Soils above the groundwater table are considered non-susceptible. Composition involves properties such as soil type and gradation. Clayey soils are generally considered non-susceptible to liquefaction (Kramer 1996, p. 354). Finally, state criteria relate to in-situ properties of soils, density and stress. If a soil is too dense, it will not liquefy.

For this research, I_c and B_q are used to screen out layers that are too clay-rich to liquefy using a chart by Hayati and Andrus (2008a) based on modified criteria recommended by Robertson and Wride (1998). Figure 6.1a presents the CPT based susceptibility chart proposed by Hayati and Andrus (2008a) with data from the Hobcaw Borrow Pit site. This chart indicates that Layer A and Layer C are susceptible to liquefaction. These layers both consist of poorly graded sand with silt. Layer B is not susceptible because the layer had I_c's greater than 2.6, indicating that Layer B is too clay rich to liquefy.

Figure 6.1b presents the I_c-B_q chart proposed by Hayati and Andrus (2004a) with data from the Rest Area Ponds site. According to this chart, Layers A, B, C, and E are susceptible to liquefaction. Layers D, F, and G plot in the test required range or the non-susceptible region, suggesting low susceptibility.

The I_c-B_q chart proposed by Hayati and Andrus (2008a) is shown in Figure 6.1c. with data from the Lowcountry Sand & Gravel site. From this chart, it is seen that Layers A, C, and E are susceptible. Layers B, D, and F are non-susceptible.

6.3 Liquefaction Potential Procedure

There are three general steps to predicting liquefaction potential. The first step is to determine the earthquake loadings, which involves obtaining moment magnitudes (M_w) and peak ground accelerations (PGA). The second step is to calculate CSR's for the layer of interest using the determined earthquake loadings. The third step is to calibrate the CRR curves for 30% probability of liquefaction (P_L) and K_{DR}. After these three steps are complete, the CSR values are plotted on the CRR curves using the corresponding penetration resistance or shear wave velocity (i.e., $(N_1)_{60cs}$, q_{t1Ncs}, or V_{s1cs}). Points that plot above the curves indicate that the soil will liquefy at the given earthquake parameters.

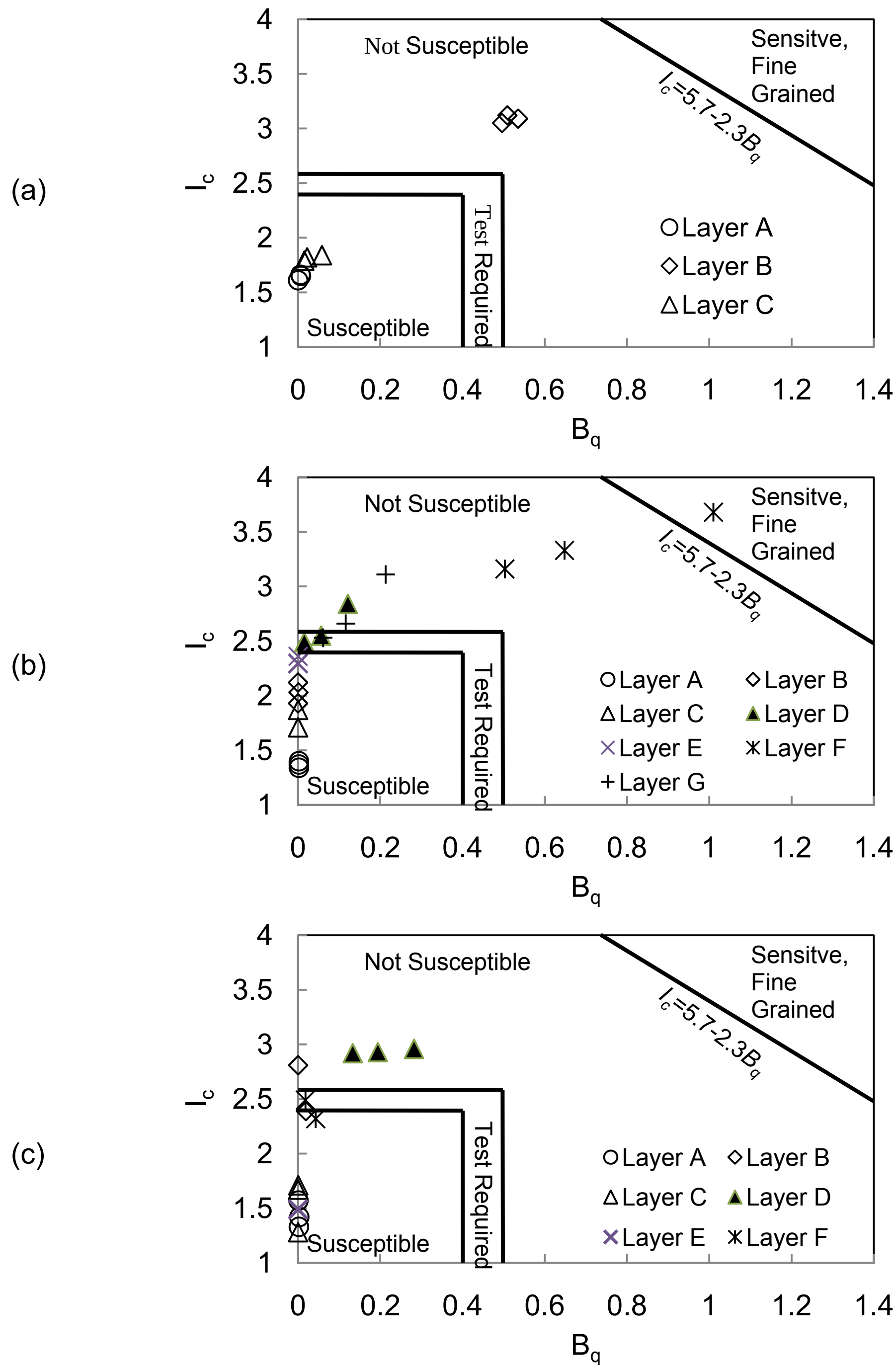

Figure 6.1 CPT-based liquefaction susceptibility chart by Hayati and Andrus (2008a) with data from the (a) Hobcaw Borrow Pit site (b) Rest Area Ponds site, and (c) Lowcountry Sand & Gravel site.

6.3.1 Earthquake Scenarios

Two earthquake scenarios were considered for the evaluation. The first earthquake scenario was taken from the 2008 USGS Earthquake Hazard Map for a 2% occurrence in 50 years (http://gldims.cr.usgs.gov/). The moment magnitudes were selected using the beta version of the 2008 interactive deaggregations from the USGS (http://eqint.cr.usgs.gov/deaggint/2008/). Table 6.1 presents the summary of parameters for this scenario.

The second earthquake scenario that will be considered is the 1886 earthquake. Two approaches are used to estimate the 1886 earthquake's PGAs for each site. First, the PGAs from the 2008 USGS 2% probability of exceedance in 50 years scenario (see Table 6.1) are scaled using a base value of PGA=0.26g for the Charleston peninsula in 1886 based on the model suggested by Chapman et al. (2006). A scaling factor of 0.36 was determined from comparing the PGA for the Charleston peninsula from Chapman's model and the USGS 2008 Hazard Map's predicted PGA. This scaling factor was applied to PGAs for the other sites to obtain PGAs for the 1886 earthquake. The second approach is picking off PGAs from the 1886 PGA map by Silva et al. (2003). For this study, the M_w value of 6.9 estimated by Heidari and Andrus (2010) is used for the 1886 earthquake. Then the two sets of PGA estimates for 1886 are compared with each other. The middle of the range between the scaled PGAs and the PGA's from Silva et al. (2003) was adopted as the PGA for each site. These values are presented in Table 6.1.

Table 6.1 Summary of earthquake scenarios for liquefaction potential analysis.

	2008 USGS 2% Probability of Exceedance in 50 years		1886 Charleston Earthquake		
			Scaled 2008 USGS PGA	Silva et al. (2003) PGA	Middle Range Value PGA Adopted for this Study
Site	PGA (%g)	M_w	(%g)	(%g)	(%g)
Hobcaw Borrow Pit	0.4	7.4	0.14	0.17	0.15
Walterboro Rest Area Ponds	0.37	7.4	0.13	0.26	0.2
Lowcountry Sand & Gravel	0.45	7.4	0.16	0.30	0.23
Charleston	0.72	7.4	0.26	0.3	-

6.3.2 CSR Calculation

In order to determine the liquefaction potential, CSR values must be determined for each point. CSR for a M_w of 7.5 can be calculated by the following equation (modified from Seed & Idriss 1971):

$$CSR=0.65(a_{max}/g)*(\sigma_v/\sigma'_v)r_d/MSF \qquad 6.1$$

where r_d is the stress reduction coefficient and MSF is the magnitude scaling factor. r_d is calculated using the following relationship suggested by Liao and Whitman (1986):

$$r_d = 1.0\text{-}0.00765z,\ z \leq 9.15\ \text{m} \qquad 6.2$$

$$r_d = 1.174\text{-}0.0267z,\ 9.15 < z \leq 23\ \text{m} \qquad 6.3$$

where z is the depth below the ground surface. The magnitude scaling factor is used to adjust a given M_w to a normalized M_w of 7.5. The more conservative relationship recommended by Youd et al. (2001) is used and can be expressed as:

$$(M_w/7.5)^{-2.56} \qquad 6.4$$

6.3.3 CRR Curves

There are several CRR curves that have been proposed to determine liquefaction potential based on either V_{s1cs}, $(N_1)_{60cs}$, and q_{t1ncs}. The following paragraphs present the CRR curves for M_w=7.5 used in the liquefaction potential analysis, along with a brief discussion on attempts to calibrate them.

One CRR curve was used for analysis with the values of V_{s1cs}. This curve was developed by Andrus and Stokoe (2000) and their equation is presented below.

$$CRR=0.022[V_{s1cs}/(100*MEVR)]^2+2.8[1/(215-V_{s1cs}/MEVR)-1/215] \qquad 6.5$$

This equation was characterized by Juang et al. (2002) as a 26% P_L curve. Juang et al. (2002) proposed the following calibration equation for Equation 6.5.

$$P_L=1/[1+(FS/0.73)^{3.4}] \qquad 6.6$$

where FS is the factor of safety used to adjust the CRR curve.

Four SPT-based CRR curves were used for the liquefaction potential analysis. The first SPT-based curve was developed by Idriss and Boulanger (2004) and expressed as:

$$\ln (CRR) = (N_1)_{60cs}/14.1+[(N_1)_{60cs}/126]^2-[(N_1)_{60cs}/23.6]^3+[(N_1)_{60cs}/25.4]^4-2.8 \qquad 6.7$$

This curve has been characterized as a 30% P_L curve and is only corrected using K_{DR} as shown in Equation 1.1. The second SPT-based curve was proposed by Cetin et al. (2004). It is characterized as a 30% P_L curve and expressed as:

$$\ln (CRR)=[(N_1)_{60cs}*(1-0.004FC)-29.53*\ln(M_w)-3.70*\ln(\sigma'_v/P_a)$$
$$+0.05*FC+16.85+2.70*\phi^{-1}(P_L)]/13.32 \qquad 6.8$$

where $\phi^{-1}(P_L)$ is the inverse of the standard cumulative normal distribution. It is entered into Microsoft Excel spreadsheets as "NORMINV(P_L, 0.1)." This curve is adjusted using K_{DR}. The third SPT-based curve is presented in Youd et al. (2001) and is expressed below:

$$CRR=1/(34-(N_1)_{60cs} + (N_1)_{60cs} /135+50/[10*(N_1)_{60cs}+45]^2-1/200 \qquad 6.9$$

This curve is also characterized as a 30% P_L curve (Juang et al. 2002) and is corrected using K_{DR}. The final SPT-based curve is one used by Andrus et al. (2009). This curve takes the curve proposed by Andrus and Stokoe (2000) (see Equation 6.5) and uses the corrected SPT blowcount $(N_1)_{60cs}$ to estimate a velocity using Equation 1.3 for use in the curve proposed by Andrus and Stokoe (2000). The equation is a shear wave velocity based equation, which Juang et al. (2002) characterized as a 26% P_L curve. Therefore, the curve must be adjusted from a P_L of 26% to a P_L of 30% using Equation 6.6. No additional age correction is necessary.

Four CPT-based CRR equations were used for liquefaction potential analysis. The first CPT-based curve is by Idriss and Boulanger (2004). This curve is plotted without any adjustment other than K_{DR} and is expressed as the following:

$$\ln (CRR) = (q_{t1ncs}/540)+(q_{t1ncs}/67)^2-(q_{t1ncs}/80)^3+(q_{t1ncs}/114)^4-3 \qquad 6.10$$

The second CPT-based equation used was proposed by Robertson and Wride (1998). It is characterized as a 26% P_L curve, so it is corrected using a relationship from Juang et al. (2002). These equations are expressed as the following:

$$P_L=1/(1+FS^{3.3}) \quad 6.11$$

$$CRR=0.833*(q_{t1ncs}/1000) + 0.05,\ q_{t1ncs}<50 \quad 6.12$$

$$CRR=93*(q_{t1ncs}/1000)^3 + 0.08,\ 50\le q_{t1ncs}<160 \quad 6.13$$

Robertson and Wride's (1998) curve is also corrected for age using K_{DR}. The third CPT-based CRR curve is from Moss et al. (2006). This equation is characterized as a 30% P_L curve and requires an age correction. The curve is expressed as the following:

$$\ln(CRR)=[(q_{t1ncs}\ 0.10135)^{1.045}+ q_{t1ncs}\ 0.10135*0.11R_f +0.001R_f +c(1+0.85R_f)-0.848*\ln(7.5)-0.002\ln(101.35)-20.923+1.632\ \phi^{-1}(P_L)]/7.177 \quad 6.14$$

where q_{t1ncs} is the corrected tip resistance in units of MPa, 0.10135 is the conversion factor used to adjust the tip resistance to a dimensionless normalized tip resistance, R_f is the friction ratio assumed to be 0.5%, and c is the normalization exponent. This exponent is calculated using the following equations.

$$c = f_1\left(\frac{R_f}{f_3}\right)^{f_2} \quad 6.15$$

$$f_1=0.78(q_{t1ncs}*0.10135)^{-0.33} \quad 6.16$$

$$f_2= 0.32*-[q_{t1ncs}*0.10135]^{-0.35}-0.49 \quad 6.17$$

$$f_3= abs[\log[10+(q_{t1ncs}*0.10135)]^{1.21}] \quad 6.18$$

The final CPT-based curve is another curve proposed by Andrus et al. (2009) that involves using tip resistance to estimate shear wave velocity for use in the CRR curve proposed by Andrus and Stokoe (2000) (see equation 6.5). Again, no additional age correction is required and the curve must be adjusted from a P_L of 26% to a P_L of 30% using Equation 6.6.

6.4 Liquefaction Potential Analysis

Average values of q_{t1ncs}, $(N_1)_{60cs}$, and V_{s1cs} are presented in various summary tables in Chapters 3, 4, and 5 for each site. CSR values were determined for each of these average properties using the procedure mentioned earlier. They were plotted against the calibrated CRR curves to assess the liquefaction potential of the layer of primary interest. The potential for each site is summarized in the following sections.

6.4.1 Hobcaw Borrow Pit

Since Layer A exhibits lower penetration resistance than Layer C and is closer to the ground surface, Layer A below the groundwater table will be considered in the liquefaction potential analysis. Figures 6.2, 6.3, and 6.4 present the liquefaction potential charts for shear wave velocity testing, SPT, and CPT for Layer A at the Hobcaw Borrow Pit site. These are modified from the CRR charts presented by Geiger et al. (2010). It can be seen that Layer A most likely did not liquefy or was marginal during the 1886 earthquake, but will likely liquefy during the earthquake predicted by the 2008 USGS Hazard Maps. Layer A has an average FS of 1.53 for the 1886 earthquake and 0.49 for the 2% in 50 years event.

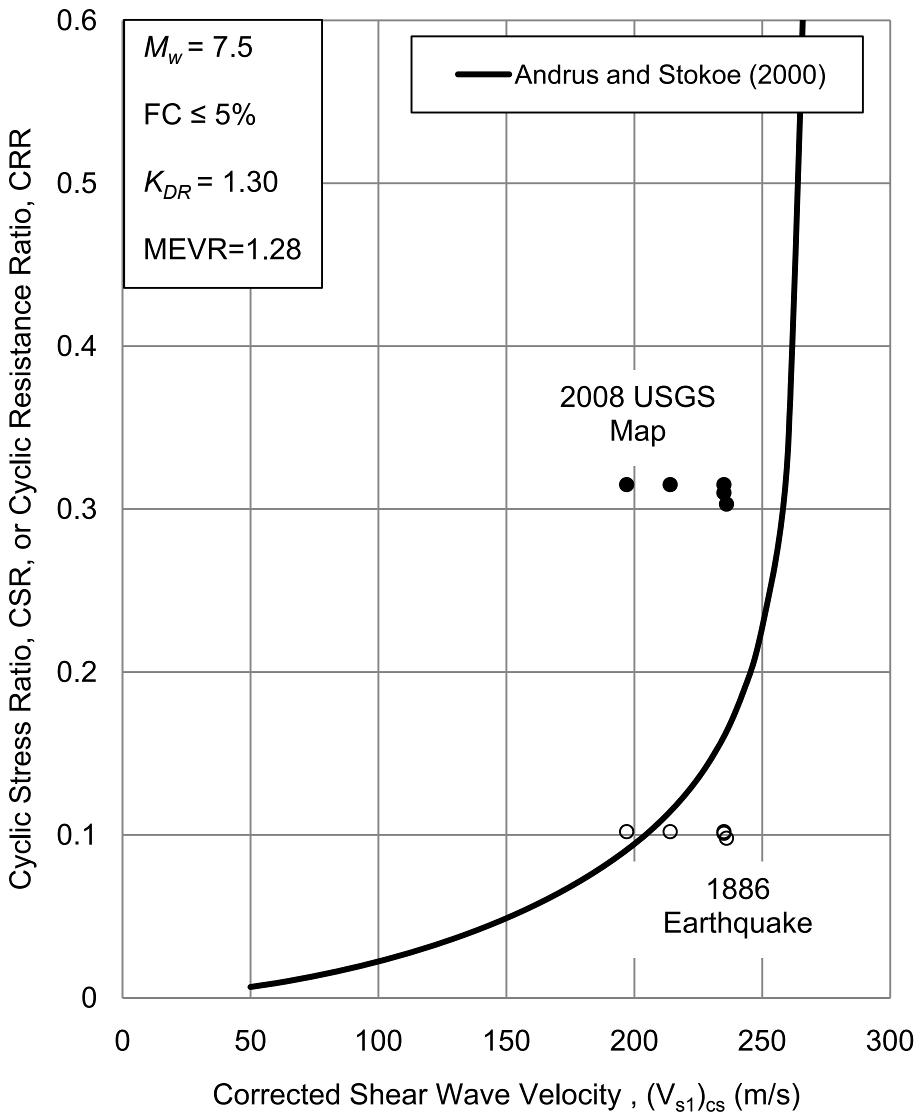

Figure 6.2 Shear wave velocity CRR curve corrected for age and clean sands with data points from Layer A at the Hobcaw Borrow Pit site (Modified from Geiger et al. 2010).

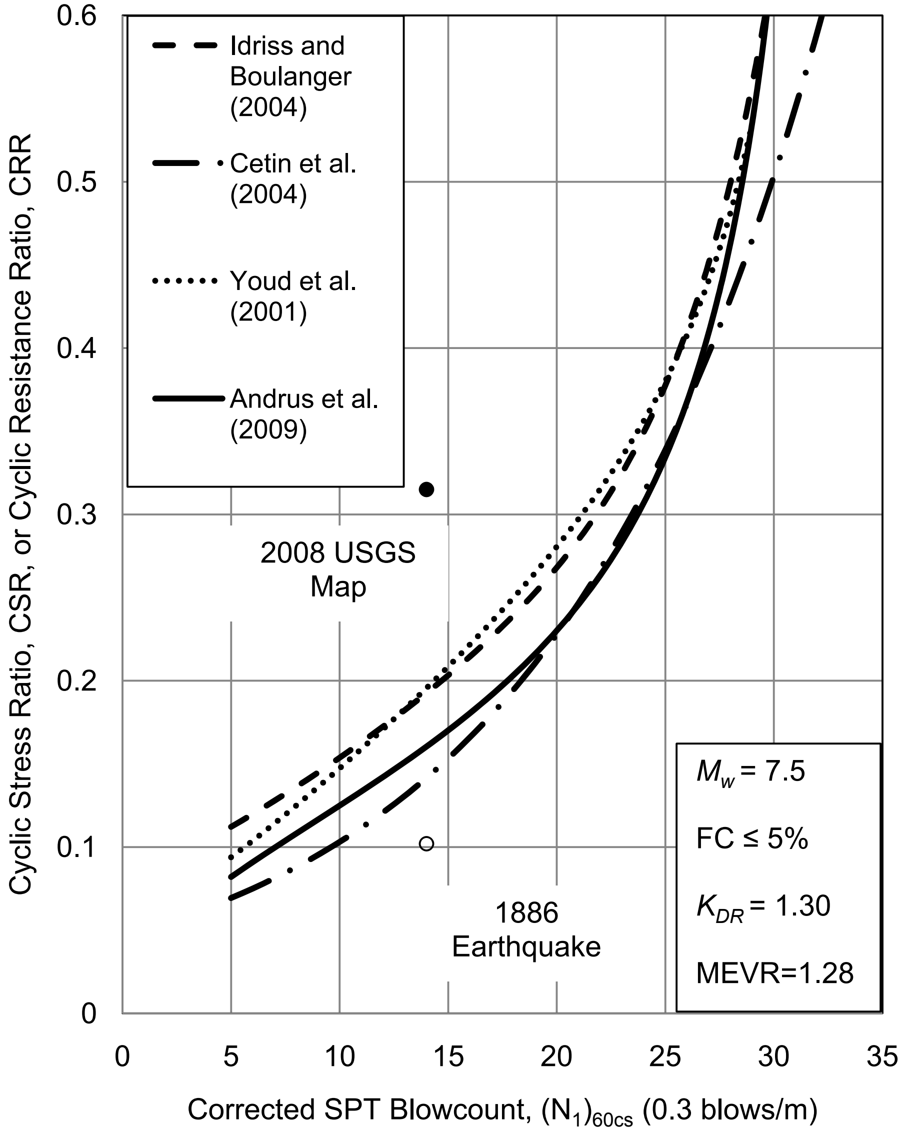

Figure 6.3 SPT blowcount CRR curves corrected for clean sands and age with data points from Layer A at the Hobcaw Borrow Pit site (Modified from Geiger et al. 2010).

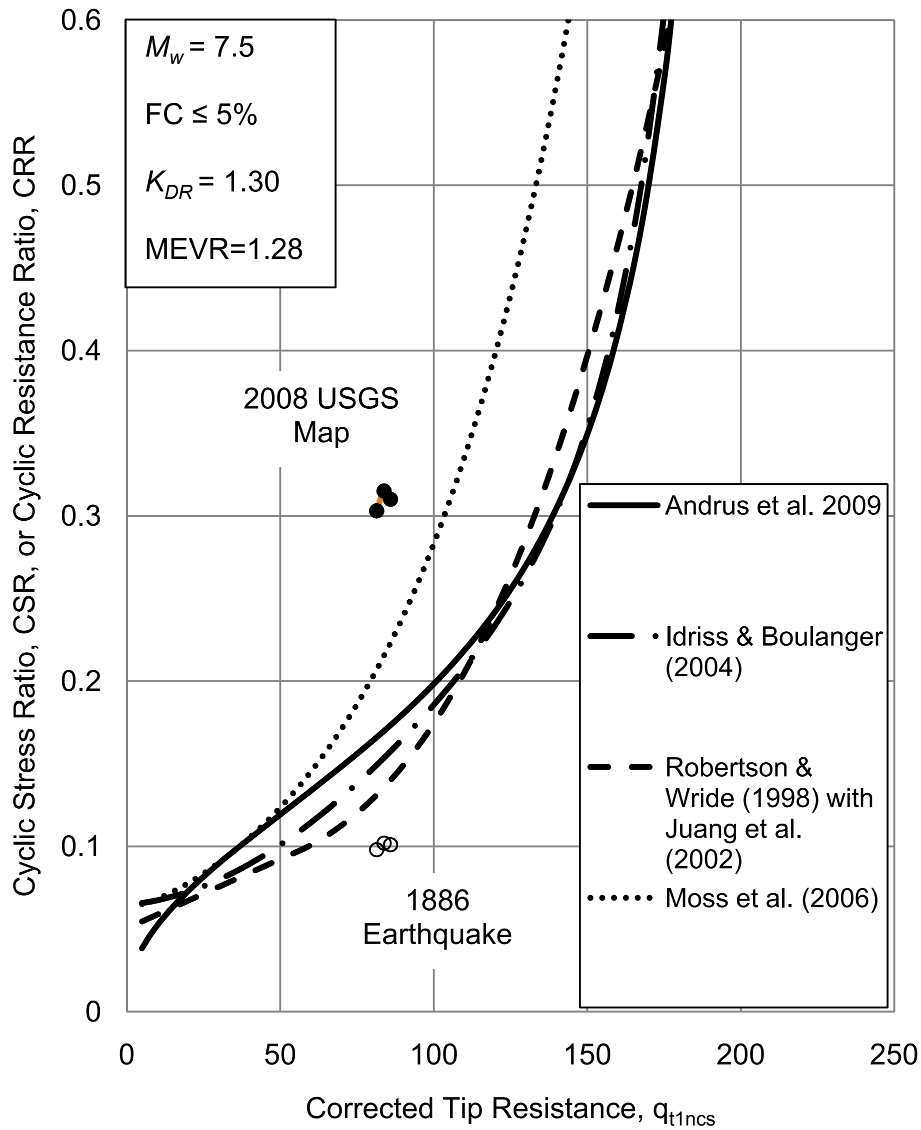

Figure 6.4 CPT tip resistance CRR curves corrected for clean sands and age with data points from Layer A at the Hobcaw Borrow Pit site (Modified from Geiger et al. 2010).

6.4.2 Rest Area Ponds

Of the susceptible layers, Layer C is the layer closest to the ground surface that is saturated and has lower penetration resistance. For these reasons, Layer C will be considered in the liquefaction potential analysis. Figures 6.5, 6.6, and 6.7 present the liquefaction potential charts for V_{s1cs}, $(N_1)_{60cs}$, and q_{t1Ncs} for Layer C at the Rest Area Ponds site. Most of the points in these charts indicate that Layer C did not liquefy or was marginal during the 1886 earthquake. The average FS for the 1886 event and the 2% in 50 years event are 1.27 and 0.59, respectively. This does not include the CRR curve by Moss et al. (2006) because this curve is much higher than the other CPR-based curves. It provides a mixed result for liquefaction potential in this event, but the other curves support the conclusion that liquefaction will occur in the future earthquake. Figure 6.6 does suggest the possibility of marginal liquefaction during the 1886 earthquake, but the other points support the conclusion that liquefaction did not occur in 1886. It can also be seen that Layer C will likely liquefy during the earthquake estimated by the 2008 USGS Hazard Maps.

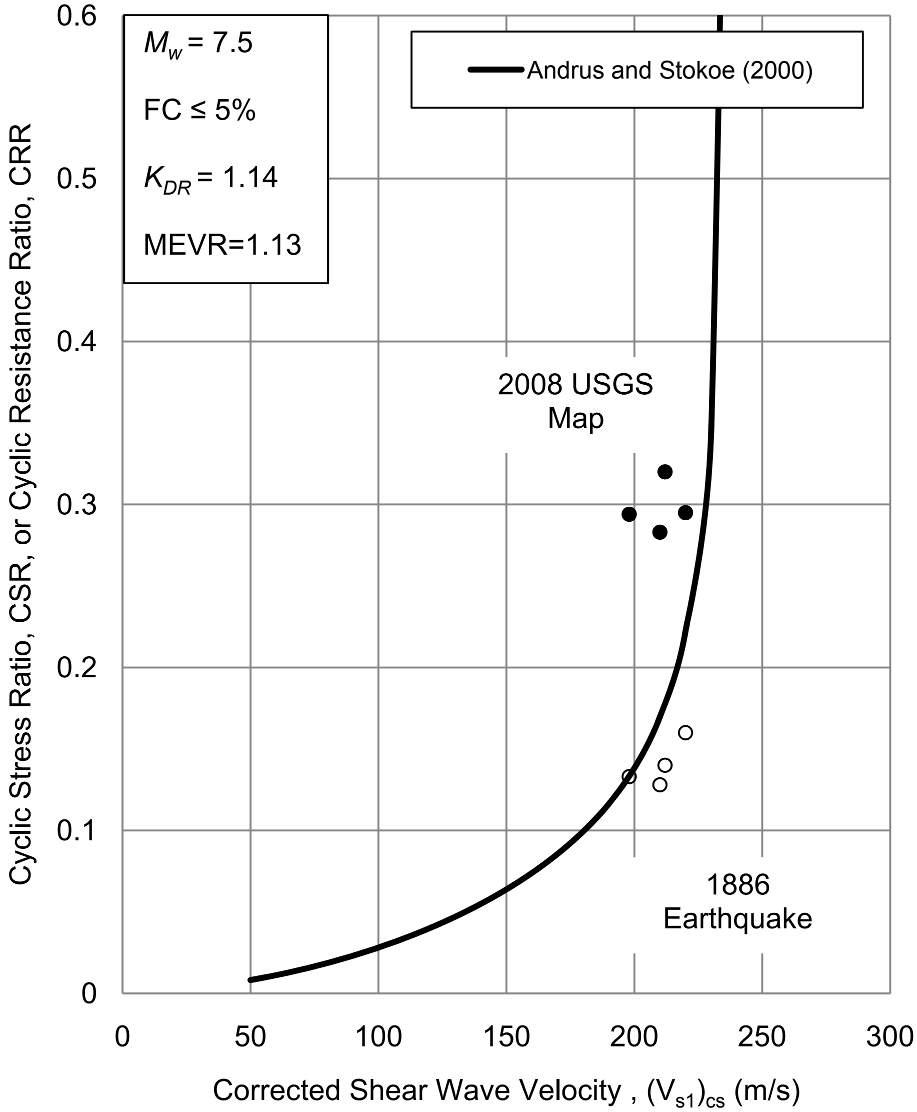

Figure 6.5 Shear wave velocity CRR curve corrected for age and clean sands with data points from Layer C at the Rest Area Ponds site.

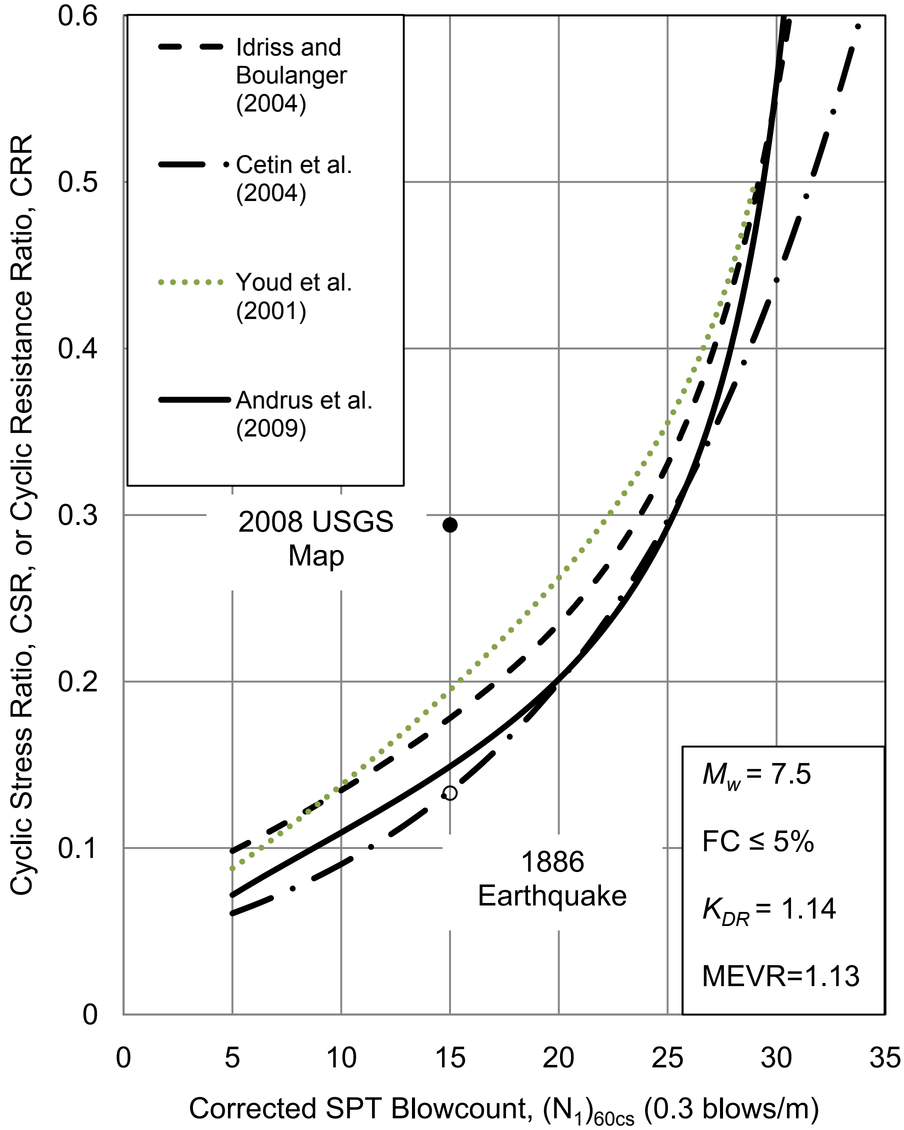

Figure 6.6 SPT blowcount CRR curves corrected for clean sands and age with data points from Layer C at the Rest Area Ponds site.

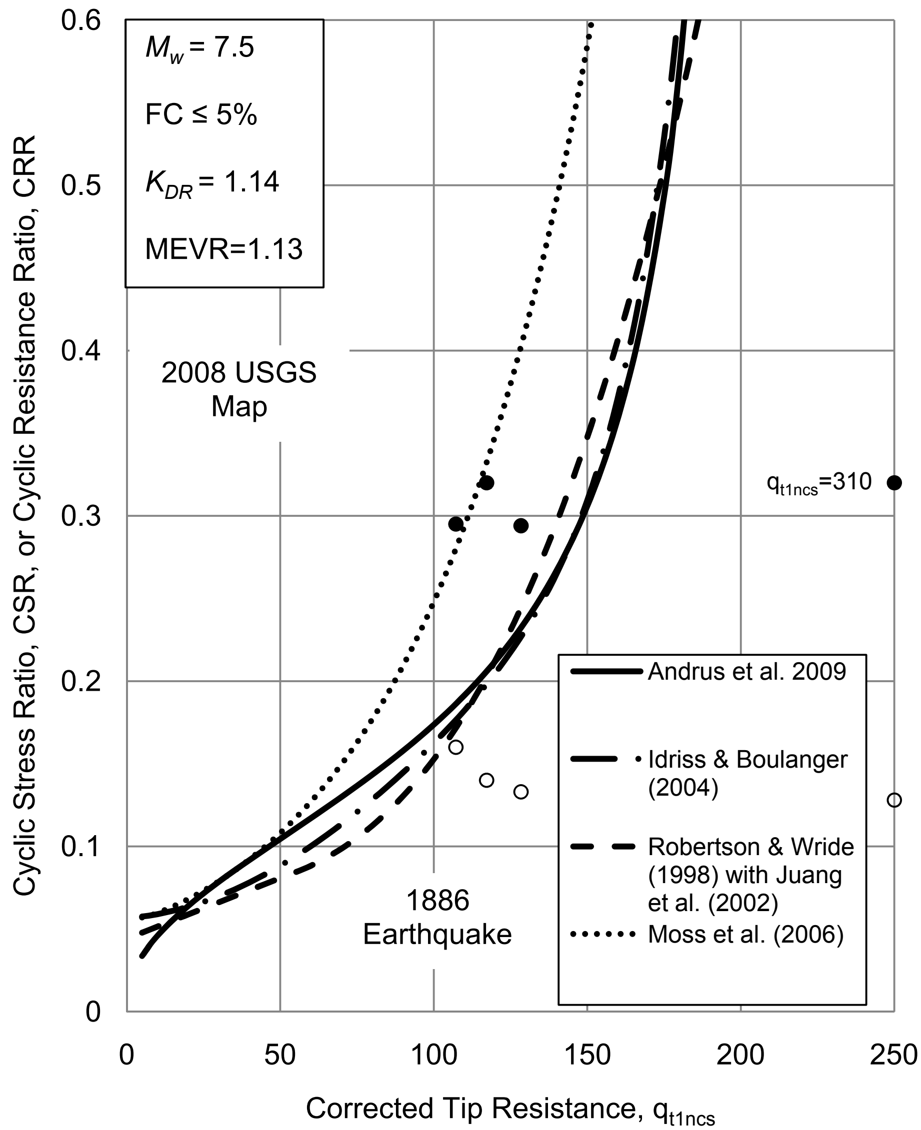

Figure 6.7 CPT tip resistance CRR curves corrected for clean sands and age with data points from Layer C at the Rest Area Ponds site.

6.4.3 Lowcountry Sand & Gravel

Of all the susceptible layers, Layer C is below the water table, is close to the surface, and exhibits lower tip resistances than other susceptible layers. For these reasons, Layer C is the critical sand layer to be analyzed for liquefaction potential.

Figures 6.8 and 6.9 present the liquefaction potential charts for V_{s1cs} and q_{t1Ncs} for Layer C at the Lowcountry Sand & Gravel site. These figures suggest that Layer C did not liquefy or was marginal in the 1886 earthquake. In addition, Layer C near cone soundings SC-2L and SC-3L indicates that liquefaction would occur during the estimated earthquake predicted by the 2008 USGS Hazard Maps. Average factors of safety for the 1886 event and the 2% in 50 years event are 1.59 and 0.67, respectively. However, some of these points indicate only marginal liquefaction. The portion of Layer C found in SC-1L was added to the charts to show that it will not liquefy due to its very high tip resistance.

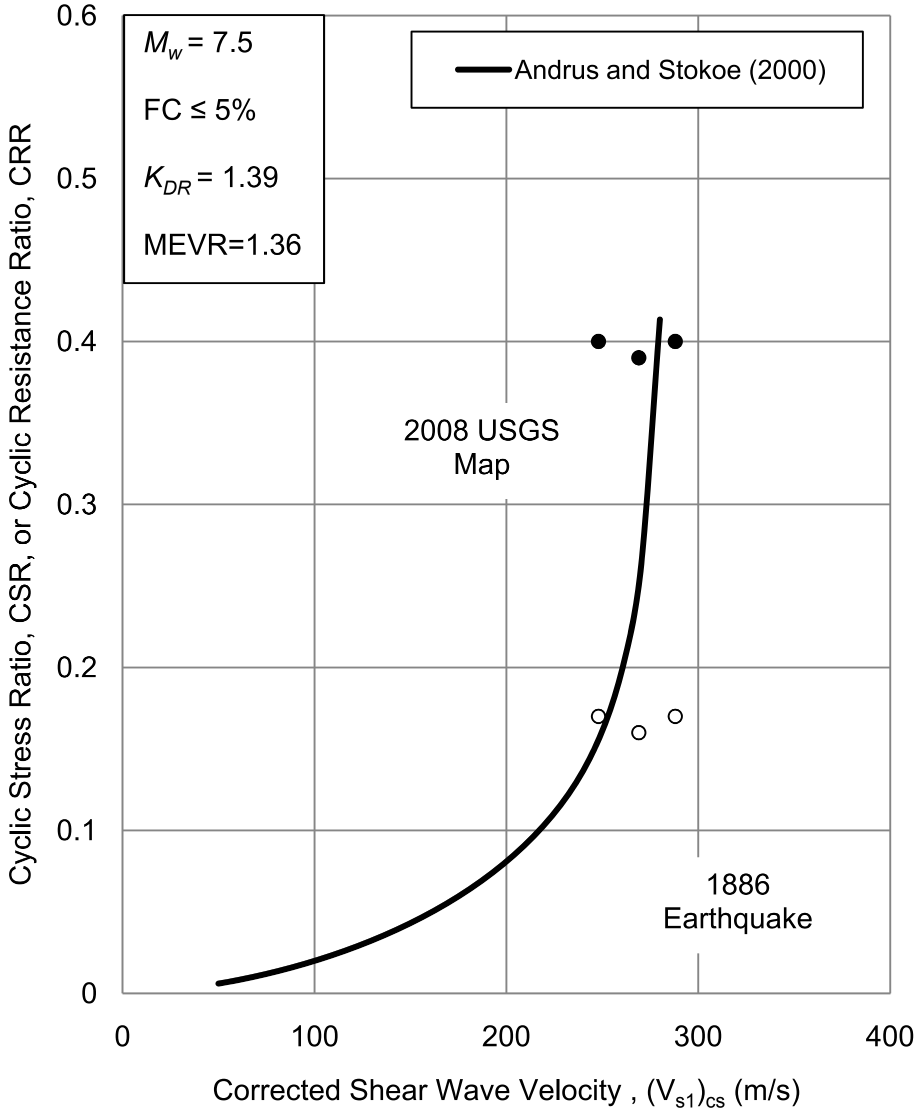

Figure 6.8 Shear wave velocity CRR curve corrected for age and clean sands with data points from Layer C at the Lowcountry Sand & Gravel site.

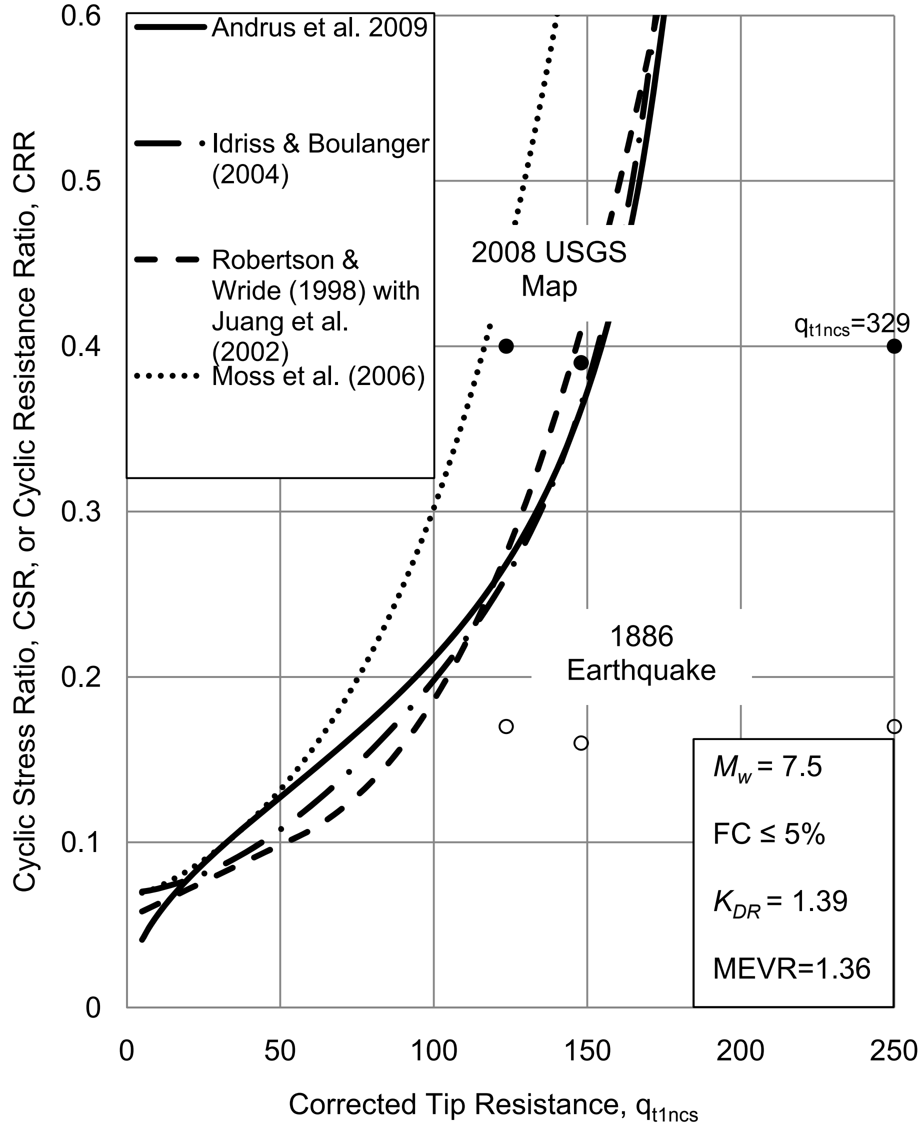

Figure 6.9 CPT tip resistance CRR curves corrected for clean sands and age with data points from Layer C at the Lowcountry Sand & Gravel site.

6.5 Summary

The surface layers at the Hobcaw Borrow Pit, Rest Area Ponds, and Lowcountry Sand & Gravel were screened for liquefaction susceptibility using the I_c-B_q chart created by Hayati and Andrus (2008a) based on modified criteria recommended by Robertson and Wride (1998). After identifying the susceptible layers, the critical sand layer for liquefaction was determined and used for liquefaction analysis.

Two earthquake scenarios were used in the liquefaction potential analysis. The first is the 2008 USGS Hazard Map for 2% probability of exceedance in 50 years. The M_w for this scenario was determined using the beta version of the USGS 2008 interactive deaggregation application. The second scenario used the 2008 USGS PGA's for 2% in 50 years and scaled them to a PGA of 0.26 for the Charleston peninsula based on the model proposed by Chapman et al. (2006). In addition, these scaled values were compared with PGA's picked off the map created by Silva et al. (2003) for a 1886 scenario earthquake. The magnitude of the 1886 earthquake was assumed to be 6.9, as was done by Heidari and Andrus (2010).

A total of nine CRR curves were used in the liquefaction potential analysis: one Vs-based curve, four SPT-based curves, and four CPT-based curves. Each curve was calibrated for P_L as necessary and also adjusted for age using the calculated MEVR for the critical sand layers.

The liquefaction evaluation was completed after plotting the critical sand layers on the CRR curves. The results are indicated in Figures 6.2 to 6.9. Each of the three sites is believed to have not liquefied during the 1886 earthquake. The liquefaction potential analysis supports this belief for each site. The liquefaction analysis also indicates that the sites would liquefy during the 2008 USGS predicted earthquake for 2% probability of exceedance in 50 years, suggesting that liquefaction might have occurred at these sites might have occurred at these sites during the past 100,000 or so years. Overall, these results support the use of shear wave velocity-based and penetration-based CRR curves being used together to perform liquefaction analyses.

CHAPTER SEVEN

SUMMARY AND CONCLUSIONS

Geotechnical investigations were conducted at three sites located in the South Carolina Coastal Plain that were believed to have not liquefied during the 1886 Charleston earthquake. These sites are the Hobcaw Borrow Pit located near Georgetown and the Rest Area Ponds and Lowcountry Sand & Gravel sites located near Walterboro. Testing at the sites included SCPTu, SPT, DMT, seismic crosshole, and fixed piston sampling. The overall goal of the investigations at each site was to characterize the liquefaction potential of the near-surface critical sand layers. The results of the liquefaction potential analysis are summarized in Table 7.1.

Near-surface sands at the Hobcaw Borrow Pit site were estimated to have a geologic age of 200,000 years by May (1978) and McCartan et al. (1984). Results of SCPTus and a DMT conducted at the Hobcaw Borrow Pit site were presented by Boller (2008). Additional testing conducted for this study included SPTs, fixed piston sampling, seismic crosshole, and laboratory testing. The portion of Layer A below the groundwater table was identified as the critical sand layer at the site, ranging in depth from 2.4 m to 8.9 m. This layer has an average MEVR of 1.28, which is in the expected range as seen in Figure 7.1. Using nine CRR curves, it was determined that Layer A did not liquefy during the 1886 event and it would experience moderate liquefaction during the earthquake predicted by the USGS 2008 Hazard Maps for 2% probability of exceedance in 50 years. The factors of safety with respect to the 30% probability of liquefaction curves are presented in Table 7.1. These results are similar to the preliminary results presented in Geiger et al. (2010).

Table 7.1 Summary of liquefaction evaluation for critical sand layers at the three investigation sites.

Site	Critical Layer	Critical Layer Depth (m)	Soil Type	Average MEVR	Average FS Based on Motion for 2% Probability of Exceedance in 50years and P_L=30%	Average FS Based on 1886 Earthquake and P_L=30%
Hobcaw Borrow Pit	A (below ground-water table)	2.4-8.9	Poorly graded sand with silt	1.28	0.49	1.53
Walterboro Rest Area Ponds	C	2.5-6.2	Poorly graded sand with silt	1.13	0.59	1.27
Walterboro Lowcountry Sand & Gravel	C	2.6-4.3	Sand to Silty Sand	1.36	0.67	1.59

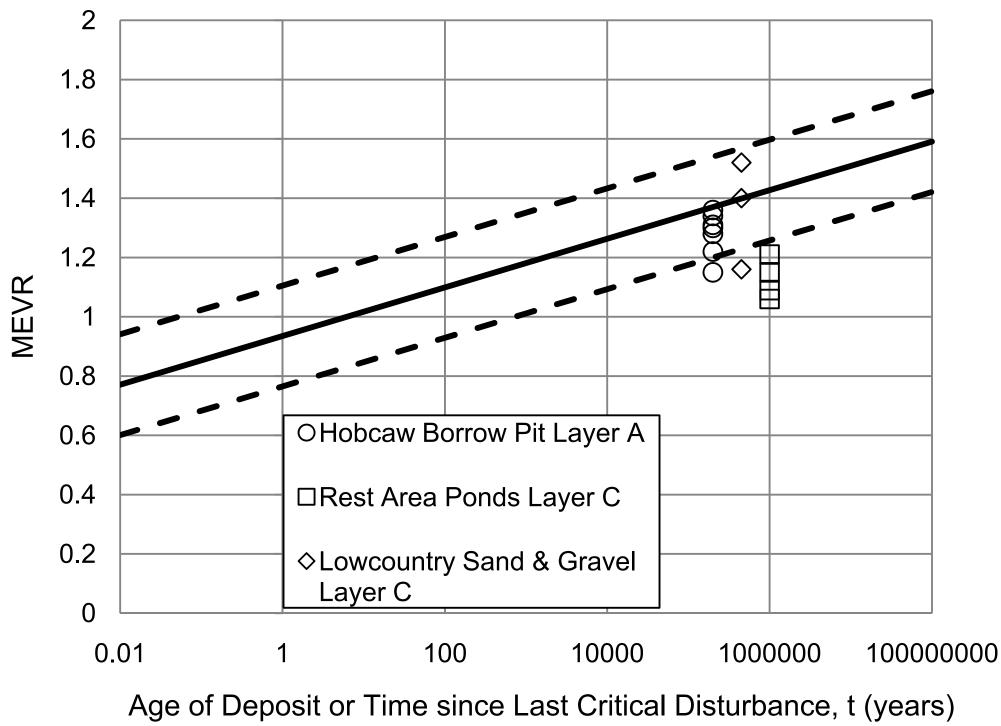

Figure 7.1 Relationship between MEVR and time since initial deposition or critical disturbance by Andrus et al. (2009) based on estimating equations by Andrus et al. (2004a) with results from the critical sand layers at the three investigation sites.

Near-surface soils at the Walterboro Rest Area Ponds site were estimated to be at least 1,000,000 years old based on a map by McCartan et al. (1984). Testing conducted at this site included three SCPTu soundings, one DMT, one SPT borehole, fixed piston sampling, and laboratory testing. Seismic crosshole testing conducted at this site will be presented in a later report. Layer C was identified as the critical sand layer at the Rest Area Ponds site. This layer has an average MEVR of 1.13, which is lower than the expected range as seen in Figure 7.1. Possible reasons for this low MEVR include horizontal variation in the soil, possible disturbance during a previous earthquake, or less than typical diagenetic processes. Based on nine CRR curves, it was determined that Layer C likely did not liquefy in 1886. It was also shown that liquefaction will likely occur in parts of Layer C in an earthquake equivalent to the 2008 USGS 2% probability of exceedance in 50 years event.

Near-surface sands at the Lowcountry Sand & Gravel site have an age of approximately 450,000 years, as indicated on the map by McCartan et al. (1984). McCartan et al. (1984) also indicated this site to be a river deposit. Investigations at this site only consisted of three SCPTu soundings and one DMT profile. Layer C was identified as the critical sand layer and has an average MEVR of 1.36, which is within the expected range shown in Figure 7.1. Five CRR curves were used to analyze the liquefaction potential of the site. It was determined that Layer C did not liquefy during the 1886 earthquake, and may only experience marginal liquefaction during an earthquake similar to the 2008 USGS 2% probability of exceedance in 50 years event. For most of Layer C at SC-1L, cone tip resistances indicated densities too great for liquefaction to occur.

The results of this study support the use of shear wave velocity-based and penetration resistance-based CRR curves together in conducting a liquefaction potential analysis. When corrections were made for age/cementation, all three methods all gave similar results. In addition, the study supports the use of MEVR as an indicator of age and cementation for liquefaction potential analysis.

For future study, it is recommended that MEVR be investigated for relationships in high density soils, soils with significant fine-grained materials, and non-saturated regions (specifically above the groundwater table). The critical sand layers at each site are close enough to the ground surface to provide favorable conditions for future testing with a vibrating truck to further improve liquefaction evaluation procedures.

APPENDIX A
SUMMARY OF DATA FROM THE HOBCAW BORROW PIT SITE

Table A.1 Soil index properties from samples collected in borings B-1 and B-3 at the Hobcaw Borrow Pit site.

				Percent Retained												
				Gravel (mm)		Sand (mm)										
Depth (ft)	C_u	C_c	D_{50}	#4	#10	#20	#40	#60	#80	#100	#200	% Fines	LL	PL	w(%)	Soil Type
B-1																
0-1.5	1.83	1.37	0.21	0	0.14	0.42	4.68	28.09	40.31	12.34	8.59	5.43	np		-	SP-SM
	2.30	1.57	0.21	0	0.02	0.30	5.35	29.13	38.89	11.75	7.57	6.99	np		-	SP-SM
3.5-5.0	1.77	1.23	0.22	0	0.00	0.28	5.17	29.77	41.44	12.73	5.69	4.92	np		-	SP
6-7.5	2.10	1.38	0.19	0	0.00	0.30	1.53	13.75	46.50	21.55	8.93	7.44	np		-	SP-SM
8.5-10	1.67	1.20	0.19	0	0.02	0.11	1.04	15.58	44.65	23.36	10.22	5.02	np		-	SP-SM
11-12.5	2.63	1.72	0.19	0	0.20	3.42	10.04	12.83	32.93	21.64	10.18	8.76	np		-	SP-SM
13.5-15	2.29	0.73	0.31	0	0.60	13.08	23.49	23.95	25.64	5.93	2.04	5.27	np		-	SP-SM
16-17.5	1.88	0.89	0.28	0	0.46	7.96	17.71	32.27	27.14	7.92	3.24	3.30	np		-	SP
18.5-20	107.5	23.3	0.32	0.26	2.74	16.25	21.29	18.20	17.00	5.69	3.15	15.42	np		-	SM
21-22.5	1.4	0.92	0.2	0	0.00	0.90	1.22	9.86	56.91	22.13	5.11	3.87	np		-	SP
23.5-25	1.75	0.98	0.24	0	0.75	6.76	12.13	29.87	36.19	8.11	2.46	3.73	np		-	SP
26-27.5	1.81	1.04	0.25	0	0.75	7.09	12.64	31.07	36.74	8.75	0.51	2.45	np		-	SP
28.5-30	133.3	0.36	0.083	0	0.10	0.85	1.86	3.71	11.93	16.05	18.96	46.54	34.2	21.5	42	SC
	63.3	29.65	0.17	0	0.36	1.69	2.62	6.11	33.02	24.71	14.11	17.38	<24	22.3	32	SM
	2.5	1.98	0.16	0	0.01	0.65	0.51	2.29	38.16	30.90	17.30	10.18	np		34	SP-SM
31-32.5	2.5	1.51	0.16	0	0.23	0.60	0.76	2.71	28.39	35.42	20.71	11.18	np		31	SP-SM
33.5-35	2.18	1.75	0.18	0	0.03	0.24	0.71	8.63	42.24	26.79	14.23	7.13	np		28	SP-SM
36-37.5	2.15	1.74	0.19	0	0	0.09	0.37	3.41	50.75	26	13.27	6.11	np		-	SP-SM
B-3 Fixed Piston Sampler																
28.5	-	-	-	-	-	-	-	-	-	-	-	62.9	90	52	48.7	MH
29	-	-	-	-	-	-	-	-	-	-	-	77.7	88	42	45.7	MH

[a] C_u=Coefficient of Uniformity.

[b] C_c=Coefficient of Gradation.

[c] D_{50}=Median grain size.

[d] LL=Liquid Limit water content (%) ASTM D 4318.

[e] PL=Plastic Limit water content (%) ASTM D 4318, np=non-plastic.

[f] Moisture content.

[g] Soil type based on United Soil Classification System ASTM D 2487.

Table A.2 Hydrometer test results from samples collected in B-1 at the Hobcaw Borrow Pit site.

Depth:	18.5-20 ft	Depth:	28.5-29 ft	Depth:	29-29.5 ft
Particle Size (mm)	Percent Finer	Particle Size (mm)	Percent Finer	Particle Size (mm)	Percent Finer
0.077	15.7	0.071	44.4	0.071	16.7
0.055	15.3	0.050	44.4	0.050	16.7
0.039	15.3	0.036	43.4	0.036	16.3
0.028	14.9	0.025	42.5	0.026	16.0
0.020	14.5	0.019	39.8	0.018	15.3
0.014	13.7	0.013	37.9	0.013	14.2
0.010	12.9	0.010	34.2	0.010	13.6
0.008	11.3	0.007	32.4	0.007	12.5
0.005	10.6	0.005	27.8	0.005	11.5
0.004	10.2	0.004	24.1	0.004	10.5
0.003	9.8	0.003	20.4	0.003	9.1
0.001	9.0	0.001	13.0	0.001	6.3
0.001	8.6	0.001	9.4	0.001	5.0

Figure A.1 Boring log for B-1 at the Hobcaw Borrow Pit site.

Site Name: Hobcaw Barony Borrow Pit		**Drilling Contractor:** S&ME, Inc.	**Drill Rig Type:** CME 550X, mud rotary
Location: Georgetown, SC	**SPT Borehole** B-1	**Hammer Type:** Automatic Trip	**Bit Diameter:** 4.5 inches
Date of Drilling: Aug. 5-6th, 2008		**Hammer Weight:** 140lb	**Total Depth of Boring:** 37.5ft
WOH=Weight of Hammer	**GWT at 1/18/10:** 7.5ft	**GWT at 8/6/08:** 8.6ft	**GWT at 11/2/08:** 6.7ft

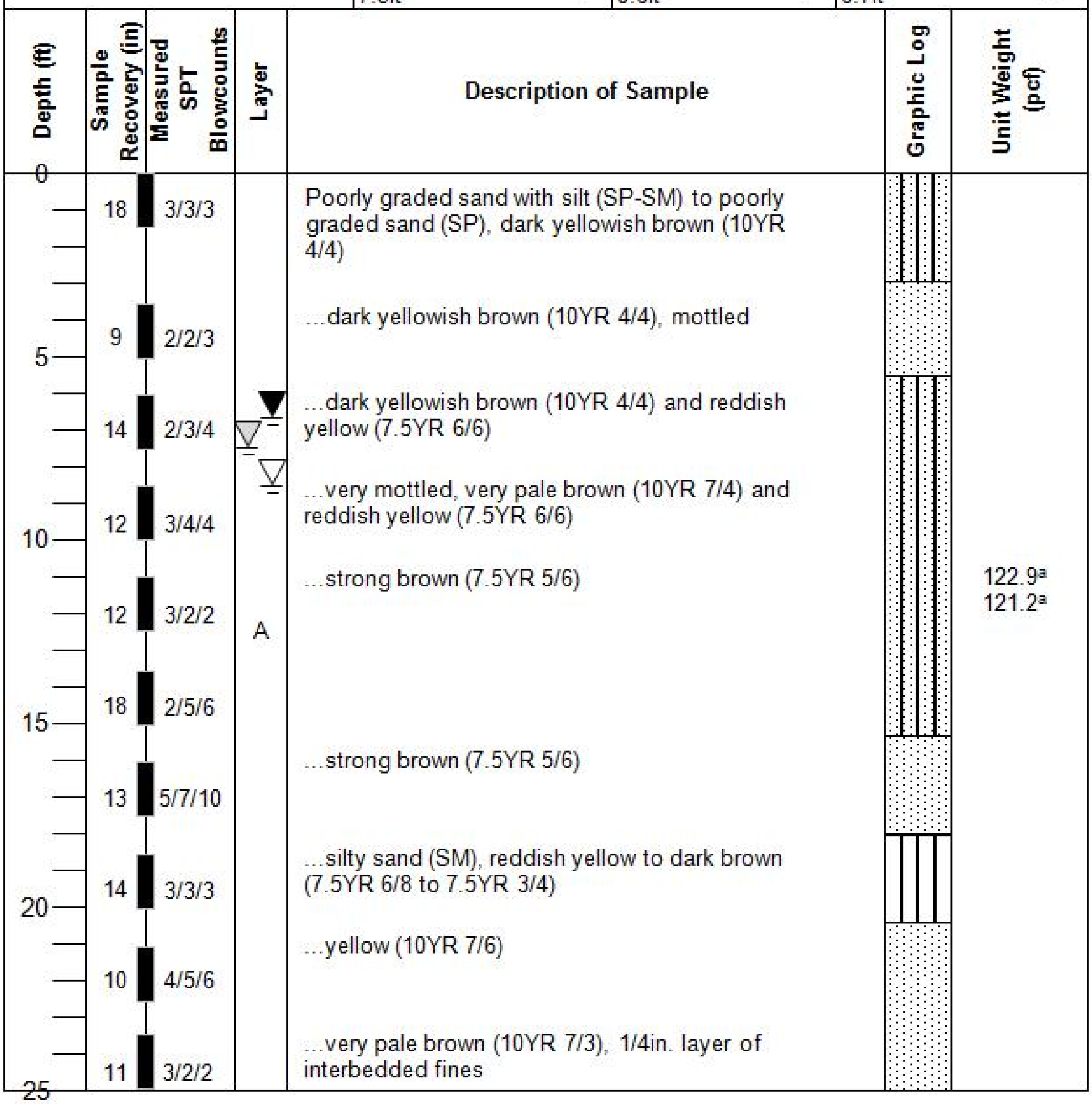

Continued on next page

Site Name: Hobcaw Barony Borrow Pit		**Drilling Contractor:** S&ME, Inc.	**Drill Rig Type:** CME 550X, mud rotary
Location: Georgetown, SC	**SPT Borehole** B-1	**Hammer Type:** Automatic Trip	**Bit Diameter:** 4.5 inches
Date of Drilling: Aug. 5-6th, 2008		**Hammer Weight:** 140lb	**Total Depth of Boring:** 37.5ft
WOH=Weight of Hammer	**GWT at 1/18/10:** 7.5ft ▽	**GWT at 8/6/08:** 8.6ft	**GWT at 11/2/08:** 6.7ft

Depth (ft)	**Sample Recovery**	**Measured SPT Blowcounts**	**Layer**	**Description of Sample**	**Graphic Log**	**Moist Unit Weight (pcf)**
25						
	12	2/2/4	A	...reddish brown (2.5YR 5/3) to light olive green (5Y 6/2), shell fragments		106.1[a] 106.8[a]
30	24	WOH/ WOH/ 2	B	Poorly graded sand with silt (SP-SM), silt of high plasticity (MH) found in B-3, gray (10YR 5/1)		
	15	1/2/2	C	Poorly graded sand with silt (SP-SM), gray (7.5Y 5/1) ...shell fragments		
35	15	5/7/7		...gray (2.5Y 5/0), white shell fragments		
	11	7/7/11		...dark gray (2.5Y 4/0), white shell fragments		
				END OF BOREHOLE		
40						
45						
50						

[a]Based on fixed piston samples taken from B-1.

Table A.3 Unit weight values determined from fixed piston samples taken from B-3 at the Hobcaw Borrow Pit site.

Depth (ft)	Sample Type	Moist Unit Weight (pcf)	Moisture Content (%)	Dry Unit Weight (pcf)	Void Ratio, e	Saturated Unit Weight (pcf)
11.5	Fixed Piston (5.40 in. high)	121.1	24.7	97.1	0.703	122.9
11.5	Consolidation (1.00 in. high)	117.7	24.7	94.4	0.752	121.2
28.5	Consolidation (1.00 in. high)	104.3	48.7	70.1	1.358	106.1
29	Consolidation (1.00 in. high)	104.0	45.7	71.4	1.317	106.8

[a] $\gamma = [\frac{G_s+Se}{1+e}]\gamma_w$, where G_s=specific gravity (assumed 2.65), S=degree of saturation, e=void ratio, and γ_w=unit weight of water

Table A.4 SPT energy measurements and corrected blowcounts for B-1 at the Hobcaw Borrow Pit site.

Test Depth (ft)	N_m	Range of Energy Efficiency in Last 12 in. (%)	Average Energy Efficiency (%)	C_E	C_B	C_S	N_{60}	C_N	$(N_1)_{60}$	$(N_1)_{60cs}$
0-1.5	6	72-78	75	1.25	1	1	8	1.70	13	13
2.5-4.0	5	57-89	71	1.18	1	1	6	1.58	9	9
6.0-7.5	7	59-79	71	1.18	1	1	8	1.39	11	12
8.5-10	8	76-207	105	1.75	1	1	14	1.29	18	18
11-12.5	4	70-75	73	1.22	1	1	5	1.24	6	7
13.5-15.0	11	70-107	86	1.43	1	1	16	1.19	19	19
16.0-17.5	17	75-209	95	1.58	1	1	27	1.14	31	31
18.5-20.0	6	75-85	80	1.33	1	1	8	1.10	9	12
21.0-22.5	11	73-88	82	1.37	1	1	15	1.06	16	16
23.5-25.0	4	49-96	75	1.25	1	1	5	1.03	5	5
26.0-27.5	6	12-89	71	1.18	1	1	7	0.99	7	7
28.5-30.0	2	78-85	81	1.35	1	1	3	0.96	3	7
31.0-32.5	4	68-84	75	1.25	1	1	5	0.93	5	6
33.5-35.0	14	68-98	79	1.32	1	1	18	0.90	17	17
36.0-37.5	18	9-120	74	1.23	1	1	22	0.88	19	20

[a] Rod length correction included in C_E; energy efficiency measured at constant intervals per blow

[b] $C_N=2.2/(1.2+\sigma'_{vo}/P_a)$, where P_a=2000 lb/ft^2 (Kayen et al., 1992)

[c] GWT=8.6ft on August 6th, 2008

[d] Assumed unit weight of soils: 110pcf above GWT, 122pcf from below GWT to 29.2ft, 106pcf from 29.2ft to 30.5ft, and 122pcf from 30.5ft to bottom of borehole

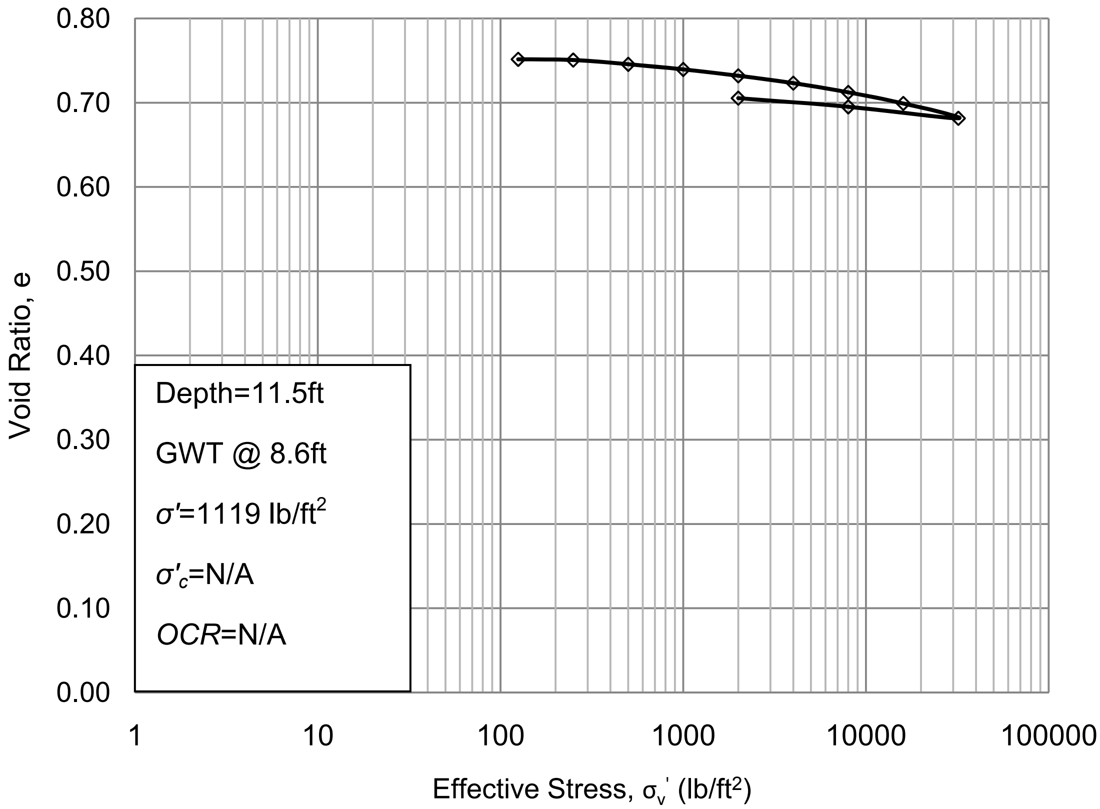

Figure A.2 Consolidation results for sample collected at 11.5ft from B-3 at the Hobcaw Borrow Pit site.

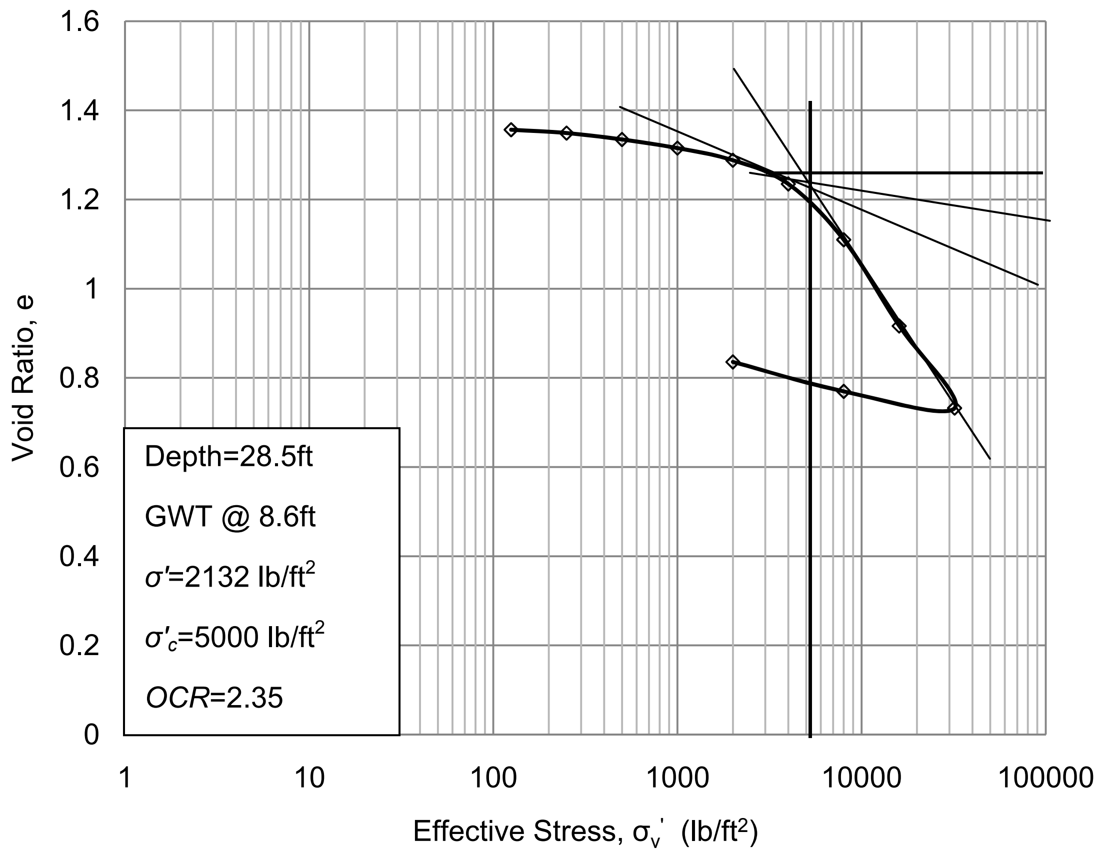

Figure A.3 Consolidation results for sample collected at 28.5ft from B-3 at the Hobcaw Borrow Pit site.

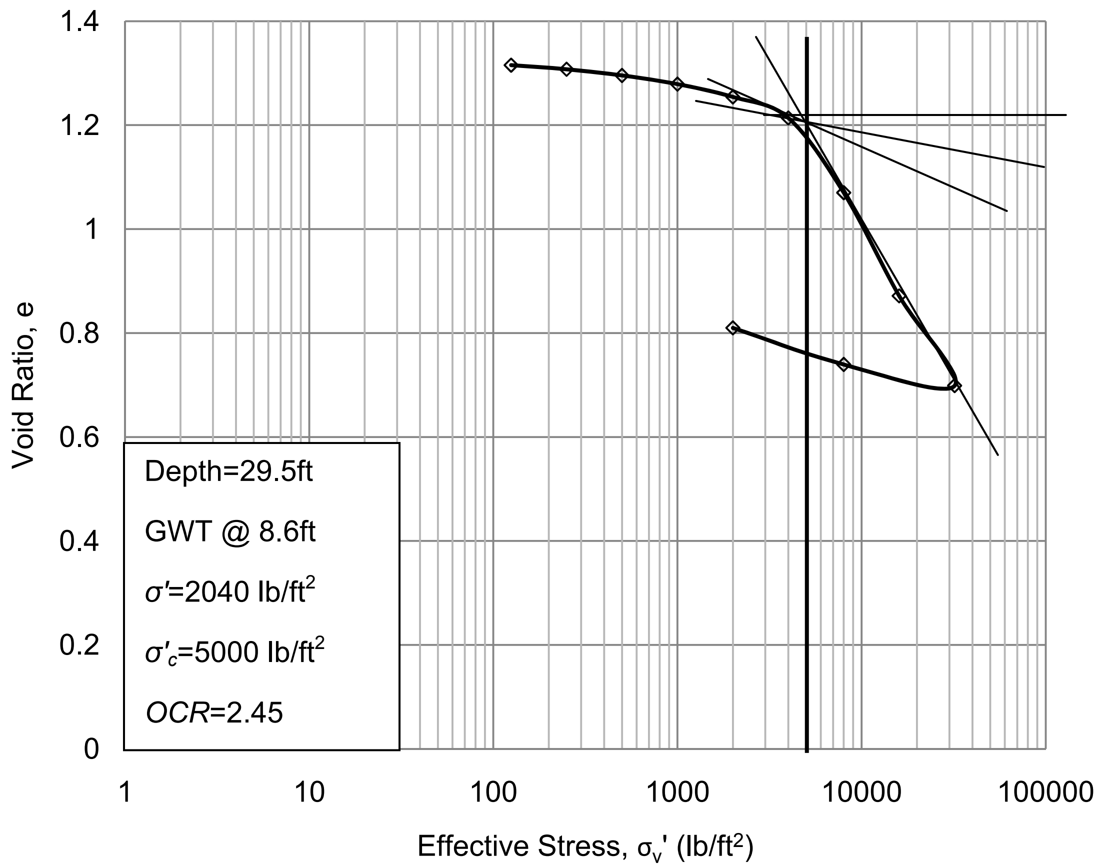

Figure A.4 Consolidation results for sample collected at 29ft from B-3 at the Hobcaw Borrow Pit site.

Table A.5 Direct measurements of P-wave velocity in crosshole testing with source in B-1 and receiver in B-2 at the Hobcaw Borrow Pit site. Measurements conducted Nov. 2008.

Depth (ft)	Corrected[a] Edge-to-Edge Distance (ft)	Travel Time (ms)	Adjusted Time[b] (ms)	Record Quality	P-wave Velocity (ft/s)
2	9.562	10.254	10.2151	Fair	936
4	9.562	16.113	16.0741	Fair	595
6	9.562	11.352	11.3131	Fair	845
8	9.562	9.948	9.9091	Fair	965
10	9.562	2.075	2.0361	Fair	4696
12	9.562	2.106	2.0671	Good	4626
14	9.562	1.953	1.9141	Fair	4996
16	9.562	2.075	2.0361	Fair	4696
18	9.562	2.044	2.0051	Good	4769
20	9.562	1.983	1.9441	Good	4919
22	9.562	2.045	2.0061	Fair	4767
24	9.562	2.075	2.0361	Fair	4696
26	9.562	2.075	2.0361	Fair	4696
28	9.562	2.075	2.0361	Fair	4696
30	9.562	2.136	2.0971	Good	4560
32	9.562	2.045	2.0061	Good	4767
34	9.562	2.014	1.9751	Good	4841
36	9.562	1.892	1.8531	Good	5160

[a] Corrected for inclination and thickness of grout.
[b] Correction of -0.0389ms for travel time through grout.

Table A.6 Interval measurements of P-wave velocity in crosshole testing with first receiver in B-2 and second receiver in B-3 at the Hobcaw Borrow Pit site. Measurements conducted Nov. 2008.

Depth (ft)	Corrected[a] Center-to-Center Distance (ft)	Travel Time (ms)	Record Quality	P-wave Velocity (ft/s)
2	9.733	9.643	Fair	1009
4	9.735	15.259	Good	638
6	9.732	10.681	Fair	911
8	9.726	No or Poor Record		
10	9.727	No or Poor Record		
12	9.734	No or Poor Record		
14	9.740	1.967	Good	4763
16	9.741	1.906	Fair	4910
18	9.739	No or Poor Record		
20	9.733	1.967	Fair	4759
22	9.728	1.906	Fair	4903
24	9.727	No or Poor Record		
26	9.729	No or Poor Record		
28	9.730	No or Poor Record		
30	9.729	No or Poor Record		
32	9.726	No or Poor Record		
34	9.727	No or Poor Record		
36	9.728	No or Poor Record		

[a] Corrected for inclination.

Table A.7 Direct measurements of P-wave velocity in crosshole testing with source in B-3 and receiver in B-2 at the Hobcaw Borrow Pit site. Measurements conducted Nov. 2008.

Depth (ft)	Corrected[a] Edge-to-Edge Distance (ft)	Travel Time (ms)	Adjusted Time[b] (ms)	Record Quality	P-wave Velocity (ft/s)
4	9.360	No (Poor) Record			
12	9.359	No (Poor) Record			
16	9.366	No (Poor) Record			
26	9.354	No (Poor) Record			
36	9.353	1.923	1.8841	Fair	4964

[a] Corrected for inclination and thickness of grout.
[b] Correction of -0.0389ms for travel time through grout.

Table A.8 Interval measurements of P-wave velocity in crosshole testing with first receiver in B-2 and second receiver in B-1 at the Hobcaw Borrow Pit site. Measurements conducted Nov. 2008.

Depth (ft)	Corrected[a] Center-to-Center Distance (ft)	Travel Time (ms)	Record Quality	P-wave Velocity (ft/s)
4	9.937	No or Poor Record		
12	9.937	No or Poor Record		
16	9.937	No or Poor Record		
26	9.937	No or Poor Record		
36	9.937	2.136	Fair	4652

[a] Corrected for inclination.

Table A.9 Direct measurements of P-wave velocity in crosshole testing with source in B-3 and receiver in B-1 at the Hobcaw Borrow Pit site. Measurements conducted Nov. 2008.

Depth (ft)	Corrected[a] Edge-to-Edge Distance (ft)	Travel Time (ms)	Adjusted Time[b] (ms)	Record Quality	P-wave Velocity (ft/s)
4	19.067	26.855	26.8161	Good	711
12	19.066	4.059	4.0201	Good	4743
16	19.074	No or Poor Record			
26	19.062	No or Poor Record			
36	19.060	4.059	4.0201	Fair	4741

[a] Corrected for inclination and thickness of grout.
[b] Correction of -0.0389ms for travel time through grout.

Table A.10 Direct measurements of SV wave velocity in crosshole testing with source in B-1 and receiver in B-2 at the Hobcaw Borrow Pit site. Measurements conducted Nov. 2008.

Depth (ft)	Corrected[a] Edge-to-Edge Distance (ft)	Up Travel Time (ms)	Up Adjusted Time[b] (ms)	Up Record Quality	Down Travel Time (ms)	Down Adjusted Time[b] (ms)	Record Quality	SV-wave velocity (ft/s)
2	9.562	17.456	17.373	Fair	17.456	17.373	Fair	550
4	9.562	15.747	15.664	Good	11.962	11.879	Good	708
6	9.562	16.113	16.030	Fair	16.723	16.640	Good	586
8	9.562	16.357	16.274	Fair	16.479	16.396	Fair	585
10	9.562	18.067	17.984	Good	18.066	17.983	Very Good	532
12	9.562	16.48	16.397	Fair	16.723	16.640	Fair	579
14	9.562	15.493	15.410	Good	15.625	15.542	Good	618
16	9.562	15.371	15.288	Good	15.991	15.908	Good	613
18	9.562	14.038	13.955	Good	14.404	14.321	Good	676
20	9.562	14.038	13.955	Good	13.916	13.833	Good	688
22	9.562	17.334	17.251	Good	19.287	19.204	Good	526
24	9.562	16.724	16.641	Very Good	17.028	16.945	Very Good	569
26	9.562	16.846	16.763	Good	16.601	16.518	Good	575
28	9.562	15.93	15.847	Good	16.174	16.091	Good	599
30	9.562	16.419	16.336	Good	16.174	16.091	Good	590
32	9.562	15.503	15.420	Good	15.197	15.114	Fair	626
34	9.562	14.526	14.443	Fair	13.671	13.588	Fair	683
36	9.562	14.312	14.229	Good	14.16	14.077	Good	676

[a] Corrected for inclination and thickness of grout.
[b] Correction of -0.0835ms for travel time through grout.

Table A.11 Interval measurements of SV wave velocity in crosshole testing with the first receiver in B-2 and the second receiver in B-3 at Hobcaw Borrow Pit site. Measurements conducted Nov. 2008.

Depth (ft)	Corrected[a] Center-to-Center Distance (ft)	Up Travel Time (ms)	Up Record Quality	Down Travel Time (ms)	Record Quality	SV-wave velocity (ft/s)
2	9.733	16.846	Good	18.799	Good	548
4	9.735	16.602	Good	21.119	Good	524
6	9.732	16.846	Good	16.602	Good	582
8	9.726	17.579	Good	17.945	Good	548
10	9.727	15.869	Good	16.235	Good	606
12	9.734	No or Poor Record				
14	9.740	14.282	Good	14.648	Good	673
16	9.741	14.038	Good	13.55	Good	706
18	9.739	13.184	Good	13.428	Good	732
20	9.733	13.55	Good	14.16	Good	703
22	9.728	17.456	Good	17.334	Good	559
24	9.727	No or Poor Record				
26	9.729	No or Poor Record				
28	9.730	No or Poor Record				
30	9.729	No or Poor Record				
32	9.726	No or Poor Record				
34	9.727	No or Poor Record				
36	9.728	No or Poor Record				

[a] Corrected for inclination.

Table A.12 Direct measurements of SV wave velocity in crosshole testing with source in B-3 and receiver in B-2 at Hobcaw Borrow Pit site. Measurements conducted Nov. 2008.

Depth (ft)	Corrected[a] Edge-to-Edge Distance (ft)	Up Travel Time (ms)	Up Adjusted [b] Time (ms)	Up Record Quality	Down Travel Time (ms)	Down Adjusted[b] Time (ms)	Record Quality	SV-wave velocity (ft/s)
4	9.360	No or Poor Record						
12	9.359	No or Poor Record						
16	9.366	No or Poor Record						
26	9.354	19.043	18.960	Fair	12.573	12.490	Fair	621
36	9.353	15.625	15.542	Very Good	15.625	15.542	Very Good	602

[a] Corrected for inclination and thickness of grout.
[b] Correction of -0.0835ms for travel time through grout.

Table A.13 Interval measurements of SV wave velocity in crosshole testing with first receiver in B-2 and second receiver in B-1 at the Hobcaw Borrow Pit site. Measurements conducted Nov. 2008.

Depth (ft)	Corrected[a] Center-to-Center Distance (ft)	Up Travel Time (ms)	Up Record Quality	Down Travel Time (ms)	Record Quality	SV-wave velocity (ft/s)
4	9.937	No or Poor Record				
12	9.937	No or Poor Record				
16	9.937	No or Poor Record				
26	9.937	19.043	Fair	18.066	Fair	536
36	9.937	15.015	Good	14.892	Good	665

[a] Corrected for inclination.

Table A.14 Direct measurements of SV wave velocity in crosshole testing with source in B-3 and receiver in B-1 at Hobcaw Borrow Pit site. Measurements conducted Nov. 2008.

Depth (ft)	Corrected[a] Edge-to-Edge Distance (ft)	Up Travel Time (ms)	Up Adjusted[b] Time (ms)	Up Record Quality	Down Travel Time (ms)	Down Adjusted[b] Time (ms)	Record Quality	SV-wave velocity (ft/s)
4	19.067	33.039	32.956	Good	32.959	32.876	Good	579
12	19.066	30.395	30.312	Good	30.761	30.678	Good	625
16	19.074	30.274	30.191	Fair	29.785	29.702	Fair	637
26	19.062	38.086	38.003	Fair	30.639	30.556	Fair	563
36	19.060	30.64	30.557	Good	30.517	30.434	Good	625

[a] Corrected for inclination and thickness of grout.
[b] Correction of -0.0835ms for travel time through grout.

Table A.15 Direct measurements of SH wave velocity in crosshole testing with source in B-1 and receiver in B-2 at Hobcaw Borrow Pit site. Measurements conducted Nov. 2008.

Depth (ft)	Corr.[a] Edge-to-Edge Distance (ft)	Up Travel Time (ms)	Up Adj. Time[b] (ms)	Up Record Quality	Down Travel Time (ms)	Down Adj. Time[b] (ms)	Record Quality	SH-wave velocity (ft/s)
2	9.562	18.188	18.105	Very Good	17.944	17.861	Excellent	532
4	9.562	21.362	21.279	Good	20.264	20.181	Good	462
6	9.562	18.433	18.350	Excellent	19.287	19.204	Very Good	510
8	9.562	18.31	18.227	Good	18.554	18.471	Good	521
10	9.562	20.996	20.913	Excellent	21.118	21.035	Excellent	456
12	9.562	18.799	18.716	Excellent	18.677	18.594	Fair	513
14	9.562	18.066	17.983	Fair	No or Poor Record			532
16	9.562	18.677	18.594	Excellent	18.677	18.594	Excellent	514
18	9.562	No or Poor Record						
20	9.562	20.508	20.425	Fair	21.728	21.645	Poor to Fair	455
22	9.562	19.531	19.448	Very Good	19.775	19.692	Excellent	489
24	9.562	20.874	20.791	Very Good	20.508	20.425	Good	464
26	9.562	17.578	17.495	Fair	18.066	17.983	Fair	539
28	9.562	No or Poor Record			19.409	19.326	Fair	495
30	9.562	19.043	18.960	Good	19.531	19.448	Very Good	498
32	9.562	17.456	17.373	Good	19.409	19.326	Very Good	523
34	9.562	15.747	15.664	Fair	15.381	15.298	Fair	618
36	9.562	15.015	14.932	Very Good	15.015	14.932	Good	640

[a] Corrected for inclination and thickness of grout.
[b] Correction of -0.0835ms for travel time through grout.

Table A.16 Interval measurements of SH wave velocity in crosshole testing with first receiver in B-2 and second receiver in B-3 at Hobcaw Borrow Pit site. Measurements conducted Nov. 2008.

Depth (ft)	Corrected[a] Center-to-Center Distance (ft)	Up Travel Time (ms)	Up Record Quality	Down Travel Time (ms)	Record Quality	SH-wave velocity (ft/s)
2	9.733	No or Poor Record		20.264	Good	480
4	9.735	No or Poor Record		18.31	Fair	532
6	9.732	17.089	Good	16.602	Fair	578
8	9.726	No or Poor Record		17.457	Fair	557
10	9.727	18.188	Good	18.921	Good	524
12	9.734	No or Poor Record				
14	9.740	No or Poor Record				
16	9.741	No or Poor Record				
18	9.739	No or Poor Record				
20	9.733	No or Poor Record				
22	9.728	21.24	Fair	No or Poor Record		458
24	9.727	17.7	Fair	No or Poor Record		550
26	9.729	No or Poor Record				
28	9.730	No or Poor Record				
30	9.729	17.578	Good	No or Poor Record		553
32	9.726	19.165	Fair	18.799	Good	512
34	9.727	No or Poor Record				
36	9.728	14.648	Fair	15.014	Good	656

[a] Corrected for inclination.

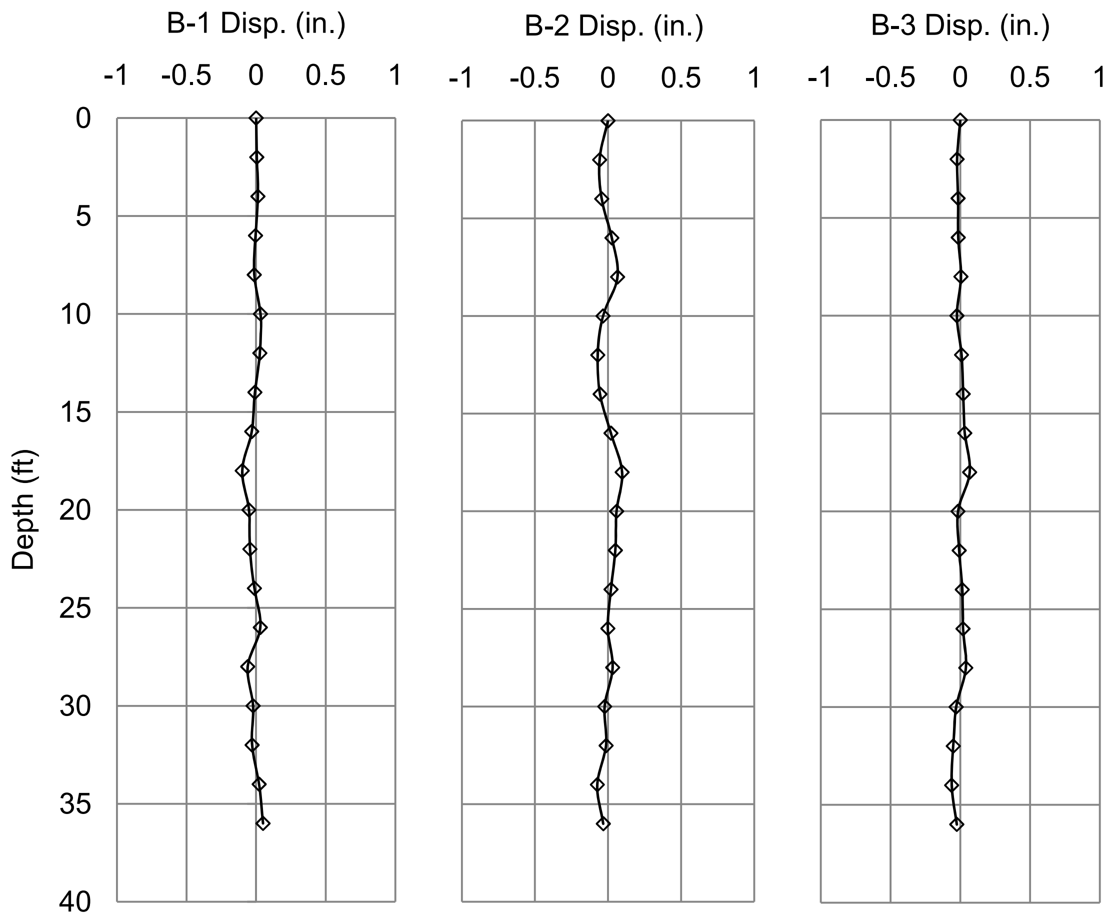

Figure A.5 Borehole displacements in the “A” direction at the Hobcaw Borrow Pit site.

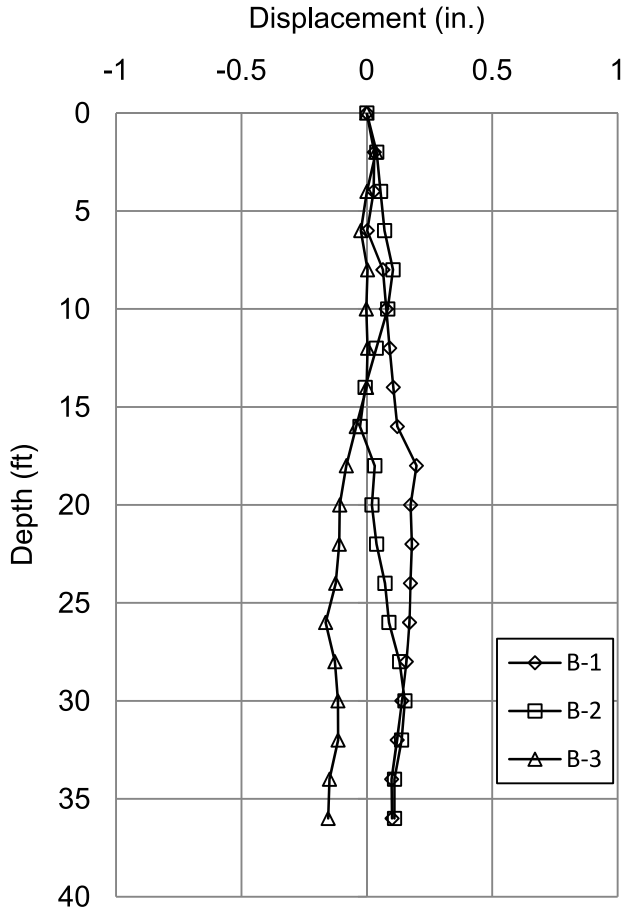

Figure A.6 Borehole deviations in the “B” direction at the Hobcaw Borrow Pit site when looking from B-1 to B-3.

Table A.17 Borehole locations[a] at the Hobcaw Borrow Pit site relative to reference points identified in Boller (2008).

Point	Point	Distance (ft)	Point	Point	Distance (ft)
Ref. 1	B-1	69.5	Ref. 2	B-3	45.3
Ref. 1	B-2	62.9	Ref. 2	B-4	39.4
Ref. 1	B-3	57.8	Ref. 3	B-1	20.1
Ref. 1	B-4	54.9	Ref. 3	B-2	25.7
Ref. 2	B-1	60.7	Ref. 3	B-3	33.1
Ref. 2	B-2	52.6	Ref. 3	B-4	39.8

[a] Map Coordinates: 33°20’44” N, 79°14’9” W

APPENDIX B
SUMMARY OF DATA FROM THE WALTERBORO REST AREA PONDS SITE

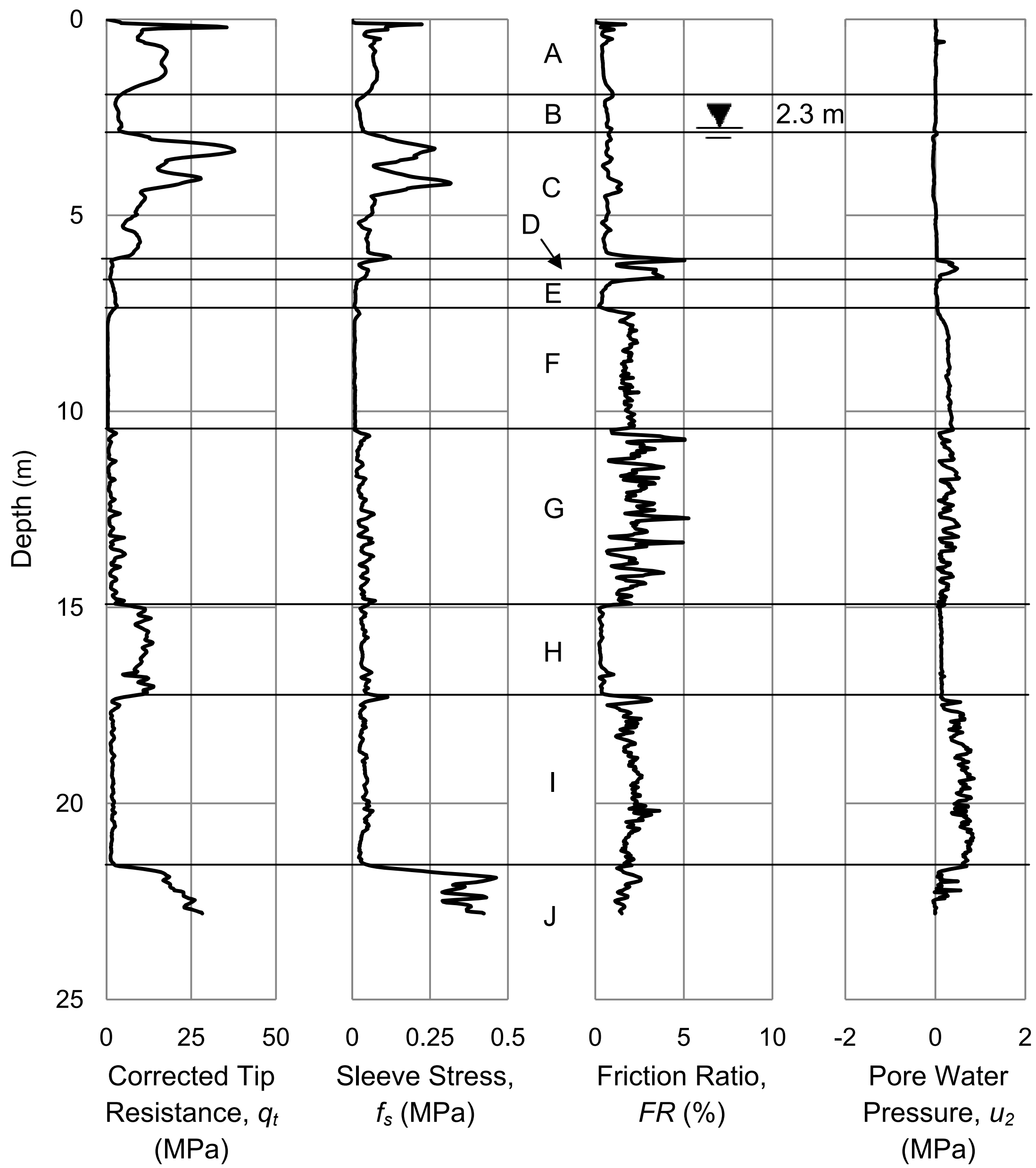

Figure B.1 Composite Profile of SCPT SC-1 at the Rest Area Ponds site.

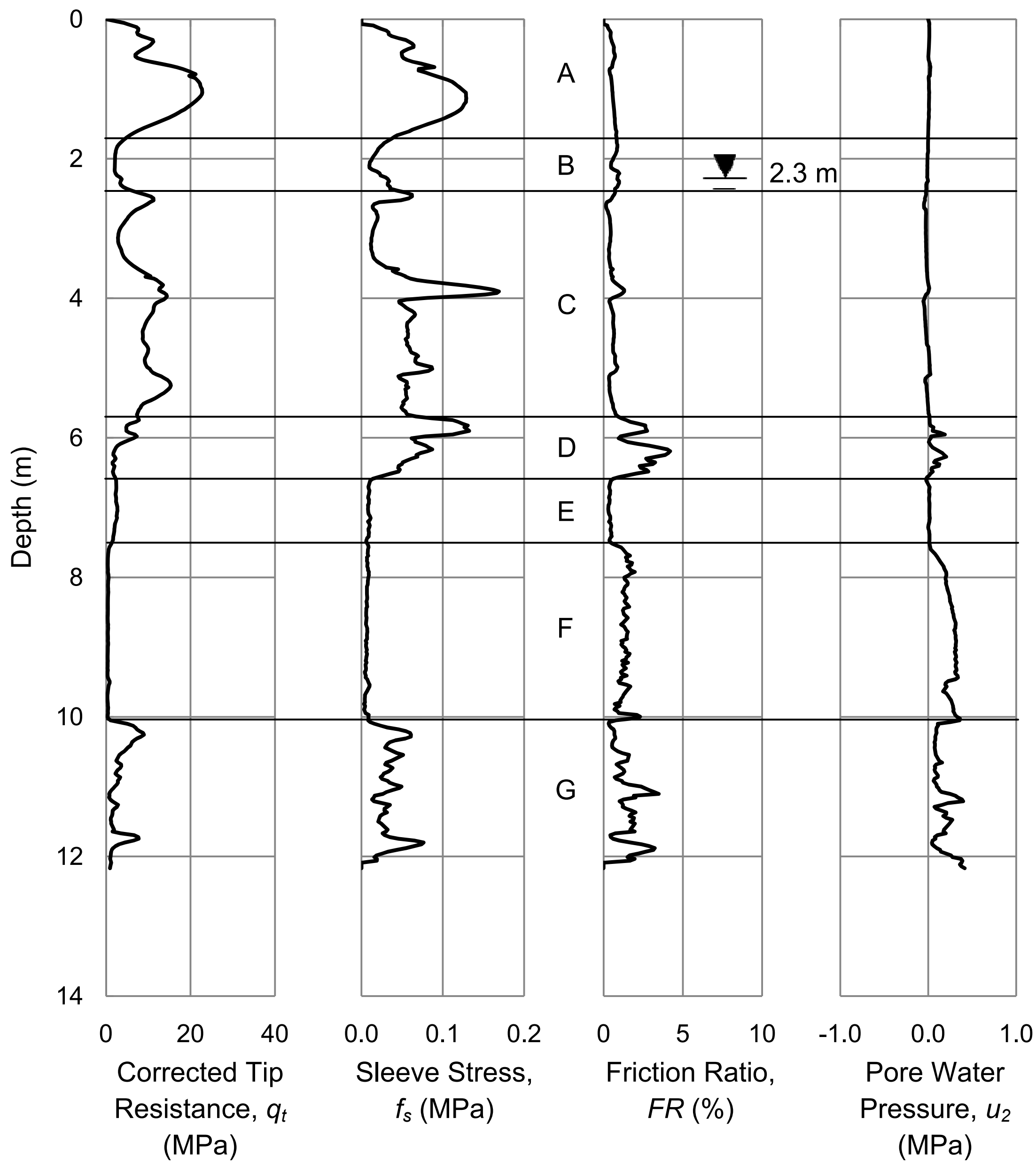

Figure B.2 Composite Profile of SCPT SC-2 at the Rest Area Ponds site.

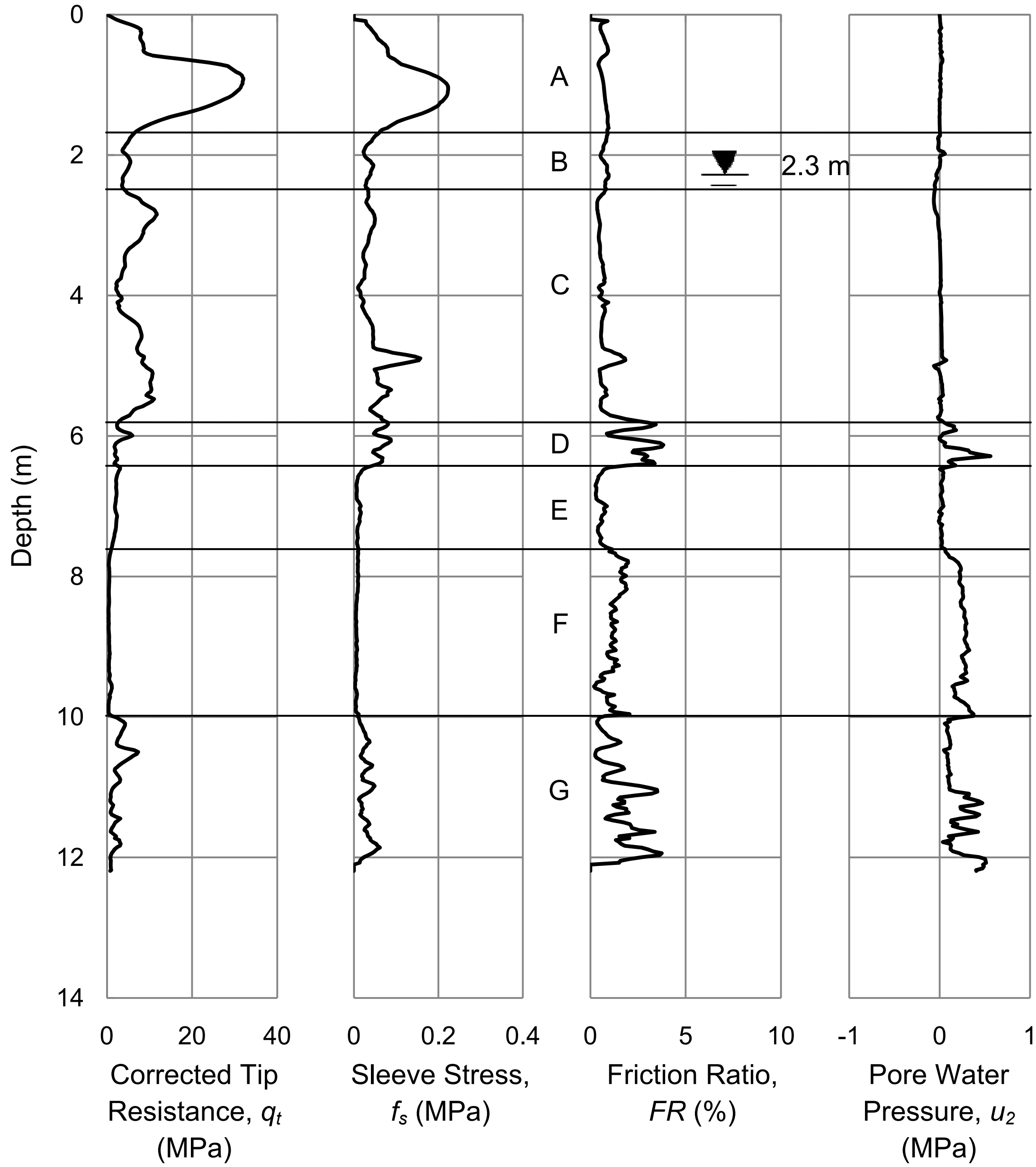

Figure B.3 Composite Profile of SCPT SC-3 at the Rest Area Ponds site.

Table B.1 Results of DMT D-1 performed at the Rest Area Ponds site

(Continued on following page)

Start of DMT		End of DMT		Average		Z_m					
ΔA	ΔB	ΔA	ΔB	ΔA	ΔB						
-0.1	0.7	0.15	0.6	0.03	0.65	0	GWT: 7.5ft				
Depth (ft)	A (bar)[a]	B (bar)	C (bar)	P_1 (psf)	P_0 (psf)	σ'_v (psf)[b]	q_t (tsf)	I_D	K_D	K_0[c]	E_D (bar)
1	2.9	7.8	-	14936	5669	110.0	83.27	1.63	135.79	5.71	154
2	5.15	14.6	-	29142	9894	220.0	157.00	1.95	132.46	5.82	320
3	8.1	35.2	-	72175	14213	330.0	331.89	4.08	218.71	11.10	963
4	10.2	34	-	69668	18945	440.0	278.14	2.68	158.34	9.10	843
5	7.9	24.2	-	49196	14923	550.0	121.47	2.30	89.45	6.66	569
6	5.45	16.4	-	32902	10364	660.0	50.09	2.17	49.85	4.35	374
7	6.1	15.2	-	30395	11915	770.0	54.65	1.55	39.47	3.42	307
8	2.4	11.6	0	22875	4175	853.8	40.03	4.51	26.75	2.45	311
9	4.45	25.6	-	52121	7210	911.4	105.43	6.31	57.08	4.64	746
10	10.4	32.4	0	66326	19550	969.0	92.71	2.41	68.29	5.91	777
11	8.4	28.2	-	57552	15602	1026.6	54.03	2.73	55.85	5.16	697
12	4.45	19.4	0	39169	7857	1084.2	35.95	4.13	35.87	3.45	520
13	5.2	25.8	-	52538	8834	1141.8	28.65	5.15	45.71	4.47	726
14	6.1	24.6	0	50032	10933	1199.4	41.55	3.71	41.38	3.96	650
15	6.15	19.6	-	39587	11565	1257.0	83.50	2.53	31.12	2.67	466
16	5.4	19.8	-	40004	9899	1314.6	84.40	3.21	30.03	2.59	500
17	5.7	24.4	-	49614	10077	1372.2	109.41	4.17	35.72	2.97	657
18	6.2	20.2	-	40840	11612	1429.8	102.69	2.67	28.11	2.33	486
19	4.6	15.4	0	30813	8604	549.9	35.23	2.82	54.73	4.93	369
20	4.3	15.2	-	30395	7967	604.5	28.78	3.12	48.99	4.55	373
21	7	11.4	0	22457	14286	659.1	25.76	0.61	32.79	3.66	136
22	2.5	6.5	-	12221	4927	713.7	23.02	1.81	15.86	1.56	121
23	2.1	6.45	0	12116	4055	768.3	21.12	2.61	14.51	1.48	134
24	2.3	7.5	0.2	14310	4384	822.9	21.53	2.96	16.14	1.65	165
25	2.4	6.3	0.2	11803	4729	1814.1	9.65	1.94	5.90	0.88	118
26	3.1	4.1	-	7207	6494	1871.7	5.93	0.13	3.23	0.83	12
27	3.1	3.9	-	6789	6515	1929.3	5.20	0.05	2.89	0.76	5
28	3.05	3.9	1.55	6789	6405	1986.9	4.58	0.07	2.77	0.73	6
29	3.2	4.2	1.8	7416	6703	2044.5	5.43	0.13	2.97	0.78	12
30	3.3	4.5	1.5	8043	6891	2102.1	6.10	0.21	3.16	0.82	19
31	3.7	4.6	0.6	8252	7758	2159.7	7.72	0.08	3.14	0.82	8
32	2.7	5.2	-	9505	5502	2217.3	5.79	1.01	3.60	0.91	67

Table B.1 Continued

Depth (ft)	A (bar)[a]	B (bar)	C (bar)	P_1 (psf)	P_0 (psf)	σ'_{vo} (psf)[b]	q_t (tsf)	I_D	K_D	K_0[c]	E_D (bar)
33	4	5	1.6	9087	8374	2274.9	34.52	0.11	3.30	0.85	12
34	3.8	10.6	0.45	20786	7351	2332.5	29.86	2.36	8.20	1.03	223
35	3.5	9.2	0.55	17861	6839	2390.1	37.71	2.15	6.75	0.86	183
36	3.2	8.6	0.45	16608	6243	2447.7	21.10	2.32	6.06	0.87	172
37	4.5	7.1	1.05	13474	9252	2505.3	11.46	0.57	4.64	1.10	70
38	3.8	5.8	0.6	10758	7852	2562.9	15.80	0.49	3.46	0.88	48

[a] 1 bar=2089 psf
[b] Assumed unit weights: 110pcf from surface to 9.3ft, 120pcf from 9.3ft to 18.7ft, 117pcf from 18.7ft to 24.8ft, and 120pcf from 24.8ft to the bottom of the borehole.
[c] $K_0=0.376+0.095K_D-0.005q_t/\sigma_v'$ for sand, $I_D\geq1.2$ (Baldi et al. 1986 as recommended by Marchetti et al. 2001); $K_0=(K_D/1.5)^{0.47}-0.6$ for clay and silt, $I_D<1.2$ (Marchetti 1980)

Table B.2 Measured shear wave velocity using true interval method for sounding SCPT SC-1 at the Walterboro Rest Area Ponds site.

Upper Geophone Depth (ft)	Lower Geophone Depth (ft)	Calculated V_s[a] (ft/s)	Standard Deviation[b] of V_s (ft/s)	Quality of Record
0.75	4.03	300	16	Very Good
4.75	8.03	511	62	Good
7.75	11.03	546	52	Very Good
10.75	14.03	572	37	Very Good
13.75	17.03	620	50	Very Good
16.75	20.03	596	78	Good
19.75	23.03	695	99	Good
23.75	27.03	580	54	Very Good
26.75	30.03	629	67	Good
29.75	33.03	616	84	Good
32.75	36.03	604	49	Very Good
35.75	39.03	634	137	Fair
38.75	42.03	598	82	Good
41.75	45.03	630	57	Very Good
44.75	48.03	534	39	Very Good
48.75	52.03	590	25	Excellent
51.75	55.03	715	168	Fair to Poor
54.75	58.03	-	-	Poor
57.75	61.03	-	-	Poor
61.75	65.03	754	109	Fair to Good
64.75	68.03	-	-	Poor
67.75	71.03	997	236	Fair to Poor

[a] Calculated using travel times based on first crossover and first peak arrival times and horizontal distance between source and cone rod of 3.83 ft.
[b] Standard deviation based on four estimates of V_s determined from first crossovers and first peaks for two hits with opposite polarity.

Table B.3 Measured shear wave velocity using the true interval method for sounding SCPT SC-2 at the Walterboro Rest Area Ponds site.

Upper Geophone Depth (ft)	Lower Geophone Depth (ft)	Calculated V_s[a] (ft/s)	Standard Deviation[b] of V_s (ft/s)	Quality of Record
1.75	5.03	331	39	Good
4.75	8.03	624	31	Very Good
7.75	11.03	647	138	Fair
10.75	14.03	471	109	Fair
14.75	18.03	479	70	Good
17.75	21.03	586	124	Fair
20.75	24.03	581	84	Good
23.75	27.03	512	80	Fair
26.75	30.03	754	35	Excellent
30.75	34.03	665	93	Good
33.75	37.03	717	49	Very Good
35.75	39.03	764	18	Excellent

[a] Calculated using travel times based on first crossover and first peak arrival times and horizontal distance between source and cone rod of 3.83 ft.
[b] Standard deviation based on four estimates of V_s determined from first crossovers and first peaks for two hits with opposite polarity.

Table B.4 Measured shear wave velocity using the true interval method for sounding SCPT SC-3 at the Walterboro Rest Area Ponds site.

Upper Geophone Depth (ft)	Lower Geophone Depth (ft)	Calculated V_s[a] (ft/s)	Standard Deviation[b] of V_s (ft/s)	Quality of Record
1.75	5.03	360	80	Fair
4.75	8.03	-	-	Poor
7.75	11.03	635	37	Very Good
10.75	14.03	554	34	Very Good
14.75	18.03	592	79	Good
17.75	21.03	719	71	Very Good
20.75	24.03	767	188	Fair
24.75	28.03	740	192	Fair
27.75	31.03	775	333	Fair to Poor
30.75	34.03	669	163	Fair
33.75	37.03	846	319	Fair to Poor
35.75	39.03	806	241	Fair to Poor

[a] Calculated using travel times based on first crossover and first peak arrival times and horizontal distance between source and cone rod of 3.83 ft.
[b] Standard deviation based on four estimates of V_s determined from first crossovers and first peaks for two hits with opposite polarity.

Table B.5 Soil index properties from split spoon and fixed piston samples collected from B-1 and B-3 at the Rest Area Ponds site.

				Percent Retained												
				Gravel		Sand										
Depth (ft)	C_u	C_c	D_{50}	#4	#10	#20	#40	#60	#80	#100	#200	% Fines	LL	PL	w(%)	Soil Type
B-3 Split Spoon Sampler																
0-1.5	2.50	1.41	0.18	1.16	0.54	1.99	6.72	14.59	25.81	22.64	17.53	9.02	np		-	SP-SM
2-3.5	2.71	1.69	0.17	0.23	0.24	1.36	6.20	14.49	24.41	22.49	19.67	10.91	np		-	SP-SM
4-5.5	2.50	1.60	0.19	2.12	0.04	0.82	5.81	15.70	27.68	18.96	19.65	9.22	np		-	SP-SM
6-7.5	3.00	1.74	0.19	1.24	0.02	0.63	6.58	16.72	30.38	20.80	12.30	11.34	np		-	SP-SM
8-9.5	2.63	1.52	0.19	0	0.01	0.34	5.62	16.66	34.76	22.56	11.46	8.59	np		26.0	SP-SM
10-11.5	2.20	1.31	0.2	0	0.11	3.41	8.70	16.82	30.33	21.45	14.23	4.95	np		27.9	SP
12-13.5	2.71	1.27	0.17	0	0.16	2.67	6.54	9.25	24.33	22.98	22.02	12.05	np		21.7	SM
14-15.5	2.07	1.29	0.17	0	0.01	0.46	5.32	12.70	27.61	25.28	25.73	2.89	np		24.5	SP
16-17.5	2.13	1.06	0.16	0	0.32	1.31	3.79	6.96	17.61	24.22	37.77	8.02	np		25.9	SP-SM
18-19.5	2.83	1.19	0.15	0	1.22	6.80	6.14	6.18	12.54	18.74	33.23	15.15	np		26.9	SM
20-21.5	-	-	0.09	0	0.05	0.46	7.22	8.80	16.99	8.96	11.19	46.33	53.3	31.3	31.9	SC or CH
22-23.5	2.71	1.27	0.17	0	0.80	7.12	7.00	9.18	18.32	22.63	22.88	12.08	np		26.5	SM
25-26.5	2.86	1.03	0.17	0	0.14	4.57	14.53	12.01	13.67	12.99	30.19	11.9	np		35.4	SP-SM
30-31.5	-	-	0.13	0	0.14	5.79	18.65	8.19	5.87	5.36	33.98	22.02	28.1	23.6	36.2	SM
34-35.5	2.74	0.83	0.15	0.05	0.65	5.17	14.53	13.33	9.51	8.51	37.37	10.88	np		33.3	SP-SM
B-1 Osterberg Fixed Piston Sampler																
26.9	-	-	0.15	0	0.09	2.9	8.81	9.32	10.68	16.61	29.71	21.88	np		32.8	SM
27.6	-	-	0.2	0	0.03	2.09	7.6	7.7	8.7	15.2	37.4	21.28	np		31.7	SM

[a] C_u=Coefficient of Uniformity
[b] C_c=Coefficient of Gradation.
[c] D_{50}=Median grain size.
[d] LL=Liquid Limit water content (%) ASTM D 4318
[e] PL=Plastic Limit water content (%) ASTM D 4318, np=non-plastic.
[f] In-situ moisture content.
[g] Soil type based on United Soil Classification System ASTM D 2487.

Table B.6 Boring log for B-3 at the Rest Area Ponds site.

Site Name: Walterboro Rest Area Ponds Site		**Drilling Contractor:** S&ME, Inc.	**Drill Rig Type:** CME 550X, mud rotary
Location: Walterboro, SC	**SPT Borehole** B-3	**Hammer Type:** Automatic Trip	**Bit Diameter:** 4.5 inches
Date of Drilling: October 13-14, 2009		**Hammer Weight:** 140lb	**Total Depth of Boring:** 37.5ft
W.O.H.=Weight of Hammer	**GWT at 6/25/09** ▽ 7.5ft	**GWT at 10/13/09:** ▽ 9.3ft	**GWT at 1/18/10:** ▼ 5.7ft

Depth (ft)	Sample Recovery (in)	Measured SPT Blowcounts	Layer	Description of Sample	Graphic Log	Moist Unit Weight (pcf)
0						
	22	3/3/6	A	Poorly graded sand with silt (SP-SM), dark brown (7.5YR 3/2), topsoil with organic content, likely fill		
	19	6/10/10	A	...yellowish brown (10YR 5/6)		
5	16	5/5/4	A	...yellowish brown (10YR 5/4), mottled		
	13	2/2/3	B	Poorly graded sand with silt (SP-SM), black (10YR 2/1) to very dark brown (10YR 2/2), difficult to cut, likely pedogenic horizon		
	17.5	3/4/10	C	Poorly graded sand to poorly graded sand with silt (SP to SP-SM), dark brown (7.5YR 3/4), likely barrier island sand (Q6b, inferred from McCartan et al. 1984)		
10						
	15	2/2/3	C	...light yellowish brown (10YR 6/4)		
	15	3/2/7	C	...very pale brown (10YR 7/4)		
15	15	5/5/5	C	...very pale brown (10YR 8/3)		
	15	3/5/5	C	...white (10YR 8/1)		
	18	3/2/5	D	Silty to clayey sand (SM to SC), white (10YR 8/2); based on fixed piston sample, interbedded clayey sand layers are hard and appear to be dessicated		
20			D			118.3[a]
	19	3/2/3	D			
	24.5	1/0/1	E	Silty sand (SM), white (10YR 8/2) ...mottling		
25						

Continued on next page

Site Name: Walterboro Rest Area Ponds Site		Drilling Contractor: S&ME, Inc.	Drill Rig Type: CME 550X, mud rotary
Location: Walterboro, SC	**SPT Borehole** B-3	**Hammer Type:** Automatic Trip	**Bit Diameter:** 4.5 inches
Date of Drilling: October 13-14, 2009		**Hammer Weight:** 140lb	**Total Depth of Boring:** 37.5ft
WOH=Weight of Hammer	**GWT at 6/25/09** ▽ 7.5ft	**GWT at 10/13/09:** ▽ 9.3ft	**GWT at 1/18/10:** ▼ 5.7ft

Depth (ft)	Sample Recovery	Measured SPT Blowcounts	Layer	Description of Sample	Graphic Log	Moist Unit Weight (pcf)
25–26	27	W.O.H.	F	Silty sand to poorly graded sand with silt (SM to SP-SM), light gray (10YR 7/2), reddish yellow mottling (7.5YR 6/8)		118.5[a] 120.4[a]
30–31	22.5	W.O.H.	F	...gray to light gray (10YR 6/1)		
35	16	2/1/1	G	Poorly graded sand with silt (SP-SM), gray (2.5Y 5/0)		
37.5				***END OF BOREHOLE***		

[a] Based on fixed piston samples taken from B-3.

Table B.7 Unit weights from fixed piston samples in B-1 at the Rest Area Ponds site.

Depth (ft)	Sample Type	Moist Unit Weight (pcf)	Moisture Content (%)	Dry Unit Weight (pcf)	Void Ratio, e	Saturated Unit Weight (pcf)
20	Fixed Piston (2.469in. high)	116.0	29.2	89.8	0.842	118.3
26.7	Consolidation (1.003in. high)	119.7	32.9	90.1	0.836	118.5
27.6	Consolidation (1.003in. high)	122.7	31.7	93.2	0.775	120.4

[a] $\gamma = [\frac{G_s+Se}{1+e}]\gamma_w$, where G_s=specific gravity (assumed 2.65), S=degree of saturation, e=void ratio, and γ_w=unit weight of water.

Table B.8 SPT energy measurements and corrected blowcounts for B-1 at the Rest Area Ponds site.

Test Depth (ft)	N_m	Range of Energy Efficiency in Last 12 in. (%)	Average Energy Efficiency (%)	C_E[a]	C_B	C_S	N_{60}	C_N	$(N_1)_{60}$	$(N_1)_{60cs}$
0-1.5	9	50-71	67	1.12	1	1	10	1.70	17	18
2-3.5	20	61-78	72	1.20	1	1	24	1.61	39	41
4-5.5	9	63-75	69	1.15	1	1	10	1.49	15	16
6-7.5	5	55-70	64	1.07	1	1	5	1.39	7	9
8-9.5	14	69-108	74	1.23	1	1	17	1.29	22	23
10-11.5	5	65-75	70	1.17	1	1	6	1.25	7	7
12-13.5	9	63-82	74	1.23	1	1	11	1.21	13	15
14-15.5	10	65-78	73	1.22	1	1	12	1.17	14	14
16-17.5	10	75-110	87	1.45	1	1	15	1.14	17	17
18-19.5	7	67-81	73	1.22	1	1	9	1.11	9	12
20-21.5	5	70-76	73	1.22	1	1	6	1.08	7	5
22-23.5	1	N/A	73	1.22	1	1	1	1.05	1	3
25-26.5	W.O.H[e]	N/A	73	1.22	1	1	-	1.01	-	-
30-31.5	W.O.H	N/A	73	1.22	1	1	-	0.95	-	-
34-35.5	2	N/A	73	1.22	1	1	2	0.90	2	3

[a] Rod length correction included in C_E; energy efficiency measured at constant intervals per blow.
[b] $C_N=2.2/(1.2+\sigma'_{vo}/P_a)$, where $P_a=2000$ lb/ft^2 (Kayen et al., 1992).
[c] GWT at 9.3ft on October 13th, 2009.
[d] Assumed unit weights: 110pcf from surface to 9.3ft, 120pcf from 9.3ft to 18.7ft, 117pcf from 18.7ft to 24.8ft, and 120pcf from 24.8ft to the bottom of the borehole.
[e] W.O.H.=Weight of hammer

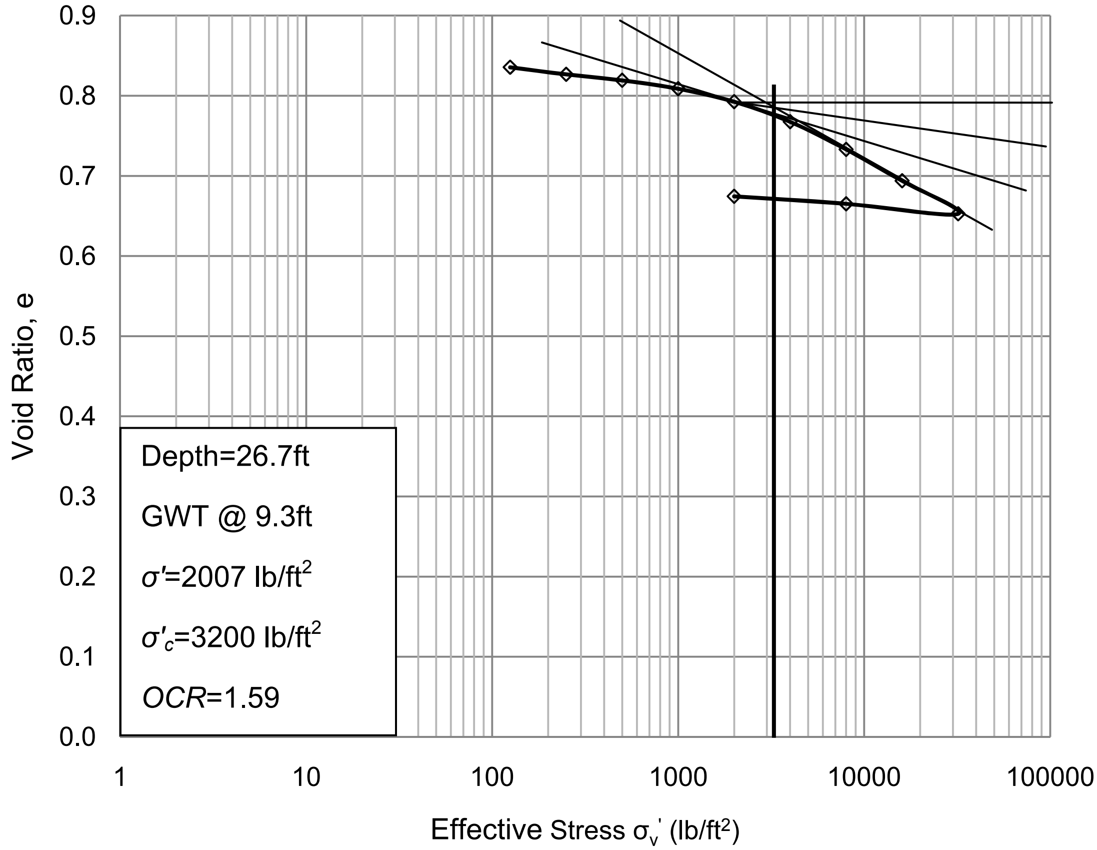

Figure B.4 Consolidation results for sample collected at 26.9ft from B-1 at the Walterboro Rest Area Ponds site.

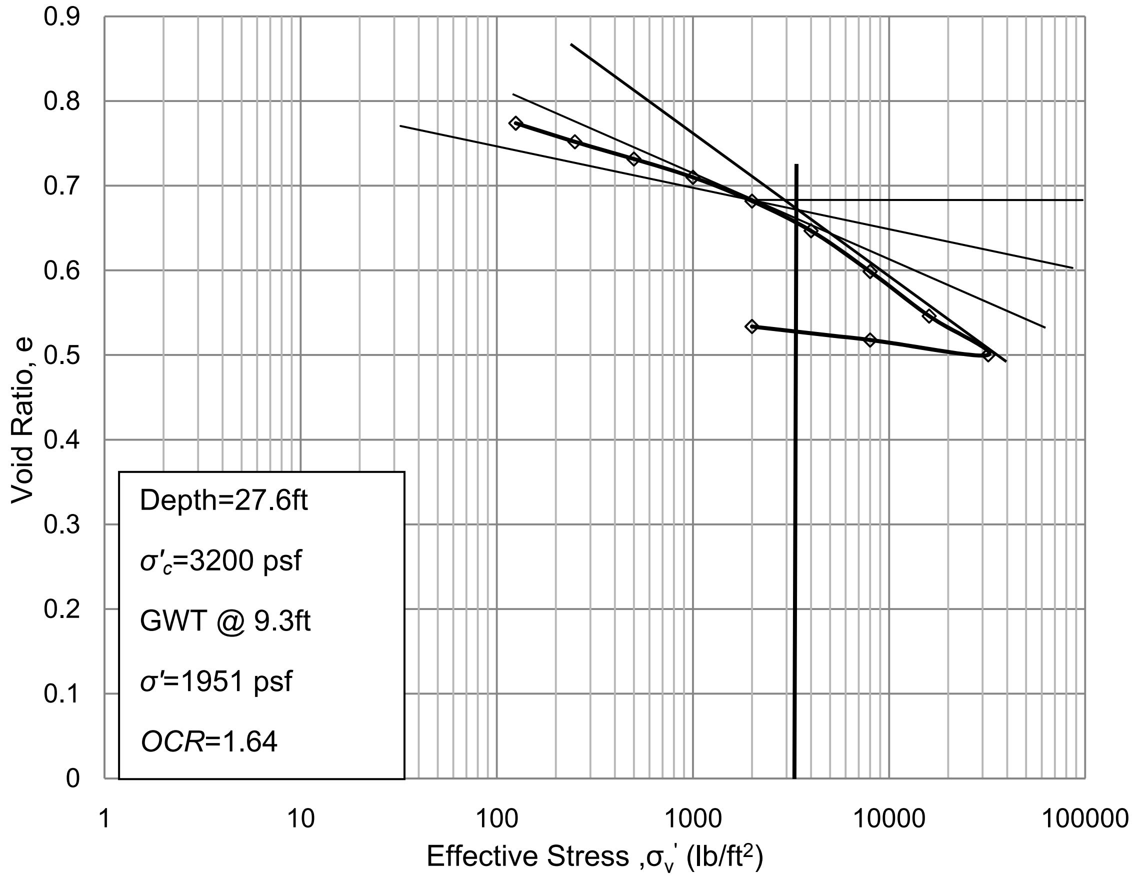

Figure B.5 Consolidation results for sample collected at 27.6ft from B-1 at the Walterboro Rest Area Ponds site.

Table B.9 Local site coordinates[a] for the geotechnical investigation at the Walterboro Rest Area Ponds site.

Point	X (ft)	Y (ft)
Corner of Fence by Gate	0	0
SC-1	294.3	-7.8
SC-2	482.1	-7.6
SC-3	540.1	-6.9
D-1	552.3	-7.3
B-1	528.7	-6.5
B-2	519.8	-6.8
B-3	510.8	-7.0
B-4 (Standpipe)	502.0	-6.7

[a] Map Coordinates: 32°48’15” N, 80°45’59” W

APPENDIX C
SUMMARY OF DATA FOR THE WALTERBORO LOWCOUNTRY SAND & GRAVEL SITE

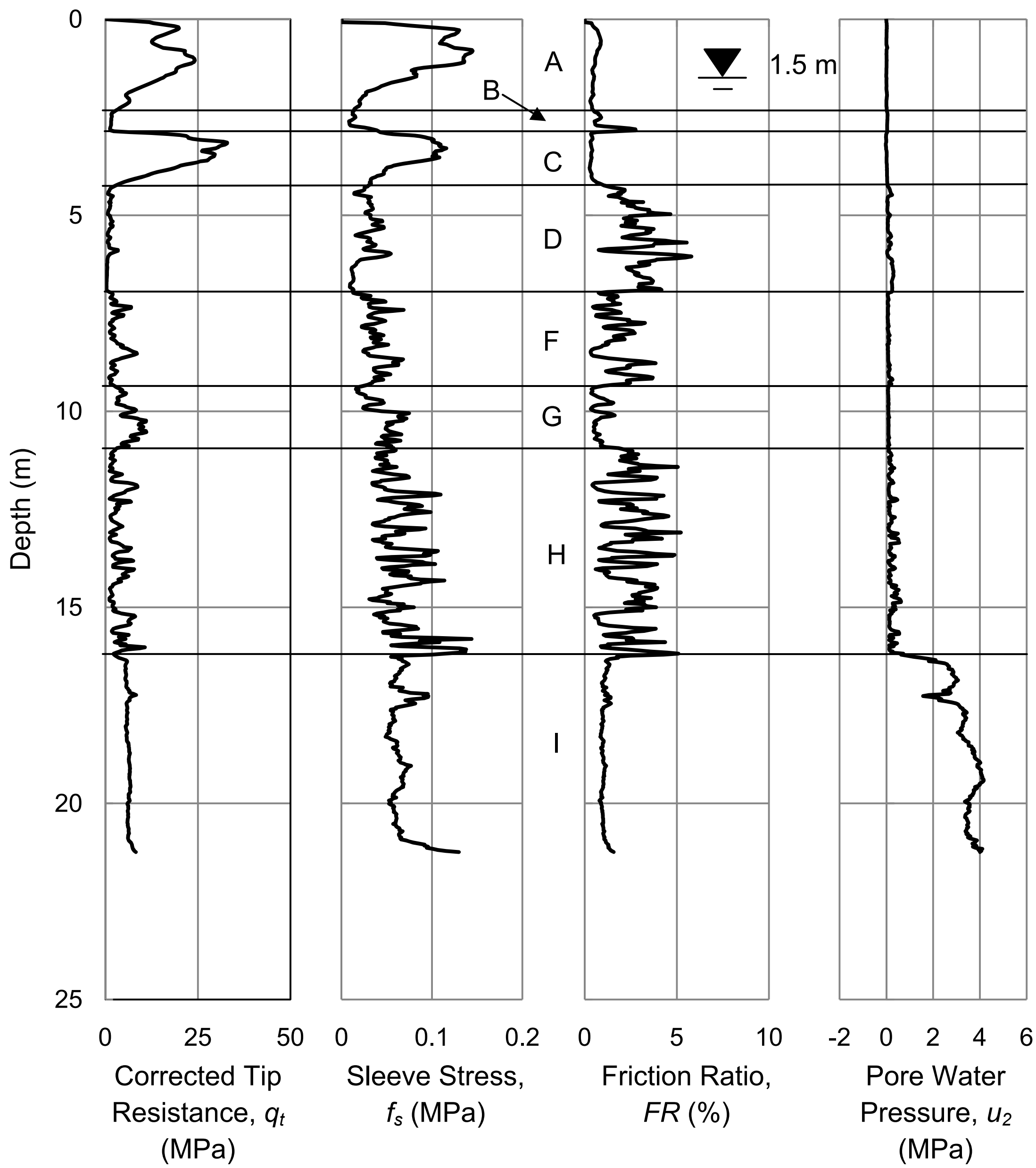

Figure C.1 Composite Profile of SCPT SC-1L at the Lowcountry Sand & Gravel site.

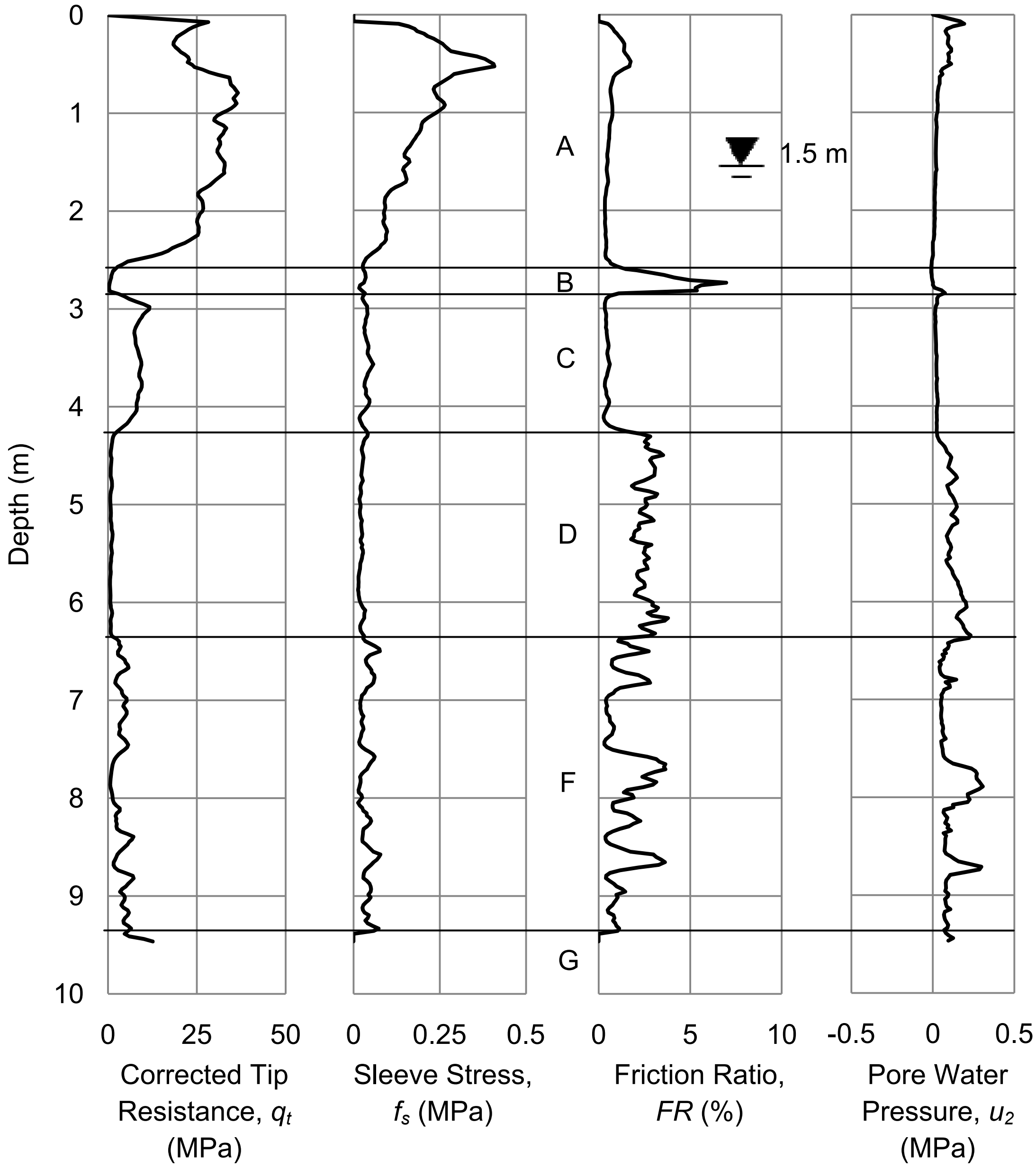

Figure C.2 Composite Profile of SCPT SC-2L at the Lowcountry Sand & Gravel site.

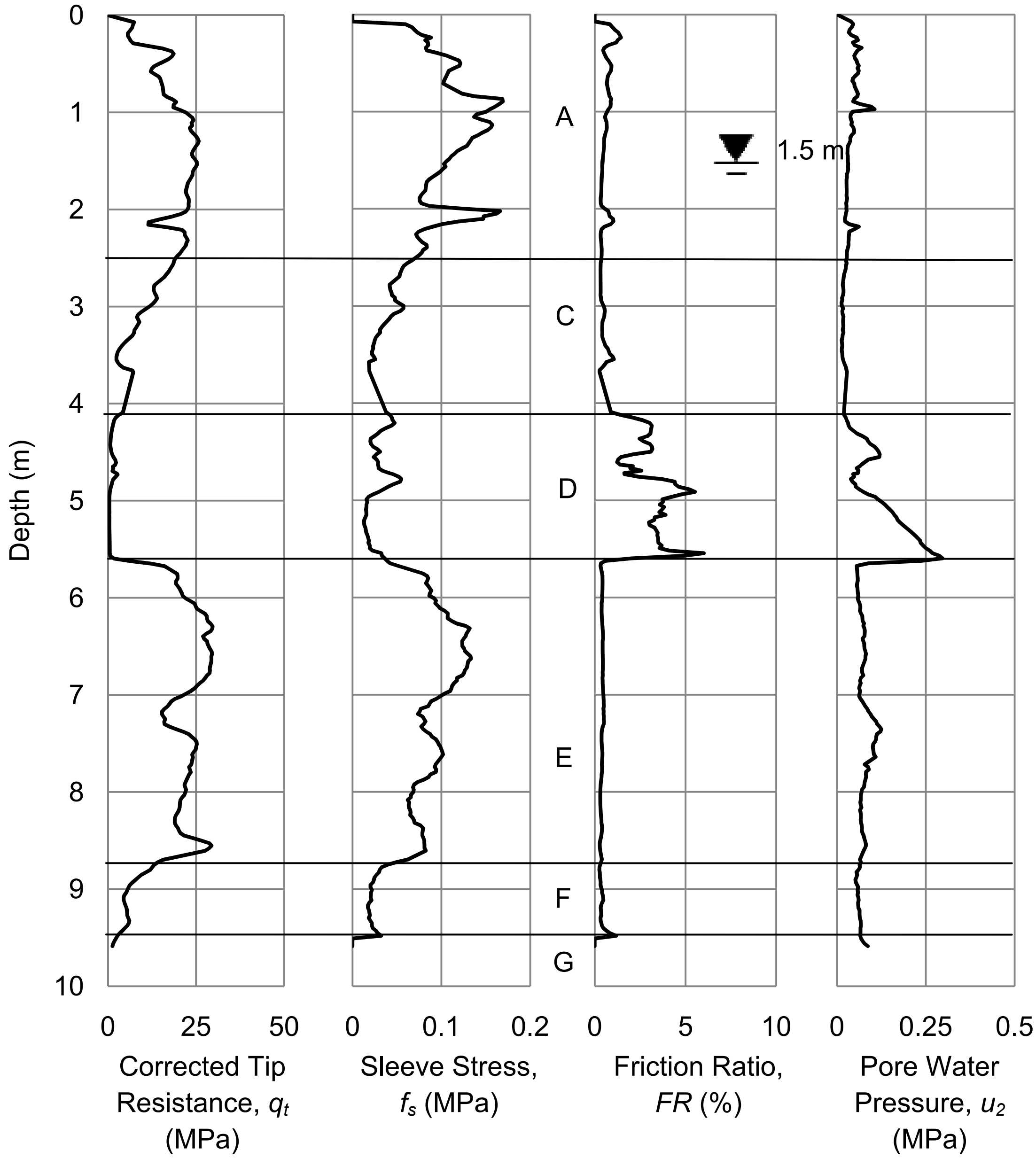

Figure C.3 Composite Profile of SCPT SC-3L at the Lowcountry Sand & Gravel site.

Table C.1 Results of DMT D-1L performed at the Lowcountry Sand & Gravel site

(Continued on following page)

Start of DMT		End of DMT		Average							
ΔA	ΔB	ΔA	ΔB	ΔA	ΔB	Z_m					
0.15	0.6	0.15	0.55	0.15	0.58	0	GWT: 4.6ft				
Depth (ft)	A (bar)[a]	B (bar)	C (bar)	P_1 (psf)	P_0 (psf)	σ'_{vo} (psf)[b]	q_t (tsf)	I_D	K_D	K_0	E_D (bar)
1	5.5	20.8	-	42250	10280	110	190.13	3.11	384.09	19.58	531
2	4.4	22.8	-	46428	7659	220	145.72	5.06	211.04	13.80	644
3	5.5	24.2	-	49353	9925	330	233.47	3.97	149.55	7.51	655
4	5.6	22.4	-	45592	10333	440	211.03	3.41	103.62	5.42	586
5	3.4	11.8	-	23449	6614	528	155.79	2.56	44.35	1.64	280
6	6.55	24.6	-	50188	12187	586	74.26	3.14	85.53	7.23	631
7	4.45	18.2	-	36819	8249	643	61.68	3.53	57.00	4.83	475
8	4.1	20	0	40579	7293	701	19.26	4.70	57.59	5.57	553
9	3.2	12.8	-	25538	6071	759	14.60	3.36	33.30	3.35	323
10	3.5	16.8	0	33894	6311	816	263.85	4.62	41.12	1.05	458
11	3.4	13.2	-	26374	6468	874	294.49	3.28	29.73	-0.17	331
12	4.4	16.6	-	33476	8306	931	255.44	3.21	35.45	1.00	418
13	1.3	3.3	-	5693	2896	989	120.98	1.18	5.23	1.20	46
14	2.35	8	0.05	15511	4708	1047	24.96	2.62	14.26	1.49	179
15	3.8	8	0.05	15511	7889	1104	15.41	1.05	13.46	2.20	127
16	2.55	7.2	0.05	13840	5230	1162	9.38	1.91	11.30	1.37	143
17	4.35	15.8	-	31805	8280	1219	17.29	3.13	25.45	2.65	391
18	4.2	15	-	30134	8035	1277	8.76	3.07	22.94	2.49	367
19	5.2	10.6	0.2	20942	10688	1335	15.40	1.05	15.02	2.35	170
20	4.7	7.6	1.7	14675	9904	1392	6.91	0.53	9.85	1.82	79
21	4.1	5.1	-	9453	8850	1450	4.75	0.08	5.81	1.29	10
22	4.1	6.05	1.6	11437	8750	1507	3.52	0.35	6.87	1.44	45
23	3.2	4.2	0.3	7573	6969	1565	15.67	0.10	4.10	1.00	10
24	3.5	14	0.3	28045	6604	1623	44.99	3.98	16.54	1.67	356
25	4.65	9.2	-	18018	9628	1680	32.48	1.00	9.97	1.84	139
26	5.95	18.6	0.2	37654	11497	1738	17.56	2.57	20.90	2.26	435
27	4.3	13.8	-	27627	8380	1795	29.00	2.76	14.61	1.60	320
28	3.65	14.6	0.45	29298	6870	1853	70.06	4.15	15.02	1.43	373
29	4.35	14	-	28045	8468	1911	20.52	2.82	13.88	1.59	325
30	5.75	14.2	0.5	28463	11518	1968	16.13	1.71	13.66	1.59	282
31	3.1	8.3	-	16138	6322	2026	43.79	2.10	7.15	0.84	163
32	3.4	15.4	0.55	30969	6238	2083	35.72	5.46	14.04	1.54	411

Table C.1 Continued

Depth (ft)	A (bar)[a]	B (bar)	C (bar)	P_1 (psf)	P_0 (psf)	σ'_{vo} (psf)[b]	q_t (tsf)	I_D	K_D	K_0[c]	E_D (bar)
33	5.5	19.4	-	39325	10427	2141	63.08	3.34	17.54	1.75	480
34	4.1	14.8	0.6	29716	7836	2199	99.55	3.65	12.68	1.13	364
35	4.05	14.6	-	29298	7748	2256	81.15	3.68	12.14	1.17	358
36	5.95	18	0.5	36401	11560	2314	35.07	2.59	14.89	1.64	413
37	7.4	27.2	0.75	55620	13780	2371	19.86	3.56	22.60	2.44	695
38	6.9	13.4	0.7	26791	14124	2429	25.46	1.05	10.17	1.86	210

[a] 1 bar=2089 psf

[b] Soil Unit Weight: 110psf above GWT, 120psf below GWT

[c] $K_0=0.376+0.095K_D-0.005q_t/\sigma_v'$ for sand, $I_D \geq 1.2$ (Baldi et al. 1986 as recommended by Marchetti et al. 2001); $K_0=(K_D/1.5)^{0.47}-0.6$ for clay and silt, $I_D<1.2$ (Marchetti 1980)

Table C.2 Measured shear wave velocity using true interval method for sounding SCPT SC-1L at the Lowcountry Sand & Gravel site.

Upper Geophone Depth (ft)	Lower Geophone Depth (ft)	Calculated V_s[a] (ft/s)	Standard Deviation[b] of V_s (ft/s)	Quality of Record
0.75	4.03	237	28	Fair
4.75	8.03	568	64	Good
7.75	11.03	576	23	Excellent
10.75	14.03	721	273	Fair
14.75	18.03	757	165	Fair
17.75	21.03	766	175	Fair
20.75	24.03	810	165	Fair
23.75	27.03	719	161	Fair
26.75	30.03	612	57	Very Good
30.75	34.03	592	78	Good
33.75	37.03	652	56	Very Good
36.75	40.03	671	27	Excellent
40.75	44.03	633	38	Very Good
43.75	47.03	630	42	Very Good
46.75	50.03	619	50	Very Good
49.75	53.03	556	39	Very Good
52.75	56.03	613	34	Very Good
56.75	60.03	643	64	Good
59.75	63.03	620	74	Good
62.75	66.03	642	55	Very Good
65.75	69.03	650	99	Fair to Good

[a] Calculated using travel times based on first crossover and first peak arrival times and horizontal distance between source and cone rod of 3.83 ft.
[b] Standard deviation based on four estimates of V_s determined from first crossovers and first peaks for two hits with opposite polarity.

Table C.3 Measured shear wave velocity using true interval method for sounding SCPT SC-2L at the Lowcountry Sand & Gravel site.

Upper Geophone Depth (ft)	Lower Geophone Depth (ft)	Calculated V_s[a] (ft/s)	Standard Deviation[b] of V_s (ft/s)	Quality of Record
0.75	4.03	-	-	Poor
4.75	8.03	660	47	Very Good
7.75	11.03	687	93	Good
10.75	14.03	754	51	Very Good
13.75	17.03	797	93	Good
16.75	20.03	747	33	Excellent
20.75	24.03	683	41	Very Good
23.75	27.03	691	44	Very Good
26.75	30.03	663	47	Very Good

[a] Calculated using travel times based on first crossover and first peak arrival times and horizontal distance between source and cone rod of 3.83 ft.
[b] Standard deviation based on four estimates of V_s determined from first crossovers and first peaks for two hits with opposite polarity.

Table C.4 Measured shear wave velocity using true interval method for sounding SCPT SC-3L at the Lowcountry Sand & Gravel site.

Upper Geophone Depth (ft)	Lower Geophone Depth (ft)	Calculated V_s[a] (ft/s)	Standard Deviation[b] of V_s (ft/s)	Quality of Record
1.75	5.03	397	104	Fair
4.75	8.03	519	36	Very Good
7.75	11.03	642	57	Very Good
10.75	14.03	689	25	Excellent
14.75	18.03	671	33	Excellent
17.75	21.03	602	48	Very Good
20.75	24.03	608	53	Very Good
23.75	27.03	558	48	Very Good
26.75	30.03	657	94	Good

[a] Calculated using travel times based on first crossover and first peak arrival times and horizontal distance between source and cone rod of 3.83 ft.
[b] Standard deviation based on four estimates of V_s determined from first crossovers and first peaks for two hits with opposite polarity.

Table C.5 Local site measurements for the geotechnical investigation at the Lowcountry Sand & Gravel site with reference points shown in Figure C.5.

Point	Point	Distance (ft)	Point	Point	Distance (ft)
Ref. 1	SC-1L	220.9	Ref. 2	SC-1L	296.6
Ref. 1	SC-2L	269.8	Ref. 2	SC-2L	259.1
Ref. 1	SC-3L	351.7	Ref. 2	SC-3L	230.2
Water's Edge	SC-1L	29.4	Water's Edge	SC-3L	29.2
Water's Edge	SC-2L	39.8	Water's Edge	D-1L	22
SC-1L	SC-2L	63.3	SC-2L	SC-3L	93.2
			SC-1L	D-1L	18.2

[a]Map coordinates: 32°51’39”N, 80°38’39”W

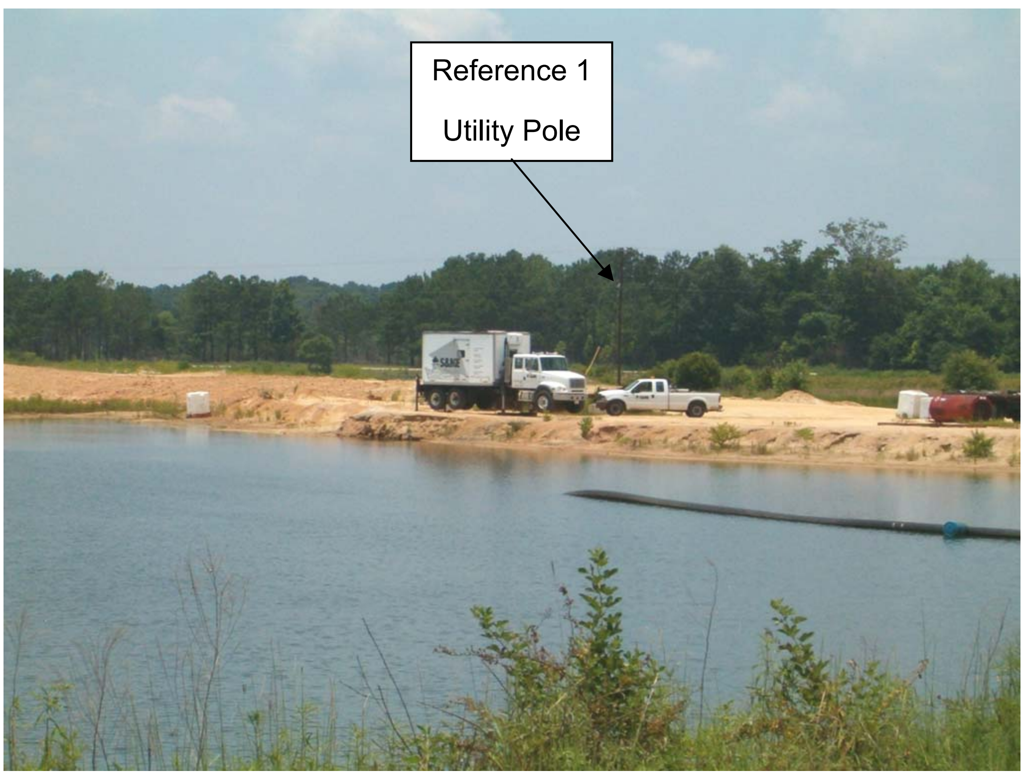

Figure C.4 Lowcountry Sand & Gravel site photograph showing location of Reference 1.

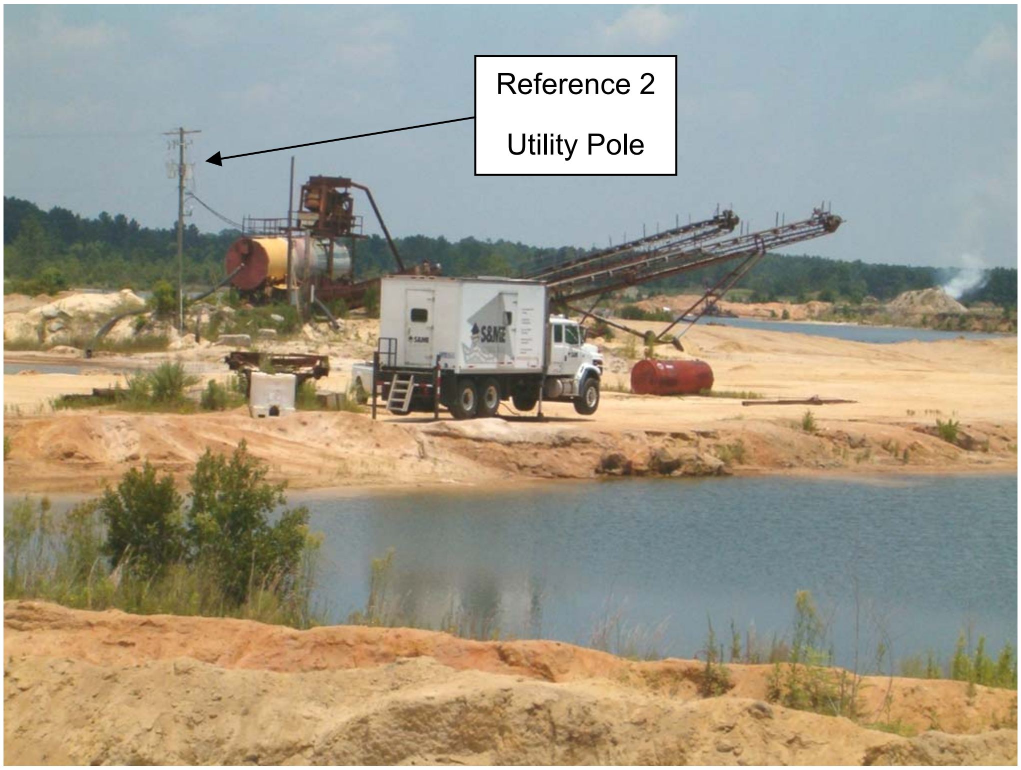

Figure C.5 Lowcountry Sand & Gravel site photograph showing location of Reference 2.

APPENDIX D
CPT DATA FROM TESTING AT THE HOBCAW BORROW PIT, REST AREA, AND LOWCOUNTRY SAND & GRAVEL SITES

Table D.1 CPT Data for HB-1 at the Hobcaw Borrow Pit site.

z	f_s	q_u	q_t	u_2	z	f_s	q_u	q_t	u_2
(ft)	(tsf)	(tsf)	(tsf)	(tsf)	(ft)	(tsf)	(tsf)	(tsf)	(tsf)
0.00	0	0	0	0	4.62	0.08	80.8	80.8	0.01
0.23	0	24.5	24.5	0.04	4.73	0.09	79.6	79.6	0.02
0.36	0.06	34.2	34.2	0.04	4.85	0.08	78.5	78.5	0.01
0.50	0.07	42.9	42.9	0.04	4.96	0.09	77.6	77.6	0.01
0.63	0.07	50.1	50.1	0.04	5.08	0.08	76.8	76.8	0.01
0.76	0.07	57.6	57.7	0.04	5.19	0.09	76.8	76.8	0.02
0.88	0.07	63.8	63.9	0.03	5.30	0.08	76.6	76.6	0.02
1.01	0.07	67.4	67.4	0.03	5.43	0.09	75.8	75.8	0.01
1.13	0.07	69.7	69.7	0.02	5.54	0.09	75.9	75.9	0.02
1.25	0.07	71.2	71.2	0.03	5.66	0.09	76.2	76.2	0.02
1.37	0.07	70.4	70.4	0.02	5.77	0.08	76.2	76.2	0.02
1.49	0.07	69.4	69.4	0.02	5.88	0.08	76.9	76.9	0.02
1.61	0.06	67.1	67.1	0.01	5.99	0.08	78.4	78.4	0.02
1.73	0.08	65.6	65.6	0.01	6.10	0.09	78.9	78.9	0.02
1.85	0.08	65	65	0.02	6.21	0.08	77.5	77.5	0.01
1.97	0.07	64.2	64.2	0.02	6.33	0.08	75.4	75.4	0.01
2.00	0.07	16.9	16.9	0.03	6.44	0.08	73.9	73.9	0.01
2.12	0.08	63.6	63.6	0.02	6.56	0.09	72.7	72.7	0.02
2.24	0.08	65.3	65.4	0.03	6.67	0.09	71.7	71.7	0.03
2.36	0.08	69.3	69.3	0.02	6.78	0.08	69.5	69.5	0.01
2.47	0.08	75.8	75.8	0.02	6.89	0.08	68.7	68.7	0.02
2.59	0.08	82.9	82.9	0.03	7.01	0.08	67.5	67.5	0.02
2.71	0.08	88.6	88.6	0.02	7.12	0.08	67.1	67.1	0.02
2.82	0.08	91.9	91.9	0.02	7.23	0.09	67.1	67.1	0.02
2.93	0.07	93.1	93.1	0.01	7.34	0.09	67.5	67.5	0.02
3.04	0.08	93.8	93.8	0.02	7.46	0.09	67.4	67.4	0.02
3.16	0.08	94.6	94.6	0.01	7.57	0.09	68.2	68.2	0.02
3.27	0.08	94	94	0.01	7.77	0.08	70.4	70.4	0.02
3.38	0.09	93.2	93.2	0.02	7.88	0.08	71.6	71.6	0.02
3.50	0.08	91.7	91.7	0.01	7.99	0.08	73	73	0.02
3.61	0.09	91	91	0.02	8.11	0.08	74.5	74.5	0.02
3.72	0.09	90.1	90.1	0.02	8.22	0.08	75.5	75.5	0.02
3.83	0.08	88.1	88.1	0	8.33	0.08	76.3	76.3	0.03
3.95	0.09	87.2	87.2	0.02	8.44	0.08	76.4	76.4	0.02
4.06	0.09	86.3	86.4	0.02	8.55	0.08	77.8	77.8	0.03
4.17	0.08	84.7	84.7	0.01	8.65	0.08	77.2	77.2	0.03
4.28	0.07	83.3	83.3	0	8.76	0.08	78.6	78.6	0.02
4.40	0.08	82.4	82.4	0.01	8.87	0.08	79.1	79.1	0.04
4.51	0.08	81.2	81.2	0.01	8.98	0.08	77.1	77.1	0.04

Table D.1 Continued

z	f_s	q_u	q_t	u_2	z	f_s	q_u	q_t	u_2
(ft)	(tsf)	(tsf)	(tsf)	(tsf)	(ft)	(tsf)	(tsf)	(tsf)	(tsf)
9.09	0.08	73.5	73.5	0.03	13.55	0.08	66.2	66.2	0.05
9.20	0.08	69.4	69.4	0.02	13.66	0.08	68.6	68.6	0.02
9.31	0.08	66.8	66.8	0.03	13.77	0.07	69.3	69.3	0
9.42	0.08	64.1	64.1	0.03	13.88	0.08	69.6	69.6	0.01
9.53	0.08	62.2	62.2	0.04	13.99	0.07	69.7	69.7	0.01
9.65	0.08	60.9	60.9	0.03	14.10	0.08	71	71	0.04
9.76	0.08	60.9	60.9	0.04	14.21	0.07	71.4	71.4	0.02
9.87	0.08	62.4	62.5	0.04	14.32	0.08	73.1	73.1	0.03
9.98	0.08	64.2	64.2	0.03	14.43	0.08	74.4	74.4	0.03
10.10	0.07	65.4	65.4	0.02	14.54	0.08	76	76	0.03
10.21	0.08	67.2	67.2	0.04	14.65	0.08	77.6	77.6	0.04
10.32	0.08	68.9	68.9	0.04	14.75	0.08	78.7	78.7	0.06
10.43	0.08	71.3	71.3	0.04	14.86	0.08	78.4	78.4	0.05
10.54	0.08	73.5	73.5	0.05	14.97	0.07	78.7	78.7	0.05
10.65	0.08	75.3	75.3	0.04	15.08	0.08	81.1	81.1	0.08
10.76	0.08	77	77	0.05	15.19	0.08	84.1	84.1	0.09
10.87	0.08	78.5	78.5	0.05	15.23	0.08	12.9	12.9	0.13
10.98	0.08	79.3	79.3	0.06	15.31	0.07	86	86	0.1
11.09	0.08	79.7	79.7	0.05	15.42	0.07	89	89	0.1
11.20	0.08	79.5	79.5	0.05	15.53	0.07	91.6	91.6	0.11
11.31	0.08	78.5	78.5	0.05	15.64	0.07	94.2	94.2	0.11
11.42	0.08	77.8	77.8	0.06	15.74	0.07	96	96.1	0.12
11.53	0.08	76	76.1	0.05	15.85	0.07	97.4	97.5	0.13
11.64	0.08	75.4	75.4	0.06	15.96	0.07	98.3	98.3	0.12
11.75	0.08	73.5	73.5	0.07	16.06	0.07	99.1	99.1	0.13
11.86	0.08	70.3	70.3	0.07	16.17	0.07	100.8	100.8	0.13
11.91	0.08	67.3	67.3	0.07	16.28	0.08	101.2	101.2	0.14
12.02	0.08	63.8	63.9	0.06	16.39	0.08	100.5	100.5	0.14
12.13	0.08	60.1	60.2	0.08	16.50	0.07	100.5	100.5	0.15
12.24	0.08	58.1	58.1	0.09	16.60	0.08	98.6	98.6	0.15
12.35	0.08	58	58.1	0.07	16.71	0.08	96	96	0.16
12.46	0.08	60.6	60.6	0.07	16.82	0.08	92.9	93	0.17
12.57	0.07	63.4	63.4	0.04	16.93	0.08	90.4	90.4	0.16
12.68	0.08	65.3	65.3	0.02	17.03	0.07	89	89	0.17
12.78	0.08	65.4	65.4	0	17.14	0.07	87.6	87.6	0.17
12.89	0.08	65.2	65.2	0.02	17.25	0.08	86.8	86.9	0.18
13.00	0.08	63.4	63.4	0.03	17.36	0.08	87.4	87.4	0.18
13.11	0.08	60.9	60.9	0.05	17.47	0.08	89.2	89.2	0.19
13.22	0.08	59	59	0.05	17.57	0.08	92.3	92.3	0.19
13.33	0.08	59.9	60	0.06	17.68	0.08	95	95.1	0.2
13.44	0.08	62.8	62.8	0.05	17.79	0.08	96.7	96.7	0.21

Table D.1 Continued

z	f_s	q_u	q_t	u_2	z	f_s	q_u	q_t	u_2
(ft)	(tsf)	(tsf)	(tsf)	(tsf)	(ft)	(tsf)	(tsf)	(tsf)	(tsf)
17.90	0.08	96.3	96.4	0.21	22.49	0.07	106.4	106.5	0.37
18.01	0.08	95.4	95.4	0.21	22.60	0.07	107.9	108	0.38
18.12	0.07	94.2	94.2	0.21	22.70	0.07	108.3	108.3	0.38
18.22	0.07	90.6	90.7	0.21	22.81	0.07	106.7	106.8	0.38
18.33	0.07	83	83.1	0.22	22.91	0.07	105.5	105.6	0.38
18.44	0.08	83.3	83.3	0.22	23.02	0.08	105.3	105.3	0.4
18.51	0.07	82	82.1	0.19	23.12	0.07	101.7	101.8	0.38
18.62	0.07	78.3	78.3	0.22	23.23	0.07	97.1	97.1	0.39
18.73	0.07	70.5	70.6	0.23	23.33	0.07	94.3	94.4	0.39
18.84	0.07	61.2	61.3	0.24	23.44	0.07	93.9	94	0.39
18.95	0.07	52	52	0.24	23.54	0.07	93.2	93.3	0.39
19.04	0.06	45.9	46	0.23	23.65	0.07	92.8	92.9	0.4
19.15	0.07	40.8	40.8	0.26	23.75	0.07	92.1	92.2	0.4
19.27	0.07	36.5	36.5	0.33	23.86	0.07	89.8	89.9	0.4
19.38	0.07	31	31.1	0.43	23.96	0.07	86.7	86.8	0.4
19.50	0.07	29.4	29.5	0.68	24.07	0.07	84.5	84.5	0.4
19.62	0.07	34.5	34.7	1.33	24.17	0.07	83	83	0.42
19.73	0.07	50.5	50.7	1.08	24.28	0.07	80	80.1	0.41
19.92	0.07	56.8	56.9	0.39	24.38	0.07	77.8	77.8	0.41
20.03	0.07	64	64	0.36	24.49	0.07	73.5	73.5	0.41
20.14	0.06	53	53.1	0.36	24.60	0.07	67.9	68	0.42
20.25	0.07	45.8	45.8	0.37	24.70	0.07	64.8	64.8	0.42
20.37	0.07	49.3	49.3	0.38	24.81	0.07	63.7	63.8	0.42
20.48	0.07	40.7	40.8	0.37	24.92	0.07	63	63.1	0.42
20.59	0.07	31	31	0.37	25.02	0.07	64.9	65	0.43
20.70	0.07	42.2	42.2	0.37	25.15	0.07	66.1	66.2	0.43
20.82	0.06	44.8	44.9	0.52	25.25	0.08	67.8	67.9	0.45
20.93	0.07	40.5	40.6	0.47	25.36	0.07	68.3	68.4	0.43
21.04	0.07	36.4	36.5	0.48	25.47	0.07	69.2	69.3	0.44
21.15	0.07	41.6	41.7	0.54	25.58	0.08	70.4	70.4	0.47
21.26	0.07	62.9	63	0.6	25.68	0.07	67.7	67.8	0.44
21.37	0.07	75.8	75.9	0.57	25.79	0.06	66.3	66.4	0.44
21.48	0.07	97.5	97.6	0.55	25.90	0.07	64.8	64.9	0.44
21.58	0.07	113.7	113.8	0.55	26.01	0.07	62.4	62.5	0.45
21.69	0.07	117.4	117.5	0.54	26.12	0.06	58.9	58.9	0.44
21.97	0.07	111.6	111.7	0.39	26.23	0.07	54.2	54.3	0.44
22.07	0.07	108.1	108.1	0.38	26.34	0.08	56	56.1	0.47
22.18	0.07	106.6	106.7	0.37	26.45	0.07	66.1	66.2	0.45
22.28	0.07	105.9	106	0.37	26.56	0.07	86.7	86.8	0.45
22.39	0.07	105.9	106	0.37	26.67	0.07	92	92.1	0.46

Table D.1 Continued

z	f_s	q_u	q_t	u_2	z	f_s	q_u	q_t	u_2
(ft)	(tsf)	(tsf)	(tsf)	(tsf)	(ft)	(tsf)	(tsf)	(tsf)	(tsf)
26.77	0.07	87.6	87.7	0.47	31.76	0.07	9.4	9.9	2.43
26.88	0.07	81.8	81.9	0.46	31.95	0.06	5.9	6.1	1.16
26.99	0.06	75.6	75.7	0.45	32.09	0.06	4.9	5.2	1.5
27.10	0.06	70	70.1	0.45	32.21	0.07	7.1	7.4	1.76
27.20	0.08	66.1	66.2	0.47	32.35	0.06	12.9	13.3	1.88
27.31	0.07	62	62.1	0.45	32.47	0.07	20	20.3	1.6
27.42	0.06	65.1	65.2	0.46	32.60	0.08	28.1	28.4	1.28
27.53	0.06	79.7	79.8	0.48	32.72	0.07	32.8	33	1.03
27.63	0.07	79.1	79.2	0.48	32.85	0.07	35.6	35.8	0.96
27.74	0.08	61.5	61.6	0.51	32.97	0.06	40.1	40.2	0.87
27.85	0.06	38.4	38.5	0.45	33.10	0.07	44.1	44.3	0.79
27.96	0.06	23.9	23.9	0.43	33.22	0.07	51.3	51.4	0.78
28.07	0.07	17.7	17.8	0.43	33.34	0.07	60.4	60.6	0.78
28.19	0.06	14.9	15	0.49	33.46	0.07	65	65.1	0.78
28.30	0.06	13.4	13.5	0.61	33.58	0.07	66.1	66.3	0.75
28.58	0.06	11.5	11.9	2.03	33.70	0.07	66	66.2	0.73
28.70	0.09	13.9	14.3	2.07	33.82	0.08	68.2	68.3	0.72
28.83	0.06	12.5	12.9	2.1	33.94	0.07	69.6	69.7	0.71
28.95	0.06	9.4	9.9	2.27	34.06	0.06	65	65.2	0.69
29.08	0.07	7.4	7.9	2.49	34.18	0.07	60.8	60.9	0.69
29.20	0.06	6.2	6.8	2.8	34.29	0.07	59.1	59.3	0.71
29.33	0.06	5.6	6.2	3.09	34.41	0.06	62.8	63	0.71
29.45	0.06	5.3	5.9	3.13	34.53	0.07	67.5	67.6	0.72
29.58	0.1	7.7	8.3	3.24	34.65	0.07	66.7	66.8	0.74
29.71	0.07	6.9	7.6	3.25	34.76	0.07	62.3	62.5	0.75
29.83	0.06	6.5	7.1	3.26	34.88	0.06	58.7	58.8	0.75
29.96	0.07	6.3	6.9	3.39	35.00	0.07	55.9	56.1	0.76
30.09	0.07	6.3	7	3.57	35.11	0.07	52.6	52.8	0.76
30.22	0.1	8.2	8.9	3.75	35.19	0.07	48.8	48.9	0.68
30.34	0.07	6.3	7.1	3.76	35.31	0.06	39.1	39.2	0.69
30.47	0.06	6.2	7	3.81	35.42	0.06	33.1	33.2	0.69
30.60	0.06	6.3	7	3.86	35.54	0.06	32.9	33	0.71
30.73	0.07	6.3	7	3.89	35.66	0.06	39.3	39.4	0.72
30.85	0.06	5.7	6.5	3.89	35.77	0.07	65.4	65.5	0.71
30.98	0.06	5.5	6.3	3.87	35.88	0.07	93.5	93.7	0.7
31.11	0.07	5.4	6.1	3.85	35.99	0.06	105.4	105.6	0.72
31.24	0.07	5	5.7	3.83	36.10	0.07	104.3	104.5	0.73
31.37	0.07	5.3	6	3.77	36.20	0.07	96.9	97.1	0.73
31.50	0.06	6.7	7.4	3.43	36.31	0.07	84.7	84.9	0.72
31.63	0.08	10.4	10.9	2.92	36.42	0.07	65.8	65.9	0.68

Table D.1 Continued

z	f_s	q_u	q_t	u_2	z	f_s	q_u	q_t	u_2
(ft)	(tsf)	(tsf)	(tsf)	(tsf)	(ft)	(tsf)	(tsf)	(tsf)	(tsf)
36.53	0.06	51.3	51.4	0.66	40.45	0.07	112.8	113	0.9
36.65	0.07	51.1	51.2	0.66	40.55	0.23	81.7	81.9	0.88
36.76	0.07	67.1	67.2	0.74	40.66	0.54	54.5	54.7	0.87
36.87	0.07	109	109.2	0.79	40.76	0.58	36.5	36.7	0.96
36.97	0.07	149.2	149.3	0.81	40.86	0.47	28.9	29.1	0.96
37.07	0.07	162	162.1	0.77	40.97	0.35	22.8	23	1.11
37.18	0.07	164.1	164.2	0.73	41.07	0.27	17.7	18	1.32
37.28	0.06	163.6	163.8	0.75	41.18	0.17	15.8	16.2	2.17
37.38	0.06	161.1	161.3	0.75	41.28	0.08	13.3	14.2	4.66
37.48	0.06	154.8	155	0.75	41.39	0.08	13.4	14.6	6.2
37.58	0.07	148.6	148.7	0.75	41.49	0.07	20	21.6	8.07
37.68	0.06	141.4	141.5	0.73	41.60	0.07	86.2	87.6	7.12
37.79	0.07	134.9	135.1	0.71	41.69	0.08	171.3	171.7	1.89
37.89	0.07	131.5	131.7	0.7	41.74	0.1	175.5	175.8	1.32
37.99	0.07	133.7	133.8	0.69	41.85	0.15	213.6	213.8	0.94
38.09	0.07	141.9	142	0.7	41.95	0.12	216.1	216.2	0.97
38.19	0.06	145	145.1	0.72	42.04	0.1	208.1	208.3	0.98
38.29	0.06	144.3	144.4	0.73	42.14	0.12	196	196.2	0.98
38.40	0.07	149	149.2	0.76	42.23	0.24	174.4	174.6	0.97
38.44	0.07	27.6	27.8	0.91	42.33	0.44	133.2	133.4	0.94
38.47	0.06	143.9	144	0.66	42.43	0.59	91	91.2	0.93
38.57	0.07	163.6	163.7	0.75	42.54	0.63	60.3	60.4	0.9
38.67	0.07	181.2	181.4	0.78	42.64	0.66	46.2	46.4	0.92
38.77	0.07	194.1	194.2	0.8	42.74	0.77	44.3	44.5	1
38.86	0.06	194.4	194.5	0.81	42.85	0.78	44.6	44.8	1.12
38.96	0.07	190	190.2	0.81	42.95	0.64	36.3	36.5	1.08
39.06	0.07	185.7	185.8	0.78	43.06	0.49	29.1	29.3	1.22
39.16	0.07	176.8	177	0.77	43.16	0.37	24	24.3	1.63
39.25	0.06	158.6	158.8	0.78	43.24	0.32	28.8	29.2	2.08
39.35	0.07	145.2	145.4	0.77	43.41	0.22	25.6	26	2.09
39.45	0.06	132.1	132.2	0.75	43.52	0.19	18.3	18.8	2.2
39.55	0.06	120.8	120.9	0.76	43.63	0.15	15.2	15.7	2.47
39.65	0.06	113.3	113.5	0.78	43.73	0.1	13.4	13.9	2.79
39.75	0.06	111.3	111.4	0.79	43.84	0.08	12.3	12.9	2.97
39.85	0.07	114.6	114.7	0.84	43.95	0.08	11.7	12.3	3.14
39.96	0.07	121.1	121.3	0.85	44.06	0.08	11.4	12	3.28
40.06	0.06	126.5	126.7	0.88	44.16	0.09	11.8	12.4	3.45
40.16	0.07	132.1	132.3	0.9	44.27	0.08	13.6	14.3	3.61
40.25	0.07	139.2	139.4	0.91	44.38	0.08	15.4	16.1	3.7
40.35	0.07	135.7	135.9	0.92	44.49	0.08	16	16.7	3.76

Table D.1 Continued

z	f_s	q_u	q_t	u_2	z	f_s	q_u	q_t	u_2
(ft)	(tsf)	(tsf)	(tsf)	(tsf)	(ft)	(tsf)	(tsf)	(tsf)	(tsf)
44.60	0.08	15	15.7	3.79	48.29	1.67	99.4	100.3	4.83
44.71	0.1	13.3	14.1	4.1	48.51	1.26	38.7	39.6	4.84
44.82	0.11	22.7	23.6	4.35	48.60	1.75	159.3	160.9	8.33
44.93	0.21	43.2	44	4.12	48.70	1.96	98.6	99.6	4.84
45.03	0.44	37.8	38.3	2.45	48.80	1.74	91.6	92	2
45.15	0.54	39.8	40.1	1.37	48.89	1.62	80.5	80.9	2.36
45.25	0.73	55.1	55.5	1.99	48.99	1.66	55.8	56.4	3.09
45.36	0.93	87.3	87.5	1.38	49.09	2.08	57.9	59.1	6.34
45.46	2.01	125.6	125.8	1.28	49.19	2.35	112.6	114.1	7.56
45.55	1.92	220.3	220.6	1.36	49.28	2.39	152.9	154.2	6.43
45.65	1.14	279.9	280.1	1.18	49.38	2.23	144	144.3	1.53
45.74	0.83	363.4	363.6	1.17	49.47	1.81	82	82.3	1.57
45.83	1.6	394.3	394.5	0.78	49.57	1.42	58.1	58.4	1.54
46.06	2.71	322.2	322.5	1.43	49.67	1.25	45.5	46	2.48
46.16	2.88	302.2	302.4	1.12	49.77	1.12	43.3	44	3.5
46.25	3.04	325.5	325.7	1.14	49.87	0.95	47.1	47.9	4.35
46.35	2.64	312.2	312.4	1.13	49.96	0.88	55.2	56.2	5.35
46.44	2.08	260.1	260.4	1.38	50.06	1.1	48.5	50	7.74
46.54	2.33	192.9	193.1	1.24	50.16	1.66	49.8	51.1	7.07
46.64	2.77	156.6	156.8	0.69	50.26	1.86	93.3	94.9	8.2
46.74	2.26	106.3	106.4	0.59	50.36	2.89	118.2	119.6	6.97
46.85	1.93	106.2	106.4	0.79	50.45	3.72	212.1	213	4.9
46.95	2.12	50.8	51.1	1.46	50.54	3.87	176.5	177.3	4.35
47.06	1.93	35.6	36.3	3.4	50.64	4.06	142.9	143.1	1.03
47.16	1.23	31.6	32.6	4.95	50.73	4.34	121.3	121.7	2.08
47.27	0.85	58.1	59	4.42	50.82	4.72	195.2	196.3	5.65
47.37	0.77	42.3	42.3	-0.03	50.92	4.47	164.8	165.4	2.8
47.48	1.48	31.2	31.6	1.62	51.01	4.12	139.3	139.7	2.07
47.58	2.44	72.1	72.7	2.82	51.10	3.67	134.2	134.8	3.01
47.68	2.5	119.4	120	3.25	51.20	3.31	92.1	92.7	3.01
47.79	2.74	114.8	115.1	1.27	51.29	0	112.4	113.3	4.51
47.89	3.1	91.2	92.1	4.93	51.39	0	114.8	116	6.26
47.99	2.69	115.4	116	3.18	51.48	0	95.3	96.2	4.78
48.09	2.16	75.8	76.1	1.43	51.57	0	89.1	90.9	9.37
48.19	1.73	75.1	75.6	3.08	51.57	0	89.1	90.9	9.37

Table D.2 CPT Data for HB-2 at the Hobcaw Borrow Pit site.

z	f_s	q_u	q_t	u_2	z	f_s	q_u	q_t	u_2
(ft)	(tsf)	(tsf)	(tsf)	(tsf)	(ft)	(tsf)	(tsf)	(tsf)	(tsf)
0.00	0	0	0	0	5.14	0.63	135	135.1	0.05
0.41	0.01	55.5	55.6	0.04	5.25	0.62	134.1	134.2	0.04
0.54	0.02	57.1	57.1	0.04	5.35	0.63	133.2	133.2	0.02
0.66	0.02	59.5	59.5	0.04	5.46	0.63	132.4	132.4	0.04
0.79	0.02	59.9	59.9	0.05	5.57	0.67	133.3	133.3	0.1
0.92	0	58	58	0.01	5.68	0.62	128.2	128.2	0.04
1.05	0	56.5	56.5	0.01	5.78	0.63	128.3	128.3	0.07
1.17	0	54.6	54.6	0.02	5.89	0.6	127.1	127.1	0.07
1.30	0.01	54	54	0.01	6.00	0.6	128.8	128.9	0.08
1.43	0	52	52	0	6.11	0.59	129.7	129.7	0.02
1.76	0.01	48	48	0.02	6.22	0.6	133.9	133.9	0.01
1.89	0.01	46.8	46.8	0.02	6.33	0.64	140.1	140.1	0.05
2.02	0	48.5	48.5	0.01	6.43	0.63	142.3	142.3	0.03
2.15	0.01	57	57	0.03	6.54	0.68	147.8	147.8	0.06
2.27	0.02	72.2	72.2	0.04	6.65	0.74	154.5	154.5	0.08
2.39	0.01	86.2	86.2	0.01	6.75	0.72	156.6	156.6	0.04
2.51	0	94.3	94.3	0.04	6.86	0.75	162.5	162.5	0.03
2.62	0	97.2	97.3	0.03	6.97	0.78	166.1	166.1	0.04
2.74	0.01	96.4	96.4	0.04	7.07	0.83	168.2	168.2	0.05
2.85	0	96	96	0.03	7.18	0.87	170.5	170.5	0.05
2.97	0	97	97	0.02	7.28	0.89	171.2	171.2	0.02
3.08	0.03	97.1	97.1	0.04	7.38	0.91	171.2	171.3	0.06
3.20	0.03	101.8	101.8	0.05	7.49	0.89	168.1	168.2	0.04
3.31	0.03	105.4	105.4	0.03	7.59	0.85	165.3	165.4	0.05
3.42	0.03	105.5	105.5	0.04	7.70	0.8	164.1	164.1	0.03
3.54	0.06	108.6	108.6	0.02	7.80	0.75	163.7	163.7	0.05
3.65	0.08	112.9	112.9	0.03	7.91	0.72	161.7	161.7	0.04
3.76	0.08	112.9	112.9	0.02	8.01	0.31	159.7	159.7	0.04
3.87	0.12	114.2	114.2	0.02	8.12	0.46	157.9	157.9	0.06
3.98	0.18	119	119	0.02	8.22	0.42	153.2	153.2	0.03
4.09	0.24	125.9	125.9	0.02	8.32	0.41	148.4	148.4	0.04
4.20	0.29	128.2	128.2	0.04	8.38	0.4	34.8	34.8	0.06
4.31	0.34	130.8	130.8	0	8.43	0.39	135.4	135.4	0.04
4.42	0.4	134.7	134.7	0.01	8.54	0.38	128.5	128.5	0.04
4.53	0.49	138.1	138.1	0.03	8.64	0.36	119.1	119.1	0.05
4.64	0.59	142.1	142.1	0.03	8.75	0.33	110.7	110.7	0.03
4.74	0.62	141.4	141.4	0.02	8.85	0.3	105.4	105.4	0.04
4.85	0.65	140.7	140.7	0.01	8.96	0.25	102.6	102.6	0.03
4.95	0.67	129.6	129.6	0.06	9.07	0.22	101.6	101.6	0.03
5.03	0.64	136.2	136.2	0.06	9.18	0.19	101.5	101.5	0.02

Table D.2 Continued

z	f_s	q_u	q_t	u_2	z	f_s	q_u	q_t	u_2
(ft)	(tsf)	(tsf)	(tsf)	(tsf)	(ft)	(tsf)	(tsf)	(tsf)	(tsf)
9.29	0.18	102.1	102.1	0	13.61	0.04	69.6	69.6	-0.05
9.39	0.19	103	103	0.01	13.72	0.04	69.9	69.9	-0.05
9.50	0.2	103.4	103.4	0.01	13.83	0.04	71	71	-0.05
9.61	0.21	103.4	103.4	0	13.94	0.04	73.4	73.4	-0.05
9.72	0.24	103.5	103.5	-0.01	14.05	0.04	76.7	76.7	-0.06
9.82	0.27	103.2	103.2	0.01	14.16	0.06	81.7	81.7	-0.05
9.93	0.28	101.5	101.5	0	14.27	0.05	86.2	86.2	-0.04
10.04	0.3	99.2	99.2	0	14.38	0.07	89.3	89.3	-0.06
10.15	0.3	96	96	0	14.49	0.09	92.1	92.1	-0.04
10.26	0.3	93	93	0	14.60	0.09	91	91	-0.05
10.34	0.31	91.2	91.2	0	14.71	0.1	88.5	88.5	-0.04
10.45	0.3	88.9	88.9	0	14.81	0.11	86.4	86.4	-0.02
10.56	0.29	86.6	86.6	-0.01	14.93	0.11	83.4	83.4	-0.03
10.66	0.29	84.7	84.7	-0.02	15.03	0.1	81.8	81.8	-0.05
10.77	0.3	83	83	0	15.16	0.1	81.7	81.7	0.02
10.88	0.28	81.2	81.2	-0.01	15.27	0.1	81.1	81.1	0.02
10.99	0.27	77.5	77.5	-0.03	15.37	0.11	79.7	79.7	0
11.10	0.26	73.3	73.3	-0.02	15.48	0.12	78	78	0.01
11.21	0.25	68.9	68.9	-0.02	15.59	0.11	77.6	77.6	0.02
11.32	0.23	65.2	65.1	-0.03	15.70	0.11	80.8	80.9	0.03
11.42	0.19	62.4	62.4	-0.02	15.81	0.1	81.7	81.7	-0.01
11.53	0.06	61.5	61.5	-0.03	15.92	0.1	83.6	83.6	0.01
11.64	0.06	63.1	63.1	-0.01	16.03	0.11	84.1	84.1	0.02
11.75	0.04	63.2	63.2	-0.03	16.15	0.11	82.3	82.3	0.03
11.86	0.02	61.1	61.1	-0.02	16.26	0.1	82	82	0.01
11.97	0.02	62.4	62.4	-0.02	16.37	0.11	83.6	83.6	0.04
12.07	0.01	63.8	63.8	-0.04	16.48	0.12	83.8	83.8	0.01
12.18	0.02	65.9	65.9	-0.03	16.59	0.12	83.8	83.8	0.03
12.29	0.02	66.9	66.9	-0.05	16.70	0.13	83.6	83.6	0.04
12.40	0.02	68.3	68.3	-0.03	16.81	0.14	84.7	84.7	0.01
12.51	0.01	68.4	68.4	-0.05	16.92	0.15	89.1	89.1	0.05
12.62	0.02	68.5	68.5	-0.05	17.03	0.17	91.3	91.3	0.03
12.73	0.03	68.8	68.8	-0.05	17.14	0.17	91.9	91.9	0.04
12.84	0.04	69.6	69.6	-0.05	17.25	0.19	92	92.1	0.04
12.95	0.03	70	70	-0.07	17.36	0.19	91.3	91.3	0.03
13.06	0.03	71.4	71.3	-0.06	17.47	0.2	91.6	91.6	0.05
13.17	0.06	72.6	72.6	-0.04	17.58	0.19	90.7	90.7	0.04
13.28	0.05	72.6	72.6	-0.03	17.69	0.19	91	91	0.04
13.39	0.03	71.4	71.4	-0.06	17.80	0.21	95.2	95.2	0.07
13.50	0.03	70.4	70.4	-0.06	17.91	0.2	101.5	101.5	0.05

Table D.2 Continued

z	f_s	q_u	q_t	u_2	z	f_s	q_u	q_t	u_2
(ft)	(tsf)	(tsf)	(tsf)	(tsf)	(ft)	(tsf)	(tsf)	(tsf)	(tsf)
18.02	0.23	109.6	109.6	0.08	22.22	0.35	96.1	96.2	0.25
18.12	0.21	113.9	113.9	0.07	22.33	0.33	88.4	88.5	0.24
18.23	0.18	117.5	117.5	0.07	22.44	0.3	84.1	84.1	0.23
18.34	0.19	117	117	0.08	22.54	0.29	87.5	87.6	0.23
18.41	0.2	105	105.1	0.08	22.65	0.29	89	89	0.23
18.52	0.21	113.3	113.3	0.12	22.76	0.29	87.2	87.2	0.24
18.63	0.22	109.7	109.7	0.12	22.87	0.29	87.5	87.5	0.24
18.73	0.23	105.5	105.6	0.12	22.97	0.29	87.8	87.8	0.24
18.84	0.25	95.7	95.8	0.11	23.08	0.29	88.3	88.3	0.24
18.95	0.25	85.5	85.5	0.11	23.19	0.28	90.5	90.6	0.25
19.05	0.25	78.6	78.6	0.1	23.30	0.27	92	92	0.25
19.16	0.24	73.5	73.5	0.11	23.40	0.28	92.8	92.8	0.27
19.27	0.19	77.2	77.2	0.12	23.51	0.26	91.3	91.3	0.25
19.38	0.15	83	83.1	0.13	23.62	0.27	88.9	89	0.27
19.49	0.13	82.7	82.7	0.12	23.72	0.26	85.9	85.9	0.28
19.60	0.25	74.4	74.4	0.14	23.83	0.24	84.9	84.9	0.26
19.71	0.36	59.2	59.2	0.14	23.94	0.26	90.1	90.2	0.29
19.83	0.33	42.7	42.7	0.1	24.04	0.24	91.9	91.9	0.27
19.94	0.46	34.2	34.2	0.12	24.15	0.24	91	91	0.29
20.06	0.37	36.4	36.5	0.15	24.26	0.23	88.5	88.6	0.27
20.17	0.39	34.7	34.8	0.18	24.36	0.22	87.2	87.2	0.27
20.28	0.4	37.4	37.4	0.18	24.47	0.23	86.6	86.6	0.27
20.40	0.37	43.9	44	0.2	24.58	0.21	86.6	86.7	0.27
20.51	0.31	41.9	41.9	0.2	24.68	0.19	87	87	0.28
20.62	0.24	45.3	45.3	0.21	24.79	0.15	84.3	84.4	0.28
20.73	0.23	62.7	62.7	0.22	24.90	0.16	82.6	82.6	0.32
20.84	0.21	88.2	88.2	0.22	25.01	0.13	77.3	77.3	0.29
20.95	0.19	94.6	94.6	0.21	25.08	0.13	73.1	73.1	0.28
21.06	0.2	96.6	96.6	0.22	25.18	0.12	68.8	68.8	0.28
21.16	0.22	98.1	98.2	0.22	25.29	0.11	63.6	63.7	0.28
21.27	0.27	102.2	102.2	0.22	25.40	0.11	62.2	62.3	0.28
21.38	0.32	104.2	104.2	0.23	25.51	0.13	67.4	67.5	0.3
21.48	0.29	102.3	102.3	0.23	25.62	0.11	68.5	68.5	0.29
21.59	0.31	98	98.1	0.22	25.73	0.13	68.1	68.1	0.29
21.70	0.32	94.8	94.8	0.22	25.84	0.14	66.5	66.6	0.29
21.73	0.32	78.8	78.8	0.24	25.95	0.17	62.7	62.7	0.29
21.79	0.33	93.3	93.3	0.24	26.06	0.19	54.9	55	0.3
21.90	0.32	94.5	94.5	0.23	26.17	0.17	48	48	0.32
22.01	0.33	97.5	97.6	0.23	26.28	0.11	48.6	48.6	0.29
22.11	0.32	97.3	97.4	0.22	26.39	0.11	59.3	59.4	0.29

Table D.2 Continued

z	f_s	q_u	q_t	u_2	z	f_s	q_u	q_t	u_2
(ft)	(tsf)	(tsf)	(tsf)	(tsf)	(ft)	(tsf)	(tsf)	(tsf)	(tsf)
26.50	0.1	67.8	67.9	0.3	31.47	0.02	46.4	46.6	0.68
26.61	0.1	71.2	71.2	0.31	31.59	0.03	46.3	46.4	0.62
26.72	0.09	68	68.1	0.31	31.64	0.05	15.8	15.9	0.58
26.83	0.08	63.5	63.6	0.31	31.69	0.07	41.1	41.2	0.57
26.94	0.08	58.6	58.7	0.3	31.81	0.15	31.7	31.8	0.57
27.05	0.08	56.7	56.8	0.31	31.93	0.2	25.2	25.3	0.57
27.17	0.07	55.5	55.6	0.31	32.05	0.18	24.8	24.9	0.57
27.28	0.07	54.5	54.6	0.32	32.17	0.15	28	28.1	0.6
27.39	0.08	56.1	56.2	0.32	32.29	0.16	41.8	41.9	0.66
27.50	0.08	59.8	59.9	0.32	32.41	0.11	48.4	48.5	0.6
27.61	0.09	62.5	62.6	0.32	32.52	0.1	52	52.2	0.59
27.72	0.1	65.5	65.6	0.34	32.64	0.08	60.5	60.7	0.58
27.83	0.11	68.9	68.9	0.35	32.75	0.09	71.2	71.3	0.62
27.94	0.1	69.4	69.5	0.34	32.86	0.09	71.5	71.6	0.58
28.05	0.09	72.1	72.2	0.34	32.97	0.12	72.6	72.7	0.62
28.16	0.11	73.2	73.3	0.38	33.09	0.13	72	72.1	0.62
28.27	0.13	66.5	66.6	0.34	33.20	0.12	71	71.1	0.59
28.58	0.34	32	32	0.36	33.31	0.14	71.5	71.6	0.59
28.69	0.28	22.5	22.6	0.37	33.42	0.18	73.3	73.4	0.62
28.81	0.22	16.1	16.2	0.45	33.54	0.19	78.5	78.6	0.62
28.94	0.13	11.7	11.8	0.48	33.65	0.19	87.8	87.9	0.61
29.06	0.1	11.1	11.3	0.62	33.76	0.21	93.8	93.9	0.62
29.19	0.05	8.6	8.7	0.65	33.86	0.22	98.2	98.3	0.62
29.32	0.05	7.8	8	0.69	33.97	0.24	102.1	102.2	0.65
29.45	0.08	10.6	10.8	0.77	34.08	0.26	92.8	93	0.63
29.58	0.06	11.5	11.7	0.73	34.19	0.26	84	84.1	0.66
29.71	0.05	12	12.2	0.76	34.30	0.24	70.1	70.3	0.64
29.84	0.04	14.7	14.9	0.78	34.41	0.21	56.7	56.9	0.59
29.97	0.04	18.8	18.9	0.79	34.53	0.19	49.8	49.9	0.59
30.10	0.03	20.2	20.4	0.79	34.64	0.2	53.3	53.4	0.63
30.22	0.06	21.4	21.6	0.82	34.75	0.09	57.9	58	0.61
30.35	0.05	21.7	21.9	0.79	34.87	0.14	55.8	55.9	0.61
30.48	0.05	21.1	21.3	0.8	34.96	0.18	53	53.2	0.63
30.61	0.06	26.6	26.8	0.81	35.08	0.17	65.7	65.9	0.64
30.73	0.09	36.3	36.5	0.83	35.19	0.18	79.1	79.2	0.66
30.86	0.11	35	35.1	0.74	35.30	0.18	100.5	100.6	0.67
30.98	0.16	32.3	32.5	0.78	35.41	0.21	117	117.1	0.66
31.11	0.16	32.2	32.3	0.81	35.51	0.22	119.3	119.4	0.6
31.23	0.1	33.3	33.4	0.76	35.62	0.27	110.9	111	0.56
31.35	0.06	40.6	40.8	0.76	35.67	0.28	103.8	103.9	0.54

Table D.2 Continued

z	f_s	q_u	q_t	u_2	z	f_s	q_u	q_t	u_2
(ft)	(tsf)	(tsf)	(tsf)	(tsf)	(ft)	(tsf)	(tsf)	(tsf)	(tsf)
35.84	0.31	93.5	93.6	0.55	38.16	0.4	44.3	44.5	0.65
35.95	0.31	96.1	96.2	0.54	38.27	0.34	38.8	39	0.66
36.06	0.32	105.7	105.8	0.55	38.33	0.3	37	37.1	0.72
36.14	0.35	111.7	111.8	0.58	38.38	0.28	57.7	57.9	0.73
36.25	0.36	110.7	110.8	0.59	38.49	0.25	98.8	98.9	0.77
36.35	0.36	105.9	106	0.59	38.59	0.22	109.5	109.6	0.73
36.46	0.34	98.2	98.3	0.58	38.69	0.27	107.7	107.8	0.73
36.57	0.33	93.2	93.3	0.58	38.80	0.44	102.5	102.6	0.73
36.67	0.32	95.7	95.8	0.6	38.90	0.57	84.7	84.9	0.71
36.78	0.31	101.8	101.9	0.6	39.01	0.5	64.7	64.8	0.71
36.89	0.33	103	103.2	0.63	39.12	0.41	51.9	52	0.69
36.99	0.33	95	95.1	0.63	39.22	0.4	64.3	64.4	0.71
37.10	0.31	88.3	88.4	0.61	39.33	0.42	89.5	89.7	0.74
37.20	0.3	93.9	94	0.64	39.43	0.56	88.8	88.9	0.71
37.31	0.28	112	112.2	0.65	39.54	0.9	94	94.2	0.7
37.41	0.28	128.1	128.2	0.66	39.64	1.44	89.2	89.4	0.73
37.52	0.33	125.8	126	0.65	39.75	1.86	69.3	69.5	0.72
37.62	0.5	107.1	107.2	0.65	39.86	0	55.3	55.4	0.75
37.73	0.69	84.8	85	0.64	39.96	0	43.9	44.1	0.87
37.83	0.75	61.9	62	0.64	40.07	0	61.3	61.6	1.58
37.94	0.88	41.8	42	0.61	40.17	0	221.1	221.6	2.31
38.05	0.53	35.6	35.7	0.61	40.17	0	221.1	221.6	2.31

Table D.3 Cone penetration test log for HB-3 at the Hobcaw Borrow Pit site.

z	f_s	q_u	q_t	u_2	z	f_s	q_u	q_t	u_2
(ft)	(tsf)	(tsf)	(tsf)	(tsf)	(ft)	(tsf)	(tsf)	(tsf)	(tsf)
0.00	0	0	0	0	5.01	0.37	71.7	71.7	0.01
0.25	0	38.2	38.2	0.02	5.13	0.4	73	73	0.02
0.39	0.09	52.6	52.6	0.02	5.24	0.38	73.7	73.7	0.01
0.52	0.1	63.2	63.2	0.02	5.36	0.37	74.9	74.9	0.01
0.64	0.12	73	73	0.01	5.47	0.36	75.4	75.4	0
0.76	0.16	80.1	80.1	0.05	5.75	0.36	75.8	75.8	0
0.88	0.15	80.4	80.4	0.01	5.86	0.35	76	76	0
1.00	0.17	81.9	81.9	0.03	5.97	0.35	76.3	76.3	0
1.12	0.19	81.8	81.8	0.05	6.09	0.34	76.7	76.7	-0.01
1.24	0.15	77.5	77.5	0.01	6.20	0.35	78.4	78.4	0
1.36	0.15	74.5	74.5	0.01	6.31	0.35	79.1	79.1	0
1.48	0.13	71	71	0.01	6.43	0.36	80.3	80.3	0
1.60	0.12	67.8	67.8	0.01	6.54	0.36	80.7	80.7	0
1.72	0.11	64.5	64.5	0	6.65	0.36	80.6	80.6	0
1.84	0.09	62.1	62.1	0	6.77	0.37	80.8	80.8	0
1.96	0.07	59.2	59.2	0	6.88	0.37	80.2	80.2	0.01
2.09	0.07	57.7	57.7	0.01	6.99	0.36	78.5	78.5	-0.01
2.21	0.06	56.4	56.4	0	7.11	0.35	76.9	76.9	-0.01
2.31	0.04	56	56	0.01	7.22	0.34	75.5	75.5	0
2.44	0.06	55.9	55.9	0.01	7.31	0.34	73.9	73.9	0
2.56	0.05	56.2	56.2	0.01	7.42	0.33	72.4	72.4	0
2.68	0.05	56.5	56.5	0	7.53	0.32	71.3	71.3	0
2.81	0.07	57.3	57.3	0	7.65	0.31	70.4	70.4	0
2.93	0.09	57.5	57.5	0	7.73	0.29	69.4	69.4	0
3.06	0.11	57.7	57.7	0	7.85	0.29	68.2	68.2	0
3.18	0.14	57.4	57.4	0.01	7.96	0.29	66.8	66.8	0.01
3.31	0.18	58.1	58.1	0.03	8.07	0.27	65.1	65.1	-0.01
3.43	0.17	56.5	56.5	-0.01	8.19	0.26	64.6	64.6	0.01
3.56	0.21	57.5	57.6	0.04	8.30	0.25	65	65	0.02
3.68	0.23	58	58	0.04	8.49	0.08	64.7	64.7	0
3.81	0.21	57	57	0	8.60	0.15	64.7	64.7	0
3.93	0.24	58.7	58.7	0.01	8.71	0.18	65	65	0
4.05	0.24	59.9	59.9	0	8.76	0.2	3.6	3.6	0.03
4.18	0.28	62.6	62.6	0.04	8.89	0.2	64.4	64.4	-0.03
4.30	0.27	62.9	62.9	0	9.01	0.21	66	66	-0.02
4.42	0.32	66.5	66.5	0.04	9.12	0.22	67.6	67.6	-0.03
4.54	0.31	67.2	67.2	0	9.23	0.24	69.8	69.8	-0.02
4.66	0.34	68.6	68.6	0.01	9.34	0.25	71.3	71.3	-0.03
4.78	0.35	69.9	69.9	0	9.45	0.28	74.2	74.2	0
4.89	0.37	71.3	71.3	0.01	9.56	0.29	75.7	75.7	-0.02

Table D.3 Continued

z (ft)	f_s (tsf)	q_u (tsf)	q_t (tsf)	u_2 (tsf)	z (ft)	f_s (tsf)	q_u (tsf)	q_t (tsf)	u_2 (tsf)
9.67	0.3	77.2	77.2	-0.02	13.91	0.22	90	90	0.04
9.78	0.31	78.8	78.8	-0.01	14.02	0.23	93.8	93.8	0.03
9.89	0.32	79.3	79.3	-0.01	14.13	0.25	98.3	98.3	0.05
10.00	0.33	80.5	80.4	-0.02	14.23	0.26	103.1	103.1	0.04
10.11	0.34	82.1	82.1	-0.01	14.34	0.28	107.7	107.8	0.03
10.20	0.35	83.6	83.6	-0.01	14.44	0.3	112.5	112.5	0.04
10.31	0.35	84.7	84.7	0	14.55	0.32	115.5	115.5	0.04
10.42	0.34	85.1	85.1	-0.01	14.65	0.33	117.2	117.2	0.06
10.53	0.35	86.6	86.6	-0.01	14.76	0.35	119	119	0.06
10.64	0.35	87.7	87.7	-0.01	14.86	0.37	120.8	120.8	0.06
10.74	0.34	88.9	88.9	0	14.96	0.38	122.2	122.3	0.07
10.85	0.32	89.4	89.4	0	15.07	0.38	124.4	124.4	0.08
10.96	0.31	90	90	0	15.17	0.45	127.3	127.3	0.07
11.06	0.31	90.6	90.6	0.01	15.27	0.36	129.3	129.3	0.06
11.17	0.31	89.4	89.4	0.01	15.38	0.35	132.3	132.3	0.08
11.28	0.31	85.9	85.9	-0.01	15.48	0.36	135.7	135.7	0.08
11.38	0.31	83.2	83.2	-0.01	15.53	0.37	122	122	0.08
11.49	0.31	79.8	79.8	0	15.64	0.37	136.6	136.6	0.07
11.60	0.3	74.7	74.7	-0.01	15.74	0.38	138.9	138.9	0.07
11.71	0.29	70.1	70.1	0	15.85	0.38	141	141	0.07
11.82	0.26	67.3	67.3	0	15.95	0.39	140.8	140.9	0.07
11.93	0.19	66.9	66.9	0	16.05	0.39	139.4	139.5	0.08
12.04	0.16	67.4	67.4	0	16.16	0.39	138.9	138.9	0.08
12.12	0.15	68.1	68.1	0	16.26	0.4	141.6	141.7	0.08
12.19	0.15	54.5	54.5	0.03	16.36	0.42	146.9	146.9	0.1
12.30	0.15	67.7	67.8	0.02	16.46	0.44	152.6	152.6	0.09
12.40	0.14	66.9	66.9	0.01	16.57	0.47	159.3	159.3	0.1
12.51	0.14	65.8	65.8	0	16.67	0.48	165	165	0.1
12.62	0.13	65.2	65.2	0	16.77	0.5	169.7	169.8	0.1
12.73	0.14	66.2	66.2	0.01	16.88	0.52	172.4	172.4	0.11
12.84	0.15	66.7	66.7	0.01	16.98	0.52	173.5	173.6	0.11
12.94	0.15	67.7	67.7	0.01	17.08	0.51	172.1	172.1	0.12
13.05	0.15	68.3	68.3	0.01	17.18	0.49	170.4	170.4	0.12
13.16	0.15	69.4	69.4	0.01	17.29	0.47	169.3	169.3	0.12
13.27	0.16	70.9	70.9	0.02	17.39	0.46	167.5	167.5	0.12
13.38	0.15	71.9	71.9	0.02	17.49	0.46	164.2	164.2	0.13
13.48	0.15	73.7	73.7	0.02	17.59	0.44	156.8	156.9	0.12
13.59	0.16	76.2	76.2	0.03	17.70	0.45	147.5	147.5	0.13
13.70	0.18	80.8	80.8	0.02	17.80	0.45	138.4	138.4	0.14
13.81	0.2	85.7	85.7	0.03	17.90	0.44	132.8	132.8	0.13

Table D.3 Continued

z	f_s	q_u	q_t	u_2	z	f_s	q_u	q_t	u_2
(ft)	(tsf)	(tsf)	(tsf)	(tsf)	(ft)	(tsf)	(tsf)	(tsf)	(tsf)
18.01	0.41	129.1	129.2	0.12	22.39	0.33	72.3	72.4	0.24
18.11	0.4	125.5	125.6	0.13	22.50	0.34	71.8	71.8	0.25
18.21	0.39	122.1	122.2	0.13	22.61	0.34	79.8	79.8	0.25
18.32	0.39	116.5	116.5	0.14	22.71	0.35	79.4	79.4	0.25
18.43	0.42	107.7	107.8	0.13	22.82	0.34	73.7	73.8	0.25
18.53	0.36	96.8	96.9	0.13	22.93	0.34	72.8	72.9	0.25
18.64	0.33	83.6	83.6	0.13	23.04	0.32	73.3	73.4	0.25
18.74	0.3	69.9	69.9	0.13	23.14	0.28	70.2	70.3	0.24
18.82	0.28	51.7	51.7	0.12	23.25	0.26	66.3	66.4	0.25
18.88	0.27	51.1	51.1	0.15	23.36	0.26	71.5	71.5	0.26
18.99	0.23	40.8	40.8	0.13	23.46	0.24	76	76.1	0.25
19.10	0.25	36	36	0.14	23.57	0.24	75.8	75.9	0.26
19.21	0.33	35.5	35.5	0.13	23.68	0.24	74.7	74.8	0.26
19.32	0.34	33.6	33.6	0.13	23.79	0.24	75.5	75.5	0.27
19.43	0.2	29.7	29.7	0.13	23.89	0.25	79.6	79.6	0.27
19.55	0.11	23.8	23.8	0.14	24.00	0.25	79.8	79.8	0.26
19.66	0.06	33.4	33.5	0.16	24.11	0.25	76.3	76.3	0.27
19.77	0.04	40.2	40.2	0.17	24.22	0.25	70.6	70.6	0.27
19.88	0.06	38	38	0.17	24.33	0.24	64.5	64.6	0.27
19.99	0.19	42.8	42.9	0.18	24.43	0.22	60.5	60.5	0.27
20.11	0.27	34.3	34.3	0.18	24.54	0.21	61.2	61.2	0.27
20.22	0.17	24	24.1	0.18	24.65	0.2	62.2	62.2	0.27
20.33	0.14	19.8	19.8	0.18	24.76	0.2	62.4	62.4	0.28
20.45	0.13	29	29	0.2	24.87	0.19	62.3	62.4	0.28
20.56	0.16	34	34.1	0.19	24.98	0.2	59.3	59.4	0.28
20.67	0.16	31.5	31.5	0.21	25.09	0.21	54	54.1	0.28
20.78	0.15	31.4	31.4	0.2	25.21	0.17	47.4	47.4	0.28
20.90	0.23	41.5	41.5	0.22	25.32	0.16	40.8	40.9	0.28
21.01	0.25	53	53.1	0.21	25.43	0.16	41.9	42	0.28
21.12	0.27	52.6	52.6	0.22	25.51	0.15	46.1	46.2	0.3
21.23	0.31	59.1	59.1	0.22	25.62	0.14	46.2	46.3	0.3
21.34	0.34	82.8	82.9	0.22	25.73	0.13	43.4	43.5	0.3
21.44	0.38	96.6	96.7	0.25	25.84	0.11	40.1	40.2	0.3
21.55	0.4	99.4	99.4	0.23	25.95	0.1	37.5	37.5	0.3
21.65	0.42	100.5	100.5	0.24	26.07	0.09	36.4	36.5	0.3
21.76	0.41	98.8	98.8	0.24	26.18	0.07	34.5	34.6	0.3
21.87	0.39	96.7	96.8	0.25	26.29	0.08	32.8	32.9	0.34
21.97	0.37	93.3	93.4	0.24	26.41	0.05	30.9	30.9	0.31
22.08	0.38	89	89	0.24	26.52	0.04	31.3	31.3	0.31
22.29	0.36	78.9	79	0.26	26.64	0.06	32.2	32.3	0.35

Table D.3 Continued

z	f_s	q_u	q_t	u_2	z	f_s	q_u	q_t	u_2
(ft)	(tsf)	(tsf)	(tsf)	(tsf)	(ft)	(tsf)	(tsf)	(tsf)	(tsf)
26.75	0.05	28.5	28.5	0.31	31.76	0.11	26.3	26.5	1.05
26.87	0.05	25.2	25.2	0.32	31.89	0.02	40.9	41.1	1.04
26.99	0.05	21.7	21.8	0.31	32.02	0.04	54.9	55.1	0.95
27.11	0.07	20.2	20.2	0.31	32.07	0.05	48.5	48.7	0.9
27.23	0.11	17.7	17.8	0.34	32.20	0.09	59.6	59.7	0.63
27.35	0.08	14.5	14.6	0.3	32.31	0.14	63.5	63.6	0.63
27.48	0.1	15.9	15.9	0.32	32.43	0.22	71.2	71.3	0.67
27.60	0.2	19.6	19.6	0.34	32.54	0.24	73.4	73.6	0.65
27.72	0.27	21.5	21.5	0.33	32.66	0.26	78.3	78.4	0.64
27.85	0.27	16.2	16.3	0.33	32.77	0.31	81.7	81.8	0.69
27.97	0.23	12.3	12.3	0.34	32.89	0.3	75.9	76	0.67
28.10	0.19	8.9	9	0.38	33.00	0.26	69.7	69.8	0.64
28.22	0.12	7.2	7.3	0.41	33.12	0.25	68.1	68.2	0.65
28.35	0.06	6.5	6.5	0.47	33.23	0.27	65.7	65.8	0.64
28.48	0.03	6.4	6.5	0.5	33.35	0.27	58.8	59	0.65
28.61	0.04	6.5	6.6	0.54	33.46	0.25	54.1	54.2	0.64
28.74	0.05	7.2	7.3	0.6	33.58	0.26	53.7	53.9	0.67
28.78	0.06	4.8	5	1.05	33.70	0.22	50.9	51	0.65
28.83	0.07	8.1	8.3	1.07	33.81	0.14	52.8	52.9	0.65
28.96	0.05	7.2	7.4	1.08	33.93	0.1	53.3	53.4	0.67
29.09	0.04	7.1	7.3	1.09	34.05	0.12	53.6	53.8	0.66
29.22	0.04	6.8	7	1.14	34.16	0.18	47.2	47.3	0.64
29.35	0.03	6.3	6.6	1.16	34.28	0.24	39.9	40.1	0.65
29.48	0.03	6.1	6.3	1.18	34.40	0.23	42.4	42.5	0.66
29.62	0.03	6.1	6.3	1.21	34.51	0.21	58.6	58.8	0.72
29.75	0.03	5.3	5.5	1.21	34.62	0.19	85.7	85.9	0.7
29.89	0.04	5.9	6.2	1.22	34.73	0.21	105.1	105.3	0.64
30.02	0.03	7.9	8.1	1.22	34.84	0.28	110.9	111	0.61
30.16	0	7.1	7.3	1.2	34.95	0.4	107.2	107.3	0.61
30.29	0.01	5.8	6	1.23	35.06	0.6	91.7	91.8	0.63
30.43	0.06	6.7	7	1.29	35.16	0.54	69.8	69.9	0.6
30.56	0.06	8.1	8.4	1.28	35.28	0.54	57.4	57.5	0.59
30.70	0.06	10.6	10.9	1.24	35.38	0.51	52.8	52.9	0.6
30.83	0.07	9.2	9.5	1.28	35.46	0.49	69	69.1	0.6
30.97	0.06	10.2	10.4	1.31	35.56	0.46	102.7	102.8	0.66
31.10	0.05	17.6	17.9	1.23	35.67	0.5	108.2	108.3	0.61
31.23	0.07	24.8	25	1.12	35.77	0.59	93.8	93.9	0.57
31.37	0.13	24.8	25	1.05	35.88	0.52	77.9	78	0.53
31.50	0.15	21.4	21.6	1.06	35.99	0.46	66.3	66.4	0.53
31.63	0.15	21.7	21.9	1.11	36.10	0.42	76.8	76.9	0.53

Table D.3 Continued

z	f_s	q_u	q_t	u_2	z	f_s	q_u	q_t	u_2
(ft)	(tsf)	(tsf)	(tsf)	(tsf)	(ft)	(tsf)	(tsf)	(tsf)	(tsf)
36.20	0.4	103.3	103.4	0.56	39.74	1.76	26.5	26.6	0.58
36.31	0.42	114.6	114.7	0.57	39.84	1.96	25.3	25.5	0.87
36.41	0.44	118.9	119	0.56	39.94	2.51	82.8	83	0.94
36.52	0.44	116	116.1	0.58	40.04	3.5	217	217.3	1.57
36.62	0.44	123.6	123.7	0.58	40.25	4.79	214.1	214.3	0.95
36.73	0.47	141.4	141.5	0.61	40.33	4.34	166.2	166.4	1.31
36.83	0.5	144.2	144.3	0.6	40.42	3.89	142.5	142.8	1.65
36.93	0.53	138.1	138.2	0.6	40.50	3.49	93.2	93.6	2.14
37.04	0.56	123.4	123.5	0.59	40.58	2.48	72.8	73.3	2.92
37.14	0.62	105.5	105.6	0.59	40.67	1.97	66.4	67.1	3.46
37.25	0.7	91.4	91.5	0.57	40.75	2	70.1	70.9	4.01
37.35	0.72	80.2	80.3	0.58	40.84	1.86	93.9	94.9	5.19
37.46	0.62	71.3	71.4	0.57	40.92	2	117.2	118.4	6.15
37.56	0.54	75.5	75.6	0.59	41.01	2.08	116.6	117.7	5.99
37.67	0.47	104.7	104.9	0.62	41.09	2.11	134.8	135.5	3.62
37.77	0.43	155.2	155.3	0.68	41.18	2.35	102.2	102.5	2.01
37.87	0.44	190.6	190.7	0.66	41.26	2.12	90	91	5.13
37.97	0.54	204	204.1	0.61	41.34	1.97	80.8	81.7	4.58
38.07	0.64	203.9	204	0.58	41.43	1.84	82	82.9	4.82
38.17	0.66	196.1	196.2	0.59	41.52	2.18	107.7	108.5	4.31
38.27	0.69	183.8	183.9	0.58	41.60	2.17	189.6	190.7	5.32
38.36	0.73	179.3	179.4	0.58	41.84	3.93	203.7	203.9	1.19
38.46	0.72	194.6	194.7	0.6	41.93	2.95	130.5	130.7	1.22
38.56	0.69	216.4	216.5	0.61	41.97	2.53	52.5	52.8	1.45
38.66	0.75	228.8	228.9	0.64	42.02	2.14	113.4	113.8	1.92
38.93	1.08	230	230	0.47	42.07	1.84	79.3	79.7	2.06
39.03	1.15	213.3	213.4	0.47	42.13	1.4	77.3	77.7	2.18
39.12	1.2	174.3	174.4	0.45	42.22	0.75	63.8	64.3	2.23
39.22	1.32	130.5	130.6	0.43	42.31	0.38	57.6	58.1	2.49
39.32	1.5	89.9	90	0.43	42.54	0.84	209.6	209.9	1.54
39.43	1.45	63.4	63.5	0.38	42.63	0	214.4	214.6	1.34
39.53	1.32	48.7	48.8	0.42	42.89	0	66.4	66.7	1.53
39.63	1.5	35.6	35.7	0.49	42.89	0	66.4	66.7	1.53

Table D.4 CPT Data from SC-1 at the Rest Area Ponds site.

z (ft)	f_s (tsf)	q_u (tsf)	q_t (tsf)	u_2 (tsf)	z (ft)	f_s (tsf)	q_u (tsf)	q_t (tsf)	u_2 (tsf)
0.00	0	0	0	0	3.85	0.7409	171.69	171.7	0.074
0.17	0	31.72	31.73	0.027	3.93	0.7589	174.31	174.34	0.126
0.25	0	42.79	42.81	0.069	4.02	0.778	178.18	178.22	0.176
0.34	0.1142	45.98	45.99	0.065	4.10	0.7969	180.09	180.12	0.148
0.43	2.3321	136.28	136.29	0.04	4.18	0.8089	181.26	181.3	0.174
0.51	1.5527	227.76	227.76	0.018	4.26	0.8201	182.35	182.39	0.186
0.60	1.176	341	341	0.023	4.34	0.8367	182.85	182.89	0.183
0.69	1.1229	370.34	370.35	0.079	4.43	0.8429	182.98	183.01	0.183
0.78	1.168	160.02	160.04	0.102	4.51	0.8335	181.89	181.93	0.187
0.88	1.1879	112.18	112.22	0.24	4.59	0.8339	180.2	180.22	0.145
0.97	0.6789	109.04	109.11	0.328	4.67	0.8354	177.35	177.38	0.157
1.05	0.4789	109.81	109.86	0.254	4.76	0.8281	174.54	174.56	0.113
1.15	0.4346	109.01	109.04	0.178	4.84	0.8344	169.7	169.71	0.034
1.23	0.4099	106.55	106.57	0.114	4.92	0.8268	166.62	166.63	0.031
1.32	0.3983	104.09	104.13	0.193	5.01	0.8249	161.17	161.18	0.028
1.40	0.4374	99.95	99.98	0.144	5.09	0.8176	153.15	153.14	-0.046
1.48	0.5451	96.47	96.47	0.041	5.17	0.7881	145.87	145.87	0.016
1.57	0.7527	97.43	97.44	0.039	5.25	0.7575	134.5	134.49	-0.019
1.65	0.934	96.8	96.81	0.028	5.34	0.7264	124.08	124.08	-0.005
1.74	0.7901	96.85	96.88	0.132	5.42	0.6964	115.44	115.44	0.002
1.82	0.732	106.34	106.35	0.074	5.50	0.678	106.39	106.39	-0.008
1.90	0.7463	114.58	114.97	2.004	5.78	0.6517	81.62	81.62	0.034
1.99	0.7367	117.59	117.71	0.633	5.86	0.6247	74.96	74.97	0.01
2.07	0.6931	134.53	134.56	0.184	5.94	0.6078	68.88	68.89	0.036
2.15	0.647	149.61	149.67	0.313	6.02	0.5817	62.06	62.06	0.007
2.24	0.6036	161.55	161.6	0.252	6.10	0.5463	57.96	57.97	0.073
2.32	0.6581	170.66	170.71	0.226	6.18	0.512	51.85	51.85	0.015
2.59	0.7381	184.44	184.48	0.181	6.26	0.4622	47.86	47.86	0.021
2.67	0.7803	186.68	186.72	0.19	6.34	0.424	44.09	44.1	0.048
2.76	0.767	187.06	187.08	0.102	6.42	0.3949	39.75	39.76	0.017
2.84	0.7318	185.23	185.26	0.155	6.50	0.359	37.43	37.44	0.048
2.93	0.7072	184.46	184.51	0.243	6.58	0.3064	34.59	34.59	0.007
3.01	0.7011	183.06	183.1	0.195	6.66	0.2529	32.33	32.33	0.025
3.10	0.6912	181.43	181.45	0.115	6.74	0.2026	30.72	30.73	0.062
3.19	0.6955	179.53	179.54	0.095	6.82	0.1711	30.25	30.28	0.134
3.27	0.7022	177.39	177.4	0.046	6.90	0.1585	29.09	29.11	0.14
3.35	0.7014	174.93	174.93	0.015	6.98	0.1533	27.69	27.71	0.109
3.43	0.7095	172.36	172.36	-0.026	7.06	0.1502	27.6	27.62	0.131
3.51	0.7128	170.61	170.6	-0.026	7.14	0.1518	27.45	27.47	0.087
3.60	0.7222	169.91	169.91	0.019	7.22	0.1516	28.26	28.27	0.065
3.69	0.7348	169.74	169.75	0.049	7.30	0.1657	29.7	29.71	0.071
3.77	0.7373	169.51	169.52	0.059	7.38	0.1831	30.97	30.97	0.027

Table D.4 Continued

z (ft)	f_s (tsf)	q_u (tsf)	q_t (tsf)	u_2 (tsf)	z (ft)	f_s (tsf)	q_u (tsf)	q_t (tsf)	u_2 (tsf)
7.46	0.2025	32.65	32.66	0.051	10.97	2.6054	393.66	393.57	-0.449
7.53	0.2149	33.45	33.46	0.049	11.04	2.4915	394.74	394.65	-0.46
7.61	0.2252	35.66	35.68	0.1	11.12	2.3678	387.45	387.36	-0.474
7.69	0.235	36.92	36.94	0.107	11.19	2.2801	373.89	373.8	-0.471
7.77	0.2432	37.75	37.76	0.055	11.27	2.2272	354.39	354.29	-0.483
7.85	0.2516	38.07	38.08	0.046	11.34	2.1413	331.54	331.44	-0.508
7.93	0.2593	37.67	37.68	0.026	11.42	2.0785	298.65	298.55	-0.507
8.01	0.2576	37.02	37.03	0.048	11.50	2.0825	269.15	269.04	-0.531
8.09	0.256	36.62	36.63	0.087	11.58	2.1541	240.64	240.53	-0.546
8.17	0.2571	36.29	36.31	0.082	11.66	2.05	217.15	217.05	-0.556
8.25	0.2623	37	37.03	0.126	11.73	1.8344	200.49	200.38	-0.568
8.33	0.2665	37.03	37.05	0.098	11.81	1.6067	188.27	188.17	-0.542
8.41	0.2688	37.37	37.38	0.08	11.88	1.5523	182.92	182.81	-0.54
8.48	0.2788	38.73	38.75	0.102	11.95	1.4698	186.43	186.33	-0.526
8.56	0.2888	40.88	40.9	0.097	12.17	0.827	176.12	176.01	-0.56
8.64	0.2992	44.04	44.06	0.094	12.25	0.7166	169.44	169.33	-0.56
8.72	0.2931	46	46	-0.001	12.32	0.7202	166.07	165.96	-0.56
9.01	0.3117	46.68	46.65	-0.136	12.39	0.7721	160.62	160.52	-0.538
9.09	0.343	41.66	41.62	-0.224	12.47	0.8505	157.99	157.89	-0.506
9.18	0.363	39.15	39.1	-0.224	12.54	0.942	159.39	159.3	-0.475
9.25	0.3486	39.17	39.12	-0.26	12.62	1.064	160.87	160.79	-0.443
9.33	0.3486	40.78	40.74	-0.217	12.69	1.1835	167.28	167.2	-0.415
9.41	0.4043	48.01	48.01	0.013	12.76	1.2958	176.07	176	-0.394
9.49	0.4827	59.39	59.46	0.34	12.84	1.3882	190.01	189.94	-0.362
9.57	0.566	74.68	74.74	0.352	12.91	1.5299	207.27	207.2	-0.347
9.65	0.6875	91.63	91.7	0.352	12.98	1.6609	226.71	226.65	-0.315
9.73	0.8175	108.61	108.6	-0.053	13.05	1.7786	244.54	244.49	-0.288
9.81	0.9715	119.21	119.13	-0.426	13.13	1.8942	264.74	264.69	-0.26
9.89	1.1104	133.05	132.95	-0.564	13.21	2.0399	280.19	280.14	-0.243
9.97	1.1456	133.02	132.91	-0.574	13.28	2.2948	289.99	289.94	-0.274
10.05	1.2448	139.08	138.97	-0.578	13.36	2.5433	291.36	291.3	-0.329
10.12	1.3895	161.58	161.47	-0.554	13.43	2.7763	284.46	284.39	-0.333
10.20	1.5148	202.46	202.38	-0.433	13.50	2.9885	271.53	271.46	-0.35
10.28	1.6519	245.15	245.09	-0.337	13.58	3.1226	253.95	253.88	-0.371
10.36	1.8082	273.16	273.11	-0.257	13.65	3.2474	241.63	241.57	-0.27
10.43	1.9878	302.78	302.73	-0.257	13.72	3.3075	232.23	232.18	-0.276
10.51	2.1909	332.68	332.61	-0.338	13.79	3.2719	223.42	223.37	-0.264
10.59	2.3519	354.92	354.85	-0.369	13.87	2.9972	212.76	212.69	-0.335
10.67	2.4969	368.57	368.5	-0.392	13.94	2.6305	198.19	198.12	-0.384
10.74	2.6433	377.36	377.29	-0.396	14.02	2.2936	180.61	180.53	-0.416
10.81	2.7713	385.82	385.75	-0.341	14.09	2.0167	163.11	163.03	-0.431
10.89	2.7429	390.32	390.25	-0.338	14.16	1.8455	145.64	145.55	-0.467

Table D.4 Continued

z (ft)	f_s (tsf)	q_u (tsf)	q_t (tsf)	u_2 (tsf)	z (ft)	f_s (tsf)	q_u (tsf)	q_t (tsf)	u_2 (tsf)
14.24	1.8171	128.94	128.85	-0.477	17.75	0.572	80.2	80.24	0.205
14.31	1.7076	116.98	116.89	-0.501	17.84	0.5634	88.02	88.07	0.225
14.39	1.5556	109.67	109.57	-0.496	17.93	0.5524	89.96	90.01	0.276
14.46	1.4057	106.36	106.27	-0.492	18.01	0.5167	93.93	93.99	0.309
14.53	1.2011	105.9	105.81	-0.475	18.10	0.5108	94.14	94.18	0.212
14.61	1.032	108.59	108.5	-0.463	18.19	0.5066	97.23	97.28	0.23
14.68	0.8974	112.21	112.11	-0.536	18.27	0.5022	100.34	100.39	0.281
14.75	0.7317	115.21	115.11	-0.515	18.36	0.4586	101.25	101.31	0.315
14.83	0.6374	117.86	117.76	-0.518	18.62	0.5078	104.44	104.51	0.331
14.90	0.6657	120	119.92	-0.413	18.71	0.5291	103.3	103.36	0.31
14.98	0.694	119.24	119.18	-0.346	18.79	0.5279	100.16	100.22	0.289
15.06	0.7286	118.71	118.65	-0.314	18.88	0.5289	97.9	97.96	0.292
15.14	0.7679	116.7	116.64	-0.289	18.96	0.5262	97.02	97.08	0.31
15.38	0.7504	108.25	108.24	-0.032	19.05	0.5214	98.33	98.39	0.33
15.47	0.7425	106.02	106.03	0.037	19.14	0.5221	97.03	97.09	0.327
15.56	0.7122	104.52	104.52	0.027	19.22	0.5305	92.67	92.74	0.333
15.64	0.6787	101.34	101.35	0.045	19.31	0.5316	89.49	89.55	0.321
15.74	0.6595	97.2	97.21	0.063	19.39	0.5292	86.65	86.71	0.34
15.82	0.6669	95.7	95.71	0.091	19.48	0.5265	84.51	84.58	0.351
15.91	0.6668	93.64	93.66	0.117	19.56	0.588	82.79	82.86	0.346
15.99	0.6719	93.22	93.24	0.132	19.65	0.7363	79.11	79.18	0.344
16.08	0.6784	90.54	90.57	0.154	19.74	0.98	75.09	75.16	0.351
16.16	0.6903	89.7	89.73	0.157	19.83	1.2078	67.14	67.21	0.335
16.26	0.6611	91.79	91.82	0.144	19.91	1.2775	50.95	51.02	0.37
16.34	0.6532	95.1	95.13	0.174	20.00	1.1832	35.45	35.52	0.353
16.43	0.5914	89.79	89.82	0.193	20.09	1.0186	23.74	23.84	0.515
16.52	0.5259	80.07	80.11	0.159	20.18	0.7863	15.5	15.61	0.556
16.61	0.4806	78.65	78.69	0.181	20.26	0.5819	14.43	14.77	1.759
16.70	0.4651	73.96	73.99	0.151	20.34	0.4148	16	16.65	3.338
16.79	0.4143	66.01	66.01	-0.002	20.43	0.3124	17.06	17.83	3.975
16.87	0.3326	61.6	61.61	0.022	20.52	0.2326	18.45	19.07	3.206
16.96	0.2444	58.98	58.99	0.043	20.61	0.238	18.81	19.52	3.69
17.05	0.2132	56.97	56.98	0.04	20.69	0.2785	18.39	19.17	4.026
17.13	0.239	54.62	54.61	-0.032	20.78	0.325	15.67	16.54	4.526
17.22	0.2727	51.6	51.61	0.021	20.87	0.4099	14.12	15.1	5.062
17.31	0.301	50.45	50.45	0.04	20.96	0.5264	14.43	15.35	4.783
17.40	0.3283	51.58	51.59	0.057	21.04	0.5417	14.92	15.78	4.445
17.49	0.3912	54.32	54.34	0.089	21.13	0.5186	14.86	15.58	3.752
17.57	0.4946	60.02	60.04	0.102	21.22	0.4918	14.43	15.06	3.276
17.66	0.5992	68.6	68.63	0.157	21.31	0.4895	13.91	14.4	2.5

Table D.4 Continued

z (ft)	f_s (tsf)	q_u (tsf)	q_t (tsf)	u_2 (tsf)	z (ft)	f_s (tsf)	q_u (tsf)	q_t (tsf)	u_2 (tsf)
21.39	0.4872	13.55	13.81	1.334	25.11	0.1038	6	6.29	1.482
21.48	0.4437	11.97	12.17	1.013	25.20	0.0912	5.89	6.22	1.724
21.57	0.4363	11.23	11.44	1.079	25.28	0.0784	5.26	5.62	1.868
21.76	0.2978	12.11	12.34	1.202	25.37	0.0791	4.37	4.74	1.928
21.84	0.2375	13.66	13.82	0.812	25.45	0.0743	3.81	4.22	2.119
21.93	0.1955	14.79	14.89	0.521	25.54	0.0742	3.57	4	2.256
22.02	0.1524	16.37	16.45	0.427	25.62	0.073	2.98	3.44	2.339
22.10	0.1449	17.55	17.62	0.324	25.71	0.0733	3.19	3.67	2.474
22.19	0.153	18.75	18.79	0.206	25.79	0.0758	3.18	3.67	2.551
22.27	0.1361	19.38	19.42	0.209	25.88	0.0775	3.18	3.69	2.628
22.36	0.1233	19.56	19.62	0.314	25.97	0.0709	3.12	3.64	2.676
22.44	0.1253	21.26	21.33	0.325	26.05	0.0818	2.99	3.52	2.746
22.53	0.1365	22.8	22.82	0.087	26.13	0.0793	3.25	3.79	2.799
22.62	0.1178	22.77	22.79	0.097	26.22	0.0757	3.37	3.92	2.83
22.70	0.1012	22.52	22.54	0.125	26.30	0.0767	3.3	3.85	2.822
22.78	0.0998	23.45	23.47	0.103	26.39	0.0741	3.31	3.87	2.93
22.87	0.0933	26.48	26.51	0.112	26.48	0.0728	3.31	3.9	3.046
22.96	0.1053	27.22	27.23	0.068	26.56	0.0827	3.63	4.23	3.111
23.04	0.1057	26.36	26.39	0.182	26.65	0.0897	3.94	4.55	3.134
23.13	0.1118	26.81	26.87	0.313	26.73	0.09	3.94	4.54	3.137
23.21	0.1125	27.06	27.13	0.394	26.81	0.0943	3.94	4.5	2.895
23.30	0.1066	27.53	27.61	0.411	26.90	0.1006	3.82	4.34	2.73
23.38	0.1102	27.92	28	0.431	26.99	0.0921	3.57	4.12	2.892
23.47	0.1091	28.12	28.21	0.491	27.07	0.0889	3.18	3.74	2.909
23.55	0.1064	27.81	27.91	0.486	27.15	0.0815	3.37	3.93	2.908
23.64	0.1038	27.35	27.44	0.471	27.24	0.0746	3.25	3.81	2.925
23.73	0.1003	27.06	27.16	0.538	27.33	0.0769	3.18	3.75	2.958
23.81	0.0845	27.96	28.06	0.525	27.41	0.0764	3.18	3.75	2.934
23.90	0.0778	30.88	30.98	0.495	27.50	0.0729	3.18	3.74	2.881
23.98	0.0686	32.62	32.7	0.415	27.58	0.0709	3.3	3.85	2.86
24.07	0.0825	31.99	32.06	0.338	27.67	0.0632	3.31	3.87	2.923
24.15	0.1109	28.28	28.36	0.397	27.75	0.0647	3.57	4.13	2.923
24.24	0.1386	24.6	24.7	0.491	27.83	0.0642	3.24	3.81	2.929
24.33	0.1522	20.82	20.92	0.531	27.92	0.0758	3.18	3.76	3.011
24.41	0.1956	18.06	18.16	0.552	28.00	0.0763	3.12	3.71	3.087
24.50	0.213	16.3	16.42	0.612	28.08	0.0756	3.36	3.96	3.087
24.58	0.2306	13.92	14.05	0.653	28.16	0.0813	3.43	4.01	3.022
24.67	0.2486	11.33	11.47	0.702	28.24	0.0848	3.88	4.48	3.101
24.76	0.2113	10.21	10.41	1.031	28.33	0.0923	4.07	4.66	3.039
25.03	0.1231	6.7	6.95	1.294	28.41	0.0846	3.8	4.36	2.885

Table D.4 Continued

z (ft)	f_s (tsf)	q_u (tsf)	q_t (tsf)	u_2 (tsf)	z (ft)	f_s (tsf)	q_u (tsf)	q_t (tsf)	u_2 (tsf)
28.49	0.0784	3.62	4.18	2.925	31.82	0.0927	4.07	4.69	3.208
28.58	0.0779	3.23	3.8	2.946	31.90	0.0916	3.74	4.39	3.395
28.66	0.0678	3.63	4.21	3.009	31.98	0.0849	4.45	5.12	3.506
28.75	0.0663	3.37	3.96	3.062	32.07	0.0865	4.49	5.18	3.564
28.83	0.0632	3.62	4.22	3.101	32.15	0.0885	4.68	5.37	3.562
28.92	0.0662	3.43	4.04	3.159	32.23	0.091	4.76	5.42	3.462
29.00	0.063	3.11	3.73	3.23	32.31	0.0993	4.31	4.92	3.162
29.09	0.0663	3.43	4.08	3.352	32.40	0.0948	4.13	4.77	3.346
29.17	0.0747	3.62	4.26	3.308	32.48	0.094	4.25	4.9	3.336
29.26	0.0779	4.06	4.7	3.324	32.56	0.0955	4.48	5.11	3.251
29.34	0.0827	4.25	4.85	3.115	32.65	0.0953	4.81	5.44	3.274
29.43	0.0771	4.37	4.94	2.925	32.73	0.087	4.43	5.07	3.32
29.51	0.0784	4.05	4.65	3.06	32.81	0.0818	3.86	4.53	3.473
29.59	0.0816	4.31	4.91	3.081	32.89	0.0873	3.8	4.48	3.516
29.68	0.0988	4.62	5.22	3.08	32.98	0.0935	3.94	4.63	3.594
29.76	0.0976	5.82	6.38	2.881	33.06	0.0926	3.48	4.18	3.641
29.85	0.0961	6.14	6.61	2.461	33.14	0.0889	3.48	4.19	3.693
29.94	0.0862	4.48	4.97	2.518	33.22	0.0896	3.61	4.34	3.771
30.02	0.093	3.86	4.36	2.595	33.31	0.0891	4.13	4.87	3.807
30.10	0.0778	4.31	4.85	2.801	33.39	0.0909	4	4.74	3.831
30.19	0.0718	4.19	4.75	2.916	33.47	0.0917	3.86	4.59	3.785
30.27	0.0716	4.06	4.62	2.899	33.55	0.0995	3.93	4.66	3.773
30.36	0.0655	3.56	4.15	3.036	33.64	0.1012	3.86	4.57	3.644
30.44	0.0578	3.24	3.84	3.15	33.72	0.0989	3.99	4.67	3.55
30.53	0.0692	3.43	4.04	3.183	33.80	0.0944	4.05	4.73	3.513
30.61	0.0811	3.43	4.06	3.292	33.88	0.0919	4.11	4.79	3.501
30.69	0.09	3.94	4.6	3.46	33.97	0.097	3.74	4.44	3.616
30.78	0.0978	4.05	4.67	3.222	34.05	0.1022	3.94	4.65	3.717
30.86	0.0696	4.38	4.99	3.185	34.13	0.0938	3.67	4.4	3.79
30.94	0.0968	4.81	5.43	3.204	34.22	0.0855	3.98	4.75	3.963
31.03	0.1051	4.87	5.49	3.248	34.30	0.0776	4.81	5.6	4.127
31.11	0.0938	5.07	5.69	3.218	34.38	0.0815	8.14	8.93	4.094
31.20	0.0932	4.68	5.27	3.036	34.65	0.2946	30.52	30.7	0.906
31.23	0.0937	3.23	3.82	3.038	34.73	0.4456	26.93	27.13	1.037
31.33	0.0922	4.89	5.48	3.044	34.81	0.5566	19.67	19.88	1.059
31.41	0.088	4.48	5.1	3.185	34.89	0.576	15.56	15.76	1.074
31.49	0.0977	5.19	5.76	2.951	34.97	0.5084	12.78	13.05	1.398
31.58	0.0895	4.49	5.04	2.834	35.06	0.4259	9.64	9.91	1.399
31.66	0.0913	4.5	5.08	2.971	35.14	0.3956	7.5	7.84	1.75
31.74	0.0896	3.99	4.57	3.02	35.22	0.4002	7.38	7.92	2.788

Table D.4 Continued

z (ft)	f_s (tsf)	q_u (tsf)	q_t (tsf)	u_2 (tsf)	z (ft)	f_s (tsf)	q_u (tsf)	q_t (tsf)	u_2 (tsf)
35.30	0.2981	11.43	12.07	3.316	38.55	0.422	26.18	26.42	1.244
35.39	0.2753	14.93	15.33	2.086	38.62	0.3866	18.73	18.96	1.198
35.47	0.2782	13.58	13.88	1.538	38.70	0.3673	13.64	13.97	1.684
35.55	0.3179	11.58	11.92	1.759	38.79	0.3538	10.32	10.75	2.204
35.63	0.3074	10.82	11.22	2.064	38.87	0.352	9.83	10.45	3.201
35.71	0.2715	9.83	10.27	2.292	38.95	0.2834	10.57	11.13	2.916
35.80	0.2345	8.8	9.2	2.1	39.04	0.2393	9	9.67	3.472
35.88	0.2277	6.94	7.48	2.797	39.12	0.2402	7.79	8.41	3.253
35.97	0.2375	6.43	7.04	3.162	39.20	0.2477	7.91	8.61	3.624
36.05	0.1812	6.03	6.67	3.323	39.28	0.2044	6.62	7.36	3.862
36.13	0.1604	6.17	6.84	3.488	39.36	0.2035	7.13	7.91	4.017
36.22	0.1866	5.93	6.63	3.622	39.45	0.2044	7.25	7.98	3.753
36.30	0.179	6.71	7.48	4.03	39.53	0.2243	9.18	10.03	4.384
36.39	0.1829	8.13	8.91	4.034	39.61	0.2335	12.3	13.04	3.828
36.47	0.1943	8.85	9.51	3.422	39.70	0.2583	12.64	13.19	2.869
36.55	0.1927	7.06	7.73	3.474	39.78	0.3097	13.29	13.77	2.493
36.63	0.1599	7	7.76	3.953	39.86	0.3072	13.02	13.54	2.655
36.72	0.167	6.81	7.56	3.913	39.94	0.2559	13.86	14.3	2.281
36.80	0.156	9.44	10.27	4.285	40.02	0.2811	14.65	15.04	2.009
36.88	0.1566	19.27	20.04	4.009	40.10	0.3814	18.91	19.41	2.61
36.97	0.2244	29.16	29.34	0.92	40.19	0.4618	26	26.44	2.25
37.06	0.2971	25.63	25.85	1.145	40.27	0.4562	22.41	22.56	0.802
37.16	0.3388	17.56	17.83	1.393	40.35	0.4146	16.47	16.71	1.254
37.24	0.348	13.09	13.38	1.516	40.43	0.3673	12.39	12.8	2.168
37.32	0.3516	10.75	11.09	1.805	40.51	0.3492	10.08	10.5	2.165
37.40	0.3156	8.73	9.17	2.322	40.59	0.3304	9.51	10.14	3.262
37.49	0.2683	6.43	6.95	2.706	40.67	0.345	11.01	11.8	4.111
37.57	0.2282	5.94	6.58	3.341	40.75	0.3226	12.96	13.68	3.73
37.65	0.1761	5.62	6.39	3.971	40.84	0.3133	12.34	12.97	3.267
37.74	0.1515	6.35	7.18	4.301	40.92	0.3045	11.58	11.99	2.141
37.81	0.1401	5.68	6.55	4.502	41.00	0.2958	10.76	11.11	1.84
37.89	0.1474	6	6.92	4.802	41.08	0.3154	8.76	9.44	3.515
37.94	0.1498	5.52	6.48	4.967	41.36	0.7063	41.76	41.97	1.076
37.98	0.1556	6.16	7.11	4.959	41.44	0.7276	35.85	36.05	1.033
38.06	0.173	8.13	9.06	4.813	41.52	0.6531	23.86	24.06	1.038
38.14	0.1659	8.36	9.27	4.682	41.60	0.5849	17.4	17.66	1.347
38.22	0.1288	7.94	8.89	4.941	41.68	0.547	11.65	11.9	1.261
38.30	0.2141	8	8.96	4.96	41.76	0.4924	8.75	9.35	3.101
38.39	0.3894	9.82	10.89	5.526	41.84	0.3961	9.17	9.89	3.737
38.46	0.4496	22.62	23.64	5.281	41.92	0.2701	8.12	8.97	4.377

Table D.4 Continued

z (ft)	f_s (tsf)	q_u (tsf)	q_t (tsf)	u_2 (tsf)	z (ft)	f_s (tsf)	q_u (tsf)	q_t (tsf)	u_2 (tsf)
42.00	0.2142	8.37	9.24	4.475	45.26	0.5307	24.07	24.43	1.862
42.08	0.2263	8.38	9.28	4.658	45.34	0.4784	24.54	24.79	1.306
42.16	0.2123	9.49	10.44	4.934	45.43	0.4344	19.73	20.09	1.84
42.25	0.2271	8.75	9.74	5.156	45.51	0.3634	14.72	15.38	3.422
42.33	0.2424	9.5	10.45	4.917	45.59	0.2686	14.7	15.35	3.383
42.40	0.2602	11.13	12.2	5.514	45.67	0.2402	15.27	15.9	3.258
42.49	0.3693	15.9	16.78	4.591	45.75	0.3044	32.71	33.19	2.508
42.57	0.4716	20.43	21.06	3.297	45.83	0.4512	41.95	42.39	2.262
42.65	0.4975	21.29	21.74	2.329	45.92	0.489	34.87	34.97	0.555
42.73	0.5061	18.78	19.13	1.796	46.00	0.5055	23.93	24.04	0.572
42.81	0.4511	15.21	15.64	2.215	46.08	0.5098	19.3	19.48	0.953
42.89	0.3918	13.01	13.39	1.943	46.16	0.5084	15.27	15.63	1.845
42.98	0.3459	12.51	13.01	2.599	46.25	0.5043	13.79	14.05	1.377
43.06	0.2781	11.85	12.58	3.762	46.32	0.4458	11.12	11.56	2.294
43.14	0.2117	9.12	9.92	4.17	46.41	0.3632	10.67	11.35	3.547
43.22	0.204	10.49	11.39	4.654	46.49	0.3458	11.52	12.25	3.767
43.30	0.2836	34.34	35.36	5.3	46.57	0.3396	11.97	12.64	3.464
43.38	0.4898	54.53	55.2	3.444	46.65	0.287	18.81	19.6	4.097
43.46	0.6488	42.09	42.28	0.986	46.73	0.3278	26.38	26.96	3.004
43.54	0.6096	29.41	29.63	1.12	46.81	0.4402	29.57	29.85	1.47
43.62	0.5557	22.62	22.89	1.415	46.89	0.5348	30.95	31.31	1.849
43.71	0.5933	17.65	17.91	1.337	46.98	0.5083	29.32	29.52	1.06
43.79	0.6869	13.53	13.87	1.764	47.06	0.4993	21.11	21.34	1.177
43.87	0.6073	16.76	17.5	3.788	47.14	0.4683	16.91	17.22	1.606
43.95	0.4804	20.05	20.79	3.834	47.22	0.4336	14.84	15.32	2.478
44.03	0.3857	15.77	16.29	2.683	47.30	0.3985	15.91	16.49	2.992
44.11	0.3744	12.45	12.93	2.492	47.38	0.3379	13.75	14.32	2.918
44.20	0.3118	12.4	13.29	4.62	47.46	0.2997	14.29	14.87	2.985
44.28	0.3212	14.77	15.59	4.262	47.54	0.2931	13.4	13.9	2.581
44.35	0.3247	20.92	21.68	3.97	47.63	0.2796	14.11	14.63	2.727
44.45	0.3002	39.6	40.4	4.152	47.71	0.3037	17.45	18.02	2.925
44.53	0.3104	47.11	47.36	1.323	47.79	0.3309	23.71	24.09	2.016
44.61	0.3685	49.67	49.94	1.413	47.87	0.3822	28.67	28.96	1.46
44.69	0.3983	55.93	56.2	1.382	47.95	0.4026	31.06	31.31	1.284
44.78	0.5007	57.79	57.97	0.923	48.03	0.3667	29.43	29.73	1.581
44.86	0.6611	53.4	53.61	1.06	48.11	0.3086	24.82	25.04	1.115
44.94	0.7092	46.58	46.85	1.408	48.19	0.3534	19.22	19.53	1.64
45.03	0.6007	33.61	33.82	1.11	48.27	0.4045	19.41	19.82	2.147
45.11	0.5907	26.79	26.99	1.031	48.35	0.3955	21.28	21.76	2.474
45.19	0.5877	25.77	26.08	1.607	48.43	0.3519	25.49	25.72	1.216

Table D.4 Continued

z (ft)	f_s (tsf)	q_u (tsf)	q_t (tsf)	u_2 (tsf)	z (ft)	f_s (tsf)	q_u (tsf)	q_t (tsf)	u_2 (tsf)
48.51	0.4055	28.07	28.36	1.529	51.92	0.4198	119.18	119.43	1.331
48.59	0.5804	43.49	43.92	2.192	52.00	0.4093	123.11	123.38	1.391
48.67	0.7706	54.39	54.79	2.085	52.08	0.3795	137.02	137.29	1.422
48.75	0.6788	40.48	40.63	0.744	52.17	0.3343	142.84	143.14	1.536
48.83	0.5721	29.88	30.09	1.131	52.25	0.315	140.77	141.05	1.455
48.91	0.5605	26.94	27.34	2.094	52.33	0.3124	134.87	135.14	1.367
49.00	0.5344	51.85	52.26	2.141	52.42	0.3017	125.03	125.27	1.273
49.07	0.4632	72.26	72.61	1.791	52.51	0.2955	116.43	116.68	1.294
49.15	0.4103	83.26	83.36	0.562	52.59	0.2938	111.1	111.35	1.277
49.23	0.3226	103.16	103.33	0.878	52.67	0.3098	112.9	113.16	1.351
49.31	0.2681	118.67	118.88	1.085	52.76	0.3021	117.25	117.52	1.386
49.40	0.2954	119.7	119.89	0.955	52.84	0.3175	122.39	122.66	1.389
49.48	0.298	118.78	118.98	1.056	52.92	0.3398	123.7	123.97	1.388
49.56	0.3225	115.46	115.66	1.043	53.00	0.3357	123.08	123.36	1.4
49.64	0.3999	108.97	109.19	1.137	53.09	0.3433	119.26	119.52	1.389
49.72	0.4541	103.47	103.7	1.175	53.17	0.3539	117.28	117.55	1.374
49.81	0.428	98.15	98.35	1.04	53.25	0.3446	113.47	113.73	1.36
49.89	0.4015	100.44	100.65	1.102	53.33	0.3507	110.51	110.77	1.356
49.97	0.4322	111.89	112.11	1.114	53.42	0.3474	107.37	107.64	1.39
50.05	0.3566	128.16	128.43	1.386	53.50	0.3279	105.02	105.29	1.407
50.13	0.3261	136.92	137.18	1.339	53.59	0.3328	105.51	105.79	1.434
50.21	0.2929	130.08	130.3	1.174	53.67	0.3237	107.3	107.57	1.359
50.29	0.301	118.91	119.14	1.149	53.75	0.3141	109.35	109.62	1.4
50.38	0.3149	110.76	111.01	1.265	53.83	0.3051	107.34	107.61	1.379
50.46	0.308	104.07	104.33	1.363	53.92	0.2943	105.57	105.85	1.437
50.54	0.3015	93.75	93.99	1.264	54.18	0.3279	93.42	93.68	1.372
50.62	0.3216	89.11	89.33	1.138	54.26	0.3555	90.53	90.8	1.365
50.70	0.3602	89.49	89.74	1.276	54.34	0.4205	87.9	88.17	1.414
50.93	0.3588	107	107.24	1.258	54.42	0.4729	85.89	86.17	1.45
51.01	0.3387	113.13	113.4	1.414	54.50	0.5308	88.29	88.59	1.544
51.09	0.3728	117.65	117.91	1.351	54.59	0.6007	95.48	95.81	1.674
51.17	0.4423	124.89	125.18	1.475	54.67	0.6471	92.29	92.6	1.624
51.25	0.456	129.48	129.77	1.513	54.74	0.598	71.17	71.39	1.12
51.34	0.4092	127.66	127.93	1.379	54.83	0.5315	50.89	51.13	1.214
51.42	0.3929	124.96	125.24	1.437	54.91	0.4573	56.29	56.58	1.529
51.50	0.4096	124.18	124.42	1.284	54.99	0.3669	97.26	97.66	2.074
51.59	0.3951	123.45	123.7	1.276	55.07	0.3055	124.15	124.45	1.565
51.67	0.4583	124.91	125.19	1.439	55.15	0.3424	129.17	129.41	1.28
51.75	0.5253	123.63	123.91	1.442	55.24	0.4685	125.28	125.55	1.421
51.83	0.4634	121.51	121.8	1.515	55.32	0.5743	117.63	117.9	1.371

Table D.4 Continued

z (ft)	f_s (tsf)	q_u (tsf)	q_t (tsf)	u_2 (tsf)	z (ft)	f_s (tsf)	q_u (tsf)	q_t (tsf)	u_2 (tsf)
55.40	0.5607	103.7	103.97	1.403	58.86	0.4	19.07	19.94	4.498
55.48	0.5076	97.43	97.73	1.529	58.94	0.4364	17.2	18.26	5.482
55.57	0.4714	105.65	105.91	1.378	59.03	0.3653	19.34	20.38	5.411
55.65	0.4618	118.82	119.13	1.584	59.11	0.3447	18.82	19.71	4.618
55.73	0.4476	132.46	132.75	1.532	59.19	0.4442	18.39	19.22	4.325
55.82	0.4407	145.1	145.37	1.421	59.27	0.4617	19.54	20.64	5.703
55.90	0.4713	144.69	144.98	1.485	59.35	0.3922	23.68	24.48	4.146
55.98	0.5371	136.19	136.46	1.41	59.44	0.3325	22.92	23.54	3.213
56.07	0.4661	123.9	124.18	1.459	59.52	0.3131	19.66	20.51	4.402
56.15	0.4039	113.83	114.12	1.534	59.60	0.3012	15.85	16.9	5.412
56.23	0.4183	113.96	114.26	1.547	59.69	0.3307	14.39	15.61	6.299
56.31	0.4531	125.03	125.33	1.565	59.77	0.2869	16.06	17.06	5.183
56.40	0.4666	124.65	124.95	1.533	59.85	0.2812	16.66	17.61	4.915
56.48	0.5792	111.67	111.95	1.429	59.93	0.2621	20.36	21.2	4.337
56.57	0.7266	92.09	92.34	1.312	60.01	0.2671	22.04	22.88	4.349
56.65	0.9956	72.12	72.39	1.384	60.10	0.304	23.55	24.24	3.588
56.73	1.1858	53.15	53.4	1.295	60.18	0.3398	23.17	23.9	3.757
56.81	1.0139	37.95	38.28	1.709	60.26	0.3654	22.38	23.11	3.783
56.89	0.8589	27.44	27.75	1.596	60.34	0.355	18.73	19.46	3.804
56.98	0.6869	21.29	21.73	2.277	60.58	0.2899	11.83	12.88	5.446
57.06	0.5391	17.45	18.1	3.38	60.66	0.2835	11.45	12.64	6.147
57.14	0.4286	16.78	17.9	5.805	60.74	0.2569	12.64	13.89	6.499
57.39	0.278	40.48	40.77	1.505	60.82	0.2693	13.08	14.36	6.6
57.47	0.3524	38.73	39.06	1.708	60.91	0.2464	13.64	14.99	7.008
57.55	0.4255	36.35	36.72	1.919	60.99	0.2475	13.77	15.21	7.492
57.64	0.3894	31.45	31.82	1.901	61.07	0.2464	13.33	14.7	7.08
57.72	0.3513	25.31	25.71	2.108	61.15	0.2446	12.79	14.38	8.217
57.80	0.3159	22.22	22.74	2.729	61.23	0.2361	13.02	14.59	8.136
57.88	0.2888	16.4	17.11	3.679	61.31	0.2617	14.02	15.58	8.095
57.96	0.2662	13.21	14.21	5.179	61.39	0.3402	15.4	16.83	7.428
58.05	0.2685	12.22	13.35	5.858	61.48	0.3771	18.03	19.43	7.267
58.13	0.2521	12.26	13.5	6.418	61.56	0.4714	22.3	23.44	5.913
58.21	0.2803	14.57	15.83	6.497	61.64	0.4704	24.3	25.27	4.998
58.29	0.2926	17.03	18.14	5.745	61.73	0.4694	22.42	23.44	5.272
58.37	0.2643	15.34	16.48	5.916	61.81	0.496	19.91	20.8	4.584
58.45	0.2827	13.07	14.19	5.806	61.89	0.4316	17.26	18.42	6.004
58.53	0.366	12.89	14.2	6.794	61.98	0.3943	16.02	17.29	6.541
58.62	0.4199	16.49	17.79	6.729	62.06	0.3447	15.27	16.51	6.415
58.70	0.4476	19.9	20.81	4.731	62.14	0.3557	16.69	18.18	7.682
58.78	0.3671	20.36	21.05	3.583	62.22	0.4246	18.61	19.91	6.696

Table D.4 Continued

z (ft)	f_s (tsf)	q_u (tsf)	q_t (tsf)	u_2 (tsf)	z (ft)	f_s (tsf)	q_u (tsf)	q_t (tsf)	u_2 (tsf)
62.31	0.4069	19.3	20.44	5.925	65.74	0.4946	17.85	19.01	6.017
62.39	0.3991	19.94	20.98	5.393	65.83	0.5712	18.66	20.11	7.537
62.47	0.3963	19.61	20.73	5.828	65.91	0.5142	21.7	23.16	7.573
62.55	0.4212	17.4	18.69	6.685	66.00	0.4634	21.17	22.05	4.602
62.63	0.4146	16.9	18.34	7.453	66.08	0.3972	19.79	20.66	4.518
62.72	0.4249	17.22	18.56	6.944	66.16	0.4964	16.64	17.75	5.737
62.80	0.4075	17.6	18.78	6.13	66.24	0.6858	17.53	18.91	7.134
62.88	0.4302	17.89	19.23	6.966	66.33	0.657	22.63	24	7.11
62.97	0.4239	16.9	18.25	7.004	66.41	0.5966	26.56	27.3	3.816
63.05	0.4353	16.57	17.95	7.144	66.49	0.5892	22.67	23.45	4.013
63.13	0.4173	16.05	17.46	7.313	66.57	0.582	17.4	18.38	5.082
63.21	0.4391	16.28	17.82	7.996	66.65	0.5373	16.78	18.16	7.179
63.30	0.4494	15.59	17.11	7.894	66.73	0.498	17.3	18.58	6.6
63.38	0.4596	16.42	17.88	7.558	66.94	0.4148	15.4	16.86	7.593
63.46	0.4772	16.68	18.29	8.338	67.02	0.4791	16.27	17.79	7.853
63.54	0.5009	18.49	20.22	8.962	67.10	0.4438	19.22	20.77	8.074
63.78	0.5045	20.41	21.5	5.604	67.18	0.4262	23.19	24.45	6.53
63.86	0.4931	19.35	20.59	6.407	67.25	0.4751	22.8	23.98	6.12
63.94	0.4766	21.39	22.53	5.918	67.34	0.527	23.72	25.19	7.606
64.03	0.4377	18.42	19.79	7.09	67.42	0.5462	24.05	25.36	6.801
64.11	0.3953	18.26	19.59	6.885	67.50	0.5567	26.18	27.33	5.959
64.19	0.4116	16.65	17.89	6.432	67.58	0.4901	25.5	26.62	5.789
64.27	0.4217	16.02	17.46	7.464	67.66	0.4905	21.79	23.04	6.471
64.35	0.4317	17.22	18.77	7.996	67.75	0.5163	19.3	20.67	7.083
64.43	0.4385	19.86	21.01	5.993	67.83	0.4637	17.49	19.08	8.279
64.52	0.4613	19.48	20.63	5.975	67.91	0.4188	16.84	18.4	8.041
64.59	0.4667	19.55	20.74	6.153	68.00	0.3566	16.15	17.58	7.428
64.68	0.4823	21.01	22.12	5.728	68.08	0.3449	14.89	16.48	8.221
64.76	0.4671	21.15	22.1	4.915	68.16	0.3373	15.93	17.6	8.651
64.84	0.4438	18.42	19.43	5.233	68.24	0.3284	15.74	17.39	8.513
64.93	0.4276	15.77	16.92	5.938	68.33	0.309	14.39	16.05	8.561
65.01	0.4097	14.89	16.23	6.927	68.41	0.311	14.77	16.43	8.579
65.09	0.354	15.02	16.59	8.133	68.50	0.2991	15.4	17.1	8.803
65.17	0.3718	16.22	17.82	8.294	68.58	0.3053	16.3	17.89	8.218
65.25	0.3882	17.04	18.47	7.392	68.66	0.2989	15.9	17.55	8.554
65.34	0.4479	18.87	20.27	7.286	68.74	0.2866	16.02	17.68	8.568
65.42	0.5461	22.3	23.35	5.45	68.83	0.2698	15.4	16.78	7.155
65.50	0.5663	23.05	24.03	5.089	68.91	0.2689	13.99	15.47	7.668
65.58	0.5462	22.55	23.5	4.935	68.99	0.2643	13.2	14.78	8.201
65.66	0.4828	20.92	21.76	4.391	69.07	0.2495	13.71	15.25	7.968

Table D.4 Continued

z (ft)	f_s (tsf)	q_u (tsf)	q_t (tsf)	u_2 (tsf)	z (ft)	f_s (tsf)	q_u (tsf)	q_t (tsf)	u_2 (tsf)
69.15	0.2534	13.71	15.17	7.561	72.37	3.465	196.01	196.24	1.207
69.23	0.2462	12.89	14.35	7.555	72.45	3.3746	196.88	197	0.619
69.32	0.2376	12.39	13.91	7.912	72.52	3.6384	196.13	196.42	1.506
69.40	0.2314	13.64	15.11	7.597	72.60	3.7838	195.52	195.8	1.424
69.48	0.254	13.31	14.89	8.156	72.67	3.706	198.58	198.8	1.174
69.57	0.2306	14.23	15.8	8.123	72.75	3.5601	206.04	206.09	0.25
69.65	0.2515	14.26	15.73	7.644	72.82	3.4087	208.91	209.05	0.711
69.73	0.2876	14.52	15.85	6.888	72.90	3.2511	208.22	209.35	5.835
69.82	0.279	13.26	14.65	7.19	72.97	3.1114	229.76	229.87	0.533
69.90	0.2591	12.39	13.63	6.436	73.05	3.0151	237.42	237.38	-0.189
69.98	0.2547	11.38	12.69	6.759	73.12	3.1051	237.14	237.59	2.316
70.07	0.225	11.83	13.08	6.505	73.36	4.3547	237.03	237.59	2.909
70.15	0.2241	11.32	12.67	6.986	73.43	4.4387	242.43	242.72	1.538
70.23	0.2714	11.38	12.75	7.067	73.49	4.5006	247.68	247.87	0.958
70.31	0.3083	12.8	14.18	7.127	73.56	4.2181	253.72	254.13	2.152
70.39	0.2839	12.49	13.93	7.472	73.64	3.8006	264.51	264.58	0.365
70.47	0.2854	14.59	15.96	7.087	73.70	3.3346	272.52	272.49	-0.183
70.56	0.3245	17.28	18.56	6.629	73.78	3.0276	270.03	269.94	-0.497
70.64	0.3708	21.39	22.62	6.337	73.84	3.0459	265.64	265.56	-0.398
70.72	0.4601	22.18	23.4	6.315	73.92	3.1673	260.08	260	-0.418
70.80	0.5702	26.38	27.67	6.701	73.99	3.5102	256.31	256.28	-0.197
70.88	0.6828	39.23	40.62	7.222	74.06	3.7464	250.84	250.8	-0.182
70.96	0.9504	67.81	68.94	5.889	74.13	3.8895	244.71	244.68	-0.147
71.04	1.2528	101.27	102.17	4.636	74.20	3.9723	242.31	242.27	-0.203
71.12	1.58	116.12	116.8	3.5	74.27	3.9842	239.8	239.77	-0.164
71.21	1.996	133.31	133.77	2.406	74.34	3.9094	239.83	239.88	0.22
71.29	2.3667	153	153.27	1.431	74.41	3.875	250.16	250.19	0.142
71.37	2.6725	168.24	168.39	0.781	74.48	3.8393	261.37	261.37	-0.014
71.45	3.0826	176.07	176.21	0.72	74.55	3.853	269.65	269.63	-0.093
71.53	3.5076	180.72	180.87	0.775	74.62	3.8494	278.56	278.54	-0.097
71.61	3.9108	182.6	182.89	1.498	74.69	4.0167	284.45	284.44	-0.05
71.69	4.2805	189.12	189.23	0.526	74.76	4.349	293.5	293.5	0.019
71.76	4.6429	194.08	194.17	0.429	74.83	4.4161	295.49	295.48	-0.077
71.84	4.8298	190.25	190.53	1.428	74.91	0	299.67	299.67	-0.015
71.92	4.7452	184.25	184.49	1.248	74.97	0	304.02	304.02	0.004
71.99	4.6108	178.52	178.73	1.11	75.05	0	308.79	308.88	0.456
72.07	4.4814	174.39	174.85	2.349	75.11	0	328.53	328.85	1.658
72.15	4.3572	178.92	179.93	5.23	75.18	0	366.9	367.05	0.788
72.22	4.1271	185.82	186.07	1.304	75.25	0	415.53	415.71	0.905
72.29	3.7903	191.95	192.19	1.221	75.25	0	415.53	415.71	0.905

Table D.5 CPT Data from SC-2 at the Rest Area Ponds site.

z	f_s	q_u	q_t	u_2	z	f_s	q_u	q_t	u_2
(ft)	(tsf)	(tsf)	(tsf)	(tsf)	(ft)	(tsf)	(tsf)	(tsf)	(tsf)
0.00	0	0	0	0	3.37	1.3121	237.57	237.59	0.102
0.18	0	44.59	44.61	0.114	3.45	1.3412	238.18	238.2	0.115
0.24	0	52.88	52.91	0.139	3.54	1.3434	236.94	236.96	0.106
0.30	0.1506	63.47	63.5	0.12	3.62	1.3425	233.81	233.83	0.101
0.37	0.1934	74.85	74.88	0.121	3.73	1.346	229.3	229.32	0.1
0.45	0.2488	80.3	80.32	0.12	3.81	1.3424	224.25	224.27	0.102
0.54	0.3195	79.92	79.94	0.131	3.90	1.3432	218.75	218.77	0.09
0.63	0.3473	76.69	76.72	0.129	3.98	1.3241	213.59	213.61	0.084
0.71	0.3501	78.62	78.64	0.125	4.07	1.3118	207.42	207.44	0.088
0.80	0.3882	88.33	88.35	0.113	4.15	1.2974	201.16	201.17	0.077
0.89	0.4719	103.14	103.17	0.134	4.25	1.2756	194.05	194.07	0.092
0.98	0.5668	115.72	115.74	0.131	4.33	1.2415	185.19	185.2	0.074
1.06	0.6088	117.26	117.28	0.129	4.42	1.2041	176.92	176.93	0.07
1.15	0.6496	113.71	113.73	0.113	4.50	1.1565	168.78	168.79	0.062
1.23	0.671	109.19	109.2	0.074	4.58	1.1077	160.24	160.25	0.074
1.32	0.6695	101.94	101.95	0.059	4.67	1.0623	150.49	150.5	0.058
1.40	0.6002	92.85	92.86	0.054	4.76	0.9932	140.27	140.28	0.034
1.49	0.5468	84.69	84.7	0.05	4.84	0.9275	130.23	130.23	0.03
1.57	0.5163	78.53	78.54	0.046	4.93	0.8525	119.11	119.11	0.029
1.66	0.5183	72.89	72.89	0.022	5.02	0.7929	107.3	107.31	0.025
1.75	0.5243	72.72	72.72	0.02	5.11	0.7201	96	96	0.018
1.83	0.5389	78.45	78.46	0.031	5.19	0.6544	85.02	85.03	0.005
1.92	0.586	91.18	91.19	0.051	5.28	0.6105	75.23	75.23	-0.012
2.00	0.6566	109.78	109.8	0.121	5.36	0.539	67.15	67.15	-0.007
2.09	0.7625	132.52	132.56	0.191	5.45	0.4676	59.82	59.81	-0.01
2.17	0.8506	154.59	154.63	0.216	5.53	0.425	53.13	53.13	-0.019
2.26	0.9369	174.44	174.49	0.264	5.62	0.3883	47.28	47.28	-0.004
2.34	0.7356	188.89	188.93	0.226	5.82	0.2923	35.27	35.26	-0.023
2.42	0.735	200.76	200.81	0.232	5.91	0.2705	31.05	31.05	-0.017
2.51	0.8218	212.57	212.61	0.215	6.00	0.2419	27.77	27.76	-0.016
2.59	0.8935	221.5	221.54	0.21	6.09	0.2169	25.76	25.75	-0.016
2.66	0.9383	205.66	205.7	0.19	6.18	0.2048	24.45	24.44	-0.015
2.70	0.9666	208.47	208.48	0.071	6.27	0.1905	23.96	23.96	-0.019
2.78	1.0466	220.62	220.63	0.045	6.36	0.1737	23.05	23.04	-0.073
2.86	1.111	225.14	225.16	0.066	6.45	0.1556	22.62	22.6	-0.075
2.95	1.1648	229.16	229.18	0.077	6.53	0.14	22.74	22.73	-0.079
3.04	1.1998	232.3	232.32	0.077	6.63	0.1307	22.24	22.22	-0.089
3.12	1.2295	233.06	233.07	0.08	6.72	0.1091	22.12	22.1	-0.1
3.20	1.2576	234.68	234.7	0.088	6.81	0.1042	22.13	22.11	-0.094
3.28	1.2854	237.34	237.35	0.086	6.89	0.1007	21.86	21.84	-0.107

Table D.5 Continued

z	f_s	q_u	q_t	u_2	z	f_s	q_u	q_t	u_2
(ft)	(tsf)	(tsf)	(tsf)	(tsf)	(ft)	(tsf)	(tsf)	(tsf)	(tsf)
6.99	0.1023	21.77	21.75	-0.099	10.55	0.1199	31.19	31.15	-0.25
7.08	0.1384	21.5	21.48	-0.119	10.64	0.123	32.66	32.61	-0.265
7.16	0.1968	22	21.98	-0.122	10.73	0.1254	35.05	35	-0.258
7.26	0.235	23.58	23.56	-0.118	10.82	0.1233	37.33	37.28	-0.242
7.35	0.2463	27.59	27.56	-0.116	10.92	0.1311	38.62	38.57	-0.248
7.44	0.3075	34.8	34.77	-0.128	11.01	0.1418	39.99	39.95	-0.222
7.53	0.3383	39.09	39.08	-0.059	11.11	0.1454	42.18	42.14	-0.223
7.62	0.3551	36.43	36.43	-0.026	11.20	0.1526	44.84	44.8	-0.23
7.71	0.3378	34.75	34.71	-0.194	11.29	0.1711	48.91	48.87	-0.205
7.80	0.3368	36.81	36.76	-0.24	11.37	0.1941	53.11	53.07	-0.202
7.89	0.3667	42.78	42.74	-0.246	11.45	0.222	57.4	57.36	-0.209
7.98	0.3699	51.65	51.61	-0.228	11.52	0.2539	62.17	62.13	-0.202
8.07	0.4621	64.48	64.43	-0.252	11.60	0.2891	68.06	68.03	-0.177
8.16	0.5665	77.82	77.77	-0.278	11.68	0.3199	73.85	73.81	-0.184
8.25	0.6473	96.2	96.15	-0.265	11.76	0.4717	80.34	80.3	-0.173
8.34	0.6503	110.69	110.63	-0.333	11.84	0.4004	87.2	87.17	-0.171
8.43	0.6073	117.57	117.49	-0.399	11.92	0.4424	95.08	95.05	-0.139
8.52	0.5034	117.69	117.62	-0.385	12.00	0.5079	102.35	102.33	-0.138
8.61	0.2295	109.27	109.19	-0.462	12.08	0.5584	109.9	109.88	-0.114
8.70	0.1619	102.11	102.01	-0.508	12.11	0.5726	97.63	97.61	-0.115
8.79	0.1439	93.6	93.51	-0.498	12.20	0.6289	118.39	118.37	-0.088
8.88	0.1458	84.9	84.8	-0.494	12.27	0.7145	125.33	125.32	-0.061
8.96	0.163	75.52	75.46	-0.294	12.35	0.8629	130.54	130.53	-0.035
9.05	0.1898	69.08	69.02	-0.282	12.43	1.0762	136.23	136.23	0
9.14	0.1942	63.41	63.36	-0.258	12.50	1.283	140.9	140.91	0.023
9.22	0.2051	59.06	59.01	-0.273	12.58	1.4356	137.95	137.97	0.085
9.31	0.2096	55.01	54.96	-0.282	12.65	1.5656	132.61	132.64	0.125
9.40	0.2049	52.26	52.21	-0.27	12.73	1.7026	131.07	131.09	0.063
9.48	0.1986	48.61	48.55	-0.293	12.80	1.7664	136.38	136.39	0.03
9.57	0.1863	45.42	45.36	-0.295	12.88	1.7362	144.39	144.38	-0.043
9.66	0.1771	41.85	41.8	-0.291	12.95	1.5893	149.16	149.11	-0.25
9.75	0.1668	38.21	38.15	-0.291	13.03	1.2691	150.82	150.75	-0.353
9.84	0.1578	35.52	35.46	-0.293	13.11	0.8494	147.85	147.76	-0.43
9.93	0.1472	33.51	33.46	-0.276	13.18	0.5851	142.88	142.79	-0.485
10.02	0.1442	31.91	31.85	-0.289	13.26	0.4826	133.81	133.69	-0.586
10.11	0.1391	30.91	30.85	-0.289	13.34	0.4898	125.52	125.41	-0.53
10.20	0.1351	30.35	30.3	-0.278	13.41	0.5228	121.25	121.15	-0.498
10.28	0.1279	29.85	29.79	-0.281	13.49	0.5475	119.18	119.09	-0.472
10.37	0.1272	29.86	29.81	-0.265	13.57	0.5718	118.26	118.18	-0.436
10.46	0.1272	29.97	29.92	-0.274	13.64	0.6068	117.6	117.52	-0.414

Table D.5 Continued

z	f_s	q_u	q_t	u_2	z	f_s	q_u	q_t	u_2
(ft)	(tsf)	(tsf)	(tsf)	(tsf)	(ft)	(tsf)	(tsf)	(tsf)	(tsf)
13.73	0.6509	117.13	117.05	-0.418	17.14	0.5858	159.43	159.38	-0.256
13.81	0.679	115.03	114.96	-0.412	17.23	0.5706	160.56	160.53	-0.2
13.88	0.6903	112.67	112.59	-0.392	17.32	0.6036	158.61	158.57	-0.202
13.96	0.68	109.44	109.36	-0.393	17.40	0.5629	154.56	154.53	-0.183
14.04	0.6559	106.21	106.13	-0.387	17.49	0.5694	149.19	149.16	-0.17
14.11	0.636	103.73	103.66	-0.377	17.58	0.573	143.3	143.27	-0.131
14.19	0.6163	101.15	101.08	-0.354	17.66	0.573	135.53	135.51	-0.121
14.27	0.5906	99.14	99.07	-0.34	17.75	0.5795	128.34	128.32	-0.117
14.35	0.586	97.2	97.14	-0.335	17.84	0.5861	120.96	120.94	-0.086
14.43	0.5835	95.41	95.34	-0.327	17.92	0.5589	110.89	110.88	-0.082
14.52	0.587	94.12	94.06	-0.288	18.01	0.5327	100.09	100.08	-0.065
14.61	0.5947	91.72	91.67	-0.277	18.10	0.5436	92.14	92.13	-0.05
14.70	0.5912	90.47	90.42	-0.27	18.18	0.523	87.75	87.74	-0.018
14.78	0.5999	90.97	90.92	-0.252	18.27	0.5126	85.28	85.28	0.001
14.87	0.5977	91.26	91.22	-0.239	18.36	0.5315	81.63	81.63	-0.002
14.96	0.5963	91.18	91.14	-0.216	18.45	0.5677	79.41	79.42	0.022
15.04	0.5658	90.42	90.38	-0.216	18.54	0.5757	77.74	77.75	0.023
15.13	0.5796	92.19	92.15	-0.188	18.60	0.5917	76.23	76.26	0.107
15.22	0.589	95.2	95.17	-0.177	18.68	0.6997	77.82	77.85	0.147
15.31	0.5846	99.01	98.98	-0.157	18.77	0.8979	80.21	80.24	0.154
15.42	0.6104	102.79	102.8	0.032	18.85	1.1707	81.59	81.63	0.175
15.50	0.6221	104.74	104.74	0.03	18.94	1.2421	73.63	73.67	0.176
15.58	0.6257	104.45	104.46	0.052	19.02	1.2964	59.21	59.24	0.194
15.67	0.6413	103.48	103.5	0.083	19.11	1.3655	51.8	51.85	0.247
15.76	0.6975	101.44	101.45	0.101	19.19	1.3214	49.94	50.06	0.614
15.85	0.7295	99.39	99.41	0.124	19.28	1.3531	50.39	50.5	0.556
15.93	0.698	96.99	97.02	0.12	19.36	1.3841	50.24	50.35	0.536
16.02	0.6926	95.78	95.81	0.136	19.45	1.2722	57.05	57.33	1.423
16.11	0.69	96.16	96.19	0.129	19.53	1.1699	71.76	72.14	1.974
16.19	0.7159	97.29	97.32	0.151	19.62	0.821	76.36	76.43	0.353
16.28	0.8031	98.97	99.01	0.181	19.71	0.6445	67.73	67.79	0.289
16.36	0.9014	101.81	101.85	0.172	19.79	0.6879	56.66	56.69	0.129
16.45	0.9099	108.25	108.29	0.188	19.88	0.6927	45.65	45.66	0.068
16.54	0.8635	111.39	111.43	0.199	19.97	0.7649	35.7	35.73	0.194
16.62	0.7363	115.91	115.96	0.234	20.06	0.8279	28.68	28.74	0.333
16.71	0.5346	124.61	124.66	0.268	20.14	0.8616	24.88	24.98	0.508
16.79	0.4732	136.32	136.31	-0.073	20.23	0.9103	22.42	22.6	0.914
16.88	0.4893	144.64	144.58	-0.302	20.32	0.8482	19.94	20.19	1.294
16.97	0.5336	152.4	152.33	-0.365	20.41	0.759	18.24	18.56	1.662
17.06	0.5822	156.6	156.53	-0.363	20.49	0.7059	17.79	18.16	1.896

Table D.5 Continued

z	f_s	q_u	q_t	u_2	z	f_s	q_u	q_t	u_2
(ft)	(tsf)	(tsf)	(tsf)	(tsf)	(ft)	(tsf)	(tsf)	(tsf)	(tsf)
20.58	0.7182	21.49	21.9	2.14	24.23	0.0925	19.31	19.34	0.156
20.67	0.6436	23.69	23.98	1.488	24.32	0.093	18.04	18.07	0.154
20.75	0.5818	20.48	20.65	0.855	24.41	0.0728	17.61	17.64	0.162
20.84	0.5297	16.16	16.29	0.684	24.49	0.064	17.16	17.19	0.154
20.93	0.5192	16.53	16.79	1.334	24.58	0.0608	15.64	15.67	0.12
21.01	0.4779	20.75	20.99	1.255	24.67	0.0744	13.58	13.61	0.149
21.10	0.4714	19.99	20.08	0.447	24.75	0.0879	10.94	10.98	0.185
21.19	0.4924	18.22	18.3	0.378	24.84	0.0917	8.24	8.29	0.235
21.27	0.4767	16.79	16.89	0.547	24.92	0.0837	6.8	6.86	0.285
21.36	0.3803	18.17	18.22	0.287	25.14	0.0803	5.35	5.51	0.812
21.45	0.3014	19.66	19.69	0.138	25.23	0.0871	5.05	5.23	0.97
21.54	0.219	22.63	22.61	-0.14	25.31	0.0709	4.85	5.07	1.102
21.62	0.1408	24.18	24.13	-0.259	25.39	0.0729	4.66	4.9	1.245
21.70	0.1136	25.24	25.19	-0.228	25.48	0.0705	4.6	4.87	1.38
21.99	0.0886	25.58	25.61	0.165	25.57	0.0804	4.17	4.46	1.543
22.08	0.0929	25.33	25.35	0.143	25.65	0.0767	4.02	4.34	1.681
22.16	0.1038	24.99	25.01	0.109	25.74	0.0741	4.54	4.9	1.827
22.25	0.0988	24.32	24.34	0.105	25.82	0.0833	4.72	5.09	1.889
22.34	0.0957	23.62	23.65	0.156	25.91	0.0837	4.54	4.93	1.992
22.42	0.0884	24.43	24.46	0.141	25.99	0.0962	4.48	4.89	2.117
22.51	0.0852	25.02	25.04	0.102	26.08	0.0926	5.04	5.45	2.144
22.59	0.0974	25.13	25.15	0.104	26.16	0.0949	5.67	6.09	2.157
22.68	0.0952	24.88	24.9	0.118	26.25	0.0872	6.29	6.69	2.066
22.77	0.0943	25.9	25.93	0.155	26.34	0.0847	5.92	6.32	2.07
22.85	0.0835	26.94	26.97	0.159	26.42	0.0822	5.22	5.63	2.135
22.94	0.0847	27.96	27.99	0.147	26.51	0.0821	4.98	5.39	2.099
23.03	0.0836	28.18	28.2	0.129	26.60	0.0793	4.85	5.27	2.138
23.11	0.0847	28.34	28.37	0.14	26.68	0.0708	4.71	5.14	2.202
23.20	0.0877	27.52	27.54	0.142	26.77	0.0705	4.97	5.41	2.265
23.28	0.0937	26.96	26.99	0.161	26.86	0.0693	4.97	5.42	2.321
23.37	0.1093	26.24	26.27	0.158	26.94	0.0692	5.36	5.83	2.391
23.46	0.1176	27.34	27.37	0.193	27.03	0.0708	4.91	5.39	2.453
23.54	0.1088	25.94	25.97	0.148	27.12	0.072	4.79	5.27	2.519
23.63	0.0844	24.5	24.53	0.135	27.20	0.0744	4.6	5.09	2.546
23.71	0.0992	22.49	22.51	0.086	27.29	0.0726	4.73	5.23	2.581
23.80	0.1064	21.95	21.96	0.037	27.37	0.0644	4.4	4.9	2.586
23.89	0.102	21.61	21.61	-0.005	27.45	0.0679	4.35	4.87	2.668
23.97	0.0898	20.61	20.62	0.034	27.54	0.0705	4.09	4.62	2.746
24.06	0.0911	20.62	20.64	0.095	27.63	0.0743	4.03	4.58	2.863
24.14	0.0974	19.86	19.88	0.125	27.71	0.0628	4.34	4.88	2.799

Table D.5 Continued

z	f_s	q_u	q_t	u_2	z	f_s	q_u	q_t	u_2
(ft)	(tsf)	(tsf)	(tsf)	(tsf)	(ft)	(tsf)	(tsf)	(tsf)	(tsf)
27.80	0.0615	4.54	5.09	2.884	31.38	0.1025	5.66	6.08	2.179
27.89	0.0606	4.28	4.84	2.909	31.61	0.0694	4.54	4.88	1.757
27.98	0.0598	4.1	4.68	2.998	31.69	0.0584	3.93	4.34	2.114
28.06	0.0607	3.78	4.36	3	31.78	0.045	3.14	3.59	2.302
28.15	0.0657	3.72	4.3	3.044	31.86	0.0447	3.21	3.68	2.437
28.39	0.0578	4.09	4.72	3.258	31.95	0.0423	3.27	3.76	2.565
28.47	0.0583	4.67	5.3	3.26	32.03	0.0435	3.59	4.12	2.718
28.56	0.0654	4.47	5.09	3.216	32.12	0.045	3.64	4.18	2.793
28.64	0.0731	4.73	5.35	3.23	32.20	0.033	4.15	4.71	2.863
28.73	0.0734	4.53	5.12	3.084	32.29	0.0468	4.03	4.6	2.941
28.81	0.0751	4.27	4.88	3.165	32.38	0.0426	4.86	5.43	2.956
28.89	0.0717	4.21	4.83	3.181	32.46	0.0334	4.34	4.92	3.002
28.98	0.0705	4.16	4.79	3.264	32.55	0.0426	4.26	4.84	2.972
29.06	0.073	4.42	5.04	3.246	32.63	0.0506	4.68	5.27	3.098
29.15	0.0725	4.29	4.92	3.26	32.72	0.0934	3.84	4.45	3.185
29.23	0.0543	4.23	4.86	3.304	32.80	0.0902	3.25	3.91	3.404
29.32	0.0637	4.67	5.31	3.299	32.88	0.0905	4.27	5	3.751
29.41	0.0591	4.67	5.3	3.257	32.97	0.0858	10.49	11.21	3.725
29.49	0.0578	4.15	4.79	3.281	33.05	0.1121	32	32.5	2.59
29.58	0.0645	4.09	4.7	3.185	33.13	0.1671	52.52	52.74	1.132
29.66	0.0702	4.22	4.86	3.314	33.22	0.2494	66.91	67.13	1.168
29.75	0.0624	3.96	4.57	3.16	33.31	0.3351	72.52	72.72	1.015
29.84	0.0725	3.78	4.4	3.211	33.39	0.4761	76.16	76.34	0.962
29.92	0.0675	3.59	4.23	3.29	33.48	0.5702	82.93	83.12	0.952
30.01	0.0616	3.65	4.29	3.32	33.56	0.6238	91.64	91.84	0.997
30.09	0.0612	3.71	4.33	3.192	33.65	0.636	93.8	93.98	0.907
30.18	0.0545	4.04	4.67	3.274	33.74	0.6336	86.32	86.48	0.826
30.26	0.0666	3.65	4.3	3.383	33.82	0.5638	76.36	76.52	0.845
30.35	0.0529	3.84	4.47	3.255	33.91	0.4366	69.73	69.89	0.837
30.44	0.0554	3.72	4.35	3.234	33.99	0.3682	64.44	64.59	0.746
30.52	0.0577	3.45	4.09	3.321	34.08	0.3367	62.55	62.7	0.795
30.61	0.0564	3.97	4.62	3.364	34.17	0.3183	60.48	60.63	0.8
30.69	0.0438	3.39	4.01	3.186	34.25	0.3035	54.17	54.32	0.763
30.78	0.0462	3.4	4.03	3.242	34.34	0.357	49.44	49.59	0.804
30.87	0.0574	3.27	3.94	3.474	34.43	0.4068	44.99	45.16	0.834
30.96	0.0533	4.21	4.89	3.525	34.51	0.4569	38.37	38.53	0.864
31.04	0.0739	5.96	6.59	3.241	34.59	0.5354	33.02	33.19	0.898
31.13	0.0839	8.6	9.06	2.353	34.87	0.3855	25.35	25.6	1.299
31.21	0.0934	8.95	9.35	2.076	34.96	0.3195	30.17	30.49	1.655
31.30	0.1052	6.85	7.24	2.034	35.04	0.3033	37.21	37.4	0.953

Table D.5 Continued

z	f_s	q_u	q_t	u_2	z	f_s	q_u	q_t	u_2
(ft)	(tsf)	(tsf)	(tsf)	(tsf)	(ft)	(tsf)	(tsf)	(tsf)	(tsf)
35.13	0.3618	37.66	37.8	0.771	37.56	0.231	11.61	12.02	2.157
35.21	0.3994	35.19	35.35	0.823	37.65	0.2227	11.25	11.8	2.869
35.30	0.3781	29.61	29.76	0.745	37.73	0.2146	12.23	12.75	2.704
35.38	0.3447	25.98	26.13	0.819	37.82	0.2536	12.36	12.85	2.529
35.47	0.2865	23.23	23.42	0.989	38.12	0.3373	19.65	20.01	1.862
35.56	0.2727	27.8	28.02	1.152	38.20	0.3178	15.88	16.23	1.788
35.65	0.2456	34.83	35.05	1.122	38.28	0.2719	36.32	36.72	2.083
35.73	0.2661	32.84	32.98	0.72	38.37	0.2981	69.29	69.5	1.095
35.82	0.3346	28.99	29.11	0.633	38.46	0.3646	79.55	79.7	0.773
35.90	0.3631	29.31	29.47	0.837	38.54	0.4752	80.59	80.76	0.87
35.99	0.4272	26.57	26.76	0.991	38.63	0.6795	68.08	68.18	0.511
36.08	0.5138	21.47	21.67	1.011	38.71	0.7975	46.78	46.86	0.437
36.16	0.4835	18.39	18.63	1.223	38.80	0.7716	31.98	32.07	0.474
36.25	0.404	13.87	14.13	1.311	38.89	0.6773	23.36	23.49	0.709
36.34	0.3253	9.92	10.22	1.559	38.98	0.577	17.66	17.86	1.018
36.43	0.2781	7.5	8	2.598	39.06	0.4521	14.1	14.38	1.414
36.52	0.1677	8.17	8.79	3.227	39.15	0.3396	12.5	12.79	1.496
36.60	0.1582	7.16	7.84	3.534	39.23	0.2693	11.74	12.15	2.093
36.69	0.1352	9.95	10.72	4.015	39.32	0.1944	11.23	11.75	2.683
36.77	0.1604	15.15	15.96	4.158	39.40	0.1642	10.35	10.9	2.858
36.86	0.2623	22.33	22.78	2.327	39.49	0.1996	9.41	10.17	3.905
36.95	0.3657	29.67	29.99	1.644	39.57	0.1982	11.11	11.9	4.062
37.04	0.331	27.36	27.5	0.748	39.66	0	12.27	13.04	3.947
37.12	0.2969	20.71	20.89	0.931	39.75	0	11.08	11.8	3.755
37.21	0.2935	16.3	16.6	1.556	39.84	0	9.91	10.67	3.951
37.30	0.3288	15.85	16.27	2.149	39.92	0	9.23	10.07	4.325
37.38	0.2732	15.37	15.78	2.132	39.92	0	9.23	10.07	4.325
37.47	0.2397	14.4	14.74	1.783					

Table D.6 CPT Data from SC-3 at the Rest Area Ponds site.

z	f_s	q_u	q_t	u_2	z	f_s	q_u	q_t	u_2
(ft)	(tsf)	(tsf)	(tsf)	(tsf)	(ft)	(tsf)	(tsf)	(tsf)	(tsf)
0.00	0	0	0	0	3.59	2.324	318.9	318.93	0.128
0.23	0	21.97	21.97	0.038	3.68	2.3184	313.52	313.53	0.085
0.30	0.2963	32.73	32.74	0.049	3.77	2.3043	307.37	307.38	0.079
0.38	0.2975	44.41	44.42	0.059	3.86	2.276	299.3	299.32	0.092
0.46	0.3189	57.05	57.07	0.099	3.95	2.2386	289.14	289.14	-0.02
0.54	0.3568	67.78	67.8	0.105	4.04	2.192	278.58	278.58	0.001
0.61	0.4	76.61	76.65	0.195	4.13	2.1294	268.53	268.54	0.01
0.70	0.4315	82.94	82.95	0.06	4.22	2.0982	257.23	257.23	0.007
0.77	0.4641	82.77	82.77	-0.047	4.29	2.0584	246.81	246.81	0.001
0.85	0.4959	84.74	84.74	0.014	4.36	1.9874	237.89	237.89	0.013
0.93	0.537	83.77	83.8	0.135	4.43	1.9139	226.71	226.71	-0.005
1.01	0.5567	82.06	82.09	0.127	4.50	1.8431	212.02	212.01	-0.009
1.09	0.582	81.43	81.45	0.089	4.58	1.7512	198.7	198.7	0.009
1.17	0.6113	82.77	82.79	0.072	4.65	1.643	182.96	182.96	0.018
1.25	0.6657	85.2	85.23	0.141	4.72	1.5282	167.68	167.68	-0.005
1.33	0.7151	88.3	88.3	0.034	4.80	1.3991	152.94	152.94	-0.022
1.42	0.7747	89.34	89.37	0.113	4.87	1.2892	142.09	142.09	-0.003
1.50	0.8087	89.76	89.79	0.129	4.94	1.1737	130	130	-0.002
1.58	0.831	91.18	91.2	0.087	5.01	1.0753	119.98	119.98	-0.006
1.67	0.8379	89.56	89.58	0.111	5.09	1.0057	110.53	110.53	0.002
1.75	0.8343	91.27	91.33	0.281	5.16	0.9411	101.15	101.15	0.001
1.83	0.8467	98.22	98.24	0.076	5.23	0.8797	93.62	93.62	0.015
1.92	0.8492	112.86	112.89	0.151	5.30	0.8222	85.49	85.5	0.014
2.00	0.9032	144	144.04	0.203	5.38	0.6976	78.67	78.67	0.008
2.08	0.9977	183.57	183.63	0.332	5.45	0.6487	72.71	72.72	0.03
2.16	1.0547	218.31	218.37	0.331	5.52	0.6237	68.08	68.08	0.02
2.24	1.112	250.44	250.49	0.271	5.59	0.5851	64.72	64.73	0.043
2.33	1.1722	277.58	277.61	0.151	5.66	0.5333	61.7	61.71	0.053
2.41	1.3105	296.55	296.58	0.138	5.72	0.5066	59.36	59.33	-0.148
2.68	1.7715	317.16	317.18	0.11	5.79	0.4777	56.4	56.36	-0.191
2.76	1.8715	325.31	325.32	0.058	5.85	0.4522	55.07	55.04	-0.155
2.84	1.9715	330.87	330.88	0.072	5.92	0.44	52.98	52.96	-0.128
2.91	2.0612	332.59	332.61	0.072	5.99	0.3972	50.87	50.85	-0.107
2.99	2.1384	334.56	334.59	0.156	6.06	0.3475	47.48	47.45	-0.135
3.07	2.1922	334.11	334.11	0	6.12	0.3137	45.12	45.09	-0.154
3.14	2.2421	332.84	332.86	0.065	6.20	0.289	42.93	42.89	-0.185
3.23	2.2897	332.82	332.85	0.13	6.27	0.2736	40.07	40.03	-0.181
3.32	2.3189	329.97	329.98	0.073	6.34	0.2543	38.31	38.3	-0.054
3.41	2.3303	328.47	328.48	0.043	6.42	0.2348	39.08	39.17	0.44
3.50	2.3307	324.57	324.6	0.134	6.51	0.2497	45.09	45.21	0.608

Table D.6 Continued

z	f_s	q_u	q_t	u_2	z	f_s	q_u	q_t	u_2
(ft)	(tsf)	(tsf)	(tsf)	(tsf)	(ft)	(tsf)	(tsf)	(tsf)	(tsf)
6.60	0.2665	50.55	50.57	0.105	10.21	0.4085	89.81	89.8	-0.023
6.68	0.298	53.86	53.86	-0.009	10.30	0.3872	87.25	87.25	-0.029
6.77	0.3503	56.05	56.06	0.074	10.39	0.3737	85.41	85.4	-0.026
6.85	0.4125	57.93	57.95	0.081	10.48	0.3696	82.98	82.98	0
6.94	0.4363	57.4	57.41	0.048	10.56	0.3605	79.79	79.8	0.046
7.03	0.4814	55.55	55.55	0.05	10.65	0.3544	74.44	74.44	0.031
7.11	0.474	53.83	53.84	0.014	10.74	0.3374	67.83	67.83	0.03
7.20	0.4512	51.9	51.89	-0.035	10.82	0.3145	62.41	62.42	0.044
7.28	0.4301	49.86	49.83	-0.191	10.91	0.2862	56.45	56.46	0.052
7.37	0.4129	46.9	46.84	-0.285	11.00	0.264	51.85	51.86	0.051
7.46	0.4147	43.21	43.13	-0.388	11.08	0.2446	48.79	48.8	0.062
7.55	0.3867	40.44	40.37	-0.391	11.17	0.2316	46.25	46.26	0.071
7.64	0.3611	38.53	38.48	-0.272	11.26	0.2315	44.54	44.55	0.077
7.72	0.3203	38.81	38.75	-0.342	11.35	0.2296	43.66	43.67	0.08
7.81	0.3089	39.73	39.64	-0.475	11.43	0.2444	43.86	43.88	0.095
7.90	0.304	38.3	38.2	-0.524	11.52	0.2609	43.86	43.88	0.102
7.99	0.2834	37.05	36.94	-0.584	11.61	0.2857	44.61	44.63	0.106
8.07	0.2943	38.28	38.17	-0.536	11.69	0.3022	44.84	44.86	0.1
8.16	0.3514	42.08	41.97	-0.539	11.78	0.2899	44.89	44.91	0.119
8.24	0.3517	46.67	46.56	-0.577	11.87	0.277	41.65	41.67	0.108
8.33	0.3579	49.86	49.75	-0.62	11.95	0.265	39.11	39.13	0.122
8.42	0.3541	58.03	57.91	-0.637	12.04	0.2612	37.88	37.9	0.119
8.50	0.3638	69.79	69.66	-0.647	12.33	0.263	34.36	34.39	0.119
8.59	0.3425	78.75	78.62	-0.67	12.42	0.2041	28.99	29.02	0.148
8.68	0.3197	82.94	82.81	-0.677	12.50	0.1855	24.63	24.66	0.124
8.77	0.3046	85.87	85.74	-0.671	12.58	0.1592	22.87	22.9	0.117
8.85	0.3259	91.65	91.52	-0.65	12.67	0.1247	24.96	24.99	0.156
9.10	0.4082	115.18	115.07	-0.57	12.75	0.0997	22.86	22.88	0.104
9.18	0.4532	118.91	118.82	-0.489	12.84	0.112	22.73	22.74	0.055
9.27	0.4763	121.64	121.56	-0.407	12.93	0.1564	25.6	25.6	0
9.35	0.5014	122.58	122.52	-0.289	13.01	0.1658	27.61	27.61	-0.014
9.44	0.5109	118.91	118.87	-0.218	13.10	0.1683	29.34	29.34	0.035
9.52	0.5205	116.33	116.29	-0.185	13.19	0.1633	35.6	35.62	0.11
9.61	0.5217	111.96	111.93	-0.186	13.28	0.2118	36.72	36.75	0.157
9.70	0.5136	105.84	105.81	-0.187	13.36	0.2394	33.86	33.89	0.147
9.78	0.5093	100.98	100.95	-0.188	13.44	0.2443	25.85	25.89	0.218
9.86	0.4934	97.01	96.98	-0.165	13.53	0.2216	28.08	28.1	0.112
9.95	0.4595	93.7	93.68	-0.128	13.62	0.1962	31.02	31.05	0.125
10.04	0.4378	90.77	90.75	-0.102	13.70	0.2169	29.01	29.04	0.153
10.12	0.4194	89.6	89.59	-0.066	13.79	0.2389	30.92	30.95	0.159

Table D.6 Continued

z	f_s	q_u	q_t	u_2	z	f_s	q_u	q_t	u_2
(ft)	(tsf)	(tsf)	(tsf)	(tsf)	(ft)	(tsf)	(tsf)	(tsf)	(tsf)
13.88	0.2655	34.42	34.45	0.16	17.53	0.9201	109.33	109.39	0.32
13.97	0.2843	39.46	39.5	0.19	17.62	0.8353	107.69	107.76	0.324
14.05	0.3158	45.32	45.36	0.202	17.70	0.8261	100.58	100.64	0.337
14.14	0.3421	52.43	52.47	0.21	17.79	0.8346	96.76	96.84	0.394
14.23	0.3772	59.06	59.1	0.204	17.87	0.7083	106.47	106.5	0.133
14.32	0.3962	65.39	65.43	0.207	17.96	0.6597	115.97	115.95	-0.094
14.41	0.4243	71.33	71.37	0.209	18.05	0.6164	112.05	112.08	0.16
14.49	0.4474	75.95	75.99	0.193	18.13	0.577	104.63	104.63	-0.005
14.58	0.4644	79.29	79.33	0.211	18.22	0.5165	95.71	95.74	0.142
14.67	0.4687	81.01	81.05	0.202	18.31	0.4588	87.08	87.11	0.145
14.76	0.4739	82.27	82.31	0.213	18.39	0.408	73.1	73.13	0.149
14.84	0.4753	83.27	83.32	0.22	18.48	0.4003	66.1	66.14	0.225
14.93	0.4727	84.78	84.82	0.227	18.72	0.5828	55.59	55.6	0.028
15.02	0.4759	85.45	85.5	0.229	18.81	0.6804	46	45.95	-0.217
15.11	0.4792	84.86	84.91	0.235	18.90	0.6788	36.62	36.6	-0.141
15.19	0.4824	82.9	82.94	0.244	18.98	0.7544	31.04	31.09	0.271
15.28	0.4686	80.63	80.68	0.244	19.06	0.8403	27.49	27.6	0.544
15.55	0.4805	74.31	74.36	0.245	19.15	0.8457	24.44	24.61	0.899
15.63	0.5661	73.9	73.94	0.236	19.23	0.8012	24.83	25.15	1.678
15.72	0.8069	75.14	75.2	0.285	19.32	0.7167	25.82	26.13	1.629
15.80	0.957	76.82	76.88	0.266	19.41	0.5744	32.55	32.92	1.901
15.89	1.2831	82.65	82.7	0.269	19.49	0.5243	42.28	42.49	1.099
15.98	1.519	91.4	91.45	0.281	19.58	0.4927	57.15	57.23	0.399
16.06	1.644	90.73	90.81	0.408	19.66	0.5938	62.58	62.63	0.254
16.15	1.6086	87.55	87.7	0.778	19.76	0.8189	51.78	51.77	-0.006
16.24	1.391	85.95	86.03	0.373	19.84	0.9094	38.13	38.13	0
16.32	1.1598	88.3	88.29	-0.019	19.93	0.9148	29.79	29.83	0.236
16.41	0.8937	93.86	93.73	-0.677	20.01	0.8566	23.25	23.38	0.661
16.49	0.7079	98.14	98.04	-0.54	20.10	0.7581	19.68	19.78	0.543
16.58	0.5081	105.14	105.11	-0.146	20.19	0.6936	18.35	18.48	0.686
16.67	0.5346	111.05	111.04	-0.055	20.28	0.6487	19.61	20.06	2.34
16.76	0.5737	112.47	112.47	0.022	20.36	0.4986	21.23	21.87	3.328
16.84	0.568	111.25	111.26	0.07	20.45	0.4707	20.61	21.29	3.503
16.92	0.5838	111.12	111.15	0.129	20.54	0.5428	18.28	19.14	4.453
17.01	0.5951	109.9	109.93	0.142	20.63	0.6148	19.4	20.53	5.875
17.09	0.586	107.64	107.68	0.188	20.71	0.7104	24.58	25.26	3.505
17.18	0.5805	106.3	106.34	0.201	20.80	0.6951	25.3	25.58	1.44
17.27	0.6124	106.95	107.01	0.289	20.89	0.6994	21.05	21.25	1.032
17.36	0.7049	107.44	107.5	0.296	20.97	0.625	18.23	18.51	1.48
17.44	0.8501	108.73	108.79	0.298	21.06	0.4837	24.49	24.85	1.828

Table D.6 Continued

z	f_s	q_u	q_t	u_2	z	f_s	q_u	q_t	u_2
(ft)	(tsf)	(tsf)	(tsf)	(tsf)	(ft)	(tsf)	(tsf)	(tsf)	(tsf)
21.15	0.334	32.5	32.64	0.75	24.62	0.0778	15.21	15.26	0.275
21.23	0.2369	32.23	32.23	0.031	24.71	0.077	13.94	13.99	0.265
21.32	0.1887	29.01	29.08	0.364	24.80	0.0899	13.32	13.36	0.197
21.41	0.1667	27.45	27.54	0.456	24.90	0.1054	12.01	12.06	0.248
21.50	0.1299	25.43	25.5	0.359	24.98	0.1188	10.18	10.31	0.658
21.59	0.1023	24.24	24.32	0.42	25.09	0.0959	9.54	9.67	0.667
21.68	0.0967	23.18	23.26	0.4	25.17	0.1091	8.16	8.33	0.838
21.76	0.0819	22.36	22.42	0.308	25.26	0.099	7.16	7.36	1.034
21.84	0.0787	22.99	23.02	0.178	25.34	0.0964	6.27	6.49	1.12
21.93	0.0678	23.38	23.4	0.113	25.43	0.0975	5.39	5.7	1.608
22.01	0.0628	23.04	23.08	0.222	25.52	0.1076	5.09	5.45	1.879
22.10	0.0714	22.47	22.52	0.277	25.61	0.1014	4.71	5.12	2.143
22.19	0.073	23.13	23.18	0.296	25.69	0.0913	4.45	4.89	2.273
22.27	0.073	23.45	23.51	0.328	25.78	0.0988	4.78	5.24	2.386
22.36	0.0678	24.06	24.1	0.207	25.87	0.0963	5.41	5.88	2.467
22.45	0.068	23.75	23.77	0.095	25.95	0.095	5.33	5.8	2.438
22.54	0.0704	22.8	22.83	0.158	26.04	0.0938	5.58	6.02	2.283
22.62	0.0697	22.3	22.35	0.231	26.13	0.1031	5.7	6.16	2.333
22.71	0.0927	22.06	22.12	0.297	26.22	0.1136	5.59	6.05	2.378
22.80	0.1301	21.42	21.49	0.358	26.30	0.1061	5.9	6.37	2.394
22.88	0.1576	20.54	20.61	0.368	26.40	0.1003	5.84	6.29	2.353
22.97	0.1733	19.85	19.93	0.448	26.48	0.0977	5.58	6.01	2.248
23.06	0.143	20.04	20.09	0.242	26.57	0.1036	5.2	5.65	2.305
23.14	0.1465	20.53	20.55	0.089	26.66	0.1027	5.03	5.51	2.467
23.23	0.1707	21.66	21.65	-0.069	26.75	0.1003	4.91	5.42	2.646
23.32	0.1723	23.45	23.5	0.258	26.83	0.0965	4.52	5.03	2.654
23.41	0.1539	25.19	25.22	0.154	26.92	0.0951	4.71	5.23	2.673
23.49	0.1437	24.89	24.88	-0.006	27.01	0.0876	4.65	5.16	2.643
23.58	0.1326	24.19	24.19	-0.004	27.10	0.0756	4.4	4.92	2.689
23.66	0.1489	23.49	23.47	-0.107	27.19	0.0781	4.58	5.11	2.725
23.75	0.1349	22.97	22.97	-0.028	27.28	0.0782	5.02	5.55	2.696
23.83	0.1152	22.86	22.92	0.308	27.36	0.0747	5.28	5.77	2.509
23.93	0.0923	22.66	22.7	0.18	27.45	0.0686	5.34	5.81	2.416
24.01	0.0898	22.25	22.27	0.12	27.54	0.0582	5.09	5.57	2.462
24.10	0.0811	20.92	20.96	0.186	27.63	0.0589	4.46	4.93	2.466
24.19	0.0808	19.8	19.84	0.213	27.72	0.0577	3.89	4.41	2.646
24.27	0.0892	18.97	19.02	0.265	27.80	0.0575	3.71	4.26	2.838
24.36	0.0947	18.23	18.28	0.261	27.89	0.0525	3.95	4.51	2.905
24.45	0.1023	17.28	17.31	0.154	27.97	0.051	4.27	4.82	2.864
24.54	0.0852	16.27	16.32	0.231	28.06	0.0519	4.21	4.76	2.852

Table D.6 Continued

z	f_s	q_u	q_t	u_2	z	f_s	q_u	q_t	u_2
(ft)	(tsf)	(tsf)	(tsf)	(tsf)	(ft)	(tsf)	(tsf)	(tsf)	(tsf)
28.13	0.0503	4.14	4.68	2.819	31.65	0.0659	9.63	9.98	1.793
28.21	0.0497	3.95	4.52	2.95	31.73	0.0768	7.77	8.12	1.822
28.29	0.0568	3.95	4.54	3.031	31.78	0.0798	6.02	6.37	1.815
28.37	0.063	3.88	4.47	3.043	31.87	0.0698	7.85	8.17	1.669
28.44	0.0548	4.34	4.94	3.105	31.96	0.0613	6.58	6.99	2.115
28.52	0.0515	4.13	4.71	2.973	32.05	0.0456	4.75	5.21	2.395
28.72	0.0635	4.27	4.84	2.955	32.14	0.0458	4.59	5.13	2.803
28.80	0.0592	4.07	4.66	3.049	32.22	0.0439	3.88	4.47	3.036
28.88	0.0579	4.39	4.99	3.096	32.32	0.0546	3.57	4.21	3.322
28.96	0.0621	4.83	5.42	3.077	32.41	0.0492	3.63	4.29	3.394
29.04	0.0638	5.15	5.74	3.036	32.49	0.044	3.63	4.29	3.408
29.11	0.0668	5.33	5.9	2.94	32.58	0.0569	3.76	4.46	3.629
29.19	0.0725	5.07	5.62	2.852	32.68	0.1192	5.03	5.79	3.907
29.27	0.0765	5.14	5.71	2.913	32.76	0.0983	11.8	12.55	3.882
29.35	0.0603	4.7	5.28	3.013	32.85	0.1177	24.57	24.98	2.121
29.44	0.0603	5.08	5.69	3.164	32.94	0.1351	32.24	32.43	0.977
29.52	0.0702	5.73	6.34	3.175	33.03	0.1411	40.19	40.42	1.192
29.61	0.0768	5.54	6.17	3.279	33.12	0.1586	44.62	44.73	0.592
29.69	0.0816	5.45	6.11	3.421	33.21	0.1915	44.17	44.33	0.857
29.78	0.0621	6.34	6.93	3.07	33.29	0.2106	42.03	42.22	0.963
29.87	0.0626	6.59	7.14	2.859	33.38	0.2278	39.9	40.07	0.875
29.96	0.0584	5.88	6.37	2.542	33.47	0.2434	37.41	37.57	0.835
30.05	0.0646	5.91	6.41	2.586	33.56	0.2763	35.01	35.19	0.936
30.14	0.0748	4.81	5.34	2.744	33.64	0.2876	33.41	33.6	1.006
30.23	0.0684	4.83	5.36	2.771	33.73	0.301	31.04	31.25	1.093
30.32	0.0656	4.58	5.14	2.912	33.82	0.3163	27.72	27.94	1.117
30.40	0.0774	4.58	5.16	3.024	33.91	0.3766	25.84	26.07	1.2
30.49	0.0653	4.96	5.55	3.038	34.00	0.3904	24.27	24.51	1.208
30.58	0.063	4.83	5.4	2.947	34.09	0.3265	24.34	24.59	1.28
30.67	0.0629	4.58	5.16	3.024	34.18	0.3025	29.43	29.66	1.206
30.76	0.047	5.98	6.58	3.101	34.27	0.2513	44.79	45.02	1.166
30.85	0.0425	7.17	7.69	2.713	34.36	0.2254	66.75	66.85	0.489
30.93	0.0365	6.46	6.93	2.427	34.45	0.2191	76.79	76.91	0.647
31.02	0.0395	4.82	5.37	2.87	34.54	0.1887	73.61	73.79	0.922
31.11	0.0444	6.08	6.7	3.196	34.63	0.1639	64.24	64.42	0.892
31.20	0.0301	8.59	9.12	2.719	34.72	0.1857	57.67	57.84	0.894
31.29	0.0335	11.29	11.64	1.822	34.81	0.2549	50.27	50.46	0.969
31.38	0.0235	11.94	12.22	1.458	34.89	0.2801	42.66	42.84	0.956
31.47	0.0329	12.11	12.43	1.669	34.98	0.3756	36.43	36.62	1.003
31.56	0.0587	10.53	10.86	1.699	35.06	0.455	30.43	30.61	0.922

Table D.6 Continued

z	f_s	q_u	q_t	u_2	z	f_s	q_u	q_t	u_2
(ft)	(tsf)	(tsf)	(tsf)	(tsf)	(ft)	(tsf)	(tsf)	(tsf)	(tsf)
35.15	0.4385	25.43	25.63	1.04	37.64	0.3256	27.59	27.85	1.339
35.23	0.3537	19.78	19.97	1.005	37.73	0.3639	20.77	21.02	1.301
35.33	0.2779	18.98	19.19	1.104	37.82	0.3838	18.06	18.46	2.064
35.41	0.2511	22.08	22.3	1.129	37.91	0.3362	15.43	15.72	1.499
35.50	0.2054	25.25	25.5	1.301	38.00	0.2764	12.24	12.69	2.311
35.59	0.1971	29.23	29.41	0.913	38.09	0.2568	9.49	10.14	3.372
35.67	0.2297	31.62	31.81	1.033	38.18	0.3213	8.66	9.51	4.433
35.76	0.2117	32.67	32.87	1.035	38.38	0.3486	22.83	23.03	1.043
35.85	0.344	31.1	31.3	1.048	38.47	0.4043	19.44	19.74	1.545
35.94	0.47	24.91	25.12	1.104	38.56	0.4079	30.25	30.51	1.33
36.03	0.511	19.38	19.61	1.162	38.65	0.4694	31.22	31.29	0.354
36.12	0.4719	14.98	15.2	1.116	38.74	0.5507	34.02	34.25	1.214
36.21	0.4435	12.45	12.68	1.173	38.83	0.5826	32.05	32.3	1.33
36.30	0.3842	10.59	10.94	1.833	38.91	0.6441	23.77	24.01	1.26
36.39	0.3078	8.9	9.56	3.398	39.00	0.5657	18.45	18.69	1.246
36.48	0.2241	8.96	9.6	3.329	39.09	0.5128	15.27	15.56	1.531
36.56	0.1558	9.4	9.95	2.851	39.18	0.4509	11.6	12.04	2.276
36.65	0.1228	7.71	8.44	3.743	39.26	0.3543	9.21	9.75	2.771
36.75	0.1491	7.45	8.33	4.539	39.35	0.2552	8.33	9.2	4.473
36.83	0.1951	9.99	10.94	4.924	39.44	0.1861	7.96	8.97	5.248
36.93	0.1886	14.92	15.69	3.977	39.53	0.1536	8.73	9.76	5.303
37.01	0.1963	13.85	14.31	2.389	39.62	0.1406	8.33	9.37	5.374
37.10	0.2226	11.29	11.76	2.44	39.70	0	8.54	9.51	4.999
37.19	0.184	9.24	9.81	2.957	39.79	0	8.6	9.59	5.109
37.29	0.1892	8.59	9.36	3.982	39.88	0	9.14	10.1	4.951
37.37	0.1524	11.06	11.95	4.589	39.97	0	9.7	10.51	4.192
37.46	0.195	20.71	21.52	4.198	40.00	0	7.52	8.34	4.226
37.55	0.2598	32.69	33.15	2.382	40.00	0	7.52	8.34	4.226

Table D.7 CPT Data from SC-1L at the Lowcountry Sand & Gravel site.

z	f_s	q_u	q_t	u_2	z	f_s	q_u	q_t	u_2
(ft)	(tsf)	(tsf)	(tsf)	(tsf)	(ft)	(tsf)	(tsf)	(tsf)	(tsf)
0.00	0	0	0	0	3.60	1.4167	248.86	248.88	0.099
0.17	0	86.19	86.2	0.038	3.69	1.3717	243.45	243.47	0.102
0.25	0	125.2	125.21	0.059	3.77	1.3181	234.05	234.07	0.087
0.34	0.5027	135.39	135.42	0.178	3.86	1.2294	222.59	222.6	0.093
0.42	0.6164	156.05	156.08	0.184	3.95	1.1053	213.29	213.31	0.074
0.50	0.7454	176.44	176.48	0.183	4.03	0.9811	206.11	206.12	0.072
0.58	0.8745	195.25	195.3	0.211	4.12	0.8898	201.81	201.83	0.059
0.67	1.0396	205.9	205.94	0.191	4.20	0.8367	199.69	199.7	0.051
0.76	1.1678	207.6	207.64	0.214	4.29	0.8079	199.58	199.59	0.032
0.84	1.3002	204.6	204.63	0.188	4.37	0.8536	199.26	199.27	0.047
0.92	1.3586	198.18	198.21	0.135	4.46	0.8362	195.9	195.91	0.027
1.01	1.3515	190.98	191.01	0.155	4.54	0.8299	189.7	189.7	0.015
1.09	1.3433	183.34	183.37	0.128	4.63	0.8668	180.66	180.66	-0.011
1.18	1.3253	176.8	176.82	0.124	4.72	0.8609	171.14	171.13	-0.048
1.26	1.3085	169.23	169.24	0.073	4.80	0.8628	167.07	167.06	-0.032
1.35	1.2664	160.62	160.64	0.078	4.89	0.8245	163.24	163.25	0.053
1.43	1.2377	152.72	152.74	0.088	4.97	0.787	156.62	156.64	0.077
1.52	1.1983	145.29	145.3	0.087	5.06	0.7322	149.66	149.67	0.043
1.60	1.1846	140.77	140.78	0.053	5.15	0.6769	144.76	144.77	0.05
1.69	1.1795	136.9	136.9	0.034	5.23	0.6255	138	138.01	0.042
1.77	1.1629	132.71	132.72	0.053	5.31	0.5753	130.98	130.99	0.027
1.86	1.1527	131.05	131.05	0.035	5.59	0.4582	107.14	107.16	0.071
1.94	1.1435	131.27	131.27	0.03	5.69	0.4395	100.49	100.49	0.032
2.03	1.1342	133.81	133.82	0.043	5.78	0.4174	94.67	94.68	0.054
2.12	1.2124	139.66	139.67	0.034	5.87	0.3861	87.28	87.29	0.032
2.40	1.3038	162.91	163	0.433	5.96	0.3464	79.77	79.79	0.073
2.49	1.4211	188.48	188.53	0.256	6.05	0.2967	72.31	72.34	0.141
2.58	1.5061	213.12	213.15	0.123	6.14	0.2784	66.03	66.07	0.215
2.66	1.5133	224.7	224.72	0.123	6.22	0.2853	61.83	61.88	0.244
2.75	1.5068	224.32	224.35	0.116	6.32	0.2805	57.73	57.78	0.278
2.83	1.4881	223.44	223.46	0.091	6.41	0.2573	57.98	58.03	0.275
2.92	1.4549	224.61	224.62	0.067	6.49	0.2433	60.75	60.79	0.218
3.00	1.4257	229.26	229.28	0.074	6.57	0.2365	62.51	62.54	0.176
3.09	1.423	236.81	236.82	0.081	6.64	0.2248	66.64	66.66	0.148
3.17	1.4112	246.21	246.23	0.104	6.72	0.2185	67.62	67.64	0.096
3.26	1.4072	249.49	249.51	0.102	6.80	0.2068	68	68.01	0.068
3.35	1.4071	251.65	251.67	0.099	6.88	0.2028	67.83	67.84	0.055
3.43	1.405	252.12	252.15	0.146	6.96	0.2077	67.12	67.12	0.03
3.52	1.4172	250.87	250.89	0.114	7.03	0.2153	63.59	63.6	0.022

Table D.7 Continued

z	f_s	q_u	q_t	u_2	z	f_s	q_u	q_t	u_2
(ft)	(tsf)	(tsf)	(tsf)	(tsf)	(ft)	(tsf)	(tsf)	(tsf)	(tsf)
7.11	0.215	59.54	59.55	0.057	10.49	1.1434	337.92	337.87	-0.232
7.19	0.2078	54.66	54.67	0.04	10.56	1.125	327.37	327.33	-0.209
7.27	0.2003	50.99	51	0.041	10.65	1.1338	321.22	321.19	-0.155
7.34	0.1798	46.03	46.05	0.097	10.73	1.1687	317.18	317.16	-0.117
7.42	0.164	41.25	41.28	0.146	10.81	1.2104	311.16	311.14	-0.108
7.50	0.15	37.48	37.51	0.152	10.89	1.1765	294.16	294.14	-0.093
7.57	0.1427	34.23	34.27	0.203	10.97	1.1559	274.53	274.54	0.013
7.65	0.144	29.88	29.93	0.216	11.05	1.0863	272.27	272.29	0.115
7.73	0.1296	25.05	25.11	0.298	11.13	1.0748	289	289.04	0.172
7.80	0.1257	21.18	21.26	0.433	11.22	1.0651	303.09	303.13	0.189
7.89	0.1316	17.63	17.72	0.505	11.31	1.093	308.87	308.91	0.163
7.97	0.1251	16.69	16.8	0.566	11.39	1.0729	308.13	308.16	0.144
8.05	0.1449	17.26	17.37	0.564	11.48	1.048	306.27	306.3	0.17
8.13	0.1571	18.51	18.61	0.523	11.57	1.1307	299.32	299.35	0.13
8.21	0.1605	17.86	17.96	0.479	11.65	1.0858	294.16	294.18	0.108
8.30	0.1442	16.75	16.84	0.481	11.74	1.0296	291.15	291.17	0.104
8.38	0.1289	16.58	16.67	0.502	11.83	0.9605	286.87	286.89	0.114
8.46	0.1134	16.68	16.77	0.462	11.90	0.9002	268.24	268.26	0.088
8.54	0.0849	15.87	15.96	0.467	11.98	0.8007	259.19	259.21	0.132
8.82	0.0924	15.93	16	0.341	12.07	0.745	243.95	243.98	0.181
8.90	0.1022	15.43	15.5	0.348	12.16	0.6633	226.35	226.39	0.206
8.98	0.1612	14.86	14.93	0.347	12.25	0.6039	212.13	212.18	0.242
9.06	0.2598	13.73	13.79	0.354	12.33	0.5754	206.09	206.14	0.249
9.14	0.3155	12.92	13	0.372	12.42	0.5265	199.32	199.36	0.248
9.22	0.3589	12.97	13.04	0.358	12.51	0.5113	189.57	189.63	0.272
9.30	0.4065	14.61	14.68	0.372	12.60	0.5105	176.32	176.37	0.261
9.38	0.4258	24.26	24.33	0.41	12.68	0.4905	163.14	163.2	0.297
9.46	0.4444	68.87	68.94	0.36	12.77	0.4845	150.18	150.24	0.307
9.54	0.5009	130.26	130.29	0.139	12.85	0.4902	137.75	137.81	0.306
9.61	0.5973	178.94	178.93	-0.027	12.94	0.4882	129.44	129.5	0.31
9.69	0.7498	210.84	210.83	-0.069	13.03	0.4625	122.59	122.65	0.314
9.77	0.8846	228.24	228.21	-0.107	13.12	0.4103	112.92	112.98	0.332
9.85	0.9526	233.12	233.09	-0.143	13.21	0.3905	102.64	102.7	0.348
9.93	0.9901	234.26	234.23	-0.108	13.29	0.3566	90.93	91	0.355
10.02	1.0489	247.09	247.08	-0.066	13.38	0.3392	79.9	79.97	0.361
10.10	1.0648	268.12	268.11	-0.018	13.47	0.3358	68.83	68.91	0.386
10.17	1.0447	303.35	303.34	-0.032	13.56	0.3382	58.47	58.54	0.394
10.25	1.0514	332.93	332.92	-0.059	13.64	0.3239	50.74	50.82	0.416
10.33	1.0824	343.63	343.61	-0.119	13.73	0.3397	42.08	42.17	0.427
10.41	1.123	342.98	342.93	-0.212	13.82	0.3338	35.54	35.64	0.48

Table D.7 Continued

z	f_s	q_u	q_t	u_2	z	f_s	q_u	q_t	u_2
(ft)	(tsf)	(tsf)	(tsf)	(tsf)	(ft)	(tsf)	(tsf)	(tsf)	(tsf)
13.91	0.3105	29.9	30.02	0.588	17.55	0.4452	11.76	11.88	0.614
14.00	0.299	23.25	23.39	0.724	17.64	0.3882	10.82	10.96	0.689
14.09	0.2644	17.19	17.42	1.175	17.73	0.3316	9.76	9.91	0.768
14.18	0.2653	13.66	13.93	1.412	17.82	0.2873	7.89	8.07	0.935
14.27	0.2634	11.85	12.15	1.571	17.90	0.2345	6.55	6.84	1.544
14.36	0.242	10.84	11.16	1.634	17.99	0.198	6.12	6.45	1.735
14.44	0.1881	8.63	8.98	1.855	18.08	0.1594	6.04	6.44	2.033
14.53	0.1475	7.75	8.14	2.016	18.17	0.2092	8.71	9.14	2.214
14.62	0.1445	6.87	7.31	2.262	18.26	0.2961	14.16	14.5	1.76
14.71	0.2061	12.91	13.41	2.583	18.35	0.329	13.02	13.26	1.268
14.80	0.275	20.98	21.22	1.245	18.43	0.3279	9.75	9.91	0.836
14.89	0.3401	18.59	18.72	0.685	18.52	0.3278	7.32	7.48	0.846
14.98	0.3043	15.56	15.67	0.566	18.61	0.2957	6	6.21	1.062
15.26	0.327	13.46	13.53	0.362	18.70	0.3482	5.93	6.29	1.906
15.31	0.3168	9.82	9.96	0.742	18.78	0.3534	8.89	9.3	2.132
15.35	0.3066	15.25	15.33	0.413	18.87	0.3946	10.16	10.55	2.054
15.43	0.3205	12.48	12.6	0.61	18.95	0.384	10.02	10.29	1.376
15.52	0.3493	13.09	13.21	0.654	19.05	0.339	10.45	10.7	1.276
15.61	0.3343	14.31	14.43	0.632	19.13	0.2841	11.03	11.28	1.288
15.70	0.3475	12.72	12.81	0.484	19.22	0.2505	19.96	20.25	1.481
15.78	0.3598	12.98	13.08	0.501	19.31	0.2681	35.24	35.4	0.822
15.87	0.3638	11.92	12.01	0.46	19.39	0.3579	35.21	35.3	0.463
15.96	0.3469	9.82	9.9	0.443	19.47	0.4802	27.82	27.88	0.347
16.04	0.3085	8.68	8.77	0.457	19.55	0.5518	20.41	20.48	0.349
16.13	0.2779	7.93	8.06	0.672	19.62	0.5679	14.23	14.31	0.396
16.23	0.2724	6.99	7.15	0.849	19.70	0.5508	11.47	11.56	0.48
16.31	0.3127	6.49	6.72	1.215	19.78	0.5233	9.57	9.73	0.787
16.40	0.3367	9.83	10.16	1.723	19.86	0.4759	8.06	8.22	0.797
16.48	0.3304	13.23	13.53	1.518	19.94	0.403	7.13	7.37	1.27
16.57	0.3291	12.83	13	0.869	20.02	0.3108	5.93	6.28	1.821
16.66	0.3352	15.68	15.85	0.88	20.10	0.2263	5.3	5.77	2.458
16.75	0.3579	15.67	15.8	0.67	20.19	0.2062	4.92	5.4	2.5
16.84	0.4652	16.24	16.37	0.681	20.27	0.1937	5.05	5.58	2.795
16.93	0.4703	20.63	20.78	0.784	20.35	0.1762	5.49	6	2.667
17.02	0.4009	17.93	18.06	0.67	20.44	0.1724	4.79	5.23	2.278
17.11	0.3834	13.86	13.99	0.631	20.52	0.1675	4.29	4.77	2.507
17.20	0.3559	14.63	14.79	0.809	20.60	0.1553	4.16	4.69	2.739
17.28	0.4206	21.08	21.22	0.708	20.69	0.1433	4.42	4.95	2.767
17.37	0.4848	20.2	20.33	0.705	20.77	0.12	4.73	5.28	2.832
17.46	0.4882	15.08	15.2	0.624	20.86	0.1147	4.42	4.99	2.957

Table D.7 Continued

z	f_s	q_u	q_t	u_2	z	f_s	q_u	q_t	u_2
(ft)	(tsf)	(tsf)	(tsf)	(tsf)	(ft)	(tsf)	(tsf)	(tsf)	(tsf)
20.94	0.1141	4.29	4.86	2.943	24.41	0.5906	34.94	35.07	0.718
21.02	0.1168	3.98	4.58	3.107	24.50	0.4333	22.66	22.8	0.734
21.10	0.1203	3.98	4.6	3.223	24.58	0.378	19.08	19.23	0.795
21.19	0.1242	3.91	4.53	3.204	24.67	0.3512	29.43	29.61	0.893
21.27	0.13	3.85	4.44	3.072	24.75	0.3249	51.44	51.58	0.732
21.36	0.1283	4.11	4.72	3.138	24.83	0.3046	49.83	49.97	0.678
21.44	0.1312	4.05	4.66	3.182	24.92	0.3104	37	37.11	0.583
21.52	0.1339	3.79	4.39	3.119	25.16	0.4727	19.43	19.57	0.737
21.61	0.1349	3.66	4.24	3.01	25.25	0.5051	21.58	21.73	0.747
21.69	0.1401	3.4	3.96	2.884	25.33	0.4536	17.68	17.82	0.708
21.92	0.1351	3.16	3.64	2.443	25.42	0.4227	12.78	12.93	0.782
22.00	0.1217	2.84	3.31	2.421	25.50	0.374	12.03	12.21	0.904
22.08	0.1118	2.59	3.06	2.453	25.59	0.2709	14.27	14.44	0.861
22.16	0.0988	2.85	3.34	2.554	25.68	0.2348	18.32	18.54	1.098
22.24	0.0967	2.59	3.09	2.579	25.76	0.2327	22.45	22.62	0.92
22.32	0.0956	2.71	3.21	2.579	25.85	0.2781	25.23	25.33	0.497
22.41	0.094	2.72	3.23	2.614	25.94	0.3692	20.13	20.25	0.605
22.49	0.1073	2.53	3.04	2.634	26.02	0.3915	16.16	16.31	0.79
22.57	0.1296	2.66	3.17	2.609	26.11	0.3435	12.9	13.06	0.831
22.65	0.1373	2.79	3.29	2.623	26.19	0.3273	12.14	12.32	0.962
22.74	0.1238	4.42	4.94	2.697	26.28	0.3553	12.85	13.05	1.037
22.82	0.134	10.33	10.79	2.409	26.37	0.4524	20.21	20.46	1.263
22.90	0.1326	17.37	17.61	1.198	26.45	0.4845	25.91	26.21	1.533
22.99	0.1756	20.63	20.76	0.647	26.53	0.4099	25.86	26.02	0.817
23.07	0.2594	20.45	20.58	0.666	26.62	0.3355	20.63	20.8	0.855
23.15	0.3349	18.88	19	0.618	26.71	0.3449	15.98	16.16	0.922
23.23	0.287	15.87	16.01	0.748	26.80	0.4551	20.69	20.92	1.205
23.31	0.2311	13.97	14.13	0.872	26.88	0.4148	26.6	26.87	1.405
23.40	0.2461	19.44	19.64	1	26.97	0.3819	29.38	29.57	1.007
23.48	0.3624	25.8	26	1.03	27.05	0.3683	32.02	32.23	1.053
23.56	0.4863	30.69	30.83	0.739	27.14	0.4329	33.13	33.36	1.17
23.65	0.507	31.7	31.82	0.612	27.23	0.5395	43.8	43.88	0.435
23.73	0.3498	22.78	22.91	0.632	27.31	0.4811	49.56	49.67	0.609
23.82	0.312	15.99	16.12	0.671	27.39	0.3986	43.07	43.2	0.688
23.90	0.3249	21.13	21.3	0.876	27.48	0.3625	47.69	47.84	0.77
23.99	0.3199	48.68	48.87	0.992	27.57	0.315	60.61	60.76	0.809
24.07	0.32	72.61	72.76	0.752	27.65	0.2623	66.7	66.83	0.625
24.16	0.3625	72.23	72.37	0.717	27.73	0.2502	72.15	72.31	0.821
24.24	0.5031	60.48	60.62	0.697	27.82	0.249	77.76	77.92	0.833
24.33	0.717	48	48.13	0.68	27.91	0.2809	87.37	87.52	0.782

Table D.7 Continued

z	f_s	q_u	q_t	u_2	z	f_s	q_u	q_t	u_2
(ft)	(tsf)	(tsf)	(tsf)	(tsf)	(ft)	(tsf)	(tsf)	(tsf)	(tsf)
27.99	0.3104	89.34	89.49	0.79	31.58	0.2738	40.07	40.25	0.923
28.07	0.3031	81.83	81.99	0.824	31.67	0.2798	34.01	34.19	0.92
28.16	0.3243	70.35	70.51	0.811	31.76	0.3562	34.01	34.2	0.955
28.37	0.5794	44.98	45.14	0.828	31.84	0.426	37.23	37.42	0.988
28.45	0.7106	37.66	37.82	0.832	31.92	0.472	37.51	37.69	0.925
28.54	0.6936	29	29.17	0.852	32.01	0.4525	33.87	34.05	0.932
28.62	0.6421	20.38	20.56	0.925	32.10	0.489	31.27	31.46	1.021
28.71	0.5929	16.36	16.55	1.002	32.18	0.455	31	31.2	1.033
28.79	0.5944	15.21	15.44	1.19	32.27	0.3167	43.82	44.03	1.071
28.86	0.6556	22.57	22.79	1.124	32.36	0.2878	54.95	55.1	0.778
28.95	0.6543	27.03	27.35	1.65	32.44	0.2528	57.35	57.52	0.855
29.03	0.5311	22.95	23.13	0.938	32.53	0.2479	68.89	69.08	1
29.11	0.4307	17.29	17.51	1.121	32.62	0.2699	81.96	82.14	0.937
29.20	0.3724	15.87	16.15	1.462	32.71	0.3545	86.65	86.82	0.893
29.29	0.3767	20.94	21.24	1.567	32.80	0.463	83.18	83.35	0.899
29.37	0.3719	26.11	26.39	1.433	32.89	0.6374	72.29	72.47	0.922
29.46	0.3864	33.53	33.74	1.099	32.97	0.7794	59.88	60.06	0.928
29.55	0.4026	31	31.16	0.864	33.06	0.7216	48.12	48.31	0.98
29.63	0.521	28.09	28.29	1.027	33.15	0.6997	42.61	42.81	1.028
29.72	0.5628	25.61	25.81	1.028	33.24	0.652	47.49	47.71	1.145
29.81	0.475	16.27	16.49	1.093	33.32	0.6616	74	74.26	1.335
29.90	0.4264	12.26	12.48	1.149	33.41	0.7505	90.55	90.71	0.855
29.98	0.3762	9.87	10.18	1.574	33.50	0.7203	97.46	97.64	0.925
30.07	0.4228	11.06	11.55	2.532	33.58	0.71	114.57	114.76	0.95
30.16	0.4817	18.24	18.78	2.803	33.67	0.6146	114.45	114.64	1.002
30.25	0.4009	17.22	17.6	1.963	33.76	0.5201	103.37	103.56	0.977
30.33	0.3573	15.15	15.42	1.37	33.85	0.5921	95.28	95.48	1
30.42	0.3537	14.08	14.33	1.281	33.94	0.5601	93.56	93.77	1.065
30.51	0.3265	14.08	14.51	2.226	34.03	0.5289	102.86	103.07	1.055
30.60	0.3004	19.74	20.16	2.205	34.11	0.5153	106.89	107.08	0.988
30.69	0.2532	25.39	25.58	0.958	34.20	0.5096	98.04	98.24	1.007
30.77	0.2002	29.36	29.53	0.892	34.29	0.5084	95.5	95.68	0.959
30.86	0.1709	35.35	35.51	0.851	34.37	0.5313	100.18	100.37	1.007
30.96	0.1646	43.95	44.11	0.864	34.46	0.5401	114.09	114.27	0.973
31.04	0.1976	48.05	48.18	0.679	34.55	0.5838	115.59	115.78	0.959
31.13	0.1797	41.88	42.04	0.813	34.64	0.6338	104.55	104.74	0.966
31.22	0.1799	48.3	48.45	0.806	34.67	0.6517	95.83	96.01	0.932
31.30	0.2032	58.58	58.73	0.778	34.76	0.6901	83.8	84	0.994
31.39	0.2492	56.42	56.59	0.845	34.84	0.4808	72.54	72.74	1.049
31.50	0.2798	47.97	48.15	0.917	34.93	0.4621	70.9	71.12	1.133

Table D.7 Continued

z	f_s	q_u	q_t	u_2	z	f_s	q_u	q_t	u_2
(ft)	(tsf)	(tsf)	(tsf)	(tsf)	(ft)	(tsf)	(tsf)	(tsf)	(tsf)
35.01	0.4839	77.82	78.07	1.323	38.71	0.449	26.56	27.08	2.682
35.10	0.495	93.02	93.22	1.035	38.80	0.3542	62.11	62.73	3.195
35.19	0.6209	91.94	92.1	0.855	38.89	0.3548	77.44	77.7	1.358
35.28	0.6798	76.64	76.81	0.903	38.97	0.3639	87.49	87.77	1.422
35.36	0.5913	60.78	60.98	1.033	39.06	0.406	89.99	90.24	1.258
35.45	0.414	48.87	49.09	1.124	39.15	0.4769	90.22	90.46	1.272
35.53	0.3967	45.05	45.28	1.16	39.24	0.5035	82.84	83.06	1.129
35.62	0.4988	52.94	53.21	1.379	39.33	0.4965	71.45	71.66	1.054
35.71	0.5765	66.38	66.54	0.782	39.42	0.5394	60.86	61.06	1.066
35.80	0.5276	46.44	46.61	0.879	39.51	0.6211	56.52	56.74	1.142
35.88	0.5994	32.58	32.79	1.076	39.60	0.8251	54.83	55.06	1.193
35.97	0.6003	28.72	28.96	1.287	39.69	1.0818	44.98	45.2	1.158
36.06	0.626	27.46	27.68	1.143	39.78	1.1433	32.69	32.93	1.238
36.14	0.6049	23.1	23.29	0.967	39.86	1.0442	24.12	24.37	1.292
36.23	0.4907	19.35	19.64	1.507	39.95	0.8335	20.76	21.13	1.924
36.32	0.4078	16.75	17.15	2.074	40.04	0.5851	14.77	15.09	1.698
36.41	0.4569	15.27	15.69	2.19	40.13	0.4682	11.18	12.03	4.409
36.50	0.5185	22.06	22.51	2.376	40.22	0.4168	23.63	24.59	4.964
36.58	0.4246	21.08	21.45	1.922	40.31	0.5393	68.22	68.98	3.896
36.67	0.3901	16.06	16.27	1.091	40.39	0.5857	71.91	72.12	1.094
36.75	0.3956	13.71	14.06	1.794	40.48	0.6641	49.68	49.89	1.126
36.84	0.477	20.92	21.19	1.364	40.57	0.8012	32.09	32.3	1.105
36.93	0.5274	27.19	27.56	1.906	40.65	0.8987	34.11	34.43	1.67
37.02	0.5011	21.48	21.74	1.328	40.74	0.9295	39.83	40.18	1.816
37.11	0.5209	20.35	20.62	1.377	40.83	0.7678	32.16	32.36	0.997
37.20	0.5419	18.52	18.8	1.446	40.91	0.7669	26.76	27.04	1.472
37.28	0.4448	14.63	15.04	2.134	41.00	0.7261	36.81	37.1	1.472
37.38	0.5184	12.88	13.35	2.45	41.08	0.828	32.97	33.23	1.326
37.46	0.637	12.14	12.61	2.449	41.16	0.9495	28.84	29.07	1.199
37.55	0.559	19.11	19.81	3.629	41.25	1.0292	29.9	30.18	1.431
37.64	0.4817	19.88	20.18	1.579	41.33	0.8702	27.17	27.48	1.6
37.73	0.3999	15.43	15.92	2.551	41.41	0.7743	20.83	21.09	1.339
37.81	0.3597	11.52	12.03	2.667	41.50	0.6872	15.76	16.1	1.762
38.09	0.6016	47.01	47.23	1.14	41.59	0.6448	13.81	14.18	1.959
38.18	0.7468	37.12	37.3	0.943	41.67	0.6131	13.62	14.37	3.873
38.27	0.7702	25.45	25.66	1.076	41.75	0.5448	14.38	14.96	3.037
38.35	0.7804	19.63	19.87	1.273	41.84	0.5531	16.96	17.38	2.178
38.45	0.6902	17.57	17.84	1.411	41.93	0.4992	17.05	17.48	2.213
38.54	0.5636	15.38	15.74	1.867	42.01	0.4962	20.2	20.66	2.414
38.62	0.4557	16.15	16.67	2.678	42.10	0.4351	26.06	26.53	2.447

Table D.7 Continued

z	f_s	q_u	q_t	u_2	z	f_s	q_u	q_t	u_2
(ft)	(tsf)	(tsf)	(tsf)	(tsf)	(ft)	(tsf)	(tsf)	(tsf)	(tsf)
42.19	0.3655	32.18	32.58	2.051	45.76	0.7246	21.04	21.49	2.327
42.27	0.3584	36.81	37.03	1.145	45.85	0.5611	21.13	21.8	3.465
42.35	0.3883	42.84	43.12	1.429	45.93	0.467	47.24	48	3.927
42.44	0.4985	48.38	48.63	1.291	46.02	0.4792	80.79	81.42	3.284
42.52	0.6858	41.39	41.56	0.912	46.10	0.6048	78.65	78.91	1.321
42.61	0.9691	35.13	35.32	1.013	46.19	0.7724	65.23	65.45	1.13
42.70	0.8956	29.15	29.36	1.106	46.27	0.7668	57.47	57.72	1.302
42.78	0.7276	21.99	22.21	1.166	46.36	0.5956	54.83	55.13	1.558
42.87	0.6254	17.78	18.12	1.751	46.45	0.5596	48.3	48.6	1.597
42.95	0.6536	12.06	12.52	2.392	46.53	0.6074	51.26	51.66	2.072
43.04	0.7279	20.87	21.87	5.179	46.62	0.8014	64.35	64.57	1.126
43.13	0.6728	29.58	30.43	4.414	46.71	0.77	58.34	58.56	1.122
43.21	0.5053	19.28	19.52	1.281	46.79	0.7996	44.42	44.68	1.329
43.30	0.4685	14.83	15.3	2.42	46.88	0.9103	36.36	36.66	1.562
43.38	0.4714	12.06	12.49	2.222	46.97	1.187	41.55	41.93	1.923
43.47	0.5042	11.03	12.01	5.091	47.06	1.0248	44.15	44.53	1.948
43.55	0.3594	12.77	13.81	5.413	47.14	0.9208	34.12	34.34	1.118
43.64	0.3767	13.44	14.49	5.445	47.23	0.9132	27.17	27.51	1.769
43.73	0.4588	16.59	17.65	5.481	47.32	0.8141	20.98	21.42	2.297
43.81	0.476	32.61	33.73	5.774	47.40	0.716	19.82	20.69	4.502
43.90	0.5799	40.13	40.44	1.621	47.49	0.6372	18.79	19.25	2.404
43.99	0.5501	44	44.36	1.889	47.58	0.5534	13.38	14.03	3.328
44.07	0.5218	49.38	49.74	1.904	47.66	0.4739	11.33	12.15	4.219
44.16	0.5089	51.04	51.38	1.791	47.75	0.5276	13.06	14.14	5.564
44.24	0.5652	72.31	72.74	2.238	48.01	0.5091	16.62	17.31	3.583
44.49	1.1127	63.28	63.52	1.273	48.10	0.5735	18.29	19.24	4.908
44.57	1.0904	39.07	39.33	1.306	48.18	0.5423	20.13	20.98	4.389
44.65	0.9917	28.84	29.11	1.417	48.27	0.477	17.83	18.28	2.333
44.74	0.9488	24.5	24.91	2.146	48.36	0.4317	13.5	14.12	3.202
44.82	1.0263	20.73	21.06	1.696	48.44	0.4194	10.73	11.63	4.663
44.91	0.9698	19.58	20.32	3.825	48.52	0.3194	10.44	11.58	5.941
44.99	0.5775	23.8	24.53	3.806	48.61	0.3544	10.36	11.58	6.324
45.08	0.4062	27.19	27.72	2.745	48.70	0.4758	13.57	14.83	6.541
45.16	0.4155	28.07	28.62	2.847	48.78	0.5617	22.42	23.67	6.5
45.25	0.562	72.72	73.19	2.434	48.87	0.5293	23.83	24.38	2.843
45.33	0.7936	78.57	78.75	0.922	48.96	0.7179	21.61	22.18	2.92
45.42	0.9358	51.9	52.06	0.822	49.04	0.6483	19.47	20.11	3.325
45.51	0.9672	34.7	34.9	1.035	49.12	0.6781	19.18	19.93	3.912
45.59	1.0807	27.19	27.5	1.593	49.21	0.8363	21.04	21.58	2.844
45.67	0.8144	21.86	22.17	1.584	49.29	0.707	25.67	26.36	3.536

Table D.7 Continued

z	f_s	q_u	q_t	u_2	z	f_s	q_u	q_t	u_2
(ft)	(tsf)	(tsf)	(tsf)	(tsf)	(ft)	(tsf)	(tsf)	(tsf)	(tsf)
49.38	0.6466	28.02	28.83	4.194	52.82	1.376	45.91	46.2	1.505
49.47	0.6748	21.16	21.49	1.684	52.91	1.4316	39.52	40.07	2.834
49.55	0.548	24.12	24.74	3.214	53.00	1.368	30.03	30.45	2.181
49.64	0.4909	35.11	35.52	2.134	53.09	1.1989	22.11	23.58	7.609
49.72	0.4081	44.7	45.17	2.442	53.18	1.0348	22.92	24.21	6.658
49.81	0.3729	63.2	63.55	1.809	53.26	0.6882	26.06	27.88	9.447
49.89	0.4081	80.53	80.77	1.227	53.35	0.5709	30.58	32.93	12.151
49.98	0.4955	83.85	84.13	1.489	53.44	0.6942	35.36	38.4	15.762
50.06	0.4404	78.19	78.44	1.284	53.53	0.6559	43.92	47.61	19.088
50.15	0.5305	72.63	72.9	1.353	53.62	0.7011	53.77	58.03	22.058
50.23	0.4941	68.03	68.28	1.312	53.71	0.7007	57.72	61.38	18.969
50.32	0.4934	65.79	66.08	1.48	53.80	0.7362	56.67	61.06	22.73
50.41	0.4852	64.02	64.34	1.615	53.89	0.758	54.2	59.23	26.042
50.49	0.5197	66.77	67.06	1.478	53.98	0.7765	52.06	57.31	27.17
50.58	0.5532	71.49	71.79	1.528	54.07	0.7536	51.14	56.43	27.412
50.66	0.6843	68.64	68.92	1.45	54.15	0.7315	50.56	55.97	28.048
50.75	0.7644	58.34	58.6	1.337	54.35	0.6827	52.69	58.05	27.735
50.84	0.8617	42.24	42.5	1.334	54.44	0.6998	50.56	56.27	29.569
50.92	0.8054	30.3	30.59	1.524	54.53	0.6812	50.26	55.98	29.636
51.01	0.8841	22.54	22.89	1.772	54.61	0.6653	51.5	57.29	29.995
51.11	0.7218	20.11	20.57	2.339	54.70	0.6719	51.69	57.47	29.941
51.19	0.5851	17.52	18.23	3.711	54.79	0.6563	53.01	58.65	29.203
51.27	0.4772	17.71	18.77	5.469	54.88	0.6314	52.95	58.73	29.916
51.35	0.482	20.35	21.47	5.775	54.96	0.6143	52.55	58.37	30.157
51.44	0.6765	45.61	46.72	5.754	55.05	0.6318	51.44	57.39	30.777
51.52	0.6739	65.63	65.94	1.618	55.14	0.6357	50.22	56.26	31.314
51.61	0.5751	50.66	50.92	1.327	55.23	0.6159	50.28	56.31	31.211
51.69	0.6947	37.49	37.75	1.337	55.31	0.6142	50.93	57.12	32.049
51.77	1.1254	43.4	44	3.117	55.40	0.6104	53.84	59.9	31.393
51.86	1.5014	56.46	56.93	2.429	55.49	0.5663	54.28	60.17	30.535
51.95	0.9939	43.6	43.84	1.264	55.58	0.5579	54.53	60.34	30.086
52.04	0.9021	32.72	33.08	1.878	55.67	0.5802	53.73	59.55	30.149
52.13	1.1314	25.45	25.92	2.467	55.76	0.5854	53.15	58.96	30.089
52.21	0.9039	36.36	37.29	4.793	55.84	0.5652	52.77	58.49	29.629
52.30	0.7226	56.74	57.49	3.901	55.93	0.7083	54.48	59.91	28.143
52.39	0.5729	41.95	42.2	1.292	56.02	0.6862	58.4	63.81	27.989
52.47	0.6676	76.06	76.71	3.36	56.11	0.682	59.1	64.58	28.382
52.56	1.025	111.11	111.37	1.379	56.19	0.6671	63.61	68.51	25.374
52.64	1.3648	95.87	96.13	1.356	56.28	0.7405	61.77	66.7	25.518
52.73	1.4385	63.24	63.5	1.33	56.37	0.7941	63.66	69.21	28.742

Table D.7 Continued

z	f_s	q_u	q_t	u_2	z	f_s	q_u	q_t	u_2
(ft)	(tsf)	(tsf)	(tsf)	(tsf)	(ft)	(tsf)	(tsf)	(tsf)	(tsf)
56.47	0.9951	74.32	79.72	27.926	60.14	0.5453	53.9	60.55	34.456
56.55	0.9436	83.09	86.76	19.029	60.23	0.5636	53.7	60.32	34.289
56.64	1.0027	74.32	77.48	16.406	60.32	0.5964	53.4	60.2	35.218
56.73	0.9993	67.01	70.97	20.486	60.40	0.631	54.03	60.89	35.535
56.82	0.9592	63.72	68.29	23.674	60.49	0.6457	55.82	62.93	36.767
56.91	0.8202	63.06	67.81	24.607	60.58	0.6342	58.07	65.17	36.728
57.00	0.7358	64.44	68.98	23.514	60.79	0.6453	59	66.1	36.766
57.08	0.775	58.55	63.71	26.754	60.87	0.6361	58.05	65.42	38.19
57.17	0.8183	54.99	60.65	29.29	60.96	0.5916	59.25	66.65	38.305
57.26	0.8519	53.57	59.6	31.206	61.05	0.6015	59.3	66.81	38.89
57.35	0.8021	53.91	60.12	32.174	61.14	0.6331	59.63	67.02	38.278
57.60	0.627	55.73	62.14	33.195	61.23	0.6536	59.07	66.66	39.327
57.68	0.6296	55.3	61.9	34.154	61.31	0.6517	59.55	67.17	39.431
57.77	0.5693	54.4	60.99	34.108	61.40	0.6369	61.94	69.38	38.494
57.85	0.5663	54.12	60.87	34.952	61.49	0.6483	61.2	68.77	39.173
57.94	0.5966	54.98	61.84	35.529	61.58	0.6605	60.31	67.91	39.374
58.03	0.5893	55.81	62.74	35.925	61.67	0.664	59.46	67.09	39.523
58.12	0.5881	54.65	61.27	34.238	61.75	0.6836	59.05	66.66	39.406
58.20	0.5832	54.03	60.66	34.368	61.84	0.6809	58.67	66.34	39.687
58.29	0.6031	53.77	60.56	35.127	61.93	0.6785	58.17	65.96	40.323
58.38	0.6006	53.69	60.47	35.138	62.03	0.6553	58.42	66.34	40.987
58.47	0.602	54.32	61.23	35.758	62.11	0.6655	58.47	66.51	41.637
58.55	0.5925	54.83	61.64	35.273	62.21	0.6797	59.18	67.3	42.048
58.64	0.6135	54.67	61.52	35.446	62.29	0.7211	59.85	67.86	41.469
58.72	0.6213	53.49	60.2	34.789	62.38	0.739	60.78	68.63	40.654
58.81	0.5981	54.03	60.63	34.21	62.47	0.8023	61.22	69.06	40.599
58.90	0.5805	54.43	61.09	34.48	62.55	0.7797	61.12	68.96	40.575
58.99	0.5516	55.05	61.64	34.122	62.64	0.7648	61.56	69.53	41.264
59.08	0.5701	52.82	59.39	34.054	62.73	0.7531	61.5	69.56	41.712
59.16	0.5524	50.51	57.12	34.224	62.81	0.7373	60.83	69.02	42.429
59.25	0.5435	51.01	57.53	33.743	62.90	0.7435	60.64	68.79	42.212
59.34	0.5562	51.94	58.36	33.257	62.99	0.726	61.06	69.19	42.093
59.43	0.5504	52.17	58.7	33.819	63.08	0.7158	60.61	68.78	42.347
59.52	0.5412	53.27	59.72	33.399	63.16	0.7156	59.41	67.59	42.323
59.61	0.5593	55.03	61.32	32.591	63.25	0.7061	60.13	68.39	42.727
59.69	0.5567	55.74	61.89	31.854	63.34	0.7165	59.22	67.46	42.67
59.78	0.5302	54.91	61.22	32.659	63.43	0.6828	59.15	67.45	42.99
59.87	0.5192	53.28	59.63	32.859	63.52	0.6902	59.27	67.53	42.758
59.96	0.5174	53.02	59.56	33.887	63.61	0.7061	59.74	68.13	43.425
60.05	0.5075	53.65	60.23	34.105	63.69	0.702	61.49	69.89	43.491

Table D.8 CPT Data from SC-2L at the Lowcountry Sand & Gravel site

z	f_s	q_u	q_t	u_2	z	f_s	q_u	q_t	u_2
(ft)	(tsf)	(tsf)	(tsf)	(tsf)	(ft)	(tsf)	(tsf)	(tsf)	(tsf)
0.00	0	0	0	0	3.69	2.0598	339	339.05	0.232
0.23	0	294.57	294.91	1.765	3.78	2.0511	347.74	347.79	0.255
0.31	1.3599	269.82	270.21	2.018	3.88	2.0271	341.93	341.98	0.235
0.40	1.6667	249.98	250.23	1.293	3.96	1.9807	338.15	338.19	0.217
0.48	1.8494	236.4	236.58	0.926	4.05	1.9176	331.22	331.26	0.204
0.56	1.925	225.35	225.51	0.81	4.15	1.8663	325.08	325.13	0.209
0.64	2.1307	213.82	213.99	0.881	4.23	1.807	329.26	329.3	0.213
0.73	2.2428	202.87	203.06	1.003	4.32	1.7539	329.78	329.82	0.214
0.81	2.4258	198.22	198.41	1.003	4.41	1.7059	326.23	326.26	0.197
0.90	2.5606	193	193.18	0.961	4.50	1.6319	321.8	321.84	0.186
0.98	2.6958	192.08	192.27	0.956	4.59	1.582	321.18	321.22	0.194
1.06	2.7758	197.95	198.15	1.043	4.68	1.5415	326.47	326.51	0.199
1.15	2.857	206.15	206.38	1.181	4.76	1.5513	330.85	330.89	0.194
1.23	2.9494	213.93	214.16	1.177	4.85	1.6717	336.88	336.92	0.184
1.31	3.3163	225.75	225.94	0.987	4.94	1.6976	342.92	342.96	0.192
1.40	3.731	235.4	235.6	1.035	5.03	1.6117	343.44	343.48	0.211
1.49	3.9765	238.55	238.75	1.03	5.12	1.5264	341.79	341.83	0.22
1.57	4.1092	233.92	234.11	0.985	5.20	1.4929	340.56	340.61	0.243
1.66	4.2366	247.33	247.56	1.182	5.29	1.5484	341.8	341.84	0.186
1.74	4.2643	254	254.17	0.892	5.52	1.6093	316.28	316.32	0.166
1.82	3.8525	277.73	277.85	0.628	5.61	1.5814	307.75	307.78	0.16
1.91	3.4062	297.44	297.54	0.516	5.70	1.4434	298.96	298.99	0.168
2.00	3.042	322.68	322.8	0.621	5.79	1.2704	287.27	287.3	0.148
2.09	2.938	356.33	356.41	0.435	5.87	1.1437	273.08	273.11	0.124
2.32	2.6003	361.14	361.22	0.441	5.96	1.0733	265.03	265.06	0.143
2.42	2.4558	369.8	369.87	0.375	6.05	1.018	264.67	264.69	0.124
2.51	2.423	375.81	375.88	0.338	6.13	0.9603	271.2	271.23	0.119
2.60	2.4552	381.91	381.96	0.31	6.22	0.9485	276.98	277	0.122
2.70	2.5029	375.33	375.39	0.308	6.31	0.9407	278.61	278.64	0.143
2.79	2.5462	368.38	368.44	0.299	6.40	0.9595	279.74	279.76	0.125
2.87	2.6467	373.53	373.58	0.284	6.48	0.9598	279.99	280.01	0.117
2.95	2.7294	378.09	378.15	0.304	6.57	0.9281	277.1	277.13	0.133
3.03	2.7659	371.58	371.64	0.323	6.66	0.9163	269.69	269.71	0.13
3.11	2.7247	362.79	362.85	0.309	6.75	0.9328	266.55	266.57	0.119
3.20	2.6253	350.33	350.39	0.318	6.83	0.9409	262.78	262.8	0.134
3.28	2.5157	334.38	334.44	0.29	6.92	0.8986	261.77	261.8	0.123
3.36	2.3966	321.22	321.27	0.245	7.01	0.9112	264.16	264.19	0.111
3.45	2.2681	313.91	313.95	0.224	7.10	0.9518	267.05	267.08	0.115
3.53	2.17	312.26	312.3	0.204	7.19	0.9954	266.3	266.32	0.104
3.60	2.0905	323.2	323.24	0.224	7.28	1.0186	266.8	266.82	0.092

Table D.8 Continued

z	f_s	q_u	q_t	u_2	z	f_s	q_u	q_t	u_2
(ft)	(tsf)	(tsf)	(tsf)	(tsf)	(ft)	(tsf)	(tsf)	(tsf)	(tsf)
7.37	0.9832	263.91	263.93	0.099	10.83	0.3781	80.23	80.27	0.19
7.45	0.9815	252.09	252.11	0.082	10.92	0.3956	80.77	80.81	0.206
7.54	0.9839	240.03	240.04	0.061	11.01	0.4283	81.48	81.52	0.21
7.63	0.9366	225.84	225.84	0.007	11.09	0.4522	83.7	83.74	0.205
7.72	0.8381	206.12	206.12	0	11.19	0.4519	86.43	86.47	0.199
7.81	0.7943	188.9	188.91	0.003	11.27	0.4276	88.73	88.77	0.208
7.90	0.6998	176.84	176.84	0.003	11.36	0.4248	90.49	90.53	0.215
7.99	0.58	157.82	157.82	0.016	11.45	0.4646	92.67	92.72	0.253
8.07	0.4793	130.45	130.45	0.011	11.54	0.5085	96.15	96.19	0.243
8.17	0.3828	93.51	93.5	-0.024	11.63	0.551	97.65	97.7	0.24
8.25	0.3416	58.29	58.28	-0.061	11.72	0.5975	98.19	98.24	0.221
8.34	0.2961	44.5	44.48	-0.073	12.02	0.4348	91.33	91.37	0.234
8.43	0.2799	27.96	27.95	-0.091	12.11	0.4113	91.49	91.54	0.233
8.53	0.292	19.99	19.97	-0.101	12.20	0.3724	95.73	95.78	0.287
8.57	0.3094	15.02	15	-0.109	12.29	0.3465	99.12	99.17	0.255
8.64	0.3487	12.63	12.61	-0.101	12.38	0.3309	99.74	99.79	0.231
8.72	0.359	10.07	10.05	-0.073	12.46	0.3305	99.08	99.13	0.246
8.81	0.371	8.98	8.97	-0.062	12.55	0.3723	96.4	96.44	0.25
8.90	0.344	6.92	6.92	-0.038	12.64	0.3792	91.24	91.29	0.254
8.99	0.3166	4.54	4.54	0.008	12.73	0.3712	88.35	88.41	0.286
9.07	0.1973	3.52	3.52	0.002	12.81	0.4155	88.69	88.74	0.287
9.16	0.1678	3.15	3.17	0.122	12.90	0.4806	87.18	87.24	0.311
9.25	0.2526	4.59	4.7	0.563	12.99	0.4853	84.25	84.31	0.319
9.34	0.3473	31.03	31.18	0.782	13.08	0.4573	83.91	83.97	0.308
9.42	0.2911	47.81	47.89	0.386	13.17	0.4002	84.84	84.89	0.268
9.51	0.2637	62.86	62.91	0.272	13.25	0.3401	84.08	84.13	0.258
9.60	0.3042	82.78	82.84	0.276	13.34	0.2654	79.27	79.31	0.245
9.69	0.352	104.82	104.87	0.286	13.43	0.204	72.77	72.82	0.254
9.78	0.4102	122	122.03	0.192	13.52	0.1788	66.91	66.96	0.256
9.86	0.4093	120.71	120.74	0.165	13.61	0.1985	61.84	61.89	0.264
9.95	0.4149	111.01	111.04	0.158	13.69	0.2348	55.32	55.37	0.247
10.04	0.4262	103.3	103.32	0.135	13.78	0.2732	45.3	45.35	0.253
10.13	0.4036	98.92	98.95	0.169	13.87	0.3386	36.03	36.07	0.255
10.22	0.3672	93.25	93.28	0.156	13.96	0.3964	26.33	26.38	0.249
10.31	0.3654	89.03	89.06	0.186	14.05	0.4324	18.68	18.73	0.276
10.39	0.3447	84.5	84.53	0.161	14.14	0.4179	14.76	14.82	0.286
10.48	0.3181	80.86	80.89	0.154	14.22	0.3437	13	13.07	0.356
10.57	0.3401	77.97	78	0.161	14.31	0.3041	12	12.08	0.444
10.66	0.3334	77.13	77.16	0.174	14.40	0.293	10.69	10.81	0.612
10.75	0.3562	79.14	79.18	0.185	14.49	0.2591	10	10.14	0.759

Table D.8 Continued

z	f_s	q_u	q_t	u_2	z	f_s	q_u	q_t	u_2
(ft)	(tsf)	(tsf)	(tsf)	(tsf)	(ft)	(tsf)	(tsf)	(tsf)	(tsf)
14.58	0.2461	8.61	8.77	0.847	18.48	0.1979	7.29	7.49	1.024
14.67	0.2645	7.74	7.91	0.903	18.57	0.1967	7.11	7.33	1.145
14.76	0.2863	7.92	8.13	1.084	18.66	0.1783	8	8.24	1.246
14.85	0.3031	10.12	10.35	1.191	18.75	0.1632	7.55	7.8	1.283
14.93	0.2853	9.94	10.16	1.136	18.84	0.1511	6.86	7.12	1.37
15.19	0.2581	8.18	8.37	0.988	18.93	0.148	6.29	6.57	1.477
15.44	0.2343	7.41	7.69	1.46	19.01	0.1534	5.92	6.23	1.603
15.53	0.2654	9.3	9.6	1.558	19.10	0.1475	5.53	5.85	1.611
15.62	0.283	11.27	11.54	1.372	19.18	0.1486	5.6	5.93	1.689
15.71	0.2399	11.68	11.91	1.197	19.27	0.136	6.03	6.37	1.769
15.80	0.2124	11.56	11.74	0.915	19.35	0.1488	6.98	7.33	1.816
15.88	0.2107	10.39	10.58	0.971	19.44	0.1525	7.43	7.78	1.814
15.97	0.2272	8.05	8.26	1.044	19.53	0.1681	6.87	7.23	1.907
16.06	0.2263	6.86	7.07	1.103	19.62	0.1825	6.35	6.72	1.953
16.15	0.2061	6.41	6.65	1.243	19.70	0.208	6.61	7.02	2.107
16.23	0.1754	6.61	6.86	1.342	19.79	0.2442	7.94	8.35	2.14
16.33	0.1887	7.12	7.39	1.422	19.87	0.2861	8.41	8.83	2.173
16.41	0.214	7.76	8.05	1.491	19.96	0.3558	11	11.38	1.96
16.50	0.2117	8	8.3	1.552	20.05	0.3289	12	12.33	1.708
16.59	0.1931	8.17	8.45	1.463	20.14	0.3221	10.76	11.07	1.573
16.69	0.1888	8.2	8.45	1.335	20.22	0.3233	8.24	8.53	1.521
16.78	0.1981	7.49	7.72	1.179	20.30	0.2739	7.24	7.57	1.717
16.86	0.2197	7.37	7.65	1.439	20.39	0.2317	7.87	8.22	1.836
16.95	0.2536	8.12	8.43	1.573	20.48	0.199	8.49	8.87	1.946
17.04	0.2301	9.96	10.26	1.574	20.56	0.1981	7.93	8.31	1.979
17.13	0.2329	10.46	10.7	1.261	20.65	0.2181	7.48	7.88	2.09
17.22	0.2395	10.45	10.68	1.163	20.73	0.2637	8.11	8.54	2.195
17.31	0.2495	12.4	12.6	1.063	20.82	0.3207	11.19	11.65	2.426
17.40	0.2645	13.53	13.71	0.972	20.91	0.2907	24.68	25.13	2.319
17.49	0.2534	13.01	13.18	0.882	20.99	0.3492	32.43	32.7	1.375
17.58	0.2146	11.95	12.13	0.95	21.08	0.5093	32.14	32.33	0.969
17.67	0.2198	10.18	10.37	0.989	21.16	0.6493	37.56	37.76	1.031
17.76	0.2695	9.13	9.34	1.123	21.25	0.7761	33.72	33.91	0.967
17.86	0.2397	9.23	9.46	1.177	21.33	0.7975	28.95	29.09	0.739
17.95	0.2812	10.93	11.15	1.138	21.42	0.5918	28.99	29.15	0.845
18.03	0.2856	11.44	11.64	1.035	21.46	0.4998	30.96	31.08	0.612
18.13	0.2652	10	10.19	0.997	21.54	0.4217	41.51	41.65	0.717
18.21	0.2532	8.98	9.2	1.107	21.62	0.3696	49.6	49.73	0.674
18.30	0.2303	9.06	9.23	0.862	21.70	0.3768	51.98	52.06	0.418
18.39	0.203	7.86	8.04	0.913	21.79	0.4112	58.16	58.27	0.522

Table D.8 Continued

z	f_s	q_u	q_t	u_2	z	f_s	q_u	q_t	u_2
(ft)	(tsf)	(tsf)	(tsf)	(tsf)	(ft)	(tsf)	(tsf)	(tsf)	(tsf)
21.87	0.4831	60.35	60.43	0.426					
21.96	0.5419	50.65	50.74	0.437	25.29	0.407	10.67	11.15	2.482
22.05	0.5481	36.79	36.88	0.471	25.37	0.3101	9.55	10.08	2.731
22.13	0.6275	28.77	28.88	0.547	25.45	0.2434	8.55	9.1	2.829
22.21	0.6377	25.7	25.85	0.741	25.54	0.1969	7.73	8.27	2.789
22.30	0.6187	22.35	22.64	1.51	25.62	0.2115	7.04	7.58	2.812
22.39	0.5976	21.11	21.27	0.821	25.71	0.2143	6.22	6.79	2.968
22.47	0.5246	27.16	27.36	1.062	25.80	0.1974	6.03	6.62	3.082
22.56	0.412	34.48	34.69	1.1	25.89	0.1773	6.66	7.28	3.205
22.64	0.3705	40.33	40.47	0.722	25.97	0.1492	8.93	9.5	2.952
22.73	0.3353	41.05	41.18	0.652	26.06	0.1565	10.94	11.44	2.591
22.81	0.2502	45.15	45.26	0.542	26.14	0.2349	12.37	12.81	2.241
22.90	0.2397	54.49	54.61	0.583	26.23	0.2607	13.14	13.57	2.252
22.99	0.2138	54.77	54.88	0.54	26.32	0.1998	14.13	14.59	2.368
23.07	0.2005	47.74	47.84	0.522	26.41	0.1374	17.02	17.45	2.241
23.16	0.2106	44.83	44.93	0.527	26.50	0.1862	24.43	24.68	1.283
23.25	0.2046	50.13	50.23	0.561	26.58	0.2648	34.4	34.66	1.327
23.33	0.229	55.02	55.13	0.554	26.67	0.2908	34.23	34.37	0.725
23.42	0.2465	54.95	55.05	0.538	26.76	0.3969	25.56	25.69	0.682
23.51	0.3011	50.43	50.53	0.528	26.84	0.4023	21.74	21.89	0.792
23.59	0.2703	44.57	44.68	0.537	26.93	0.5008	24.56	24.74	0.939
23.68	0.238	38.24	38.35	0.576	27.02	0.5362	23.36	23.52	0.878
23.77	0.2495	33.42	33.53	0.568	27.11	0.4921	25.72	25.88	0.787
23.85	0.2874	33.92	34.05	0.641	27.19	0.4156	24.79	24.98	0.999
23.94	0.303	36.43	36.56	0.666	27.28	0.3076	26.42	26.6	0.936
24.03	0.2595	33.27	33.39	0.614	27.37	0.2879	37.44	37.66	1.172
24.11	0.2368	32.24	32.36	0.657	27.45	0.2841	57.29	57.42	0.691
24.20	0.2247	40.33	40.47	0.715	27.54	0.2744	74.87	75.04	0.856
24.29	0.1907	49.3	49.46	0.826	27.63	0.2646	70.64	70.8	0.795
24.37	0.1672	54.4	54.5	0.54	27.71	0.2748	62.14	62.29	0.801
24.45	0.1853	59.26	59.37	0.555	27.80	0.3737	57.79	57.94	0.8
24.54	0.2574	56.38	56.49	0.59	28.04	0.5998	34.33	34.48	0.747
24.63	0.3643	47.76	47.89	0.633	28.14	0.8127	27.07	27.23	0.844
24.69	0.4662	39.88	40	0.637	28.22	0.77	24.23	24.46	1.141
24.78	0.586	31.54	31.66	0.652	28.31	0.7047	20.33	20.59	1.377
24.87	0.6401	24.01	24.15	0.69	28.40	0.6073	16.45	16.77	1.64
24.95	0.6148	19.34	19.49	0.811	28.49	0.531	15.7	16.16	2.398
25.03	0.5398	16.09	16.28	1.017	28.58	0.4413	19.66	20.26	3.116
25.11	0.4911	13.2	13.45	1.298	28.67	0.352	29.63	30.21	2.981

Table D.8 Continued

z	f_s	q_u	q_t	u_2
(ft)	(tsf)	(tsf)	(tsf)	(tsf)
28.75	0.3144	50.48	50.89	2.124
28.85	0.3	72.53	72.74	1.111
28.94	0.2961	75.5	75.69	1
29.03	0.4045	67.71	67.88	0.87
29.12	0.4854	58.81	58.97	0.824
29.21	0.5169	52.41	52.57	0.834
29.30	0.5314	41.11	41.27	0.848
29.39	0.518	35.39	35.54	0.794
29.49	0.447	45.96	46.15	1.004
29.57	0.5165	49.42	49.61	0.96
29.66	0.4592	48.12	48.27	0.782
29.75	0.3679	43.04	43.2	0.818
29.83	0.2967	39.03	39.19	0.84
29.92	0.2689	44.98	45.15	0.898
30.00	0.283	57.51	57.72	1.127
30.09	0.3319	61.73	61.88	0.77
30.17	0.4678	57.46	57.6	0.714
30.27	0.4295	49.65	49.79	0.74
30.35	0.3561	45.3	45.46	0.794
30.44	0.4223	46.43	46.6	0.889
30.53	0.5727	59.26	59.46	0.997
30.62	0.762	67.89	68.07	0.942
30.70	0.6087	58.31	58.45	0.726
30.80	0	48.62	48.78	0.828
30.88	0	62.45	62.65	1.02
30.97	0	105.04	105.29	1.3
31.05	0	131.39	131.59	0.989
31.05	0	131.39	131.59	0.989

Table D.9 CPT Data from SC-3L at the Lowcountry Sand & Gravel site

z	f_s	q_u	q_t	u_2	z	f_s	q_u	q_t	u_2
(ft)	(tsf)	(tsf)	(tsf)	(tsf)	(ft)	(tsf)	(tsf)	(tsf)	(tsf)
0.00	0	0	0	0	3.82	1.6278	242.63	242.72	0.485
0.24	0	77.76	77.84	0.411	3.91	1.5908	245.91	246.01	0.507
0.33	0.6206	74.24	74.33	0.478	3.99	1.5252	252.68	252.78	0.503
0.43	0.6982	71.35	71.44	0.436	4.08	1.477	260.1	260.19	0.431
0.52	0.7291	65.15	65.22	0.37	4.17	1.4081	266.27	266.34	0.392
0.61	0.7621	58.87	58.94	0.353	4.26	1.3882	269.02	269.1	0.397
0.70	0.8148	58.84	58.92	0.417	4.35	1.3673	266.13	266.2	0.364
0.78	0.923	63.61	63.72	0.579	4.44	1.3468	260.49	260.55	0.327
0.87	0.8554	67.57	67.69	0.615	4.52	1.2868	255.46	255.52	0.311
0.95	0.8869	74.49	74.58	0.464	4.61	1.2316	250.43	250.49	0.312
1.04	0.8898	119.61	119.71	0.519	4.70	1.2017	248.54	248.6	0.308
1.13	0.8595	162.83	162.97	0.727	4.78	1.1627	251.69	251.75	0.321
1.22	0.8731	189.13	189.25	0.606	4.87	1.1398	257.98	258.04	0.319
1.30	0.9941	194.89	195	0.554	4.96	1.1035	262.88	262.94	0.322
1.39	1.1085	189.55	189.65	0.508	5.05	1.0761	264	264.06	0.329
1.48	1.1804	180.57	180.67	0.529	5.14	1.0951	260.1	260.16	0.323
1.56	1.2519	165.87	165.98	0.575	5.23	1.0575	253.69	253.75	0.33
1.65	1.2684	149.91	150.03	0.6	5.32	1.0299	250.81	250.87	0.314
1.73	1.2599	136.5	136.63	0.641	5.40	0.9864	250.43	250.48	0.291
1.81	1.1958	129.97	130.09	0.602	5.49	0.9401	246.03	246.09	0.294
1.90	1.1319	126.64	126.77	0.642	5.58	0.8964	241.5	241.55	0.281
1.99	1.1188	138.2	138.32	0.621	5.66	0.8709	237.1	237.16	0.281
2.07	1.1048	150.22	150.33	0.545	5.95	0.8563	230.56	230.61	0.286
2.16	1.09	155.79	155.88	0.471	6.04	0.8269	232.08	232.14	0.287
2.25	1.0755	157.98	158.07	0.455	6.12	0.8039	235.74	235.79	0.282
2.33	1.0664	160.12	160.22	0.511	6.21	0.7872	239.5	239.55	0.298
2.41	1.1172	162.23	162.33	0.515	6.29	0.7899	240	240.06	0.287
2.67	1.2885	164.94	165.06	0.616	6.38	0.81	239	239.06	0.272
2.76	1.4294	175.4	175.51	0.601	6.47	0.9027	239.37	239.43	0.28
2.85	1.7621	192.26	192.35	0.512	6.56	1.2943	236.22	236.28	0.278
2.94	1.7659	202.32	202.42	0.476	6.64	1.7347	230.32	230.37	0.285
3.02	1.7281	194.89	195.02	0.663	6.73	1.6936	214.76	214.81	0.265
3.12	1.6744	193.93	194.12	1.015	6.82	1.5429	186.96	187.01	0.25
3.20	1.618	213	213.22	1.108	6.90	1.537	152.23	152.28	0.232
3.29	1.5716	231.11	231.2	0.463	6.99	1.2485	120.64	120.69	0.241
3.38	1.457	240.53	240.61	0.403	7.08	1.055	119.76	119.83	0.357
3.46	1.4284	250.2	250.27	0.396	7.17	0.9438	176.05	176.17	0.642
3.55	1.5161	253.45	253.53	0.411	7.25	0.8474	219.16	219.26	0.521
3.64	1.6123	248.04	248.13	0.438	7.33	0.7763	227.55	227.62	0.362
3.73	1.6439	249.67	249.76	0.421	7.42	0.7463	227.44	227.5	0.357

Table D.9 Continued

z	f_s	q_u	q_t	u_2	z	f_s	q_u	q_t	u_2
(ft)	(tsf)	(tsf)	(tsf)	(tsf)	(ft)	(tsf)	(tsf)	(tsf)	(tsf)
7.51	0.7603	232.46	232.53	0.347	11.28	0.2426	33.87	33.9	0.145
7.60	0.787	236.86	236.93	0.347	11.37	0.2314	29.85	29.88	0.145
7.69	0.8184	232.71	232.78	0.34	11.46	0.2259	27.29	27.32	0.157
7.78	0.8711	231.07	231.14	0.344	11.55	0.2504	25.26	25.29	0.162
7.87	0.8739	224.93	225	0.325	11.64	0.2675	25.22	25.26	0.176
7.96	0.8286	218.91	218.96	0.304	11.73	0.1919	29.32	29.35	0.202
8.04	0.8155	213.88	213.94	0.289	11.82	0.1938	35.42	35.47	0.234
8.13	0.7818	206.06	206.12	0.295	11.91	0.1956	45.96	46.01	0.264
8.22	0.7394	199.26	199.31	0.289	12.01	0.1976	72.77	72.82	0.28
8.31	0.6944	195.81	195.86	0.267	12.06	0.1987	74.9	74.96	0.294
8.40	0.643	194.1	194.16	0.286	13.43	0.3954	44.3	44.34	0.205
8.49	0.6013	189.15	189.2	0.264	13.52	0.439	30.66	30.7	0.211
8.58	0.5846	184.34	184.39	0.259	13.61	0.4617	22.28	22.33	0.258
8.66	0.5712	180.05	180.09	0.243	13.70	0.4713	17.88	17.93	0.286
8.76	0.5572	173.06	173.1	0.216	13.79	0.4959	16.3	16.36	0.323
8.85	0.5519	167.15	167.19	0.202	13.88	0.4605	14.59	14.65	0.344
9.12	0.436	137.86	137.89	0.172	13.97	0.3923	12.51	12.58	0.385
9.21	0.4398	135.47	135.5	0.183	14.06	0.3311	10.64	10.73	0.49
9.30	0.4451	136.06	136.1	0.194	14.15	0.2976	9.57	9.69	0.589
9.39	0.459	138.61	138.65	0.193	14.24	0.257	8.7	8.85	0.75
9.48	0.463	143.29	143.33	0.178	14.33	0.2123	8.43	8.6	0.875
9.57	0.4986	145.45	145.48	0.148	14.41	0.2096	7.61	7.79	0.919
9.65	0.5001	140.49	140.52	0.157	14.50	0.2157	6.93	7.11	0.977
9.74	0.544	133.68	133.7	0.136	14.59	0.2409	7.44	7.65	1.106
9.84	0.5998	123.6	123.62	0.144	14.68	0.2933	9.01	9.24	1.174
9.93	0.5989	112.67	112.71	0.184	14.77	0.3249	10.27	10.5	1.226
10.01	0.5621	101.12	101.15	0.155	14.85	0.28	12.95	13.2	1.257
10.11	0.4856	90.19	90.22	0.165	14.94	0.2475	16.86	17.1	1.243
10.20	0.4515	85.59	85.62	0.192	15.03	0.284	21.93	22.1	0.923
10.29	0.4298	89.73	89.77	0.182	15.12	0.3013	24.33	24.49	0.82
10.37	0.4018	93.33	93.36	0.179	15.20	0.2982	21.22	21.35	0.719
10.46	0.3724	88.52	88.55	0.184	15.25	0.3043	14.33	14.47	0.675
10.55	0.3452	83.78	83.82	0.19	15.32	0.306	15.52	15.63	0.579
10.64	0.3227	78.76	78.79	0.172	15.40	0.3508	13.52	13.65	0.634
10.74	0.3237	77.29	77.33	0.192	15.48	0.4345	26.52	26.64	0.615
10.83	0.2966	72.35	72.38	0.165	15.52	0.474	28.85	28.94	0.476
10.91	0.2735	64.01	64.04	0.163	15.60	0.5431	22.57	22.67	0.504
11.01	0.2605	55.03	55.05	0.141	15.69	0.5727	15.35	15.43	0.41
11.10	0.253	47.14	47.17	0.147	15.77	0.5607	12.64	12.73	0.451
11.19	0.241	40.38	40.41	0.159	15.86	0.4823	10.76	10.87	0.542

Table D.9 Continued

z	f_s	q_u	q_t	u_2	z	f_s	q_u	q_t	u_2
(ft)	(tsf)	(tsf)	(tsf)	(tsf)	(ft)	(tsf)	(tsf)	(tsf)	(tsf)
15.95	0.4183	8.94	9.05	0.554	19.54	0.9097	219.16	219.28	0.616
16.03	0.3647	6.87	7	0.65	19.62	0.9019	222.17	222.29	0.627
16.12	0.311	5.48	5.63	0.775	19.71	0.9606	231.24	231.35	0.61
16.20	0.2405	4.86	5.04	0.921	19.80	0.9816	245.3	245.42	0.628
16.29	0.1884	4.22	4.44	1.123	19.88	0.9723	256.6	256.73	0.666
16.37	0.1634	4.16	4.39	1.209	19.97	1.0036	259.99	260.12	0.687
16.46	0.1734	4.36	4.62	1.321	20.05	1.0295	263.37	263.5	0.688
16.55	0.1633	4.3	4.57	1.411	20.14	1.0824	274.43	274.56	0.676
16.63	0.163	3.97	4.26	1.477	20.22	1.1194	287.49	287.63	0.705
16.72	0.1582	3.97	4.27	1.558	20.30	1.1175	292.65	292.79	0.745
16.81	0.162	4.24	4.55	1.634	20.39	1.1182	293.27	293.41	0.75
16.89	0.1628	3.85	4.17	1.688	20.48	1.1648	296.02	296.17	0.753
16.98	0.1515	4.24	4.58	1.749	20.56	1.2211	304.2	304.35	0.799
17.07	0.1374	3.85	4.19	1.783	20.64	1.3316	310.08	310.23	0.777
17.15	0.135	4.16	4.52	1.851	20.73	1.377	309.22	309.38	0.806
17.24	0.139	4.23	4.6	1.94	20.82	1.3601	304.33	304.49	0.818
17.33	0.1506	4.16	4.56	2.037	20.90	1.3401	290.88	291.04	0.817
17.41	0.1569	4.23	4.64	2.119	20.99	1.3313	281.84	282	0.813
17.50	0.1612	4.22	4.65	2.204	21.07	1.3092	284.98	285.12	0.752
17.58	0.1764	4.66	5.11	2.297	21.16	1.2893	293.77	293.92	0.774
17.67	0.1853	4.86	5.31	2.365	21.24	1.29	294.9	295.05	0.8
17.76	0.1928	5.05	5.52	2.441	21.33	1.2909	298.41	298.57	0.803
17.84	0.1865	4.85	5.32	2.457	21.41	1.3133	302.17	302.33	0.813
17.93	0.2019	4.98	5.47	2.534	21.50	1.3208	306.82	306.98	0.831
18.02	0.2024	5.17	5.68	2.609	21.58	1.3539	308.61	308.77	0.857
18.10	0.2343	5.17	5.7	2.729	21.67	1.3875	306.07	306.23	0.838
18.19	0.3389	5.1	5.64	2.808	21.75	1.3918	306.46	306.62	0.837
18.28	0.3464	6.49	7.07	3.011	21.84	1.361	305.94	306.1	0.813
18.36	0.3772	17.8	18.39	3.103	22.06	1.3443	301.68	301.82	0.741
18.45	0.4077	67.88	68.36	2.474	22.14	1.3198	302.31	302.45	0.734
18.53	0.4418	127.21	127.39	0.932	22.23	1.3125	301.17	301.32	0.744
18.62	0.5348	167.7	167.81	0.579	22.31	1.292	293.27	293.42	0.776
18.87	0.8229	205.23	205.34	0.597	22.40	1.2289	288.12	288.25	0.704
18.96	0.8766	206.47	206.59	0.602	22.49	1.2276	281.71	281.84	0.677
19.04	0.8901	206.58	206.7	0.61	22.57	1.1932	271.91	272.05	0.7
19.12	0.8776	202.07	202.19	0.613	22.66	1.1722	264	264.13	0.668
19.20	0.8632	200.98	201.09	0.593	22.75	1.1647	256.85	256.97	0.65
19.29	0.8878	206.71	206.82	0.586	22.85	1.1476	244.29	244.43	0.684
19.37	0.9076	212.2	212.32	0.602	22.93	1.0824	230.61	230.74	0.666
19.46	0.9271	215.63	215.74	0.607	23.02	1.0326	216.07	216.2	0.653

Table D.9 Continued

z	f_s	q_u	q_t	u_2	z	f_s	q_u	q_t	u_2
(ft)	(tsf)	(tsf)	(tsf)	(tsf)	(ft)	(tsf)	(tsf)	(tsf)	(tsf)
23.10	0.9866	198.61	198.74	0.69	26.69	0.6607	213	213.14	0.7
23.19	0.9243	187.69	187.83	0.746	26.77	0.6611	212.61	212.75	0.723
23.27	0.9057	182.31	182.46	0.787	26.86	0.6776	210.28	210.41	0.679
23.36	0.8892	176.14	176.3	0.834	26.95	0.6834	206.25	206.38	0.698
23.44	0.8017	167.3	167.47	0.892	27.03	0.6777	201.57	201.71	0.704
23.53	0.7904	160.47	160.65	0.927	27.12	0.7069	198.46	198.6	0.705
23.61	0.7685	159.44	159.63	0.984	27.21	0.7226	197.94	198.08	0.696
23.70	0.8228	164.49	164.68	1.025	27.29	0.7295	198.09	198.22	0.708
23.79	0.8409	169.71	169.92	1.084	27.38	0.7972	201.44	201.58	0.725
23.87	0.8578	166.77	167	1.153	27.46	0.828	207.33	207.48	0.737
23.96	0.839	167.73	167.95	1.178	27.55	0.8264	210.27	210.41	0.733
24.04	0.8069	182.54	182.78	1.248	27.63	0.8216	214.4	214.54	0.748
24.13	0.8301	202.37	202.63	1.307	27.72	0.8204	225.95	226.1	0.783
24.21	0.8656	223.45	223.7	1.284	27.81	0.8329	250.95	251.1	0.8
24.30	0.9131	239.64	239.87	1.173	27.89	0.8438	276.31	276.47	0.823
24.38	0.9318	247.81	248.03	1.154	27.98	0.8445	300.3	300.46	0.847
24.47	0.9778	256.97	257.19	1.149	28.06	0.8452	307.22	307.38	0.853
24.55	1.0002	262.49	262.71	1.122	28.15	0.846	299.67	299.83	0.822
24.64	1.0121	263.38	263.58	1.068	28.23	0.8617	287.37	287.52	0.785
24.72	1.0324	261.25	261.46	1.053	28.54	0.6482	163.89	164.02	0.676
24.81	1.044	260.11	260.32	1.061	28.62	0.5164	147.43	147.57	0.704
24.89	1.0555	253.97	254.18	1.076	28.71	0.4155	137.03	137.16	0.664
24.98	1.0643	249.56	249.76	1.083	28.79	0.3427	131.63	131.76	0.678
25.07	1.0459	251.82	252.04	1.139	28.88	0.3187	125.54	125.66	0.635
25.32	0.9765	246.94	247.1	0.816	28.96	0.3116	112.33	112.44	0.572
25.41	0.9658	240	240.18	0.916	29.04	0.2821	99.45	99.56	0.599
25.49	0.9828	243.02	243.2	0.939	29.13	0.2596	90.32	90.43	0.573
25.58	0.98	245.54	245.71	0.857	29.22	0.2519	81.52	81.63	0.541
25.66	0.9143	240.15	240.32	0.852	29.30	0.2408	72.57	72.68	0.556
25.75	0.8951	236.76	236.93	0.859	29.39	0.211	65.29	65.41	0.591
25.83	0.8386	232.87	233.03	0.838	29.47	0.2115	60.55	60.67	0.629
25.92	0.7654	229.85	230.01	0.814	29.56	0.2297	57.6	57.72	0.607
26.00	0.7231	226.72	226.87	0.807	29.65	0.2173	53.92	54.04	0.621
26.09	0.7113	228.94	229.1	0.793	29.73	0.2159	48.59	48.71	0.602
26.17	0.7198	231.86	232.01	0.733	29.82	0.2129	46.51	46.63	0.631
26.26	0.7138	229.47	229.61	0.724	29.90	0.2237	46.94	47.06	0.637
26.35	0.6865	226.2	226.34	0.703	29.99	0.1972	49.07	49.19	0.623
26.43	0.6856	219.8	219.93	0.699	30.08	0.1812	51.89	52.01	0.625
26.52	0.6475	214.89	215.02	0.7	30.16	0.1807	54.82	54.94	0.631
26.60	0.6679	213.5	213.64	0.686	30.25	0.1931	56.11	56.24	0.665

Table D.9 Continued

z	f_s	q_u	q_t	u_2
(ft)	(tsf)	(tsf)	(tsf)	(tsf)
30.33	0.1984	56.69	56.82	0.663
30.42	0.2038	57.11	57.24	0.665
30.51	0.19	60.14	60.27	0.672
30.59	0.2079	63.31	63.45	0.696
30.68	0.2277	62.18	62.32	0.699
30.76	0.2279	57.62	57.75	0.704
30.85	0.238	50.18	50.31	0.691
30.93	0.2751	42.92	43.05	0.693
31.02	0.2968	34.75	34.89	0.693
31.11	0.3367	28.33	28.46	0.684
31.20	0	23.82	23.96	0.711
31.28	0	19.11	19.25	0.752
31.37	0	15.65	15.8	0.81
31.46	0	13.46	13.63	0.91
31.46	0	13.46	13.63	0.91

REFERENCES

American Society for Testing and Materials, ASTM [2004], *Annual Book of ASTM Standards*, Philadelphia, PA, Vol. 4.08, ASTM D5778, D1586. D 6635, D4428M, D 421, D 422 , D 4318, D 2435.

Andrus, R.D., Hayati, H., and Mohanan, N.P. (2009) "Correcting liquefaction resistance for aged sands using measured to estimated velocity ratio," Journal of Geotechnical and Geoenvironmental Engineering, 135(6), 735-744.

Andrus, R.D., Piratheepan, P., Ellis, B.S., Zhang, J., and Juang, C.H. (2004a). "Comparing Liquefaction Evaluation Methods using Penetration-V_S Relationships." *Soil Dyn. and Earthquake Engr.*, Vol. 24, No. 6, pp. 713-721.

Andrus, R.D. and Stokoe, K.H., II (2000), "Liquefaction resistance of soils from shear wave velocity." Journal of Geotechnical and Geoenvironmental Engineering, 126(11), 1015-1025.

Arango, I., Lewis, M.R., and Kramer, C. (2000). "Updated Liquefaction Potential Analysis Eliminates Foundation Retrofitting of Two Critical Structures", *Soil Dynamic and Earthquake Engr. Conf.,* Bergen, Norway, Elsevier Publishers, Vol. 20, pp. 17 - 25.

Baldi, G., Belloiti, R., Ghionna, V., Jamiolkowski, M., Marchetti, S., and Pasqualini, E. (1986). "Flat Dilatometer Tests in Calibration Chambers." *Proc., In-Situ 1986, ASCE Spec. Conference on "Use of In Situ Tests in Geotechnical Engineering"*, Virginia Tech, Blacksburg, VA, June, ASCE Geotechnical Special Publ. No. 6, 431-446.

Boller, R.C. (2008). "Geotechnical Investigations at Three Sites in the South Carolina Coastal Plain that Did Not Liquefy During the 1886 Charleston Earthquake." *M.S. Thesis*, Clemson University, Clemson, SC.

Cetin, K.O., Seed, R.B., Kiureghian, A.D., Tokimatsu, K., Harder, L.F., Jr., Kayen, R.E., and Moss, R.E.S. (2004), "Standard Penetration Test-Based Probabilistic and Deterministic Assessment of Seismic Soil Liquefaction Potential", *J. of Geotechnical and Geoenvironmental Engr.*, Vol. 130, No. 12, pp. 1314-1340.

Chapman, M.C., Martin, J.R., Olgun, C.G., and Beale, J.N. (2006). "Site-response Models for Charleston, South Carolina and Vicinity Developed from Shallow Geotechnical Investigations." *Bulletin of the Seismological Society of America*, Vol. 96 (2), pp. 467-489.

Dutton, C.E. (1889). "The Charleston Earthquake of August 31, 1886." Ninth Annual Report 1887-1888, 203-528.

Friedman, G.M. and Sanders J.E. (1978). Principles of Sedimentology. John Wiley & Sons, New York, NY.

Geiger, A.J. (2009). "Analysis of aged sands that did not liquefy during the 1886 Charleston earthquake." *B.S. Honors Thesis*, Clemson University, Clemson, SC.

Geiger, A.J., Boller, R.C., Andrus, R.D., Heidari, T., Hayati, H., Camp, W.M., III. (2010). "Estimating liquefaction potential of a 200,000 year-old sand deposit near Georgetown, SC." *5th International Conf. on Recent Advances in Geotechnical Earthquake Engr. and Soil Dynamics*, accepted for publication.

Hayati, H. and Andrus, R.D. (2008a). "Liquefaction Susceptibility of Fine-Grained Soils in Charleston, South Carolina Based on CPT." *Proc., GeoCongress 2008*, ASCE, held March 9-12, New Orleans, LA.

Hayati, H. and Andrus, R.D. (2008b). "Liquefaction Potential Map of Charleston, South Carolina Based on the 1886 Earthquake." *J. of Geotechnical and Geo-environmental Engrg.,* Vol. 134, No. 3, pp. 815-828.

Hayati, H. and Andrus, R.D. (2009). "Updated Liquefaction Resistance Correction Factors for Aged Sands." *J. of Geotechnical and Geoenvironmental Engr.*, Vol. 135, No. 11.

Hayati, H., Andrus, R.D., Gassman, S.L., Hasek, M., Camp, W.M., III and Talwani, P. (2008). "Characterizing the Liquefaction Resistance of Aged Soils." *Proc., Geotechnical Earthquake Engr. and Soil Dynamics IV*, held May 18-22, Sacramento, CA.

Heidari, T. and Andrus, R.W. (2010). "Mapping Liquefaction Potential of Aged Soil Deposits in Mount Pleasant, South Carolina." *Engineering Geology*, Vol. 112, accepted for publication.

Idriss, I.M. and Boulanger R.W. (2004). "Semi-Empirical Procedures for Evaluating Liquefaction Potential During Earthquakes." *Proc., 11th Int. Conf. on Soil Dynamics and Earthquake Engr. (SDEE) and 3rd Int. Conf. on Earthquake Geotechnical Engr. (ICEGE)*, Berkley, CA, Vol. 1, pp. 32-56.

Idriss, I.M. and Boulanger, R.W. (2008). *Soil Liquefaction During Earthquakes,* Earthquake Engineering Research Institute, Berkeley, CA.

Juang, C.H., Jiang, T., and Andrus, R.D. (2002), "Assessing Probability-Based Methods for Liquefaction Potential Evaluations", *J. of Geotechnical and Geoenvironmental Engr.*, Vol. 128, No. 7, pp. 580-589.

Kayen, R.E., Mitchell, J.K., Seed, R.B., Lodge, A., Nishio, S., Coutinho, R. (1992). "Evaluation of SPT-, CPT-, and shear wave-based methods for liquefaction potential assessment using Loma Prieta data." *Proc., 4th Japan-U.S. Workshop on Earthquake-Resistant Design of Lifeline Facilities and Countermeasures for Soil Liquefaction,* Vol. 1, pp. 177-204.

Kramer, S.L. (1996). Geotechnical Earthquake Engineering. Prentice Hall, Upper Saddle River, NJ.

Leon, E., Gassman, S.L., and Talwani, P. (2006), "Accounting for Soil Aging when Assessing Liquefaction Potential", *J. of Geotechnical and Geoenvironmental Engr.*, Vol. 132, No. 3, pp. 363-377.

Lewis, M.R., Arango, I., Kimball, J.K., and Ross, T.E. (1999). "Liquefaction Resistance of Old Sand Deposits", *Proc., 11th Panamerica Conf. on Soil Mechanics and Geotech. Engrg.*, ABMS, San Paulo, Brazil, pp. 821-829.

Liao, S.C., and Whitman, R.V. (1986). "Overburden Correction Factors for SPT in Sand." *Journal of Geotechnical Engineering*, Vol. 112, No. 3, pp. 373-377.

May, J.P. (1978). "Quaternary Geology of Hobcaw Barony Georgetown, South Carolina." Report to the Belle W. Baruch Forest Science Institute, The Citadel, Charleston, SC.

Marchetti, S. (1980). "In-situ Tests by Flat Dilatometer." Journal Geotechnical Engineering 106 (GT3) Proc. Paper 15290, pp. 299-321.

Marchetti, S., Monaco, P., Totani, G., and Calabrese, M. (2001). "The flat dilatometer test (DMT) in soil investigations," *Proc., IN SITU 2001, International Conference on In Situ Measurement of Soil Properties, Bali, Indonesia.* 41 pp.

Martin, J.R. and Clough, G.W. (1990). "Implications from a Geotechnical Investigation of Liquefaction Phenomena Associated with Seismic Events in the Charleston, SC Area." Report to USGS Grant No. 14-08-00 1-G-1348, Virginia Tech, Blacksburg, VA.

McCartan, L., Lemon, E.M., Jr. and Weems, R.E. (1984). "Geologic Map of the Area between Charleston and Orangeburg." *Misc. Investigations Series Map I-1472,* scale 1:250,000, U.S. Geological Survey, Reston, VA.

Moss, R.E.S., Seed, R.B., Kayen, R.E., Stewart, J.P., Kiureghian, A.D. and Cetin, K.O. (2006). "CPT-Based Probabilistic and Deterministic Assessment of In Situ Seismic Soil Liquefaction Potential." *J. of Geotechnical and Geoenvironmental Engr.*, Vol. 132, No. 8, pp. 1032-1051.

Robertson, P.K. (1991). "Soil Classification using the Cone Penetration Test." *Canadian Geotechnical Journal*, 27(1), pp. 151-158.

Robertson, P.K. and Wride, C.E. (1998). "Evaluating Cyclic Liquefaction Potential Using the Cone Penetration Test." *Canadian Geotechnical J.*, Vol. 35, No. 3, pp. 442-459.

Seed, H.B. (1979). "Soil Liquefaction and Cyclic Mobility Evaluation for Level Ground During Earthquakes." *J. of Geotechnical Engr.*, Vol. 105, No. 2, pp. 201-255.

Seed, H.B. and I.M. Idriss (1971). "Simplified Procedure for Evaluating Soil Liquefaction Potential." *J. of the Soil Mechanics and Foundation Division*, Vol. 97, No. SM9, pp. 1249-1273.

Seed, H.B., Tokimatsu, K., Harder, L.F., Jr., and Chung, R.M. (1985). "Influence of SPT Procedures in Soil Liquefaction Resistance Evaluations." *J. of Geotechnical Engr.*, ASCE, Vol. 111, No. 12, pp. 1425-1445.

Silva, W., Wang, I., Siegel, T., Gregor, N., Darragh, R. and Lee, R. (2003). "Ground Motion and Liquefaction Simulation of the 1886 Charleston, South Carolina Earthquake." *Bulletin of the Seismological Society of America*, Vol. 93, No. 6, pp. 2717-2736.

Stiple, G.E. (1959). "Guidebook for the South Carolina Coastal Plain Fieldtrip of the Carolina Geological Society: Division of Geology, S.C. State Development Board." *Bulletin No. 24*, 27 p.

Troncoso, J., Ishihara, K. and Verdugo, R. (1988). "Aging Effects on Cyclic Shear Strength of Tailing Materials." *Proc., 9th World Conf. on Earthquake Engr.*, Vol. 3, pp. 121-126.

United States Geological Survey, USGS (2008). "United States National Seismic Hazard Maps." <http://gldims.cr.usgs.gov/>.

United States Geological Survey, USGS (2009). "2008 Interactive Deaggregations ,beta.)." <http://eqint.cr.usgs.gov/deaggint/2008/>.

Youd, T.L. and Perkins, D.M. (1978), "Mapping of Liquefaction-Induced Ground Failure Potential." *J. of Geotechnical Engr. Division, ASCE*, Vol. 104, No. 3, pp. 433-466.

Youd, T.L., Idriss, I.M., Andrus, R.D., Arango, I., Castro, G., Christian, J.T., Dobry, R., Finn, W.D.L., Harder, L.F., Jr., Hynes.M.E., Ishihara, K., Koester, J.P, Liao, S.S.C., Marcuson, W.F., III, Martin, G.R., Mitchell, J.K., Moriwaki, Y., Power, M.S., Robertson, P.K., Seed, R.B., and Stokoe, K.H., II (2001). "Liquefaction Resistance of Soils: Summary Report from the 1996 NCEER and 1998 NCEER/NSF Workshops on Evaluation of Liquefaction Resistance of Soils." *J. of Geotechnical and Geoenvironmental Engr.,* Vol. 127, No. 10, pp. 817-833.